LEABHARLANN CHOLÁISTE NA TRÍONÓIDE, BAILE ÁTHA CLIATH | TRINITY COLLEGE LIBRARY DUBLIN
Ollscoil Átha Cliath | The University of Dublin

Terms and Conditions of Use of Digitised Theses from Trinity College Library Dublin

Copyright statement

All material supplied by Trinity College Library is protected by copyright (under the Copyright and Related Rights Act, 2000 as amended) and other relevant Intellectual Property Rights. By accessing and using a Digitised Thesis from Trinity College Library you acknowledge that all Intellectual Property Rights in any Works supplied are the sole and exclusive property of the copyright and/or other IPR holder. Specific copyright holders may not be explicitly identified. Use of materials from other sources within a thesis should not be construed as a claim over them.

A non-exclusive, non-transferable licence is hereby granted to those using or reproducing, in whole or in part, the material for valid purposes, providing the copyright owners are acknowledged using the normal conventions. Where specific permission to use material is required, this is identified and such permission must be sought from the copyright holder or agency cited.

Liability statement

By using a Digitised Thesis, I accept that Trinity College Dublin bears no legal responsibility for the accuracy, legality or comprehensiveness of materials contained within the thesis, and that Trinity College Dublin accepts no liability for indirect, consequential, or incidental, damages or losses arising from use of the thesis for whatever reason. Information located in a thesis may be subject to specific use constraints, details of which may not be explicitly described. It is the responsibility of potential and actual users to be aware of such constraints and to abide by them. By making use of material from a digitised thesis, you accept these copyright and disclaimer provisions. Where it is brought to the attention of Trinity College Library that there may be a breach of copyright or other restraint, it is the policy to withdraw or take down access to a thesis while the issue is being resolved.

Access Agreement

By using a Digitised Thesis from Trinity College Library you are bound by the following Terms & Conditions. Please read them carefully.

I have read and I understand the following statement: All material supplied via a Digitised Thesis from Trinity College Library is protected by copyright and other intellectual property rights, and duplication or sale of all or part of any of a thesis is not permitted, except that material may be duplicated by you for your research use or for educational purposes in electronic or print form providing the copyright owners are acknowledged using the normal conventions. You must obtain permission for any other use. Electronic or print copies may not be offered, whether for sale or otherwise to anyone. This copy has been supplied on the understanding that it is copyright material and that no quotation from the thesis may be published without proper acknowledgement.

PHYSICOCHEMICAL STUDIES OF DICLOFENAC SALTS AND THE EFFECT OF BASIC EXCIPIENTS ON THEIR DISSOLUTION

by

Karen M. O'Connor, B.Sc. (Pharm.), M.P.S.I.

being a thesis submitted for the degree of

Doctor of Philosophy
in Pharmaceutics

at

University of Dublin
Trinity College

under the direction and supervision of

Professor O.I. Corrigan, B.Sc. (Pharm.), M.A., Ph.D., F.T.C.D., F.P.S.I.

September 2000

TRINITY COLLEGE
23 JAN 2001
LIBRARY DUBLIN
THESIS
6263.

DECLARATION

I give permission for the Library to lend or copy this thesis upon request.

Signed: Maria' Conor

DECLARATION

This thesis is submitted by the undersigned to the University of Dublin for examination for the degree of Doctor of Philosophy. It has not been submitted as an exercise for a degree at any other university. I carried out all the practical work except where duly acknowledged. This manuscript was written by me with the aid of editorial advice from Prof. O.I. Corrigan.

Karen O'Connor

Karen M. O'Connor

To my parents

TABLE OF CONTENTS

TABLE OF CONTENTS

Chapter 2. Some approaches to modifying drug properties

Experimental

Chapter 3. Materials and methods

Results and Discussion

Chapter 4. Physicochemical characterisation of diclofenac *N*-(2-hydroxyethyl)pyrrolidine and diclofenac diethylamine

Chapter 7. The effect of basic organic compounds on the dissolution of diclofenac salts

Chapter 8. General Discussion

ACKNOWLEDGEMENTS

I would like to thank my supervisor Professor Owen Corrigan for his guidance and support during the course of my research and in the preparation of this thesis.

I am grateful to Trinity College for providing me with a postgraduate award and travel funding. I would also like to thank Enterprise Ireland for their financial support.

I would like to thank the academic, secretarial and technical staff of the School of Pharmacy, in particular Anne Marie for all the advice, Mary, Pat, Brian and Nuala. I am also grateful to Rhona and Ray in Pharmaceutical Chemistry for their help with FT-IR and KFT.

I would like to acknowledge Dr. David Doff for his help with XRD, Dr. David Lloyd for the molecular modelling work, Sally Ann Cryan for assistance with the spectrofluorimetry, and Tara Fox for carrying out surface tension measurements.

Thanks to my fellow postgrads: Abina, Mark L., KG, Rosario, Idris, Dennis, Colleen, Sally Ann, Brendan, Bronagh, Nicole, Deirdre, Karl, Catríona, Len, Shane, Helena, Fiona, Mark H., Fergal, Anthony, Stephen, Mairéad and Tina. In particular, thanks to Anne Marie, Abina, Rosario, Catríona, Deirdre, Karl and Len for giving up their time to proof-read this thesis. Also, I would like to thank all other postgrads in the School of Pharmacy, especially those who kept me company in the Lincoln and Patrick for all the editing advice!

A special thanks to my friends Leonie, Serena, Sarah, Ger and Nuals, for knowing never to ask me when I'd be finished! Thanks to my friends from home: Vonnie, Annette and Anita. Thanks also to my house-mates and friends: Ger, Patsy, Caroline, Bríd, Catherine and Orlagh.

Finally, I would like to thank my parents and my sisters, Fiona and Ciara, for all their encouragement and support.

PRESENTATIONS ASSOCIATED WITH THIS THESIS

Oral presentation

Evaluation of biopharmaceutically relevant properties of some diclofenac salts, *23rd Annual Joint Research Seminar*, Queen's University, Belfast, March 1999 [K.M. O'Connor and O.I. Corrigan]

Poster presentation

Comparison of the physicochemical properties of sodium, diethylamine and *N*-(2-hydroxyethyl)pyrrolidine salts of diclofenac, *4th European Congress of Pharmaceutical Sciences*, Milan, September 1998 [K.M. O'Connor, M.T. Ledwidge and O.I. Corrigan]

ABBREVIATIONS AND SYMBOLS

γ	activity coefficient
θ	angle of incidence
ω	angular velocity of rotation
ρ	density
η	dynamic viscosity
δ	effective diffusion boundary layer thickness
μm	micrometre
$\pm$	plus or minus
$\in$	porosity
™	trademark
λ	wavelength
ΔG	change in free energy
ΔH	change in enthalpy
ΔS	change in entropy
$\sim$	approximately
®	registered trademark
τ	tortuosity
°	degree
°C	degree centigrade
a	activity
Å	angstrom
A	surface area
A^1_1	UV absorption of 1 %w/v solution, path length 1 cm
AMP	2-amino-2-methylpropanol
AMPD	2-amino-2-methyl-1,3-propanediol
ATR	attenuated total reflectance
B.N.	batch number
b.p.	boiling point
BA	benzylamine
C	carbon
C	concentration
c.p.m.	cycles per minute
CAC	critical association concentration
CD	coefficient of determination

cm	centimetre
cm^{-1}	frequency
CMC	critical micelle concentration
CMR	critical mixture ratio
CO_2	carbon dioxide
C_p	heat capacity
CPS	counts per second
Cu	copper
D	diffusion coefficient
DAMP	diclofenac 2-amino-2-methylpropanol
DAMPD	diclofenac 2-amino-2-methyl-1,3-propanediol
DAMPD-MH	DAMPD monohydrate
DBA	diclofenac benzylamine
DCFA	diclofenac acid
DDEA	diclofenac diethylamine
DDEA-MH	DDEA monohydrate
DDNL	diclofenac deanol
DHEP	diclofenac *N*-(2-hydroxyethyl)pyrrolidine
DHEP-A	DHEP anhydrate
DHEP-DH	DHEP dihydrate
DHEP-MH	DHEP monohydrate
DNa	diclofenac sodium
DNL	2-dimethylaminoethanol / deanol
DSC	differential scanning calorimetry
DtBA	diclofenac *tert*-butylamine
DTRIS	diclofenac tris(hydroxymethyl)aminomethane
exo	exothermic direction
FT-IR	fourier transform infrared spectroscopy
g	gram
G	intrinsic dissolution rate
h	diffusion layer thickness
H	hydrogen
H_2O	water
H_3O^+	hydronium ion
HCl	hydrochloric acid
HEP	*N*-(2-hydroxyethyl)pyrrolidine
hr	hour

HSM	hot stage microscopy
IDR	intrinsic dissolution rate
J	rate of transport per unit area
J	joule
k	Boltzmann constant (1.3806×10^{-23} J K^{-1})
K	degree Kelvin
K	dissolution rate constant
K_a	dissociation constant for a weak acid
$K_a^{'}$	apparent dissociation constant for a weak acid
K_b	dissociation constant for a weak base
KBr	potassium bromide
KFT	Karl Fischer titration
k_R	interfacial transport rate constant
K_{SP}	solubility product constant
$K_{SP}^{'}$	apparent solubility product
kV	kilovolt
L	Avogadro constant (6.022×10^{23} mol^{-1})
log	logarithm to the base 10
M	molecular weight
M	moles per litre
m.p.	melting point
mA	milliamp
mg	milligram
min	minute
ml	millilitre
mm	millimetre
mM	millimolar
mmol	mmole
mN	milliNewton
mol	mole
MSC	model selection criterion
mW	milliwat
N	nitrogen
n	number of replicates
N_2	nitrogen gas
Ni	nickel

nm	nanometre
NO_2	nitrogen dioxide
NPN	*N*-phenyl-1-naphthylamine
P	% conversion from SALT1 to SALT2
P_e	effective permeability coeeficient
pH	minus log of hydrogen ion concentration
pH_{max}	pH of theoretical maximum solubility
pK_a	dissociation exponent for a weak acid
pK_{SP}	$-\log_{10}(K_{SP})$
pK_W	dissociation exponent for water
PVP	polyvinylpyrrolidine
r	radius
R	ideal gas constant (8.314 J/K/mol)
r.p.m.	revolutions per minute
R^2	correlation coefficient
SD	standard deviation
T	temperature (degrees Kelvin)
t	time
tBA	*tert*-butylamine
TG	thermogravimetric analysis
T_g	glass transition temperature
T_m	melting point (absolute scale)
T_t	transition temperature
TRIS	tris(hydroxymethyl)aminomethane
UV	ultraviolet spectroscopy
v	kinematic viscosity
V	volume
V_m	molar volume
vs.	versus
v/v	volume per volume
W	weight
w/v	weight per volume
w/w	weight per weight
X	solubility (mole fraction)
XRD	X-ray diffraction

SUMMARY

This study involved investigation of the physicochemical properties of diclofenac salts prepared from a range of organic bases. The salts examined included five novel salts of diclofenac, prepared from the following bases: *tert*-butylamine, 2-amino-2-methylpropanol, 2-amino-2-methyl-1,3-propanediol, benzylamine and deanol. Characterisation techniques included X-ray diffraction, differential scanning calorimetry, thermogravimetric analysis, thermal microscopy, Karl Fischer titration, FT-IR spectroscopy and elemental analysis.

In the case of the salts prepared from 2-amino-2-methylpropanol and benzylamine, two polymorphic forms of each salt were identified. For three of the salts, novel pseudopolymorphic forms were identified. The behaviour in solution of the novel hydrates of diclofenac *N*-(2-hydroxyethyl)pyrrolidine and diclofenac diethylamine (DDEA) was investigated. The solubility of the anhydrous form of DDEA was estimated from the ratio of the intrinsic dissolution rates of the monohydrate and anhydrate forms.

The aqueous solubilities of the salts studied ranged from 3.95 mM to 446 mM, corresponding to 113-fold difference in solubility. Correlation was found between the inverse of the salt melting point and the logarithm of salt solubility. A log-log relationship was observed between salt solubility and hydrogen ion concentration in the salt solution. Relationships between the properties of the salt forming agents and those of the resulting diclofenac salts were explored. Reasonable correlation was found between the free base melting point and the salt melting point.

The pH-solubility profiles of three diclofenac salts were studied. In each system, supersaturation was observed at the pH_{max}. The apparent solubility product (K'_{SP}) values were calculated from the pH-solubility data for each salt system. An increase in the calculated solubility product was observed around the pH_{max}, the region in which supersaturation occurred, suggesting that the supersaturation was due to self-association of the salts. This was consistent with evidence of self-association of the salts from surface tension measurements and solubilisation experiments.

The effect of a basic excipient on the dissolution of a salt of a weakly acidic drug was investigated. Dissolution of diclofenac from compressed discs containing mixtures of a diclofenac salt and a basic excipient, in various w/w ratios, was examined. From the range of diclofenac salts, the most soluble salt and the least soluble salt were selected for inclusion in the study. Two solid organic bases with high aqueous solubilities, tris(hydroxymethyl)aminomethane and 2-amino-2-methyl-1,3-propanediol, were employed in the study. The inclusion of the basic excipients resulted in

slight enhancement in the dissolution rate of the less soluble salt and dramatic suppression in the dissolution rate of the more soluble salt. These findings were attributed to the solubilities of the salts formed between diclofenac and the basic excipients used. For each base:salt system studied, XRD analysis confirmed the presence of the new salt, formed between diclofenac acid and the basic excipient, in the discs.

The two component (salt conversion) model was developed to predict dissolution from mixtures of a salt of an ionisable drug and an ionisable excipient with the potential to form a salt with the drug. The model assumed that all the drug present, initially in the form of the salt added to the disc, interacted with available ionisable excipient to form a new salt. Dissolution from three of the four salt:base systems studied was accurately predicted by the two component (salt conversion) model. Best agreement between the observed and predicted rates was observed for the systems prepared with 40 – 90% base. Deviations from the model at high weight fractions of base and, in the case of the systems containing the more soluble drug, at low weight fractions of base were attributed to carrier controlled dissolution. Deviations from the model in the case of one of the base:salt systems studied may have resulted from the ability of the newly formed salt in the system to form supersaturated solutions. The three component (salt conversion) model was developed to predict dissolution rates when the conversion from the original salt form was less than complete.

The present work illustrates that the inclusion of a basic excipient in the formulation of an acidic drug will not always result in enhanced drug dissolution. The solubility of the salt formed between the drug and the ionisable excipient has an important influence on the dissolution of the drug.

INTRODUCTION

ORIGIN AND SCOPE OF THE THESIS

The physicochemical characteristics and resultant biological performance of a drug can be dramatically altered by conversion to a salt form (Berge et al., 1977). Studies have been carried out on the effect of salt formation on physical and chemical characteristics in an attempt to predict the influence of a particular salt forming agent on the properties of the parent compound (Berge et al., 1977; Gould, 1986). In particular, relationships between the properties of the salt-forming agent and the solubility of the resultant salt have been explored (Wells, 1988). Unfortunately, no reliable way of predicting the influence of a salt-forming agent on the behaviour of the parent compound has been reported. Therefore, selection of an appropriate counterion to produce a salt with the desired combination of properties is still carried out on an empirical basis.

Ionisable excipients, which have the potential to interact with acidic or basic drugs, have been used to enhance dissolution. Several studies on the influence of basic excipients (Levy et al., 1965; McGloughlin, 1989) or buffering agents (Javaid and Cadwallader, 1972; Doherty and York, 1989; Tirkonnen et al., 1995; Chakrabarti and Southard, 1997; Preechagoon et al., 2000) on the dissolution of acidic drugs have been reported. The effect of acidic excipients on the dissolution of salts of basic drugs has also been investigated (Ventouras et al., 1977; Ventouras and Buri, 1978; Gruber et al., 1980; Cleary, 1987; McNamara, 1988; Thoma and Zimmer, 1990; Kohri, 1991; van der Veen et al., 1991a and 1991b; Gabr, 1992; Thoma and Ziegler, 1998; Streubel et al., 2000). The dramatic enhancements in drug dissolution rate observed were not consistent with the rates predicted from existing models for two component mixtures.

McGloughlin (1989) developed two models to predict dissolution from acidic drug:basic excipient mixtures, the two component (linear solubility) model and the two component (salt formation) model. Both models predict a plateau in the dissolution rate:composition profile, corresponding to the solubility of the salt of the acid and base. Whereas several studies have investigated the influence of ionisable excipient on the dissolution of salts of acidic and basic drugs, the authors did not endeavour to predict dissolution from these systems or to investigate the influence of the solubility of the salt formed between drug and excipient on the rate of dissolution of the drug.

The objectives of the present work were:

- To examine and compare biopharmaceutically relevant properties, such as solubility, dissolution rate and membrane transport, of diclofenac salts available in pharmaceutical preparations.

- To account for variation between commercial batches of diclofenac *N*-(2-hydroxyethyl)pyrrolidine with regard to their behaviour in solution.

- To investigate the physicochemical properties of a range of salts of diclofenac, a weakly acidic drug, in order explore possible relationships between the properties of the salt-forming agent and those of the resultant salt.

- To investigate the effect of a basic excipient on the dissolution of a salt of a weakly acidic drug.

- To attempt to predict dissolution rates from mixtures of a salt of an ionisable drug and an ionisable excipient with the potential to interact with the drug.

Chapter 1

Pharmaceutically relevant properties of drugs

1.1. INTRODUCTION

The physicochemical properties of a drug govern its bioavailability and therapeutic efficacy. Consequently, extensive and systematic preformulation studies of the physicochemical characteristics of a drug entity are necessary to determine the most suitable form for formulation.

1.2. SOLUBILITY

Solubility is defined as the concentration of the dissolved solid in a saturated solution, which is in equilibrium with the solid, at a defined temperature and pressure (Grant and Brittain, 1995). The solubility of a compound depends on the physical and chemical properties of the solute, the nature and composition of the solvent medium, temperature and pressure.

For many drugs that are poorly absorbed, the rate of absorption is dissolution rate controlled. Since solubility is the driving force for dissolution (Noyes and Whitney, 1897), the aqueous solubility of a drug may have a strong influence on its bioavailability. Kaplan (1972) suggested that unless a compound has an aqueous solubility greater than 1% over a pH range of 1 to 7 at 37°C, absorption problems will be encountered.

The chemical stability of a drug can be affected by its solubility since the reactivity of a compound in solution can be very different to that in suspension. For a solution phase reaction to occur, it is usually necessary for the substrate to be fully dissolved (Yalkowsky and Banerjee, 1992).

Furthermore, the solubility of a drug has a strong influence on its ease of formulation (Anderson and Conradi, 1985). For example, a solution formulation for intravenous administration would require the drug to be highly water-soluble.

1.2.1. Factors influencing solubility

Solubility may be viewed as an equilibrium of a solute between its dissolved and undissolved states. This equilibrium is governed by the Gibbs free energy of solution (ΔG_{soln}) at constant temperature and pressure, according to the following equation:

$$\Delta G_{soln} = \Delta H_{soln} - T \Delta S_{soln} \qquad \textbf{Equation 1. 1}$$

where ΔH_{soln} is the enthalpy change or *heat of solution*, T is the absolute temperature and ΔS_{soln} is the entropy change. Negative values of ΔG_{soln} favour the dissolution process.

An ideal solution is defined as one in which no heat is evolved or absorbed when the individual components are mixed together ($\Delta H_{soln} = 0$) and the final volume is an additive property of the individual components. The molecules exhibit complete freedom of movement and randomness of distribution and there is complete uniformity of attractive forces. Ideal solubility is not affected by the nature of the solvent. The solubility of a solid in an ideal solution (in mole fraction), X_2^i, is given by the following equation:

$$-\log X_2^i = \frac{\Delta H_f}{2.303R}\left(\frac{T_m - T}{T\,T_m}\right) \qquad \textbf{Equation 1. 2}$$

where ΔH_f is the molar heat of fusion, R is the universal gas constant (8.314 J/K/mol) and T_m is the melting point of the solid solute in absolute degrees. The superscript i in the symbol X_2^i refers to an ideal solution and the subscript 2 designates the mole fraction as that of the solute. At temperatures above the melting point, the solute is in the liquid state and, in an ideal solution, the liquid solute is miscible in all proportions with the solvent. Therefore, Equation 1.2 no longer applies. Furthermore, ΔH_f varies with temperature due to the difference between the heat capacities of solid and supercooled liquid (ΔC_p). For prediction of solubility at temperatures considerably lower than T_m, a correction term can be used to account for the difference between the heats of fusion at T and at T_m (James, 1986). As T approaches T_m, the correction term becomes very small and Equation 1.2 applies.

The enthalpy of fusion, ΔH_f, is the energy required to increase interatomic or molecular distances, to facilitate an increase in disorder, to overcome crystal lattice energy, and allow melting (Wells, 1988). There is a close relationship between ΔH_f and melting point: a crystal with weak bonds has a low melting point and ΔH_f and a strong crystal lattice results in high melting point and ΔH_f values.

A solution is described as having an *activity* or effective concentration. The activity of a solute in a solution, a_2, is expressed as the concentration (in mole fraction), X_2, multiplied by the activity coefficient, γ_2:

$$a_2 = X_2 \gamma_2$$ **Equation 1. 3**

In an ideal solution, the activity coefficient is unity and the activity of the solute is equal to its concentration. The activity coefficient, γ_2, is obtained by considering the intermolecular forces of attraction that must be overcome to remove a molecule from the solute phase and deposit it in the solvent (Martin, 1993).

Equation 1.2 indicates that solute melting point and heat of fusion have an important influence on solubility. Accordingly, Yalkowsky (1981) reported a relationship between melting point and solubility for a series of polycyclic aromatic hydrocarbons.

Solubility as a function of temperature can be calculated using the heat of solution, ΔH_{soln}, instead of the heat of fusion, from an equation analogous to Equation 1.2. For electrolytes and non-electrolytes, the following equation is used (Williamson, 1944):

$$\ln\left(\frac{c''}{c'}\right) = \frac{\Delta H_{soln}}{R}\frac{(T'' - T')}{(T' T'')}$$ **Equation 1. 4**

where c' is the concentration of solute in solution at the temperature T' (Kelvin) and c'' is the concentration at the temperature T''. In the case of strong electrolytes, R in Equation 1.4 is replaced by νR, in which ν is the number of ions produced in the dissociation of the electrolyte. The heat of solution for a given solute may be endothermic or exothermic and will govern the effect of temperature on solubility. For most solids, the ΔH_{soln} is endothermic and the solubility increases with an increase in temperature, in accordance with the Le Chatelier principle (Richards, 1991).

The overall heat of solution, ΔH_{soln}, is derived from the sum of the enthalpy required to separate molecules or ions in the crystal lattice (ΔH_{cl}) and the enthalpy change on immersion of the solute molecules in the solution (ΔH_{solv}) (Richards, 1991). Different crystalline arrangements of a drug, such as polymorphs or solvates, will have different ΔH_{cl}, ΔH_{soln} and ΔS_{soln} values, resulting in different free energies and solubilities.

The molecular structure of a solid can influence its solubility. For example, the presence of hydrophilic groups can cause a significant increase in the aqueous solubility of a solute (Richards, 1991). Conversely, esterification of erythromycin to form erythromycin propionate causes a

reduction in solubility which can be attributed to the presence of the hydrophobic propionate substituent (Richards, 1991).

In a saturated solution of a slightly soluble electrolyte or organic salt, an equilibrium exists between the ionised and unionised species:

$$A_Y B_{X\,(solid)} \longleftrightarrow YA^{X+} + XB^{Y-} \qquad \textbf{Equation 1. 5}$$

The solubility is characterised by the solubility product, K_{SP}, of the compound:

$$K_{SP} = \frac{\{A^{X+}\}^Y \{B^{Y-}\}^X}{\{A_Y B_X\}} \qquad \textbf{Equation 1. 6}$$

where {X} indicates the activity of species X. Since the electrolyte dissolves only with difficulty and the ionic strength is low, the equilibrium expression may be written in terms of concentrations rather than activities:

$$K_{SP} = \frac{[A^{X+}]^Y [B^{Y-}]^X}{[A_Y B_X]} \qquad \textbf{Equation 1. 7}$$

where [X] indicates the concentration of species X.

The solubility of the solid phase is essentially constant, so that:

$$K_{SP} = [A^{X+}]^Y [B^{Y-}]^X \qquad \textbf{Equation 1. 8}$$

The introduction of ions which complex with either A^{X+} or B^{Y-} could result in an increase in the solubility of the salt. This is because a decrease in $[A^{X+}]$ or $[B^{Y-}]$ would be compensated for by further ions from the solid phase entering into solution to maintain the solubility product equilibrium.

When the ion product exceeds K_{SP}, precipitation will occur. Addition of a common ion, e.g. B^{Y-}, causes $A_Y B_X$ to precipitate to maintain the equilibrium solubility product. This *common ion effect* results in a reduction in the equilibrium solubility of sparingly soluble electrolytes. For example, Lin et al. (1972) reported that the free base of an antihypertensive drug exhibited a higher

dissolution rate than that of its hydrochloride salt in 0.1 N HCl. This was attributed to suppression of the solubility of the salt in the presence of the chloride ions. Miyazaki et al. (1975, 1979, 1980, 1981a and 1981b) carried out extensive studies on the dissolution of pharmaceutical bases and their hydrochloride salts in acidic media. The apparent dissolution rates and solubilities of the bases in dilute hydrochloric acid at pH 1 – 2 were higher than those of the hydrochloride salts. The dissolution rates of the bases increased with a decrease in pH and a corresponding increase in Cl^- concentration. The reverse was true for the hydrochloride salts. This was attributed to common ion suppression of the solubility product equilibrium.

The Setschenow equation was derived empirically to quantify the phenomena of *salting out* that can result from the addition of an electrolyte to non-electrolyte solutions (Setschenow, 1889):

$$\log f = \log \frac{S_O}{S} = k\, C_S \qquad \textbf{Equation 1. 9}$$

where S and S_O are the solubilities of the non-electrolyte in solvent with and without the electrolyte present, C_S is the molar concentration of the electrolyte solution, f is the activity coefficient of the non-electrolyte in the electrolyte solution and k is the overall salting out constant, which can be calculated from the slope of a plot of $\log f$ versus C_S. The Setschenow equation has been used to describe the effect of the chloride ion on the solubility of drug hydrochloride salts (Lin et al., 1972; Miyazaki et al., 1975, 1979, 1980, 1981a and 1981b). Bogardus (1982) examined the relationship between the empirical Setschenow equation and the solubility product equilibrium theory. The study demonstrated that the apparent Setschenow salting out constant is not a physical chemical constant and it is related to solubility or solubility product constant only at low concentrations of added salt. The solubility product (K_{SP}) was shown to be inversely proportional to the salting out constant squared. Therefore, K_{SP} is a more sensitive indicator of common ion effects than the salting out constant. One of the major disadvantages of the use of the Setschenow plots is that self-association cannot be detected. Since the initial slope is most important in a Setschenow plot and this region is most susceptible to the effects of self-association, use of this method may lead to erroneous results (Bogardus, 1982).

1.2.2. pH-solubility relationships

Weak acids or bases are only partially dissociated in solution. The pH of the solution influences the degree of ionisation and the solubility. Approximately 95% of all drugs are weak organic acids or bases (Wells, 1988), exhibiting variable equilibrium solubilities within the wide physiological

pH range. Consequently, an understanding of the pH-solubility profile of a drug is necessary in preformulation work. Dittert et al. (1964) described the phase solubility method for investigating pH-solubility profiles.

Kramer and Flynn (1972) investigated the pH-solubility profile of the free base and HCl salt forms of two amines. The pH-solubility profile obtained for each system could not be described by a single equation since it was not continuous. The equilibrium for B, a weak monoprotic base, in a saturated solution is given by:

$$BH^+ + H_2O \longleftrightarrow H_3O^+ + B \qquad \textbf{Equation 1. 10}$$

where B is the free base and BH^+ is the protonated species.

The apparent dissociation constant ($K_a^{'}$) for the reaction is given by:

$$K_a^{'} = \frac{[H_3O^+][B]}{[BH^+]} \qquad \textbf{Equation 1. 11}$$

The overall pH-solubility profile for a weak base is a combination of two individual profiles in which either the free base or the salt is solubility limiting. The point at which the ionised and unionised species are simultaneously saturated, which occurs at the juncture of these profiles, is designated the pH_{max}. The total solubility of the base in a saturated solution consists of the concentration of both the unionised form, [B], and ionised form, $[BH^+]$. At low pH, when pH < pH_{max}, the solubility of the protonated form is limiting and the total solubility (C_S) is given by:

$$C_S = [BH^+]_S + [B] = [BH^+]_S \left(1 + \frac{K_a^{'}}{[H_3O^+]} \right) \qquad \textbf{Equation 1. 12}$$

where [B] is the concentration of the unionised form of the base, or the *intrinsic solubility*, $[BH^+]$ is the concentration of the ionised form and the subscript s denotes a saturated species.

At high pH, when pH > pH_{max}, the solubility of the free base is limiting and the total solubility is given by:

$$C_S = [BH^+] + [B]_S = [B]_S \left(1 + \frac{[H_3O^+]}{K_a'}\right) \qquad \textbf{Equation 1. 13}$$

Chowhan (1978) investigated the pH-solubility relationship of organic carboxylic acids and their salts. The pH-solubility profile obtained for each system was not continuous and two equations were developed to characterise the profiles. These equations, relating to weak acids, correspond to those derived by Kramer and Flynn (1972) for weak bases. At low pH, when $pH < pH_{max}$, the total solubility is:

$$C_S = [HA]_S + [A^-] = [HA]_S \left(1 + \frac{K_a'}{[H_3O^+]}\right) \qquad \textbf{Equation 1. 14}$$

where HA is the free acid and A^- is the ionised species. At high pH, when $pH > pH_{max}$, the solubility is given by:

$$C_S = [HA] + [A^-]_S = [A^-]_S \left(1 + \frac{[H_3O^+]}{K_a'}\right) \qquad \textbf{Equation 1. 15}$$

Chowhan showed that Equations 1.14 and 1.15 adequately described the experimentally obtained pH-solubility profile of the acidic drug, naproxen. The observed solubility profile for 7-methylsulfinyl-2-xanthonecarboxylic acid and 7-methylthio-2-xanthonecarboxylic acid and their salts agreed with the calculated profile at low pH values only. At pH values equal to or greater than the pH corresponding to complete ionisation, the observed solubility values were higher than calculated. The author postulated that the enhanced solubility was due to complex formation or hydration of the salts.

By combining the known expressions for solubility as a function of pH (Kramer and Flynn, 1972; Chowhan, 1978) with the appropriate solubility product expression, Streng et al. (1984) derived equations which describe the pH-solubility profile of a weak acid or base as a function of its pK_{SP}, pK_a and uncharged species solubility. These equations can be used to estimate the change in solubility following the addition of salt to the system.

1.3. DIFFUSIVITY

Diffusion is defined as a process of mass transfer of individual molecules of a substance, brought about by random molecular motion (Martin, 1993). The process of diffusion of substances through liquids, solids and membranes is of considerable importance in pharmaceutics (Martin, 1993). Mass transfer processes relevant to drug delivery include dissolution from solid dosage forms (Nernst and Brunner, 1904) and transport across biological membranes (Florence and Attwood, 1988).

Flow of molecules through a barrier, such as a polymeric membrane, is a convenient way to study diffusion processes. The passage of matter through a barrier may occur by simple molecular diffusion, following partitioning of the permeating molecules into the bulk membrane, or by movement through solvent-filled pores and channels. In the case of the transport of drug through a porous polymeric membrane, the diffusing molecules pass through the pores. However, if the molecules are too large for such channel transport, the diffusant may dissolve in the polymer matrix and pass through by molecular diffusion (Martin, 1993).

In transport studies across membranes, the steady state flux is described by Fick's first law of diffusion, which states that the rate of transfer of diffusing substance per unit area (J) is proportional to the concentration gradient:

$$J = -D\frac{dC}{dx} \qquad \textbf{Equation 1. 16}$$

where D is the *diffusivity* or *diffusion coefficient* of the diffusant, C is its concentration and x is the distance of movement perpendicular to the surface of the barrier. The negative sign in Equation 1.16 signifies that diffusion occurs in a direction opposite to that of increasing concentration. For an homogenous film of a given cross-sectional area and a constant thickness, Fick's law can be expressed as:

$$J = P_e\,\Delta C \qquad \textbf{Equation 1. 17}$$

where P_e is the *effective permeability coefficient* and ΔC is the concentration difference across the total film thickness. Under sink conditions, ΔC is replaced with the concentration of permeant in the receptor phase, C_r:

$$J = P_e C_r \qquad \textbf{Equation 1. 18}$$

In the case of a partition-diffusion mass transfer mechanism through a nonporous membrane, the permeability coefficient, P_e, is given by:

$$P_e = \frac{D_m K_m}{h_m} \qquad \textbf{Equation 1. 19}$$

where D_m is the permeant diffusion coefficient in the membrane, K_m is the membrane-donor phase partition coefficient and h_m is the membrane thickness.

In the case of transport across a porous membrane, P_e is given by:

$$P_e = \frac{1}{\frac{2}{P_{aq}} + \frac{1}{P_m}} \qquad \textbf{Equation 1. 20}$$

where P_{aq} and P_m are the permeability coefficients due to the aqueous diffusion layer and the membrane, respectively (Ho et al., 1980). The transport of a substance through the water-filled pores of a porous membrane is dependent on the aqueous diffusivity of the compound.

From Equation 1.18, it can be seen that the maximum transport rate of a given compound across a membrane is limited by its solubility (C_S). The importance of supersaturation as a means of enhancing flux beyond the limiting value achieved with saturated systems has been recognised (Higuchi, 1960; Kondo et al., 1987; Pellet et al., 1994; Pellet et al., 1997; Iervolino, 2000; Raghavan, 2000). The use of a high-energy phase of a drug, such as those formed in drug:PVP coprecipitates, results in an enhancement of drug flux across a membrane (Corrigan et al., 1980). This is because C_S is effectively increased without altering P_e. Other solubility-enhancing strategies, such as solubilisation or cosolvent addition, generally result in a lower P_e value (Corrigan, 1995).

Other methods, both physical and chemical, have been employed to increase the transport of drug molecules across membranes. Iontophoresis involves the application of a voltage drop across a membrane to enhance the rate of penetration of ions. It has been employed for the transdermal delivery of drugs for systemic therapy (Banga and Chien, 1988). Chemical methods include the

use of penetration enhancers. These enhance transport through the membrane (the stratum corneum) by altering its barrier properties.

In some salt solutions, a mutual affinity between the cation and anion present in the salt allows the formation of a complex or weakens the ionic dissociation, resulting in *ion pairs*. The ions are in close proximity and their charges are masked or shielded by the low dielectric constant of hydrophobic moieties of the functional groups. Therefore ion pairs display a lower hydrophilicity than the two ions considered separately and offer unusual behaviour for an ionic species, such as increased partition towards a lipid phase (Inagi et al., 1981; Pandit et al., 1989; Grant and Higuchi, 1990; Fini et al., 1999). Ion pair formation is a possible explanation for the ability of quaternary ammonium compounds, which are ionised under all pH conditions, to be absorbed readily (Florence and Attwood, 1988; Takács-Novák and Szász, 1999). Many authors have reported the flux of ionisable drugs across synthetic lipophilic membranes and biological membranes (under pH conditions which minimise the contribution of the unionised form) and attributed this to ion pair formation (Inagi et al., 1981; Maitani et al., 1994; Valenta et al., 2000).

1.4. DISSOLUTION RATE

Dissolution is often the slowest of the various stages involved in the release of a drug from its dosage form and passage into the systemic circulation. Therefore, it is frequently the limiting or rate-controlling step in bioabsorption for drugs of low solubility (Martin, 1993).

1.4.1. Single component dissolution

Dissolution processes can be classified according to the following three types (Wurster and Taylor, 1965):

(a) The liberation of solute molecules at the interface occurs much faster than the diffusion of solute from the interfacial boundary to the body of the solution. Therefore, the transport process determines the dissolution rate. Dissolution is said to be *diffusion controlled*.

(b) The reaction at the interface is much slower than the transport process. In this case, the processes of liberation and solvation of solute molecules at the interface determine the dissolution rate. Dissolution is said to be *surface reaction controlled*.

(c) The rate of the interfacial reaction and the rate of transport are of the same order of magnitude so that the dissolution rate is a function of both processes.

1.4.1.1 Diffusion controlled dissolution

In most cases of the dissolution of solids in liquids, dissolution is diffusion controlled (Carstensen, 1972; Nicklasson, 1981). That is, the surface reaction is instantaneous and the transport of solute molecules from the interfacial boundary to the bulk solution is the rate-limiting step in the dissolution process.

The rate at which a solid dissolves in a solvent was described quantitatively by Noyes and Whitney in 1897:

$$\frac{dC}{dt} = K\,(C_S - C) \qquad \textbf{Equation 1. 21}$$

where C_S is the equilibrium solubility of the solid at the experimental temperature, C is the concentration of the solute in the solution at time t and K is a constant with the dimensions of t^{-1}.

Nernst and Brunner (1904) subsequently interpreted the dissolution of a solid as a diffusion controlled process and postulated the existence of an *aqueous diffusion layer* or *stagnant liquid film*, of thickness h, at the surface of a solid undergoing dissolution. The diffusion controlled dissolution model of Nernst and Brunner, also referred to as the *film theory*, is represented schematically in Figure 1. 1.

The thickness h represents a stationary layer of solvent in which the solute molecules exist in concentrations from C_S to C. Beyond the static diffusion layer, at x greater than h, mixing occurs in the solution and the drug is found at a uniform concentration, C, throughout the bulk phase. At the solid surface-diffusion layer interface, $x = 0$, the solid drug is in equilibrium with drug in solution in the diffusion layer. The gradient or change in concentration with distance across the diffusion layer is constant, as shown by the straight downward-sloping line in Figure 1. 1.

Fick's first law of diffusion (Equation 1.16) was applied by Nernst and Brunner (1904) to quantify the dissolution rate of a single component solid dissolving in a solvent without disintegration or chemical reaction. The weight of solute dissolved, W, with respect to time is given by:

$$\frac{dW}{dt} = \frac{D\,A\,(C_S - C)}{h} \qquad \textbf{Equation 1. 22}$$

where D is the diffusion coefficient of the solute in cm^2/sec and A is the surface area of the dissolving solid. Equation 1.22 can be rewritten as follows:

$$\frac{dC}{dt} = \frac{D\,A}{V\,h}(C_S - C)$$ **Equation 1. 23**

where V is the volume of solution.

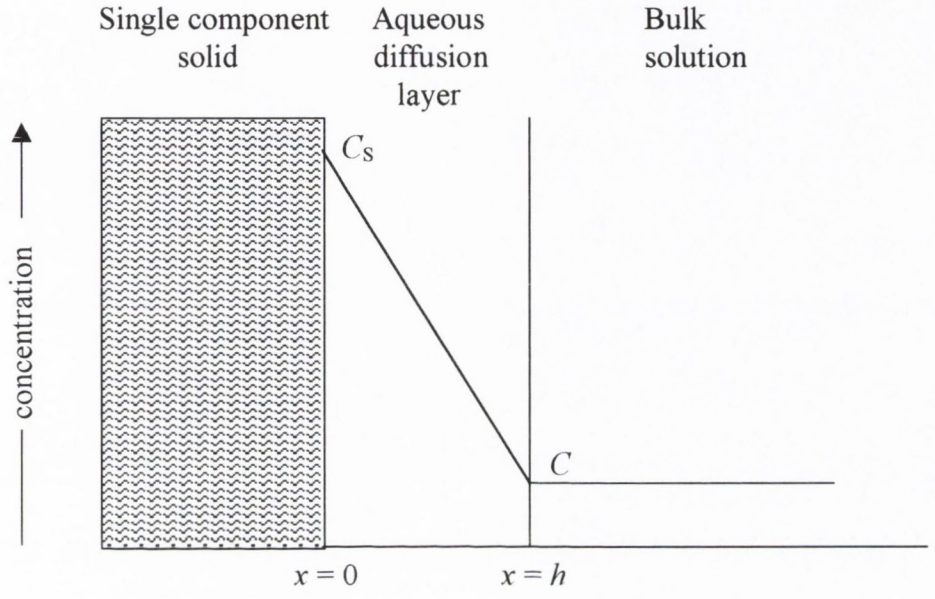

Figure 1. 1 Dissolution of a drug from a solid, showing the stagnant diffusion layer between the solid surface and bulk solution

If the absorption is rapid (or if the absorption mass transfer coefficient is much larger than DA/h), C becomes negligible compared to C_S and dissolution occurs under *sink conditions*. Absorption is then said to be *dissolution rate limited*, which applies to most poorly soluble drugs. In such cases, the concentration term, C, may be eliminated from Equation 1.22, giving the following equation:

$$\frac{dW}{dt} = \frac{D\,A\,C_S}{h}$$ **Equation 1. 24**

or

$$G = \frac{dW/dt}{A} = \frac{D\,C_S}{h}$$ **Equation 1. 25**

where G is the dissolution rate per unit surface area or the *intrinsic dissolution rate*.

The limitation of the model developed by Nernst and Brunner lies in the fact that it does not describe the actual situation since in reality no stagnant layer exists (Grijseels et al., 1981). As well as molecular diffusion, convective transport plays an important role in mass transport. Levich (1962) developed a dissolution model based on hydrodynamics, called the *convective diffusion theory*. This model assumes that only in the immediate vicinity of the surface, where liquid motion is almost absent, does a region exist where molecular diffusion is involved. This zone is termed the *effective diffusion boundary layer*, of thickness δ. The value of δ can be calculated from hydrodynamic theory, independently of dissolution rate data. It is a function of the physical properties of the liquid, its velocity and the diffusion coefficient of the dissolving solid. Within the diffusion boundary layer, the concentration of the solution shows a rapid change. At a first approximation, a linear concentration gradient may be assumed and the expression for the diffusion flux is then approximated by:

$$J = \frac{D(C_S - C)}{\delta}$$ **Equation 1. 26**

This equation is of the same form as that derived by Nernst and Brunner, assuming a stagnant liquid layer.

1.4.1.2 Surface reaction controlled dissolution

Deviations from the Nernst-Brunner model occur if the interfacial reaction is not instantaneous. For solutes with a high activation free energy for the interfacial reaction, the rate of release of solute molecules at the interface may be much slower than the diffusion across the boundary layer. As a result, solute-solution equilibrium at $x = 0$ may not be assumed. This consideration is accounted for by the *interfacial barrier model* (Higuchi, 1967), as represented schematically in Figure 1. 2. As illustrated in Figure 1. 2, C represents the concentration in the aqueous boundary layer from where diffusion starts as well as the concentration in the bulk solution. The rate of the interfacial reaction, which determines the overall dissolution rate, is:

$$G = k_R (C_S - C)$$ **Equation 1. 27**

where k_R is the effective interfacial transport rate constant. Under sink conditions, Equation 1.27 may be written as:

$$G = k_R C_S$$ **Equation 1. 28**

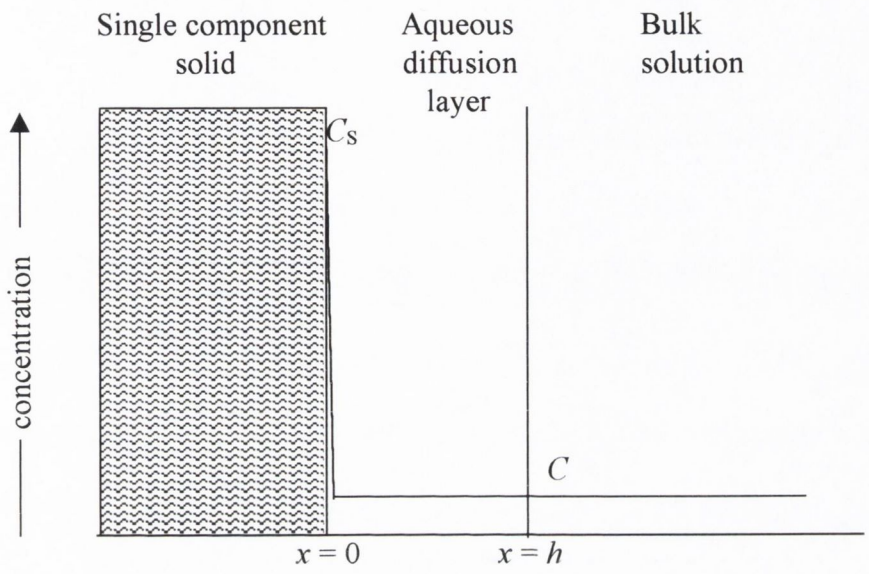

Figure 1. 2 The interfacial barrier model for the dissolution of a drug from a solid

When the diffusion rate constant and the interfacial reaction rate constant are of similar magnitude, both processes contribute to the dissolution rate (Higuchi, 1967). In this case, a double barrier model applies, as illustrated in Figure 1. 3. C_i represents the concentration where diffusion begins.

Under sink conditions, the dissolution rate is given by:

$$G = \frac{D C_S}{h\left[1 + \frac{D}{h k_R}\right]}$$ **Equation 1. 29**

This equation becomes reduced to Equation 1.25 when $k_R >> D/h$ or Equation 1.28 when $k_R << D/h$ (Higuchi, 1967).

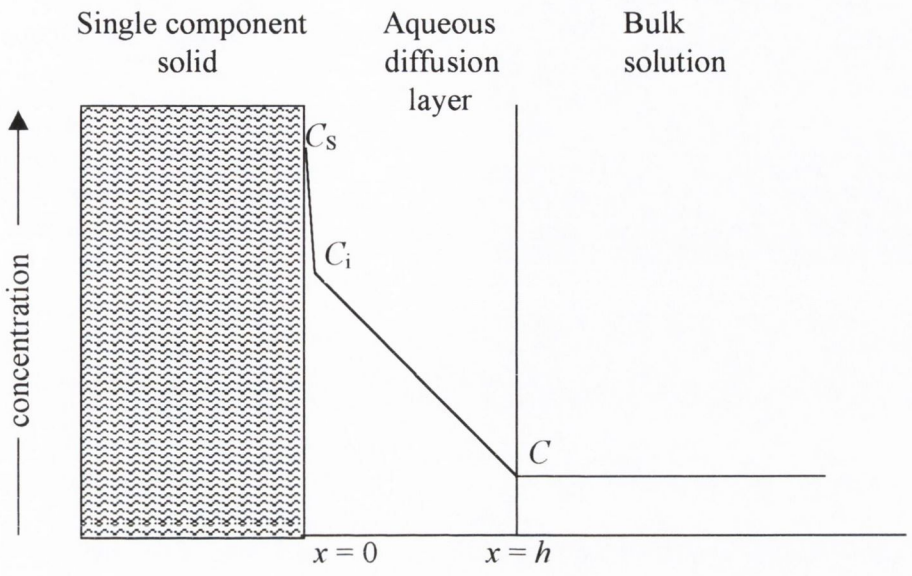

Figure 1. 3 The double barrier model for the dissolution of a drug from a solid

Agitation rate effects can be used to identify the process controlling the dissolution rate of a solute (Levy, 1963; Touitou and Donbrow, 1981). Under sink conditions and under conditions of laminar flow, the mass transport from a rotating disc in which only diffusion and convection are important is given by the Levich equation (Levich, 1962):

$$\frac{dW}{dt} = 0.62\, A\, D^{2/3}\, v^{-1/6}\, \omega^{1/2}\, C_s \qquad \textbf{Equation 1. 30}$$

where $\frac{dW}{dt}$ is the dissolution rate, v is the kinematic viscosity and ω is the angular velocity of rotation. The rate of dissolution per unit surface area, G, may be expressed as:

$$G = \mathrm{a}\,(\omega)^{0.5} \qquad \textbf{Equation 1. 31}$$

where $\mathrm{a} = 0.62\, D^{2/3}\, v^{-1/6}\, C_s$.

The following empirical relationship is used to identify the process controlling dissolution:

$$G = a(\omega)^b$$ **Equation 1. 32**

The value of b can be obtained from the slope of the plot of log G versus log ω. In the case of surface reaction controlled dissolution under laminar flow, the agitation intensity would not be expected to influence the dissolution rate and the exponent b approaches zero. If both the surface reaction and the transport process are influential in the control of dissolution rate (under laminar flow), b should fall between 0 and 0.5.

Equation 1.32 can also be used to characterise the type of fluid motion in the system, i.e. turbulent or laminar. Levich (1962) found that when flow was laminar b had a value between 0 and 0.5 and that a value of b greater than 0.5 indicated turbulence in the system.

1.4.2. Dissolution of salts

A pharmaceutical salt can exhibit a higher dissolution rate than the corresponding conjugate acid or base at the same pH, even though they may have the same equilibrium solubility (Berge et al., 1977).

Nelson (1957) carried out a study on the dissolution of theophylline salts and showed a correlation between diffusion layer pH and dissolution rate, concluding that salts often speed up dissolution by acting as their own buffers to alter the pH of the diffusion layer. Results of a subsequent study (Nelson, 1958) supported the hypothesis that salts exert a self-buffering action in their diffusion layers. By this reasoning, the dissolution rates of acids and bases would be determined by the pH values of the diffusion layers and would be independent of the bulk pH of the medium used. The difference in dissolution rates between an acid and its salt in a particular medium is therefore accounted for by the difference in the diffusion layer pH.

Hamlin et al. (1965) studied the dissolution rates of a wide range of drugs and found that the Noyes-Whitney equation was obeyed. However, the authors did not explain the differences observed between the dissolution rates of acids and their salts at a particular pH. The role of the solute in changing the pH of the saturated solution was not considered. For example, in the case of a sodium salt dissolving in a medium of pH 2, the saturated solution of the salt could have a pH as high as 7. The Noyes-Whitney equation is followed if the intrinsic dissolution rate at pH 2 is calculated using the C_S determined at pH 7.

Serajuddin and Jarowski (1985a and 1985b) investigated the dissolution mechanism of acids and their salts at different bulk pH. They obtained good conformity of their dissolution data with the Noyes-Whitney equation when the saturated solubility at pH_0, the pH at the interface, was used rather than the solubility at the bulk solution pH. Therefore, the intrinsic dissolution rate under sink conditions is given by:

$$G = \frac{D\,C_{S\,h=0}}{h} \qquad \textbf{Equation 1. 33}$$

where $C_{S\,h=0}$ is the saturated solubility at pH_0.

Using Equation 1.14, which describes the total solubility of a weak monoprotic acid (C_S) in aqueous solution, Equation 1.33 can be rewritten as:

$$G = \frac{D\,C_{SO}\left(1+\dfrac{K_a^{'}}{[H_3O^+]}\right)}{h} \qquad \textbf{Equation 1. 34}$$

where C_{SO} is the intrinsic solubility of the acid. If D/h is known, the dissolution rate of the acid at the pH of the interface (pH_0) can be calculated from Equation 1.34. The calculated dissolution rates for benzoic acid at different pH_0 values (Serajuddin and Jarowski, 1985b) were found to agree well with experimental values obtained by Mooney et al. (1981). Serajuddin and Jarowski also measured the pH of saturated solutions of benzoic acid under different bulk pH and their results agreed with the theoretical pH_0 values obtained by Mooney et al. (1981). The ratio of the dissolution rates of benzoic acid (Mooney et al., 1981) to the solubilities of benzoic acid determined at pH_0 were constant. The pH of the dissolution medium in equilibrium with an excess of the dissolving material was shown to be a good approximation for the pH at the solid-liquid interface.

Morozowich et al. (1962) studied the release of benzphetamine, a basic amino compound, from pellets of benzphetamine pamoate in 0.1 N HCl. They proposed that the dissolution rate was controlled by a layer of pamoic acid deposited on the surface of the pellet. Higuchi and Hamlin (1963) investigated this phenomenon and proposed that some time after the pellet was placed in the acid solution, a layer of pamoic acid of thickness s had formed on the surface. The H^+ ions had to diffuse through this layer and react with the pamoate ion to precipitate more acid, thus releasing the benzphetamine cation, which then diffused out through the acid layer. Some of the

benzphetamine cation could also diffuse out without being released by H^+. Higuchi et al. (1965a) studied the dissolution of an acidic drug, tolazamide, and its sodium salt in phosphate buffers and reported that surface conversion of the sodium salt to the acid occurred in media of low pH. The authors suggested that appreciable conversion took place only after the solid-solution interface is supersaturated with respect to acid tolazamide by more than 20 times the equilibrium solubility. Under conditions of much greater initial surface supersaturation ratios, a relatively impermeable acid surface coating was formed which controlled the dissolution rate of the drug. In a dissolution study of sodium salicylate in 0.1 N HCl (Serajuddin and Jarowski, 1985b), precipitation of salicylic acid was detected on the surface of the sodium salicylate pellet.

1.4.3. Two component non-interacting model

A physical model has been developed by Higuchi et al. (1965b) to describe dissolution from a uniform, intimate, non-disintegrating mixture of two crystalline compounds, A and B, assuming diffusion controlled kinetics. According to the model, when the mixture is exposed to a solvent, both phases should initially begin to dissolve at rates proportional to their solubilities and diffusion coefficients, as described by the Nernst-Brunner equation (Equation 1.25). After a short period of time, if $\frac{N_A}{N_B}$ is not equal to $\frac{D_A C_{SA}}{D_B C_{SB}}$, one of the phases will become depleted from the solid-liquid interface region of the solid mass. N_A and N_B are the amounts of A and B in the mixture, D_A and D_B are the respective diffusion coefficients and C_{SA} and C_{SB} are the solubilities. As a result of this, a surface layer of just one of the phases is formed. The three possible cases after time $t > 0$ are illustrated in Figure 1. 4.

Most mixture ratios would lead to Cases I or II. Case III, where the two components coexist at the solid-liquid interface, is obtained only when the two components are combined in the *critical mixture ratio* (CMR), where:

$$\frac{N_A}{N_B} = \frac{D_A C_{SA}}{D_B C_{SB}} \qquad \textbf{Equation 1. 35}$$

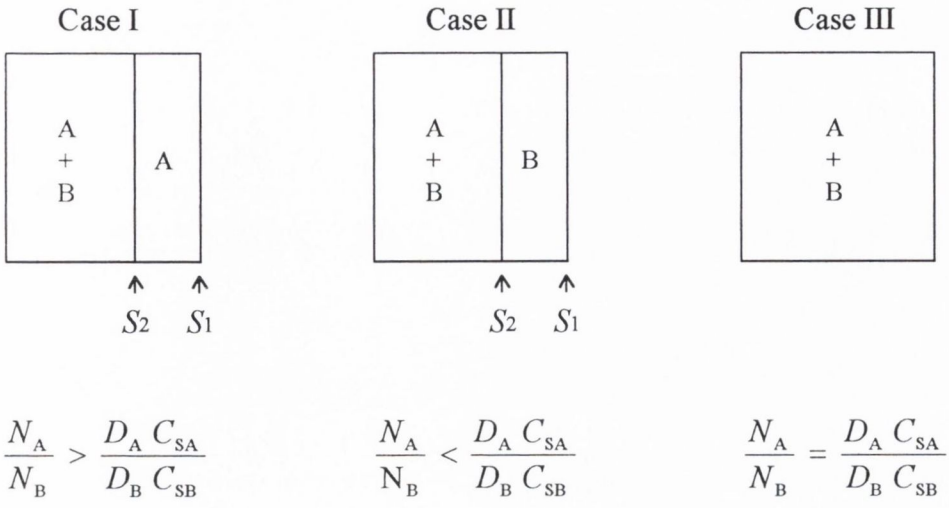

Figure 1. 4 Dissolution behaviour of mixtures of A and B. Case I: phase B dissolves fast enough to leave a layer of pure A at the surface; Case II: phase A dissolves fast enough to leave a layer of pure B at the surface; Case III: the two phases coexist at the solid-liquid interface

In Case III, the dissolution rate, under sink conditions, for each component is given by the Nernst-Brunner equation describing the dissolution rate for a pure component:

$$G_A = \frac{D_A C_{SA}}{h} \qquad \textbf{Equation 1. 36}$$

and

$$G_B = \frac{D_B C_{SB}}{h} \qquad \textbf{Equation 1. 37}$$

The following equations relate to mixtures of the two components, A and B, in ratios such that phase B dissolves fast enough to leave a layer of pure A behind, i.e. Case I. S_1 and S_2 in relation to Case I (Figure 1. 4) are the co-ordinate values representing the phase A-solution boundary and the A + B mixture-phase A boundary, respectively. At time $t = 0$, $S_2 = S_1 = 0$. At time $t > 0$, ΔS, the thickness of the phase A layer is equal to $(S_2 - S_1)$. Since A is always on the surface, the dissolution rate of A, G_A, is given by Equation 1.36.

As molecules of B must diffuse through the phase A layer, as well as through the liquid diffusion layer, the dissolution rate of B, G_B, is calculated from the following equation:

$$G_B = \frac{D_B C_{SB}}{h + \left(\frac{\tau}{\in}\right)(S_2 - S_1)}$$ **Equation 1. 38**

where τ and $\in$ represent the tortuosity and porosity of layer A, respectively.

The dissolution rates of A and B can also be written as:

$$G_A = A_A \left(\frac{dS_1}{dt}\right)$$ **Equation 1. 39**

$$G_B = A_B \left(\frac{dS_2}{dt}\right)$$ **Equation 1. 40**

where A_A and A_B are the amounts per unit volume of A and B in the mixture. Equation 1.39 can be combined with Equation 1.36 and integrated to give:

$$S_1 = \left(\frac{D_A C_{SA}}{A_A h}\right) t$$ **Equation 1. 41**

Substituting Equation 1.41 into Equation 1.38 and combining with Equation 1.40 results in:

$$A_B \left(\frac{dS_2}{dt}\right) = \frac{D_B C_{SB}}{h + \left(\frac{\tau}{\in}\right)\left[S_2 - \left(\frac{D_A C_{SA}}{A_A h}\right) t\right]}$$ **Equation 1. 42**

The solution to Equation 1.42 when $S_2 = S_1 = 0$ at $t = 0$ is:

$$t = K_1 \left\{ S_2 - \frac{\in}{\tau}\left(\frac{K_1}{K_2} - h\right)\left[1 - \exp\left(-\frac{K_2 \tau}{K_1 \in} S_2\right)\right]\right\}$$ **Equation 1. 43**

where $K_1 = \frac{A_A h}{D_A C_{SA}}$ and $K_2 = \frac{A_B}{D_B C_{SB}}$.

When $S_2 >> \frac{\in K_1}{\tau K_2}$, Equation 1.43 may be written as:

$$t \approx K_1 \left[S_2 - \frac{\in}{\tau} \left(\frac{K_1}{K_2} - h \right) \right] \qquad \textbf{Equation 1. 44}$$

From Equations 1.40 and 1.44, the dissolution rate of B, G_B, becomes constant in the steady state:

$$G_B = \frac{A_B D_A C_{SA}}{A_A h} = \frac{N_B}{N_A} G_A \qquad \textbf{Equation 1. 45}$$

In Case II, when $\frac{N_A}{N_B} < \frac{D_A C_{SA}}{D_B C_{SB}}$ and a layer of B exists on the surface of the solid mass (Figure 1. 4), the dissolution rate of B, G_B, can be calculated from Equation 1.37 and the dissolution rate of A in the steady state, G_A, can be calculated from the following equation:

$$G_A = \frac{N_A}{N_B} G_B \qquad \textbf{Equation 1. 46}$$

Higuchi et al. (1965b) investigated the dissolution of benzoic acid:salicylic acid mixtures in 0.1 N HCl. Discs were prepared by compression of mechanical mixes and of melts of mixes. The observed dissolution rates were in good agreement with the steady state rates predicted by the model. However, some deviations from theoretical values were observed near the critical mixture ratio. The experimentally obtained dissolution rates were lower than those predicted. This was thought to be due to small local variations in composition. Accordingly, the data obtained for the melt systems showed better agreement with theoretical values and was attributed to more intimate mixing of the two phases in the melt preparations, resulting in better definition of the boundaries, S_1 and S_2.

Shah and Parrott (1976) examined the dissolution in water of salicylic acid:aspirin spheres and aspirin:phenacetin spheres, prepared by compression of mechanical mixes. The observed dissolution rates agreed well with the theoretical rates calculated from the two component non-interacting model. Again, deviations from the model were observed at compositions near the critical mixture ratio, thought to be due to small local variations in composition since the mixtures were not prepared by a melt method.

In a study of the mechanism of dissolution of gallstones in cholelitholytic solvents, O'Reilly (1990) investigated dissolution from two component compacts consisting of gallstone components. Dissolution from compacts of cholesterol monohydrate and palmitic acid in single solvent systems was shown to follow the two component non-interacting model. The model was modified to predict dissolution from two-component compacts in a range of mixed solvent systems.

1.4.4. Interacting two component model

The two component non-interacting model was extended to two component systems in which the components, A and B, interact to form a soluble complex, AB (Higuchi et al., 1965b). As for the previous model, three cases analogous to those illustrated in Figure 1. 4 are expected in the steady state.

Assuming the interaction involves the solution reaction A + B $\leftrightarrow$ AB, the equilibrium constant, K_i, is calculated from:

$$K_i = \frac{C_{SAB}}{C_{SA}\, C_{SB}} \qquad \textbf{Equation 1. 47}$$

where C_{SAB} is the solubility of the 1:1 complex. The composition of the critical mixture ratio is:

$$\frac{N_A}{N_B} = \frac{D_A\, C_{SA} + D_{AB}\, K_i\, C_{SA}\, C_{SB}}{D_B\, C_{SB} + D_{AB}\, K_i\, C_{SA}\, C_{SB}} \qquad \textbf{Equation 1. 48}$$

where D_{AB} is the diffusion coefficient of the 1:1 complex (Shah and Parrott, 1976). The dissolution rates of A and B at the critical mixture ratio are:

$$G_A = \frac{D_A\, C_{SA} + D_{AB}\, K_i\, C_{SA}\, C_{SB}}{h} \qquad \textbf{Equation 1. 49}$$

and

$$G_B = \frac{D_B\, C_{SB} + D_{AB}\, K_i\, C_{SA}\, C_{SB}}{h} \qquad \textbf{Equation 1. 50}$$

Since the absolute increase in dissolution rate ($D_{AB}\ K_i\ C_{SA}\ C_{SB}\ /\ h$) is the same for both components, the relative increase in maximum dissolution rate is greatest for the least soluble component.

When the ratio of the components is such that pure A is the surface phase, the dissolution rates in the steady state may be determined by:

$$G_A = \frac{D_A\ C_{SA}}{h\left[1 - \frac{N_B\ D_{AB}\ K_i\ C_{SA}}{N_A\left(D_B + D_{AB}\ K_i\ C_{SA}\right)}\right]} \qquad \textbf{Equation 1. 51}$$

and

$$G_B = \frac{D_A\ C_{SA}}{h\left[\frac{N_A}{N_B} - \frac{D_{AB}\ K_i\ C_{SA}}{D_B + D_{AB}\ K_i\ C_{SA}}\right]} \qquad \textbf{Equation 1. 52}$$

Higuchi et al. (1965b) investigated the dissolution behaviour in water of discs prepared from melts of benzocaine:caffeine mixtures. The experimentally obtained dissolution rates agreed well with the rates predicted from the model.

Shah and Parrott (1976) applied the interacting two component model to aspirin:caffeine compressed spheres of mechanical mixes. There was good agreement between predicted and observed dissolution rates of aspirin for systems containing <0.3 and >0.8 mass fraction of aspirin and between predicted and observed dissolution rates of caffeine for spheres containing >0.7 mass fraction of aspirin. Deviation from the model at other compositions was attributed to minute flaking of the spheres due to the high solubility of caffeine relative to aspirin.

Corrigan and Stanley (1981) investigated the dissolution of phenobarbitone and of β-cyclodextrin from mixtures prepared by freeze drying and reported agreement with the interacting two component model.

1.4.5. Three component non-interacting model

Carmichael et al. (1981) developed a mass transfer model for the dissolution of *n*-component, non-disintegrating mixtures. They investigated dissolution of two and three component spheres and compared experimental and theoretical sphere weights and the average flux of each dissolving

component after 2 hours. They reported reasonable qualitative agreement with theoretical predictions. However, in some cases observed dissolution rates were four times higher than the predicted rates.

In a subsequent study, Simpson and Parrott (1983) developed equations to predict the steady state dissolution rates of each component from three component mixtures. Assuming that the Nernst-Brunner film theory applies, there are thirteen possible dissolution behaviours (Figure 1. 5).

As dissolution proceeds in Case I, the boundaries of the three components recede at the same rate and the three components co-exist at the solid-liquid interface. This dissolution behaviour occurs at the critical composition of the components at which:

$$\frac{N_A}{N_B} = \frac{D_A C_{SA}}{D_B C_{SB}} \qquad \textbf{Equation 1. 53}$$

$$\frac{N_A}{N_C} = \frac{D_A C_{SA}}{D_C C_{SC}} \qquad \textbf{Equation 1. 54}$$

and

$$\frac{N_B}{N_C} = \frac{D_B C_{SB}}{D_C C_{SC}} \qquad \textbf{Equation 1. 55}$$

where N_A, N_B and N_C are the mass fractions of components A, B and C, C_{SA}, C_{SB} and C_{SC} are their solubilities and D_A, D_B and D_C are their diffusion coefficients, respectively. Since all three components are dissolving from the surface, equations for the dissolution rates of components A, B and C (G_A, G_B and G_C, respectively) are the same as those for the dissolution of the pure components. Therefore, G_A and G_B can be calculated from Equations 1.36 and 1.37, respectively, and G_C is calculated as follows:

$$G_C = \frac{D_C C_{SC}}{h} \qquad \textbf{Equation 1. 56}$$

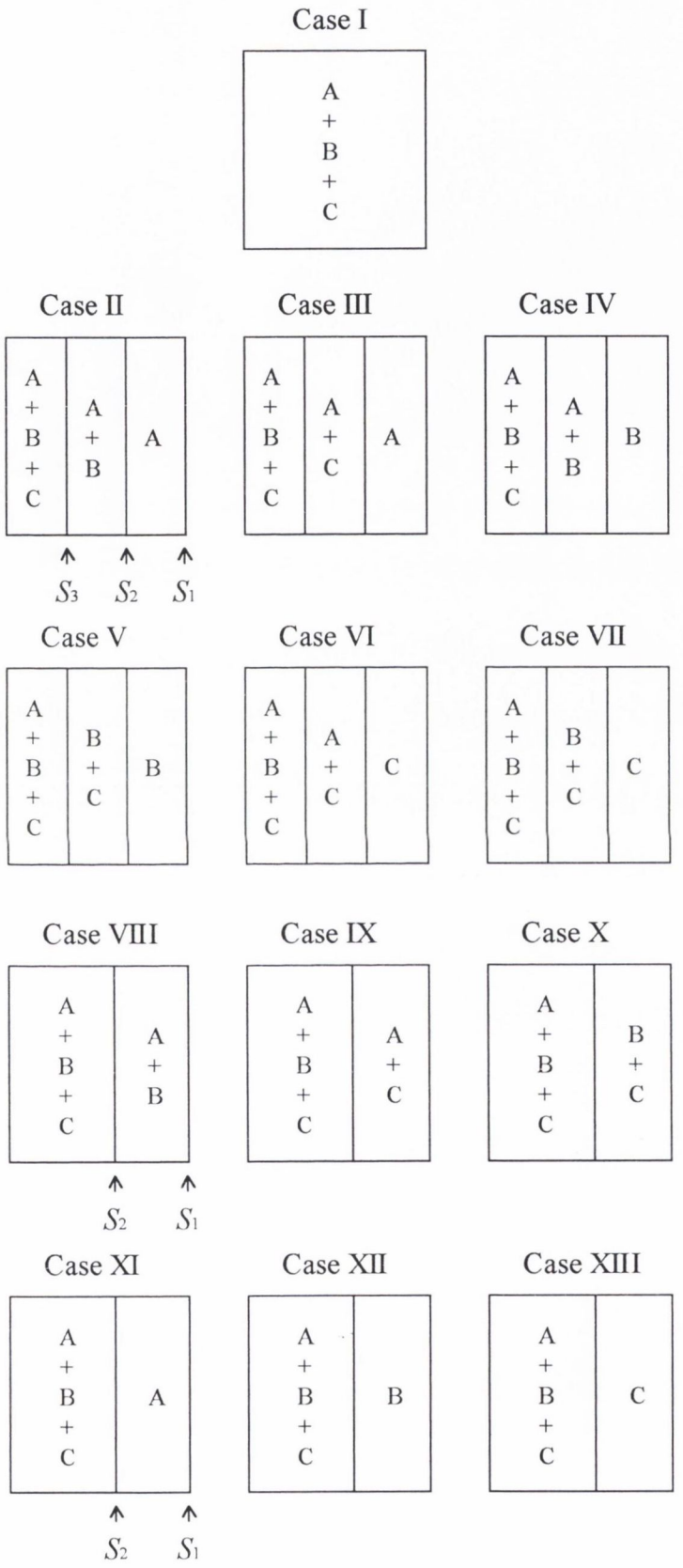

Figure 1. 5 Dissolution behaviours of three component solids of components A, B and C

In Case II (Figure 1. 5), component C dissolves faster than components A and B and the dissolving boundary of component C recedes into the solid. Component B dissolves faster from the solid surface than component A and the dissolving boundary of component B recedes into the solid, leaving a surface layer of component A. S_1, S_2 and S_3, in relation to Case II, represent the co-ordinate values for the component A-solution boundary, component A-components A and B boundary and components A, B and C-components A and B boundary, respectively. Case II dissolution behaviour occurs when:

$$\frac{N_A}{N_B} > \frac{D_A C_{SA}}{D_B C_{SB}} \qquad \textbf{Equation 1. 57}$$

$$\frac{N_A}{N_C} > \frac{D_A C_{SA}}{D_C C_{SC}} \qquad \textbf{Equation 1. 58}$$

and

$$\frac{N_B}{N_C} > \frac{D_B C_{SB}}{D_C C_{SC}} \qquad \textbf{Equation 1. 59}$$

Since component A is always on the surface, its dissolution rate is given by Equation 1.36. Component B must diffuse out through the layer of component A, of thickness $S_2 - S_1$, and the aqueous diffusion layer. The dissolution rate equation for component B may be derived as:

$$G_B = \frac{N_B}{N_A} G_A \qquad \textbf{Equation 1. 60}$$

Component C must diffuse through the layer of components A and B, of thickness $S_3 - S_2$, through the layer of component A, of thickness $S_2 - S_1$, and through the liquid diffusion layer. Its dissolution rate may be derived as:

$$G_C = \frac{N_C}{N_A} G_A \qquad \textbf{Equation 1. 61}$$

Cases III, IV, V, VI and VII describe dissolution behaviours similar to Case II. However, the order of dissolving and the receding of the boundaries are different with different mass fractions of components A, B and C.

In Case VIII (Figure 1. 5), component C dissolves faster than the other two components. As dissolution proceeds, the boundary of component C recedes within the solid, leaving a layer of components A and B, which coexist at the surface. S_1 and S_2, in relation to Case VIII, represent the co-ordinate values for the components A and B-solution boundary and the components A, B and C-components A and B boundary, respectively. Case VIII dissolution behaviour occurs under the condition that:

$$\frac{N_A}{N_C} > \frac{D_A C_{SA}}{D_C C_{SC}} \qquad \textbf{Equation 1. 62}$$

$$\frac{N_B}{N_C} > \frac{D_B C_{SB}}{D_C C_{SC}} \qquad \textbf{Equation 1. 63}$$

and

$$\frac{N_A}{N_B} = \frac{D_A C_{SA}}{D_B C_{SB}} \qquad \textbf{Equation 1. 64}$$

The dissolution rates for components A and B from Case VIII mixtures are given by Equations 1.36 and 1.37, respectively. The dissolution rate for component C can be calculated from Equation 1.61 or from the following equation:

$$G_C = \frac{N_C}{N_B} G_B \qquad \textbf{Equation 1. 65}$$

Cases IX and X describe dissolution behaviours similar to Case VIII. The order of dissolving and the receding of the boundaries are different with different mass fractions of the three components.

In Case XI (Figure 1. 5), both components B and C dissolve at the same rate, faster than component A. The boundaries of components B and C recede at the same rate and both coexist at the same boundary, leaving a surface layer of component A. S_1 and S_2, in relation to Case XI, represent the co-ordinate values for the component A-solution boundary and the components A, B and C-component A boundary, respectively. Case XI dissolution occurs when:

$$\frac{N_A}{N_B} > \frac{D_A C_{SA}}{D_B C_{SB}} \qquad \textbf{Equation 1. 66}$$

$$\frac{N_A}{N_C} > \frac{D_A C_{SA}}{D_C C_{SC}}$$ **Equation 1. 67**

and

$$\frac{N_B}{N_C} = \frac{D_B C_{SB}}{D_C C_{SC}}$$ **Equation 1. 68**

In Case XI, the dissolution rates for components A, B and C are given by Equations 1.36, 1.60 and 1.61, respectively.

Cases XII and XIII describe dissolution behaviours similar to Case XI. However, the order of dissolving and the receding of the boundaries are different with different mass fractions of components A, B and C.

Figure 1. 6 shows a composition diagram for a mixture of three hypothetical components having equal solubilities and diffusion coefficients. Case I dissolution behaviour at the critical mixture of the three component mixture is represented by point M. Points P, J and K represent the critical mixtures of components A and B, components B and C and components A and C, respectively. The line AMJ represents a three component mixture which contains components B and C, in a mass fraction the same as the critical mixture ratio for a two component mixture of components B and C, with component A.

Simpson and Parrott (1983) studied dissolution from ethylparaben:phenacetin:salicylamide compressed spheres of various compositions. The experimental dissolution rates substantiated their model for the dissolution kinetics of a three component, non-disintegrating solid. A study by Parrott et al. (1983) involved investigation of dissolution kinetics from benzoic acid:salicylic acid:salicylamide compressed spheres. The observed dissolution rates compared favourably to the predicted dissolution rates calculated from the three component non-interacting model. O'Dowd and Corrigan (1999) examined the dissolution characteristics of three component compacts, of constant surface area, containing theophylline, benzoic acid and salicylamide over a wide range of compositions. Benzoic acid and theophylline were found to interact to form a soluble complex. Consequently, the authors modified the three component model in order to account for two components interacting to form soluble complexes. Reasonable agreement between individual component steady state dissolution rates and those predicted by the model was reported.

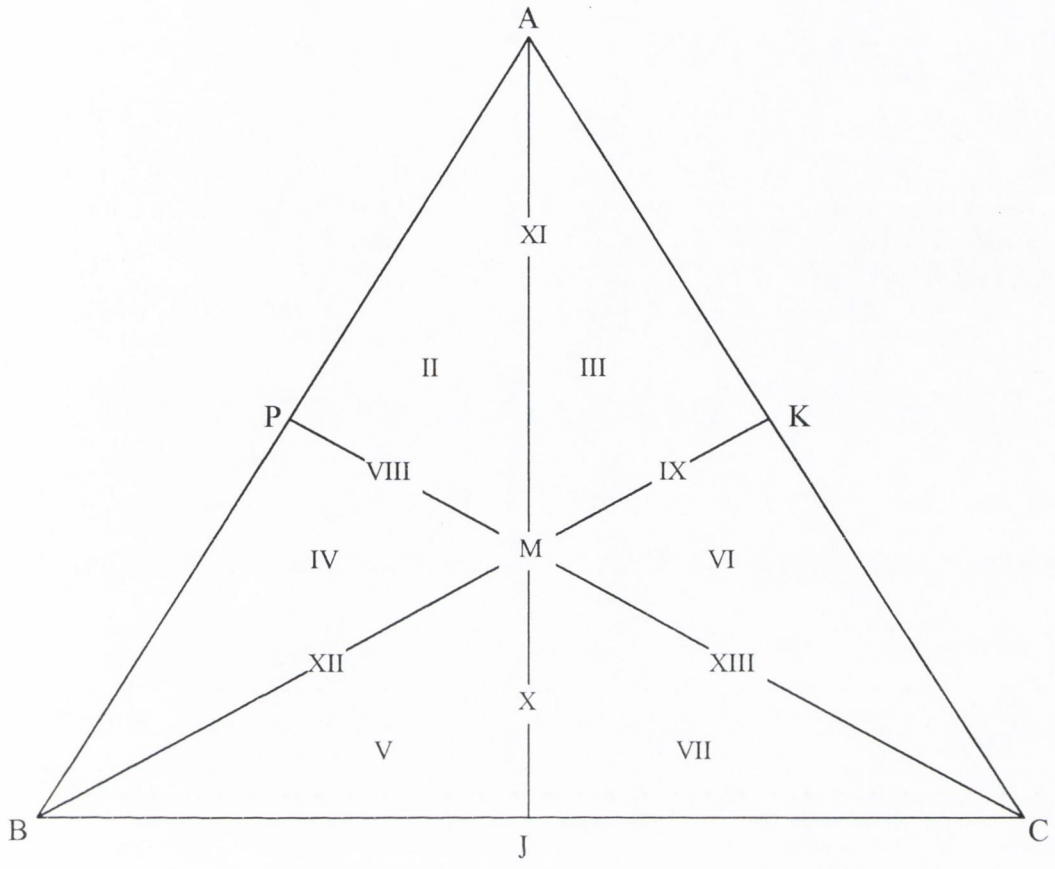

Figure 1. 6 Composition diagram for a three component mixture of components having equal solubilities and diffusion coefficients, showing the regions corresponding to the thirteen dissolution behaviours

1.4.6. Effect of ionisable excipients on the dissolution of ionisable drugs

A study by Nelson (1958) revealed enhancement in the dissolution rate of poorly soluble weak acids (benzoic acid, theophylline, theobromine and phenobarbital) following the addition of tribasic sodium phosphate. The author attributed this effect to the ability of the base to create an environment near the dissolving solid in which the solubility of the acid was higher than that in the dissolution medium. As the mole fraction of the acid was increased, the dissolution rate increased to a maximum rate. A further increase in the mole fraction of the acid decreased the dissolution rate.

Cleary (1987) investigated dissolution from discs of drug:acid mechanical mixes where the drug was basic and present in the salt form. Propranolol hydrochloride, nicardipine hydrochloride and

quinidine sulphate were the drugs investigated. The acid excipients used were fumaric acid and succinic acid. It was shown that the inclusion of an acid could increase the dissolution rate of the salts. The effect was dependent on the properties of the acid and on the proportion present. For each drug, the acid found to have the greatest overall effect on dissolution rate was that which was closest in solubility to that of the drug in a saturated solution of the acid. The acid to cause the highest increase in solubility also tended to decrease the pH of the saturated solution to the greatest extent. In cases where the effect of the acid was small (e.g. propranolol hydrochloride:fumaric acid systems), the dissolution rates were reasonably well quantified by the two component non-interacting model if the solubility of the drug in the saturated acid solution was used. Inclusion of an acid had the greatest effect on the dissolution of quinidine sulphate, with succinic acid having the greatest effect over the widest range of acid weight fractions. The maximum enhancement in dissolution rate due to succinic acid was 14 times that of the pure salt. This degree of enhancement was less than that expected from the saturated solubility data. Furthermore, the data could not be explained in terms of the two components interacting to form a soluble complex.

Ramtoola (1988) investigated the dissolution from mixtures of two weak acids in phosphate buffer solution. The limiting rates obtained were found to deviate from the rates predicted from the two component non-interacting model. The deviations were explained in terms of pH changes occurring in the microenvironment at the solid-liquid interface. The two component model was modified to take into account the pH changes at the interface and the resulting change in solubility and dissolution rate of the surface component. The rates predicted by the model agreed well with observed limiting rates from benzoic acid / salicylic acid discs. The model predicted dissolution profiles with positive curvatures for acids with very different dissociation constants and/or intrinsic solubility values. Subsequently, the dissolution of a weakly acidic drug, indomethacin, from mixtures of the drug with a strongly acidic excipient was investigated. The excipients used were adipic acid, citric acid and glutamic acid and the results obtained were consistent with the model. The limiting dissolution rates for indomethacin decreased with increasing proportion of acid excipient and at certain compositions, the dissolution profiles were positively curved. However, the experimental rates for indomethacin were higher than the predicted rates at certain compositions. It was proposed that the higher rates observed from the indomethacin / citric acid and the indomethacin / adipic acid discs resulted from the depletion of the acid excipient from the disc before steady state was reached. Accordingly, the experimental release rates of the acids were shown to be higher than the predicted rates.

McNamara (1988) investigated the effect of a range of ionisable excipients (mostly acids) on the dissolution rate of quinidine sulphate, the salt of a basic drug. The excipients used were citric acid, tartaric acid, maleic acid and sodium citrate. In all cases, increasing the acid content resulted in an

increase in drug dissolution rate to a maximum, followed by a decrease in dissolution rate. A significant enhancement in dissolution rate (10- to 16-fold increase relative to the pure drug) was achieved with each acid examined. In contrast, the use of the salt sodium citrate was not effective in enhancing the dissolution rate of the drug. The maximum relative enhancement was achieved with maleic acid, at the 75:25 drug:acid ratio. The drug:acid ratio at which the maximum dissolution rate occurred varied with each acid. The shape of the rate versus composition profile was found to be dependent on both the solubility and the pK_a of the acid. Maleic acid and citric acid yielded the broadest rate versus composition profiles, i.e. they were effective in enhancing dissolution rate over a wider composition range. Both these acids have wide pK_a ranges and have similar solubilities. Fumaric and tartaric acids, with similar pK_a values and different solubilities, yielded similar maximum relative enhancements and enhanced dissolution rate over narrow composition ranges. However, the maximum dissolution rates occurred at lowest (15%) and highest (50%) acid weight fractions for the fumaric acid and tartaric acid systems, respectively.

Dissolution from discs containing mixtures of an acidic drug and a basic excipient was investigated by McGloughlin (1989). Two new models were proposed to account for deviations from the two component non-interacting model.

(a) The two component (linear solubility) model incorporated an expression relating the solubility of the dissolving acid in the diffusion layer and the concentration of the base. The model predicted a plateau in the dissolution rate when the diffusion layer was mutually saturated with the acid and the base, determined by the solubility of the salt form. Results obtained from mixtures of benzoic acid and tris(hydroxymethyl)aminomethane (TRIS) in phosphate buffer were consistent with results predicted from the model.

(b) The two component (salt formation) model assumed that the salt formation reaction between the acid and the base went to completion. Therefore, at the acid:base 1:1 molar ratio, the system was thought to consist entirely of the salt form. For 0 to 0.5 mole fraction of the base, the acid was present in excess and the two component non-interacting model was applied to the acid:salt system. For higher mole fractions of base, the two component non-interacting model was applied to the base:salt system. This model also predicted a plateau in the dissolution rate in some situations, depending on the relative solubilities of the acid, the base and the salt. Experimental rates obtained for naproxen:procaine systems were in good agreement with rates calculated from the model.

The experimental dissolution rates determined for naproxen:TRIS and phenylbutazone:TRIS systems were intermediate between the rates predicted by the two models.

Healy (1995) investigated dissolution (in phosphate buffer) from discs containing mixtures of ibuprofen, a weakly acidic drug, and an acidic excipient in varying weight fraction ratios. The

excipients used were adipic, succinic, maleic, tartaric and citric acids. The dissolution profiles for the acid excipient showed a downward curvature, consistent with the two component non-interacting model. However, ibuprofen dissolution profiles showed a positive curvature, which was attributed to recession of the acid excipient from the disc surface, leading to a rise in microenvironmental pH. The two component non-interacting model was modified to include the effect of changing acid excipient concentration on ibuprofen solubility and hence dissolution rate. Best agreement between predicted and observed limiting dissolution rates was found for systems containing the acid excipients of lower solubility, adipic acid and succinic acid. The experimental limiting rates for the systems containing the more soluble excipients were lower than predicted for ibuprofen and higher than predicted for the excipient. These deviations were attributed to the fact that steady-state conditions had not been reached prior to depletion of the excipient from the disc. Initial dissolution rates for ibuprofen were predicted by fitting the dissolution profile for the acid excipient to the two component non-interacting model. Initial dissolution rates predicted in this way were found to be lower than the experimentally determined rates.

Chakrabarti and Southard (1997) examined the release of naproxen from compacts containing ionisable buffers. Calcium salts of carbonic, citric and phosphoric acids were used as buffers. The dissolution rate of naproxen was found to increase with increasing buffer proportion to a maximum at 50 %w/w buffer. The dissolution rates were found to be inversely proportional to the buffer solubility. The authors concluded that the buffer solubility should be lower than the drug solubility since buffers with solubilities greater than or equal to the drug solubility dissolve too quickly, leaving behind particles of undissolved drug.

A recent study by Preechagoon et al. (2000) examined indomethacin dissolution following co-compression with three different buffers (calcium carbonate, sodium carbonate and sodium citrate) in media of pH 2 and pH 7. The release of indomethacin was appreciably enhanced in the presence of sodium carbonate or sodium citrate. The authors concluded that freely soluble buffers improve the dissolution rate of a poorly soluble drug better than buffers of low solubility.

Ionisable additives, which modify the microenvironmental pH, have been included in many pharmaceutical formulations. Examples include aluminium glycinate and magnesium carbonate (Levy et al., 1965) and other alkaline compounds (Javaid and Cadwallader, 1972) in aspirin formulations. Water-soluble inorganic and organic salts, such as sodium bicarbonate, sodium carbonate, disodium hydrogen citrate and trisodium citrate, and α-amino acids, such as glycine, have been included in penicillin and cephalosporin formulations to provide a range of buffered pH microenvironments (Dwight, 1972a and 1972b). The release of propoxyphene hydrochloride from a controlled release formulation, containing a buffer system in the pellet core, was shown by

Bechgaard and Baggesen (1980) to be pH-independent. This resulted in greater reproducibility of the rate of availability of propoxyphene after administration, relative to an unbuffered formulation. The patent for the formulation (Pederson, 1976) specified buffers that can be incorporated into the pellet cores: salts of phosphoric, phthalic, citric or tartaric acids or salts of amino acids, e.g. glycine, or mixtures or these buffer salts.

Several authors have described the use of organic acids as pH adjusters in the formulation for the design of sustained release dosage forms for salts of weakly basic drugs. Ventouras et al. (1977) reported that succinic acid enhanced the rate of release of vincamine hydrochloride hemihydrate from hydrophilic matrices and that the enhancement was independent of the pH of the dissolution medium. Enhancements were in the order of 5- to 9-fold. The effect was seen to increase with increasing acid content. The pH of the microenvironment of the matrix was measured using microelectrodes. The enhancement in release rates could be attributed to a decrease in the microenvironmental pH relative to the pH of the bulk medium. In a subsequent study (Ventouras and Buri, 1978), the authors carried out solubility studies on vincamine hydrochloride in buffer at pH 7.5 in the presence of succinic acid and concluded that the enhancement in release rate was not due to complex formation. The release of quinidine sulphate dihydrate and drotaverine hydrochloride from hydrophilic matrices was also examined and the range of acids extended to include tartaric and oxalic acids. Drug release from systems containing 25:75 w/w drug:acid, a hydrophilic matrix and kaolin was investigated. Quinidine sulphate release increased with decreasing acid pK_a (oxalic > tartaric > succinic). The fastest release rate for vincamine hydrochloride was obtained with oxalic acid, but the other acids did not follow the same trend observed for quinidine sulphate. The release of drotaverine hydrochloride was slowest from the oxalic acid system. Dissolution tests were performed on mixed discs of drotaverine hydrochloride and acid at different ratios. The authors concluded that the enhancement of dissolution was dependent on the nature of the acid and the amount used.

Gruber et al. (1980) coated spherical particles containing dipyridamole and acidic excipients, such as citric acid and tartaric acid. The acidic components were included in the formulation to enhance absorption of the basic drug, which is practically insoluble above pH 4, in the small intestine.

Studies on the effect of acidic excipients on the release of salts of weakly basic drugs, ketanserin tartrate and mianserin hydrochloride, from programmed release megaloporous systems in both acidic and neutral media have been published (van der Veen et al., 1991a and 1991b). An acidic excipient (citric, succinic or tartaric acid) was incorporated into the formulation with a view to enhancing the release of weakly basic drugs in neutral media, thus counteracting the occurrence of decreasing release rates with increasing pH in the gastrointestinal tract. Dramatic increases in

release rates in neutral media (pH 6.8) were observed for the dosage forms containing acidic excipients. This effect was attributed to a localised pH change in the pores of the megaloporous dosage forms, resulting in retardation of the conversion of the soluble drug to the insoluble base. Incorporation of succinic acid in the formulation resulted in much slower release rates in neutral media relative to the systems employing citric or tartaric acids. The authors attributed these lower release rates to the lower solubility and lower acidity of succinic acid compared to the other two acids.

A study by Thoma and Zimmer (1990) examined the release of noscapine hydrochloride, a weakly basic drug, from diffusion dosage forms with polymethacrylate mixture film coatings. They investigated the use a range of six organic acid excipients: succinic, adipic, tartaric, citric, ascorbic and fumaric acids. By maintaining the pH value within the diffusion coating below the precipitating pH of noscapine, an improvement in release was achieved, over the pH range 1.2 to 7.5, which depended on the type and amount of acid added. With succinic, adipic, tartaric and citric acids, pH-independent release profiles were achieved, in decreasing order of effectiveness. The authors concluded that the ability to improve the release properties of weakly basic drugs by organic acids represents the sum of several, overlapping effects. These include the solubility of the acids, their acidic strength and buffer capacity and the solubility of the salts formed with the drug. They postulated that poorly soluble acids, such as fumaric acid, only exert an effect that is of limited duration, whereas very easily soluble acids, such as tartaric and citric acids, diffuse out too rapidly through the film coating. Succinic and adipic acids, with higher pK_a values, are more successful in maintaining an acid pH inside coated diffusion dosage forms than tartaric or citric acids, whose pK_a values are lower. The authors attributed this to the tendency of strong acids to dissociate completely and display lower buffer capacities because the proportion of the undissociated species, as a necessary constituent of a buffer system, is smaller.

Kohri et al. (1991) used citric acid to enhance the rate of release of papaverine hydrochloride, the salt of a weak base, from PVP matrix tablets in neutral media. When the composition ratio of citric acid to drug was more than about 3.5, the tablets showed pH-independent release. When a bulk solution of pH 7.0 was employed, the surface pH of the tablets was shown to decrease to about 1.5, a pH value approximately equal to that of a saturated solution of citric acid in buffer pH 7.0.

Gabr (1992) reported an increase in the release of the papaverine hydrochloride from tablet matrices in buffer (pH 7.4) by the incorporation of organic acids in the formulation. The study was carried out using the same acids as those employed by van der Veen et al. (1991a and 1991b). Contrary to the findings on the megaloporous systems (van der Veen et al., 1991a and 1991b), the matrix tablets containing succinic acid demonstrated the highest release rates compared to those

containing citric or tartaric acids. These findings supported the hypothesis of Thoma and Zimmer (1990) that the very soluble acids diffused rapidly through the matrix tablet, while the moderately soluble succinic acid diffused at a relatively low rate, thus maintaining an acidic pH inside the tablets for a longer time.

Thoma and Ziegler (1998) investigated the release of fenoldopam mesylate, the salt of a weakly basic drug, from coated pellets following the incorporation of an organic acid (succinic, fumaric or adipic acid). Formulation with adipic or fumaric acid failed to enhance the release of fenoldopam in higher pH media. Despite having a higher solubility than fumaric acid, succinic acid was much more effective in improving fenoldopam dissolution. The authors concluded that it was not so much the solubility of the succinic acid but the succinic acid itself, and the amount present and released, that controlled fenoldopam release at higher pH values. Possible explanations proposed by the authors included the formation of a solid dispersion of fenoldopam in succinic acid or a complex of the two components.

In a recent study, pH-independent release of verapamil hydrochloride was observed from tablets composed of ethylcellulose or hydroxypropyl methylcellulose and an organic acid (Streubel et al., 2000). A pH indicator was used to investigate the microenvironmental pH within the tablets. The addition of fumaric, sorbic or adipic acid to the matrix former was found to result in low pH values during drug release in phosphate buffer (pH 6.8 and 7.4). The more pronounced enhancements in drug release rates were observed following the inclusion of fumaric acid in the formulations. This was attributed to the lower pK_a values of fumaric acid, relative to those of sorbic or adipic acid.

Investigations on the effect of formulating acidic drugs with buffering agents have also been reported. Doherty and York (1989) used microenvironmental pH control to modify the dissolution of a frusemide:PVP solid dispersion system. Incorporation of an internal buffer system, comprising disodium hydrogen orthophosphate and citric acid, in the formulation resulted in an increase in the dissolution rate of the weakly acidic drug in acidic media and a retardation of the dissolution rate in alkaline media. The surface pH was measured and it was shown that dissolution rate changes were as a result of controlled changes in the pH immediately surrounding the dissolving solid. The pH of the bulk medium was considered to exert only a secondary influence. A study by Tirkonnen et al. (1995) investigated the release of indomethacin, a poorly water soluble acidic drug, from ethylcellulose microcapsules following the inclusion of an internal buffer, dibasic sodium phosphate (DSP), in the core of the microcapsules. Indomethacin release was accelerated considerably with increasing amounts of DSP, to a maximum of a 600-fold increase in release rate when 50% DSP was employed. This effect was attributed to the ability of DSP to increase the pH within the core, leading to an increase in the solubility of the acidic drug.

In contrast to the above examples, in which an improvement in dissolution rate is sought after, Pagay (1988) investigated the inclusion of an appropriate buffer system in a hydroxypropylmethylcellulose (HPMC) matrix to suppress the initial release of a weakly basic drug in an acidic medium. Magnesium hydroxide or citrate buffer was employed to decrease the solubility of the drug within the environment of the matrix, thereby controlling the rate of drug release. The buffered formulations showed dramatic reductions in the amount of drug released in the first hour and prolongation of the time taken to release all of the drug present. It was shown that the release rates from HPMC matrix formulations were controlled by the presence of the buffering agent (the pH of the matrix) rather than the pH of the dissolution medium.

1.5. SURFACE ACTIVITY

Molecules or ions having two distinct regions of opposing solution affinities within the same molecule are termed *amphiphiles* or *surface active agents* (Florence and Attwood, 1988). Amphiphilic molecules may self-associate to form dimers, trimers or aggregates of larger sizes. Depending on the nature of the molecule, a high degree of association may lead to the formation of *micelles* at concentrations above the *critical micelle concentration* (CMC) (Martin, 1993). The micelle structure in aqueous solution can be viewed as an aggregate in which the molecules are oriented with the hydrophobic portions together and the hydrophilic portions in contact with the surrounding aqueous solution (Attwood and Florence, 1983). Micelles exist in equilibrium with the free molecules (monomers) in solution.

In an aqueous system, the interior core of a micelle is a hydrophobic environment and is therefore capable of dissolving hydrophobic materials. This process whereby water-insoluble or partly water-soluble substances are brought into aqueous solution in high concentration is termed *solubilisation*. Above the CMC, the amount of substance solubilised increases with an increase in concentration of the surfactant, i.e. as the number of micelles increases.

Certain physicochemical properties of the solution undergo dramatic changes at the CMC. Examples include surface tension, conductivity, light scattering and osmotic pressure. Techniques used to determine the CMC of a compound include analysis of these properties at different drug concentrations (Martin, 1993). Solubilisation of water-insoluble dyes can also be used to demonstrate micelle formation.

As the concentration of surfactant solutions is increased above the CMC, there can be a transition from the typical spherical micellar structure to a more elongated or rod-like micelles. Further

increase in concentration may cause the orientation and close packing of these elongated micelles into hexagonal arrays. A new phase (the *middle phase*), consisting of these ordered arrays, separates out from, but remains in equilibrium with, the remainder of the solution which contains randomly oriented rods. In the case of some surfactants, a further increase in concentration results in the separation of a second transition phase (the *neat phase*) which has a lamellar structure. Finally, a further increase in concentration results in separation of surfactant out of solution. Both the middle and neat phases are liquid crystalline states and are referred to as *lyotropic liquid crystals* (Florence and Attwood, 1988).

1.5.1. Pharmaceutical implications of drug surface activity

Many drugs demonstrate self-association in solution (Felmeister, 1972; Florence and Attwood, 1988). Self-association of a drug can affect its solubility, diffusion and transport through membranes.

Micelles have a much higher solubility in water than single surfactant molecules because the hydrophobic moieties in the micelles are well shielded from contact with water by the polar moieties (Attwood and Florence, 1983). In certain cases, the formation of supersaturated solutions has been attributed to the ability of a drug to self-associate (Roseman and Yalkowsky, 1973; Bogardus and Blackwood, 1979; Serajuddin and Rosoff, 1984; Serajuddin and Jarowski, 1985a and 1985b; Serajuddin and Mufson, 1985; Dahlan et al., 1987). Enhanced solubility through micelle formation will have implications in terms of the dissolution and membrane transport of drugs (Ledwidge and Corrigan, 1998).

Detergency may enhance membrane permeability and improve drug absorption, as reported in the case of drug administration in connection with bile salts (Attwood and Florence, 1983). In the case of a surface active drug, the drug itself acts as a detergent and may actively promote its own bioavailability by interacting with the membranes it encounters during the administration pathway.

Self-association of solutes in solution leads to the formation of larger molecules, which generally diffuse more slowly in solution (Grant and Higuchi, 1990). The Stokes-Einstein equation relates the diffusivity, D, to the radius of the diffusing particles, r:

$$D = \frac{kT}{6\pi\eta r}$$ **Equation 1. 69**

where k is the Boltzmann constant (1.3806×10^{-23} JK^{-1}), T is the absolute temperature and η is the dynamic viscosity. Other factors being equal, for rigid, almost spherical particles:

$$r = \left(\frac{3V_m}{4\pi L}\right)^{1/3} = \left(\frac{3M}{4\pi\rho L}\right)^{1/3}$$ **Equation 1. 70**

where V_m is the molar volume, L is the Avogadro constant (6.022×10^{23} mol^{-1}), M is the molecular weight and ρ is the density of the diffusing substance.

Equations 1.69 and 1.70 indicate that:

$$D \propto \left(\frac{1}{M}\right)^{1/3}$$ **Equation 1. 71**

and

$$D \propto \left(\frac{1}{V_m}\right)^{1/3}$$ **Equation 1. 72**

Therefore, an increase in apparent molecular weight (and apparent molar volume) due to self-association will hinder diffusion. The influence of self-association on the aqueous diffusivity of a compound will have implications in terms of drug dissolution and, consequently, the bioavailability of poorly soluble drugs. Furthermore, a reduction in diffusivity will affect transport across membranes. Nagadome et al. (1995) reported a decrease in the flux of sodium deoxycholate through a porous membrane at concentrations above the CMC. Mikkelson et al. (1980) studied the steady state flux of phenol across a high-density polyethylene film and reported negative deviations from the relationship between concentration and flux at higher concentrations. They attributed these deviations to a reduction in thermodynamic activity of the phenol arising from its self-association in the donor phase. Accumulation of drug molecules in certain sites in the body to such an extent that they reach micellar concentrations may be possible (Attwood and Florence, 1983). This would result in a change in the thermodynamic activity of the compound *in vivo*, thus affecting its transport across biological barriers.

Surface active drugs have a propensity to bind hydrophobically to proteins and to other biological macromolecules and also tend to associate with other amphiphilic substances such as dyes and other drug substances, with bile salts and with receptors (Attwood and Florence, 1983). Therefore, surface activity can influence the reactivity of a drug at a site of action (Felmeister, 1972).

Chapter 2

Some approaches to modifying drug properties

2.1. INTRODUCTION

There are many techniques available to the pharmaceutical scientist for increasing the solubility, and thereby the dissolution rate, of a poorly soluble drug. These include: (a) changing the drug molecule from a nonionised moiety into a salt form, (b) varying the counterion of the salt form, (c) changing the crystal form of the drug and (d) forming a complex of the drug with a pharmacologically inert substance (Benet, 1973). In this chapter, the methods (a) – (c) above are discussed.

2.2. SALT FORMATION

Salt formation is a simple means of endowing a drug having ionisable functional groups with unique properties in order to overcome some undesirable feature of the parent drug (Anderson and Conradi, 1985). The physicochemical characteristics and resultant biological performance of a drug can be dramatically altered by conversion to a salt form (Berge et al., 1977; Bighley et al., 1996).

2.2.1. Pharmaceutical importance of salt formation

The importance of salt formation has been documented in a review by Berge et al. (1977) which describes the use of different salt forms to modify the dissolution, solubility, organoleptic properties, stability, absorption, pharmacokinetics, pharmacology and toxicity of drugs.

The development of more soluble salt forms of a drug, with a view to improving the drug's bioavailability (e.g. Engel et al., 2000) or ease of formulation (e.g. Agharkar et al., 1976), is one of the principal motives for salt formation (Agharkar et al., 1976). Several studies compare the solubilities of different salt forms of a compound with that of the free acid or base (Dittert et al., 1964; Gu and Strickley, 1987; Anderson and Conradi, 1985; Rubino, 1989). An example of the dramatic enhancement in solubility achievable through salt formation is the lactate salt of the antimalarial drug, α-(2-piperidyl)-3,6-bis(trifluoromethyl)-9-phenanthrenemethanol, which was found to be approximately 200 times more soluble than the hydrochloride salt (Agharkar et al., 1976). Gu et al. (1987) carried out a study to select an appropriate salt form for RS-82856. The hydrogen sulphate salt was found to be more soluble than the parent drug over a wide pH range and was shown to result in an approximately 2-fold increase in bioavailability in dogs. Salt formation does not always confer greater solubility. There are many examples in the literature of

the preparation of salts to reduce the water solubility of the parent compound (Morozowich et al., 1962; Magerlein, 1965; Jones et al., 1969; Benjamin and Lin, 1985). Reasons for lowering the aqueous solubility of a drug include the attainment of dissolution-controlled absorption for controlled release from oral dosage forms (Morozowich et al., 1962; Benjamin and Lin, 1985) or masking of the parent drug's inherently bitter taste (Jones et al., 1969).

As discussed in Section 1.4.2, a pharmaceutical salt generally exhibits a higher dissolution rate than the corresponding conjugate acid or base at an equal pH by acting as its own buffer and altering the pH of the diffusion layer. Many studies illustrate the influence of the salt form on dissolution and the beneficial effects of changing unionised drugs into salts (Gu and Strickley, 1987; Fini et al., 1996).

Although different salts of the same drug are not likely to differ qualitatively in pharmacological response, quantitative differences would normally be expected, depending on their rate and site of dissolution in the gastrointestinal tract and their relative bioavailability (Anderson, 1985). For example, oral administration of tolbutamide sodium resulted in a rapid and pronounced reduction in blood glucose, whereas the free acid was found to produce a more gradual hypoglycaemic effect (Nelson et al., 1962). This was attributed to the dissolution rate of the sodium salt being about 275 times greater than that of the free acid. On consideration of these results, Gibaldi (1991) concluded that the more slowly dissolving free acid was the more useful form of the drug for the treatment of diabetes.

2.2.2. Selection of an appropriate salt form

Selecting the optimal salt form should involve consideration of all physicochemical properties that influence its physical and chemical stability, processability under manufacturing conditions, dissolution rate and bioavailability. For example, Morris and co-workers (1994) identified four selection criteria for the selection of the optimal salt form of a novel HMG-CoA reductase inhibitor including: (1) low hygroscopicity, (2) physical stability of the crystal form under different storage conditions, (3) aqueous solubility and (4) chemical stability.

Whereas salt formation may result in improved dissolution rate and bioavailability of a poorly water soluble compound, the preparation of stable salt forms for some drugs may not be feasible and free acid or base forms may be preferred. For example, Serajuddin and co-workers (1986) selected the base form of α-pentyl-3-(2-quinolinylmethoxy)benzenemethanol for dosage form design due to the physical instability of its hydrochloride salt. The selection of an optimal salt

form in terms of stability requires consideration of counterion-related factors such as crystal lattice energy (stronger crystal lattice forces generally result in superior solid-state stability), pH of the liquid microenvironment (a function of counterion pK_a) and the possibility of counterion participation in the degradation of the drug (Anderson and Flora, 1996). The stability of organic compounds in the solid-state is related to the melting point or strength of the crystal lattice (Gould, 1986). Liquefication of the solid generally occurs before degradation begins since the forces between molecules in a crystal are small relative to the energy required to break chemical bonds. Therefore, the melting point of a compound can be an important factor in determining stability (Gould, 1986). A study of the stability of a prostaglandin derivative and its sodium, potassium and tromethamine salts, when stored protected from light at 33°C, revealed a marked dependence of solid-state stability on salt form (Anderson, 1985). In addition, a low melting point of a drug salt can adversely affect its processability (Gould, 1986).

A salt with a high tendency to adsorb / desorb moisture under the ambient relative humidity conditions or high temperatures encountered during manufacture will result in problems such as batch-to-batch variation in potency, handling difficulties, tablet cracking, chemical instability or variability in dissolution rates and bioavailability (Anderson and Flora, 1996). Excessive moisture uptake is a frequent problem for salts prepared from strong acids or bases (Wells, 1988). Morris et al. (1994) rejected a variety of metal salts of a new drug candidate under investigation due to hygroscopicity or humidity-dependent changes in crystal structure, including the sodium, potassium, calcium, magnesium and zinc salts. A study by Gu and Strickley (1987) showed that the tris(hydroxymethyl)aminomethane (TRIS) salts were less hygroscopic than the sodium salts for a variety of analgesic/anti-inflammatory agents.

A balance between different salt properties needs to be taken into consideration in assessing the correct salt form to progress into drug development. Some decision-making models have been developed to aid in the selection of an appropriate salt form. Gould (1986) described a salt selection process based on melting point, solubility, stability, wettability etc. of various salt forms. However, in the absence of clear "go / no go" decisions at any particular stage of the salt selection process, this approach would lead to the generation of extensive physicochemical data on all the salts prepared. A more rational approach was adopted by Morris et al. (1994) in order to select an appropriate salt form for a novel HMG-CoA reductase inhibitor. The physicochemical properties of the salts were studied using a multi-tier approach. The studies were planned such that the least time-consuming experiments were conducted earlier. After each tier of testing, a "go / no go" decision was made, thus avoiding the accumulation of extensive data on all available salt forms. The hygroscopicities of all the salts were evaluated at tier 1 and four salts were eliminated from the study due to excessive moisture uptake. The remaining three salts were subjected to tier 2

evaluation of humidity-induced crystal structure changes and aqueous solubility in the gastrointestinal pH range, resulting in the elimination of the magnesium salt. Tier 3 involved determination of the chemical stability under accelerated conditions (temperature, humidity and presence of excipients). The two remaining salts were found to be chemically stable in the solid state. The arginine salt was selected for further development following consideration of the ease of synthesis, ease of analysis, marketing preference etc. A similar tiered approach was adopted by Engel et al. (2000) in the selection of an appropriate salt form for LY333531, a free base of low aqueous solubility.

2.2.3. Predictive relationships between counterion characteristics and properties of the salt formed

Salt forming agents are often chosen empirically. The preferred salt form is selected following consideration of practical issues such as cost of raw materials, ease of crystallisation and percent yield and other basic considerations such as stability, hygroscopicity and flowability of the resulting salt form (Berge et al., 1977).

Studies have been carried out on the effect of salt formation on physical and chemical characteristics in an attempt to predict the influence of a particular salt forming agent on the biological behaviour of the parent compound (Berge et al., 1977; Gould, 1986). In particular, relationships between the properties of the salt-forming agent and the solubility of the resultant salt have been explored (Wells, 1988). Unfortunately, no reliable way of predicting the influence of a salt-forming agent on the behaviour of the parent compound has been reported. Only qualitative "rules of thumb" are generally found. For example, increasing the hydrophilicity of the counterion has been proposed as a means of increasing the water solubility of the resultant salt, as reported for a series of erythromycin salts (Jones et al., 1969). However, these qualitative rules may not be very reliable (Anderson and Flora, 1996). Therefore, selection of an appropriate counterion to produce a salt with the desired combination of properties is still carried out on an empirical basis.

2.2.3.1. Counterion pK_a

Successful salt formation generally requires that the pK_a of the conjugate base is greater than that of the conjugate acid to ensure sufficient proton transfer from the acid to the base. The equations below describe the theoretical pH values for aqueous solutions of various salts (Anderson and Flora, 1996):

Weak acid / strong base: $$pH = \frac{1}{2}[pK_a + pK_w + \log C]$$ **Equation 2. 1**

Weak base / strong acid: $$pH = \frac{1}{2}[pK_a - \log C]$$ **Equation 2. 2**

Weak acid / weak base: $$pH = \frac{1}{2}[pK_a(\text{acid}) + pK_a(\text{base})]$$ **Equation 2. 3**

where C is the salt concentration (mM) and pK_W is the dissociation exponent for water. Consideration of these equations, and of the relationships governing the pH-solubility behaviour of weak acids (Section 1.2.2), would suggest that in general it is advantageous to select conjugate bases having pK_a values well above the pK_a of a weakly acidic drug when attempting to prepare a water soluble salt form (Anderson and Flora, 1996).

However, factors such as the K_{SP} of the salt, common-ion effects and hygroscopicity may disfavour the salts of first choice using the above criterion, e.g. hydrochloride or sodium salts. The formation of hydrochloride salts does not always enhance solubility above that of the free base. The lower solubility of a hydrochloride salt in dilute HCl, relative to that of the free base, is attributed to the common ion effect of the chloride ion on the solubility product equilibrium of the salts (Miyazaki et al., 1975, 1979, 1980, 1981a and 1981b). Additional disadvantages of using strong acids or bases in salt preparation have been reported. Salts prepared from strong acids or bases are freely soluble but can be very hygroscopic (Wells, 1988), leading to instability in solid dosage forms since some drug will dissolve in its own adsorbed films of moisture. In the case of salts of weak bases and strong acids, the strongly acidic solution may increase hydrolysis due to unfavourable pH. An excessively low / high solution pH can lead to physiological compatibility problems in the case of injectable formulations (Wells, 1988). Injections should lie in the pH range 3 – 9 to prevent vessel or tissue damage and pain at the injection site. Packaging incompatibilities can also result from strongly acidic or basic formulations (Wells, 1988).

In relation to using pK_a of the counterion for predicting salt solubility, further modification is required since the interpretation of salt solubility is complicated by the difficulty in discriminating between the energy required to remove ions from the crystal lattice and the energy of solvation (Wells, 1988). Consideration of ionic equilibria fails to account for the stereochemistry of the drug, counterion size or other polar groups which can interact (Wells, 1988).

Forbes et al. (1995) investigated the relationship between apparent solubility in water at 10°C and filtered solution pH for salts of *p*-aminosalicylic acid. The differences in solubility of the salts did not appear to be solely due to a pH effect, thus compromising a simple predictive relationship. In particular, the salts with ammonium-based cations, i.e. ethanolamine and ammonium, were more soluble than metallic salts of *p*-aminosalicylic acid at similar pH values. The authors postulated that these salts may have an increased solubility due to the ammonium based cations exerting a hydrotropic and a structuring effect upon water molecules. Their findings were in agreement with the report by Pandit et al. (1989) that the ethanolamine salt of an acidic anti-allergic drug was more soluble than the salts prepared from inorganic cations.

2.2.3.2. Counterion size / structure

Structural effects on salt solubility within a series of counterions should be considered in terms of their separate contributions to the crystal lattice energies and solvation energies. The molar free energy of solution on dissolving a salt in water, ΔG_{soln}, may be represented by:

$$\Delta G_{soln} = \Delta G_{cation} + \Delta G_{anion} - \Delta G_{lattice} \qquad \textbf{Equation 2. 4}$$

where ΔG_{cation} and ΔG_{anion} are the molar free energies of hydration of the cation and anion, respectively, and $\Delta G_{lattice}$ is the crystal lattice free energy (Anderson and Flora, 1996). The lattice energy and the hydration energy both increase with an increase in cation / anion charge and decrease with an increase in ionic radius. Both would also be expected to increase with an increase in polarity or hydrogen-bonding nature of the counterion. The overall change in solubility with a change in the counterion will depend on which terms, the hydration energies or the lattice energy, are most sensitive to the change in structure (Anderson, 1985).

In a study on the sodium, potassium, calcium and magnesium salts of three organic acids, Chowhan (1978) compared the solubilities of the salts at the pH_{max}. The order of decreasing solubility of naproxen salts was $K^+ > Na^+ > Mg^{2+} > Ca^{2+}$; the order for 7-methylsulfinyl-2-xanthonecarboxylic acid salts was $K^+ > Na^+ > Ca^{2+} > Mg^{2+}$; the order for 7-methylthio-2-xanthonecarboxylic acid salts was $Na^+ > K^+ > Ca^{2+} = Mg^{2+}$. Chowhan concluded from these results that the qualitative trends between structure and water solubility, reported for inorganic alkali and alkaline earth metal salts (Leussing, 1959), could not be used for organic carboxylic acids. It can be noted from the results that the salts of the divalent cations consistently exhibit lower water solubility than those of the monovalent cations, suggesting that the crystal lattice energy effects dominate (Anderson, 1985).

Forbes et al. (1995) compared the rank solubility order for metallic *p*-aminosalicylic acid salts with the rank order data obtained for other carboxylic acids (Chowhan, 1978; Anderson and Conradi, 1985) and observed a general trend of salts of divalent cations being less soluble than salts of monovalent cations. The rank order solubilities reported by Pandit et al. (1989) for the anti-allergic drug, *N*-[4-(1,4-benzodioxan-6-yl)-2-thiazolyl]oxamic acid ($Na^+ > K^+ > Ca^{2+}$) provides further evidence for this trend. Forbes et al. (1995) suggested that a more precise prediction of the effect of salt forming agent on the solubility of organic carboxylic acids is not possible because of modification of the solubilities of the salts due to different degrees of hydration. This explanation is further supported by the observation by Rubino (1989) that the log solubilities of a series of sodium salts were inversely related to both the melting point and stoichiometric amounts of water in the crystal hydrates.

Several reports have shown that the structure of an organic salt-forming agent influences the solubility of the resulting salt. Magerlein (1965), in a study of *N*-alkylsulfamate salts of lincomycin, reported that the solubility of the salts decreased as the size of the alkyl group attached to the acidic function increased. Jones et al. (1969) investigated the effect of the alkyl chain length of the conjugate acid on the solubility of sixteen salts of the weak base erythromycin. Increasing the length of the alkyl chain of the acid was thought to increase the hydrophobic properties of the acid as well as those of the corresponding salt. Accordingly, the water solubilities of the salts were shown to decrease with increasing size of the alkyl group of the acid. The salts prepared from acids with similar alkyl groups but with different acid strengths exhibited similar water solubilities, indicating that the strength of the acid group has little influence on the water solubility of the salts.

The stability of salt forms can also be affected by the counterion structure. A preformulation study on the stability of hydrate forms of fenoprofen salts (Hirsch et al., 1978) showed that the dihydrate of the calcium salt was more stable than the dihydrate of the sodium salt at 25°C and 1% relative humidity, indicating that the water of hydration was more tightly bound in the calcium salt crystals. Forbes and co-workers (1992) saw similar trends in relation to the stability of hydrates of *p*-aminosalicylic acid salts. The onset temperatures of dehydration for the magnesium and calcium salts were higher than that of the sodium salts, consistent with stronger ion-dipole interactions in the divalent salts. Examination of the crystal structure of the sodium salt revealed a very open structure with an observable channel of water oxygens, not apparent for the divalent salts, which was suggested by the authors as a significant factor in the stability of the hydrate.

Forbes et al. (1992) studied the potassium, sodium, calcium and magnesium salts of *p*-aminosalicylic acid and reported a general trend of increasing propensity to form hydrates with increasing ionic potential of the cations. This was evident from the increase in the number of

moles of water associated with the salts as the ionic radius decreased and the charge on the cation increased. However, the usefulness of such a generalisation is limited since salts may form several stoichiometric hydrates with different amounts of water, depending on the crystallisation conditions. Therefore, the selection of the optimal salt form with respect to hydrate stability usually requires experimental evaluation (Anderson and Flora, 1996).

2.2.3.3. Crystal properties

Since the solubility differences within a series of structurally related salts can be attributed to changes in the crystal lattice free energy, relationships between solubility and crystal properties have been explored. The relationship between the ideal mole fraction solubility of a solid, X_2^i, and its melting point, T_m, is given by Equation 1.2.

Relationships have been identified between salt melting points and the melting point of the conjugate acid or base. These indicate that those structural features leading to high-melting (e.g. planarity, symmetry) or low-melting (e.g. chain flexibility, asymmetry) salt-forming agents will be carried over in determining the crystal lattice energies of the salt (Anderson and Flora, 1996). In a study on a series of salts of a basic experimental drug candidate, Gould (1986) explored the dependence of salt melting point on the controlling effect of crystallinity from the conjugate anion. Salts prepared from planar, high melting aromatic sulphonic or hydroxycarboxylic acids yielded crystalline salts of correspondingly high melting point, whereas flexible aliphatic strong acids such as citric and dodecyl benzene sulphonic yielded oils. Gould concluded that the comparative planar symmetry of the conjugate acid appeared to be important for the maintenance of high crystal lattice forces.

Hydroxyl acids increase rigidity in flexible bases by hydrogen bonding, resulting in an increase in melting point (Wells, 1988). However, the solubility may not be compromised due to the hydrophilicity of the acid.

The effect of various counterions on the aqueous solubility of a series of salts of a high melting, basic antimalarial drug was investigated by Agharkar et al. (1976). The 2-hydroxyethane-1-sulfonate and lactate salts were considerably more soluble than the hydrochloride salt. Their lower melting points suggested that the enhanced solubility was in part due to lower crystal lattice energies. Hydrogen bonding between the hydroxyl groups of the anions and water may also have contributed to their superior solubilities.

2.2.3.4. Hydrophilicity

Results of a study by Senior (1973) illustrate the importance of considering the hydrophilic nature of the conjugate acid or base, as well as its role in controlling crystallinity, when predicting the solubility of salt forms. Salts of chlorhexidine showed increased water solubility due, not only to a lowering of the melting point, but to the presence of hydroxyl groups on the conjugate acid.

The solubilities of salts examined by Rubino (1989) were found to be unrelated to the polarity of the corresponding acid forms (as estimated from the octanol-water partition coefficients). This observation was in agreement with the conclusions from a study by Anderson and Conradi (1985). The hypothesis that higher salt solubilities can be achieved by selecting more hydrophilic counterions neglects the possibility of interactions in the compound becoming stronger as the salt-forming agent is made increasingly polar. Accordingly, a study on a range of diclofenac salts (Fini et al., 1995a) revealed that the presence of hydroxyl groups in the cation did not guarantee an improvement in solubility. This was attributed to hydrogen bond interactions existing in the solid state. These maintain the hydrophilicity of the hydroxyl groups inside the salt instead of directing it towards the dissolution medium, thus decreasing the interaction between the salt and the solvent.

2.3. POLYMORPHISM

Many pharmaceutical solids exhibit *polymorphism*, which is defined as the ability of a compound to exist as two or more crystalline phases that have different arrangements of the molecules in the crystal lattice (Haleblian and McCrone, 1969). Two polymorphs will be different in crystal structure but identical in the liquid or gaseous states.

The process of transformation from one polymorph to another is a *phase transition*, which may occur on storage or during processing. If the phase transition is reversible, the two polymorphs are *enantiotropes* and the system of the two solid phases is said to be *enantiotropic*. In the case of enantiotropy, a reversible transition can be observed at a definite transition temperature before the melting point is reached. The lower melting form is the stable form (i.e. has the lower free energy content and solubility) at temperatures below the transition temperature (T_t) and the higher melting form is the stable form at temperature above T_t. If the phase transition is irreversible, the two polymorphs are *monotropes* and the system of the two solid phases is said to be *monotropic*. In a monotropic system, the higher melting form is the most thermodynamically stable at all temperatures below the melting point, and all other polymorphs are thermodynamically unstable.

Because of differences in the dimensions, shape, symmetry, capacity (number of molecules) and void volumes of their unit cells, the different polymorphs of a given compound display different physical properties arising from differences in their molecular packing (Grant, 1999). Such properties include molecular volume, density, refractive index, thermal conductivity and hygroscopicity. Differences in melting points of different polymorphs arise from differences of the co-operative interactions of the molecules in the solid state as compared with the liquid state (Grant, 1999). Different lattice energies in polymorphs give rise to different solubilities and dissolution rates. If the solubilities of the various solid forms are sufficiently different, the crystal form of the drug present may have implications in terms of its bioavailability (Higuchi et al., 1963). Polymorphism can also have an important influence on the processing of the drug substance into drug products. For example, the behaviour of suspensions depends on the crystal form present. If the wrong polymorph is used, a phase transformation to a more stable polymorph may occur, producing a change in crystal size and possibly caking (Haleblian and McCrone, 1969). Furthermore, there have been a number of reported instances where different crystalline phases of the same compound have different chemical stabilities. For example, chemical instability was reported for some batches of an aqueous suspension of a corticosteroid (Haleblian and McCrone, 1969). Two polymorphs of the compound were subsequently identified, one of which was light-sensitive. Batches containing this crystal form decomposed with time and assayed lower than the other batches.

Many pharmaceutical solids can exist in an amorphous form, which is sometimes regarded as a polymorph (Grant, 1999). Unlike true polymorphs, amorphous forms are not crystalline. They consist of disordered arrangements of molecules and therefore possess no distinguishable crystal lattice or unit cell. The lower stability and greater reactivity of the amorphous form indicates that its molar Gibbs free energy exceeds that of the crystalline state (Grant, 1999). The high free energy content of amorphous forms means they are thermodynamically unstable and tend to revert to a more stable form (Haleblian, 1975). The amorphous form is typically obtained during lyophilisation, spray-drying, granulation, grinding or milling (Guillory, 1999).

2.4. PSEUDOPOLYMORPHISM

With some crystalline solids, solvent in the surrounding medium may become incorporated into the crystal structure, resulting in a *solvate* or *pseudopolymorph*. A *hydrate* is formed when water is the solvent of crystallisation. Pharmaceutical solids may become hydrated when they come in contact with water during processing steps such as wet granulation, aqueous film-coating or spray-drying. Alternatively, they may be exposed to water during storage in an atmosphere containing water

vapour or in a dosage form consisting of materials which contain water (Khankari and Grant, 1995).

The presence of solvent molecules in the crystal structure influences the intermolecular interactions within the solid, modifying the internal energy and therefore the enthalpy. Changes in the shape and symmetry of the unit cell also result from solvation, altering the entropy of the solid. These changes in the enthalpy and entropy result in changes in the free energy and chemical potential of the solid. Modification of the chemical potential alters the thermodynamic activity of the solid, resulting in changes in pharmaceutically important properties such as solubility, dissolution rate and physical and chemical stability (Khankari and Grant, 1995). The changes in dissolution rate and stability of a drug may ultimately modify its bioavailability. In addition, many solid-state properties are altered, resulting in changes in the behaviour of the drug during processes such as tableting and grinding (Khankari and Grant, 1995).

A general rule is that the solubility of a solvate in the solvating solvent is lower than that of the nonsolvated form (Grant and Higuchi, 1990). Thus, the hydrate of a compound is always less soluble in water than the corresponding anhydrous form which crystallised from water at the same temperature. Because the hydrate has already reacted intimately with water, the free energy released on crystal dissolution and the further interaction with water is lower for the hydrate than for the anhydrate (Khankari and Grant, 1995). On the other hand, the solubility of solvates formed from organic solvents may be many times higher in water than that of the nonsolvated form (Shefter and Higuchi, 1963). This is because the negative free energy of mixing of the organic solvent with water can contribute to the negative free energy of solution (Grant and Higuchi, 1990).

2.5. CHARACTERISATION OF SOLID-STATE FORMS

The normal approach to administering the majority of pharmaceutically active therapeutic agents is through solid dosage forms (Byrn, 1982), which are conventionally produced by the processing and formulation of powdered solids. Since any characteristic that might affect the stability or availability of a drug substance in a solid dosage form should be monitored, the physical characterisation of solids has become an extremely important area in pharmaceutics (Brittain, 1995). A variety of methods are available for the study of the solid-state chemistry of drugs.

2.5.1. Powder X-ray diffraction

Powder X-ray diffraction (XRD) is a powerful tool for the investigation of crystalline compounds. The technique is based on Bragg's Law, which describes the diffraction of a monochromatic X-ray beam impinging on a plane of atoms (Cullity, 1978). Parallel incident rays strike the crystal planes and are diffracted at angles that are related to the spacings between planes of molecules in the lattice, according to Bragg's law:

$$n\lambda = 2d\sin\theta \qquad \textbf{Equation 2. 5}$$

where n is the order of the diffraction pattern, λ is the wavelength of the incident beam, d is the distance between the planes in the crystal and θ is the angle of beam diffraction. The scattering angle is determined by slowly rotating the sample and measuring the angle of the diffracted X-rays in relation to the angle of the incident beam. Alternatively, the angle between the sample and source can be kept fixed while moving the detector to determine the angles of the scattered radiation. Knowing the wavelength of the incident beam, the spacing between the planes (d-spacing) is calculated using Bragg's Law (Brittain, 1995). To measure a powder pattern, a randomly oriented powdered sample is prepared so as to expose all planes of the sample. The resultant X-ray diffraction pattern consists of a series of peaks at characteristic scattering angles. No two compounds would be expected to form crystals in which the three-dimensional spacing of planes is totally identical in all directions (Brittain, 1995). Therefore, every crystalline compound produces its own characteristic X-ray diffraction pattern.

Powder X-ray diffraction is the primary method for demonstration of the existence of drug polymorphs or pseudopolymorphs (Brittain, 1995). Each powder pattern of the crystal lattice is characteristic for a given crystal form.

Differentiation of amorphous from crystalline solids is possible using X-ray powder diffraction (Haleblian, 1975). XRD of amorphous forms produces very diffuse reflections, without peaks, due to the absence of an ordered crystal lattice. X-ray diffraction is also widely used to determine the degree of crystallinity in materials such as polymers, which exhibit properties associated with both crystalline and noncrystalline materials (Suryanarayanan, 1995). In addition, powder X-ray diffraction is useful for the quantitative determination of phase composition in a mixture of crystalline solids (Suryanarayanan, 1995; Doff et al., 1986). Each of the components will have a characteristic diffraction pattern, independent of the other components in the mixture. Provided appropriate absorption corrections can be made, the intensities of the peaks of each of the

components will be proportional to the weight fraction of that component in the mixture (Klug and Alexander, 1974).

A useful complement to conventional powder X-ray diffraction is variable-temperature X-ray diffraction. In this technique, the sample is contained on a stage, which can be heated to any desired temperature. The method is extremely useful in the study of thermally induced phenomena.

More detailed structural information may be obtained from single crystal X-ray crystallography, which provides a precise identification and description of a crystalline substance. Unit cell dimensions and angles conclusively establish the crystalline lattice system. However, the stringent sample requirement limits its application to high-quality, single crystals. In view of this, the technique of powder X-ray diffraction is the predominant tool for the study of polycrystalline materials (Klug and Alexander, 1974) and is suited for the routine characterisation of polymorphs and solvates (Brittain, 1999).

2.5.2. Thermal Analysis

Thermal analysis generally refers to any method involving heating a sample and measuring the change in some physical property. Thermal analysis is used to characterise compound purity, polymorphism, pseudopolymorphism, degradation and excipient compatibility and is now a routine tool in preformulation work or in the quality control of drugs.

2.5.2.1. Differential scanning calorimetry (DSC)

In DSC, the sample and reference are kept at the same temperature and the heat flow required to maintain the equality in temperature is measured. DSC results are generally plotted as the differential power input (e.g. mW) against temperature. The area under a DSC peak is directly proportional to the heat absorbed or evolved by a thermal event and integration of peak area yields the heat of reaction (e.g. J/g). Endothermic processes (melting, sublimation, vaporisation, desolvation, solid-solid phase transitions and some chemical degradation reactions) are differentiated from exothermic processes (adsorption, crystallisation and oxidative decomposition).

A useful application of DSC is the determination of the absolute purity of a given compound without reference to a standard. Unfortunately, the method is limited to reasonably pure compounds (purity greater than ~97 mole%) that melt without decomposition.

DSC is extremely useful in the study of polymorphism and pseudopolymorphism (Brittain, 1995). Giron (1995) classified polymorphs according to the type of DSC curves generated:

Type 1 A solid-solid transition occurs before the melting point of the high melting form. This transition is exothermic for monotropy and endothermic for enantiotropy. No weight loss is detected by TG.

Type 2 Some substances have two melting points. After the melting of the lower melting form, crystals of the higher melting form grow from the melt, resulting in an exothermic peak in the DSC scan. Then, the higher melting form melts, giving rise to a second endothermic peak. The system can be monotropic or enantiotropic.

Type 3 Each crystalline form has a melting peak and no conversion between each form occurs.

Pseudopolymorphs were also classified according to their thermal properties (Giron, 1995):

Type 1 Desolvation or dehydration occurs in the solid state with an endothermic peak.

Type 2 The dehydration or desolvation process occurs during the melting or after the melting of the solvate. The solvate melts first and the solvent is eliminated from the liquid phase. This may be followed by an exothermic transition due to the crystallisation of the solvent-free form from the melt. The melting peak of the solvent-free form is then observed. In some cases, melting of the solvate and desolvation of the solid phase may overlap.

Type 3 Different polymorphic forms of a solvate, with the same chemical composition, may exist.

When studying the stability relationships between different polymorphic forms, the use of temperature cycling experiments can be very useful (Brittain, 1999). Samples are heated to a preset temperature, cooled back to a lower temperature, and then reheated. Alterations in the DSC curve resulting from the cycling process can provide information of the ease of phase conversion.

DSC is an important technique in the study of polymers (Brown, 1988). Most solid polymers are formed by rapid cooling to low temperatures (quenching) from the melt and are therefore initially in the glassy state. The transition from a glass to a rubber, the glass transition, is an example of a second order phase transition. Such transitions are accompanied by a change in heat capacity, but no change in enthalpy ($\Delta H = 0$). The transition appears on the DSC curve as a discontinuity in the baseline at the glass transition temperature, T_g.

An important application of DSC analysis is the determination of possible interactions between a drug substance and the excipients used in its formulation (McCauley and Brittain, 1995). One approach is to produce binary mixtures of each ingredient and to monitor changes in melting endotherms, which would indicate either a physical or chemical interaction between the two

components. An alternative approach involves stressing the formulation and using DSC to monitor any changes that may have occurred.

Oscillating or *modulated* DSC involves the superimposition of a sinusoidal temperature signal onto a conventional DSC programme (Hill et al., 1997). This allows the separation of the parent DSC signal into two distinct components, the specific heat capacity (reversible) component and the kinetic (irreversible) component. This information allows for better interpretation of simultaneous thermal events such as glass transitions (detected in the heat capacity signal) and relaxation endotherms which frequently occur over the same temperature range (detected in the kinetic signal).

2.5.2.2. Thermogravimetric analysis (TG)

TG involves measuring the thermally-induced change in mass of a sample as a function of the applied temperature. This technique is restricted to the detection of events which involve either a mass gain or loss and it is most commonly used to study desolvation processes and compound decomposition. The primary use of TG analysis is the quantitative determination of the volatile content of a solid (Brittain, 1995) and it can be used as an adjunct to Karl Fischer titrations for the determination of water content. TG also serves as a powerful adjunct to DSC. A combination of the two techniques can be used to assign observed thermal events. For example, detection by TG of weight loss over the same temperature range as an endothermic event on the DSC curve would distinguish a desolvation process from a solid-solid phase transformation. In addition, TG analysis of compound decomposition can also be used to compare the stability of similar compounds.

2.5.2.3. Thermal microscopy

Also referred to as *hot stage microscopy* (HSM), thermal microscopy can be an extremely valuable tool for the characterisation of solid state forms, including polymorphic or solvate systems (Brittain, 1999). The technique involves heating and cooling a few milligrams of a substance on a microscope slide and observing the sample. Thermal microscopy can be used to determine melting points or phase transition temperatures. During phase transformation, the optical properties of the crystals will usually undergo drastic change (Newman and Brittain, 1995). The loss of crystal birefringence is an easily observed parameter, since the transition will generally terminate in an isotropic condition. Heating and cooling a sample can generate information regarding the nature of a polymorphic transition. In addition, the loss of solvent molecules from a solvate can be detected by immersing the sample in an oil. The evolution of gases is evident in the generation of gaseous bubbles from the sample (Newman and Brittain, 1995).

2.5.2.4. Solution calorimetry

Solution calorimetry allows us to investigate processes which involve enthalpy changes. For example, the heat of solution (ΔH_{soln}) for a given system can be obtained by mixing the solute and solvent and determining the resultant heat change. If a compound exists in two or more different crystalline or amorphous forms with different lattice energies, the heat of solution in any given solvent will differ for each form. The difference in the heats of solution will be equal to the difference in lattice energy of the solids provided that the solid compounds are chemically identical (Giron, 1995). The difference in heat of solution between the two forms is equal to the heat of transition, ΔH_t. For example, the heat of hydration (ΔH_h) can be calculated from the difference between the heat of solution of an anhydrate and that of its hydrated form:

$$\Delta H_h = \Delta H_{soln\,(anhydrate)} - \Delta H_{soln\,(hydrate)} \qquad \textbf{Equation 2. 6}$$

This equation is valid for solvents that allow rapid dissolution in the calorimeter. Whereas the heats of solution of the anhydrate and the hydrated form depend on the solvent, the difference between them is independent of the solvent.

2.5.2.5. Other thermal analysis techniques

Thermal analysis techniques, which can be used as complementary methods to those described above, include *differential thermal analysis* (the difference in temperature between a sample and a reference is monitored as a function of temperature), *evolved gas analysis* (the amount and composition of volatile products are measured as a function of temperature) and *thermomechanical analysis* (deformation of the sample due to an externally applied stress is followed as a function of temperature).

2.5.3. Spectroscopy

Spectroscopic techniques are useful for the characterisation of pharmaceutical solids at the molecular level. An advantage of solid state spectroscopy over diffraction techniques is that spectroscopic analysis can be performed on crystalline and amorphous materials.

2.5.3.1. Vibrational spectroscopy

The vibrational modes of molecules can be observed directly through their absorbance in the infrared region (*infrared spectroscopy*) or through the observation of the low-energy scattered bands that accompany the passage of an intense beam of light through the sample (*Raman*

spectroscopy). In either case, the use of Fourier transform methodology has vastly improved the quality of the data that can be obtained. The vibrational spectra of solid materials reflect details of the crystal structure and therefore are used in the investigation of polymorphic and pseudopolymorphic forms (Brittain, 1999). Vibrational spectroscopy can be used to develop methods for the quantitative analysis of one polymorph (or solvate) in the presence of the other (Brittain, 1999).

In the case of infrared (IR) spectroscopy, absorption of IR energy by the sample results from transitions between molecular vibrational and rotational levels (Bugay and Williams, 1995). IR spectra can be interpreted by using group frequency compilations (Socrates, 1994; Silverstein & Webster, 1998). Since most pharmaceutical compounds are of low symmetry, Raman spectroscopy will generally produce spectra equivalent to those obtained from IR. However, differences in peak intensity can be observed, which may provide information about the structural composition of the sample (Brittain, 1995).

2.5.3.2. NMR spectroscopy

The ultimate characterisation of a pharmaceutical material concerns the chemical environment of each atom in the compound (Brittain et al., 1991). This information can be obtained through solid-state NMR, which is therefore useful for differentiating solid-state structures (Yu et al., 1998). When the crystal structure of polymorphs is such that the nuclei in their structures are magnetically nonequivalent, it will follow that the resonances of these nuclei will not be equivalent. Since organic functional groups can be assigned to observed resonances, NMR can be used to study the nature of polymorphic variations (Brittain, 1995). The investigation of polymorphism can be performed at either the bulk drug or dosage form level. Therefore, NMR can be used for the investigation of polymorphic conversion under various processing techniques such as dry blending and tableting.

EXPERIMENTAL

Chapter 3

Materials and methods

3.1. MATERIALS

Material (abbreviation)	*Supplier/Manufacturer*
2-Amino-2-methyl-1,3-propanediol (AMPD)	Sigma
2-Amino-2-methyl-1-propanol (AMP)	Sigma
2-Dimethylaminoethanol / Deanol (DNL)	Sigma
Acetone	BDH
Benzoic acid	Sigma
Benzylamine (BA)	Sigma
Deionised water	---
Diclofenac acid (DCFA)	AMSA
Diclofenac diethylamine (DDEA)	IBSA
Diclofenac *N*-(2-hydroxyethyl)pyrrolidine (DHEP)	IBSA
Diclofenac sodium (DNa)	Sigma
Diethylamine (DEA)	Aldrich
Ethyl acetate	Riedel-de Haën
Hydranal Composite 5	Riedel-de Haën
Hydranal Standard 5.00	Riedel-de Haën
Hydrochloric acid, 37% (HCl)	Merck
Indium standard	Mettler
Methanol	Riedel-de Haën
N-(2-Hydroxyethyl)pyrrolidine (HEP)	Aldrich
Nitrogen gas	Air products
N-Phenyl-1-naphthylamine (NPN)	Sigma
Paraffin wax, pastillated	BDH
Potassium bromide (KBr)	Riedel-de Haën
Silicone oil	Dow Corning
Standard buffer solution, pH 4.00	Riedel-de Haën
Standard buffer solution, pH 7.00	Riedel-de Haën
tert-Butylamine (tBA)	Aldrich
Tris(hydroxymethyl)aminomethane (TRIS)	Aldrich

3.2. METHODS

3.2.1. Powder X-ray diffraction

Powder X-ray diffraction (XRD) measurements were carried out on a Siemens D500 X-ray powder diffractometer. A DACO MP wide-range goniometer was used, with a 1.00° dispersion slit, a 1.00° anti scatter slit and a 0.15° receiving slit. The Cu anode X-ray tube was operated at 40 kV and 30 mA in combination with a Ni filter to give monochromatic Cu Kα X-rays (λ = 1.542 Å). Powdered samples were mounted in conventional cavity mounts; compressed discs were mounted in a holder with a 13 mm diameter aperture and positioned such that the surface of the disc was level with that of the holder. Samples were scanned in the 2θ range 5° to 35° at a rate of 3°/min.

3.2.2. Differential scanning calorimetry

Differential scanning calorimetry (DSC) was performed on powdered samples using one of two systems:

(a) a Mettler TA3000 Thermal Analysis System: TC10A processor, DSC20 measuring cell, with Mettler GraphWare TA72 software or

(b) a Mettler Toledo DSC 821^e, with Mettler Toledo STAR^e software Version 5.1.

Unless otherwise specified, each sample (5 – 10 mg) was run in an open pan, i.e. a hermetically sealed aluminium pan with three vent holes pierced in the lid. Each run was carried out under nitrogen purge at a heating rate of 10°C/min (unless specified otherwise). The onset temperature and enthalpy change for each thermal event was calculated. The DSC systems were calibrated for temperature and heat of fusion using an indium standard. The reproducibility of DSC results was confirmed for each system; assessment of the variability of temperature and enthalpy values obtained with the DSC 821^e system is described in Appendix I.

3.2.3. Thermogravimetric analysis

Thermogravimetric (TG) analysis was carried out on powdered samples (5 – 10 mg) using a Mettler TG 50 linked to a Mettler MT5 balance. Data was processed using either

(a) Mettler GraphWare TA72 software or

(b) Mettler Toledo STAR^e software Version 5.1 with a Solaris operating system.

Analysis was carried out under nitrogen purge at 10°C/min (unless specified otherwise). The reproducibility of TG results was confirmed using the same procedure as that used for the DSC systems.

3.2.4. *Thermal microscopy*

Thermal microscopy was carried out on a Reichert hot stage mounted on a Meopta microscope with and without crossed polarising filters. Samples were mounted in air or in silicone oil (to detect desolvation).

3.2.5. *Karl Fischer titration*

Karl Fischer titrations (KFT), for the determination of water content, were carried out on powdered samples using Metrohm 701 KF Titrino linked to a Metrohm 703 Ti stand. The KF reagent (Hydranal Composite 5) was standardised using Hydranal Standard 5.00. All analyses were performed in triplicate.

3.2.6. *Elemental analysis*

Elemental analysis (C, H, N) was carried out on powdered samples (~2 mg) by the Microanalytical Laboratory, Department of Chemistry, University College Dublin. An Exetor Analytical CE440 was used. Flash combustion of the sample caused conversion of nitrogen (N) to NO_2, hydrogen (H) to H_2O and carbon (C) to CO_2. The resulting gases were sequentially removed by traps and detected by thermal conductivity detectors.

3.2.7. *Preparation of diclofenac salts*

Salts were prepared by dissolving diclofenac acid in an appropriate solvent (Table 3. 1) and mixing in an equimolar amount of base dissolved in the solvent. The resulting product was recovered by filtration under vacuum in cases where a precipitate resulted (indicated by * in Table 3. 1). If no precipitate was formed, the product was recovered by removing excess solvent using a Büchi RE 111 Rotavapor apparatus linked to a Büchi B-169 vacuum system. All products were allowed to dry by exposure to ambient conditions for 48 hours.

Table 3. 1 Counterions and solvents used in the preparation of diclofenac salts

Counterion	*Solvent(s) used*
2-Amino-2-methyl-1,3-propanediol	acetone
	methanol
2-Amino-2-methyl-1-propanol	acetone*
Benzylamine	acetone
	methanol
	ethyl acetate*
tert-Butylamine	acetone*
Deanol	acetone*
Diethylamine	acetone*
	methanol
	water*
N-(2-Hydroxyethyl)pyrrolidine	acetone*
Tris(hydroxymethyl)aminomethane	methanol*

* precipitate formed

3.2.8. Preparation of hydrates

Hydrate forms were prepared by dissolving the anhydrate form in deionised water at ~40°C and recrystallising the hydrate form by allowing slow evaporation of water at room temperature. The resulting forms were exposed to ambient conditions for 48 hours to allow evaporation of excess moisture.

3.2.9. Fourier transform infrared spectroscopy

Fourier transform infrared (FT-IR) analysis was carried out using (a) a Nicolet 205 FT-IR spectrometer or (b) a Perkin Elmer Paragon 1000 FT-IR spectrometer (the instrument type is specified on each spectrum). Spectra were obtained from 32 scans over the range 4000 – 400 cm^{-1} or 64 scans over the range 4000 – 450 cm^{-1} on the Nicolet and Perkin Elmer spectrometers respectively. KBr discs were prepared by grinding a quantity of sample (5 – 10 mg) with 100 mg KBr in a mortar and pestle, followed by compression in a 13 mm diameter punch and die set under 8 tonnes pressure for 5 minutes. The discs were mounted in a disc holder during analysis.

The spectrum for diclofenac acid is presented in Figure 1, Appendix II. The signal at 1684 cm^{-1} can be attributed to C=O stretching of the carboxylic acid group (Silverstein and Webster, 1998; Palomo et al., 1999). FT-IR analysis was carried out on each of the salts prepared. Salt formation can be established by (a) the absence of the carboxylic acid peak at 1684 cm^{-1}, (b) the presence of bands characteristic of carboxylic acid salts, at 1650 – 1550 cm^{-1} and 1440 – 1335 cm^{-1} (Socrates, 1994) and (c) absorption at 3350 – 3150 cm^{-1}, attributable to NH_3^+ stretching of solid amine salts (Socrates, 1994). FT-IR analysis was also carried out on hydrate forms identified. Water of crystallisation can be detected by the presence of medium intensity O–H stretching vibrations between 3600 cm^{-1} and 3100 cm^{-1} (Socrates, 1994).

3.2.10. UV assay for determination of diclofenac concentration

The concentration of diclofenac in aqueous salt solutions was determined by UV assay. Absorbances were measured at λ276 nm (Adeyeye and Li, 1990) using a Hewlett Packard 8452A photodiode array spectrophotometer. Concentrations were determined by reference to a calibration curve for the particular salt. A calibration curve was plotted for each salt from the absorbance values of three series of dilutions, prepared from three stock solutions. Equations for the calibration curves are given in Appendix III.

3.2.11. Fourier transform infrared spectroscopy in the development of an assay for TRIS and AMPD

It has previously been reported that, whereas TRIS demonstrates UV absorbance at λ205 nm, the location of the peak is concentration dependent (McGloughlin, 1989). UV spectroscopy is therefore unsuitable for development of an assay for TRIS.

An assay was developed using attenuated total reflectance (ATR) FT-IR spectroscopy. Infrared absorbance was quantified using a Nicolet 205 FT-IR spectrometer with an ATR accessory consisting of a ZnSe crystal mounted in a stainless steel trough. For each sample, ~1 ml was poured onto the upper surface of the crystal and a spectrum was obtained from 200 scans over the range 4000 – 700 cm^{-1}. The reference spectrum (obtained from 200 scans of deionised water) was subtracted from the sample spectrum to correct for solvent. The absorbance at a particular wavenumber (corresponding to a peak characteristic of the base) was recorded and corrected for baseline deviation by subtracting the absorbance at a reference wavenumber. A sample spectrum

for each of the bases (following subtraction of the reference spectrum) is presented in Appendix IV.

Linear calibration curves were plotted for TRIS and AMPD in the concentration range 0.2 – 1.0 %w/v. Absorbances were too low to be quantified at concentrations lower than 0.2 %w/v. Since the samples obtained from dissolution runs are much lower in concentration than 0.2 %w/v, it was necessary to concentrate the samples using a freeze-drying process. Each 25 ml sample taken during a dissolution run was transferred to a 50 ml round-bottomed flask. The flask was immersed in a Hetofrig cooling bath (Heto) for ~15 mins, then transferred to a Hetosicc CD52 freeze-drier (Heto) and left overnight. The product obtained (in powder form) was dissolved in 1.0 ml of deionised water. The IR absorbance of the resulting solution was recorded and its concentration determined by reference to a calibration curve obtained by subjecting a series of standard solutions of the base to the freeze-drying process. Equations for the calibration curves are given in Appendix IV.

3.2.12. Solubility studies

3.2.12.1. Ampoule solubility method

Equilibrium solubilities were determined using a modification of the sealed ampoule method of Mooney et al. (1981). Excess solid (approximately 2 – 3 times the estimated solubility) was placed in 5 ml deionised water in a 10 ml glass ampoule, which was then heat sealed. Ampoules were placed in a shaker water bath (Precision Scientific) at 25°C and agitated at 150 c.p.m. At 24, 48 and 72 hours, samples were withdrawn from the ampoules, filtered through a 0.45 μm filter (Gelman Sciences), diluted appropriately and assayed for drug content (Section 3.2.10). The pH of the filtered solution was determined using an Orion Model 520A pH meter. Solubility determinations were carried out in triplicate.

In the case of DDNL, only small volumes (~0.5 ml) of solution could be recovered by filtration of the saturated solutions due to the high viscosity of the solutions. For pH determination, the suspension was centrifuged in a Sorvall RT6000B temperature-controlled centrifuge (25°C) at 5000 r.p.m. for 10 mins and the pH of the supernatant was determined. Validation of this method was carried out by determining the concentration of a sample of supernatant (as described in Section 3.2.10) to confirm that the value obtained was consistent with the concentration of the solution after filtration.

3.2.12.2. Paddle solubility method

Excess solid (2 – 3 times the equilibrium solubility) was placed with ~30 ml deionised water in a water-jacketed vessel linked to a temperature controlled water bath (Heto) held at 25°C. Solutions were agitated constantly by overhead stirrers at 500 r.p.m. (Heidolph). The solutions were analysed at hourly intervals up to eight hours, at 24 hours and at 48 hours. At each sampling time, a 2 ml aliquot was withdrawn, filtered through a 0.45 μm filter (Gelman Sciences), diluted appropriately and assayed for drug content (Section 3.2.10). Solubility determinations were carried out in duplicate.

3.2.12.3. Gravimetric solubility method

A gravimetric technique was used to determine the solubilities of AMPD and TRIS. The methods that involved saturated solutions with excess solid present were deemed inappropriate due to the very high solubilities of the bases.

A volume of deionised water (10 ml) was placed in a water-jacketed vessel linked to a temperature controlled water bath (Heto) held at 25°C. Powdered solid was added periodically in small quantities of known weight until no more solid would go into solution. The solution was agitated constantly by overhead stirrers (Heidolph) at 500 r.p.m. The final volume of the solution was noted and, from this, the solubility of the base calculated. Determinations were carried out in duplicate.

3.2.13. Intrinsic dissolution rate determination

3.2.13.1. Diclofenac salts

Intrinsic dissolution rate (IDR) studies were performed using the USP 24 paddle method (*United States Pharmacopeia*, 2000). Discs were prepared by compressing 200 mg of powder in a Perkin-Elmer hydraulic press, for 5 minutes under 8 tonnes of pressure, using a 13 mm punch and die set. Analysis of the compressed discs by XRD confirmed that the crystal form of the original powder was retained following the compression procedure. Paraffin wax was used to mount the discs in stainless steel disc holders, leaving one face exposed (surface area, 1.327 cm^2). The dissolution runs were carried out in a Sotax AT7 dissolution bath at 25°C. The drug dissolved into 900 ml deionised water and was agitated by overhead paddles (50 r.p.m.). The medium was analysed for drug content at 5-minute intervals up to 30 minutes and at 10-minute intervals thereafter. A 5 ml aliquot was withdrawn, filtered through a 0.45 μm filter (Gelman Sciences), diluted if necessary and assayed for drug content (Section 3.2.10). The withdrawn sample was replaced with 5 ml of

deionised water. All dissolution runs were carried out in triplicate, in sink conditions. The initial portion of each dissolution profile (0 – 15 min) was used to derive the intrinsic dissolution rate.
The reproducibility of the dissolution method was investigated by carrying out replicate runs on benzoic acid discs (Appendix V).
The diffusion layer thickness, h, was calculated from the experimentally determined dissolution rate of benzoic acid (Appendix VI).

3.2.13.2. Solid organic bases (TRIS and AMPD)

Discs were prepared with 400 mg of powdered base, using the compression conditions described for the diclofenac salt discs. The discs were mounted in stainless steel disc holders and the dissolution bath was set up as described above (900 ml deionised water, 50 r.p.m.). At 2-minute intervals up to 8 minutes, a 25 ml aliquot was withdrawn and assayed as described in Section 3.2.11. All dissolution runs were carried out in triplicate, in sink conditions.

3.2.14. Solution calorimetry

Integral heats of solution (ΔH_{soln}) were determined using the Setaram MicroDSC III calorimeter operated in isothermal mode at 25°C. Known amounts (~450 mg) of solvent were placed in the lower compartments of the batch mixing vessels (sample and reference vessels). The choice of solvent was based on the requirement for "rapid" dissolution of solid for accurate determination of ΔH_{soln} values (Giron, 1995). For each solid phase, preliminary experiments were carried out to select an appropriate solvent, i.e. one in which complete dissolution occurred over 5 mins. The solvents used for each solid investigated are listed in Table 3. 2. A known weight of powdered sample (~1 mg) was placed in the upper compartment of the sample batch mixing vessel. The heat of solution was determined by integration of the thermal event curve using Setaram Thermal Analysis software. This value was adjusted to account for the heat change due to mixing of the upper and lower compartments, which was estimated by integrating the thermal event generated when no sample was present in the upper compartment of the vessel. All readings were determined in triplicate. The accuracy of the method was verified by obtaining ΔH_{soln} readings for TRIS samples. The result obtained for ΔH_{soln} of TRIS (57.65 ± 0.55 Cal/g) compared well with the reference value for TRIS in 0.1 N HCl (58.75 ± 0.12 Cal/g).

Table 3. 2 Solvents used for the determination of ΔH_{soln} values

Salt studied	*Solvent used*
DHEP monohydrate	deionised water
DDEA anhydrate	deionised water:methanol 50:50 v/v
DDEA monohydrate	deionised water:methanol 50:50 v/v

3.2.15. pH-solubility studies

The pH-solubility studies of the salts were carried out using a modification of the phase solubility technique of Dittert et al. (1964). A saturated solution of diclofenac acid or diclofenac salt was prepared by dissolving an excess in deionised water. The solution was maintained at 25°C in a water-jacketed vessel linked to a temperature controlled water bath (Heto) and agitated using an overhead stirrer at 500 r.p.m. (Heidolph). The pH was adjusted above and below that of the saturated solution by the dropwise addition of the appropriate base or 0.1 / 1.0 N HCl. The solution was allowed to equilibrate after each addition, the pH of the bulk solution was recorded (Orion Model 520A pH meter) and a sample taken. The sample was filtered through a 0.45 μm filter (Gelman Sciences), diluted appropriately and assayed for drug content (Section 3.2.10). Apparent pK_a values (pK_a') were calculated from pH-solubility data fitted to Equation 1.14 using the data fitting program, Micromath® Scientist™ for Windows™ Version 1.05 (Micromath® Scientific software).

In the case of the DDNL system, the addition of DNL to diclofenac acid resulted in highly viscous solutions that could not be filtered. The centrifugation method described in Section 3.2.12.1 was carried out on these solutions and the concentration of the supernatant was determined.

3.2.16. Membrane transport studies

A modification of the diffusion cell technique of Goldberg and Higuchi (1968) was used to investigate transport through Visking®, a porous membrane of regenerated cellulose tubing (Scientific Instrument Centre). The diffusion cell (shown in Figure 3. 1) was formed from two 250 ml conical flasks which were modified to contain side-arm attachments with ground-glass ends. The Visking® membrane (2.5 cm diameter), which had been soaked overnight and rinsed several times in deionised water, was placed between these ground-glass ends and the flasks were clamped

together. A solution of drug in deionised water at 25°C, which had been allowed to equilibrate, was placed in the donor flask. The flask was completely filled with drug solution by filling the Y-tube to overflowing via one stopcock and subsequently closing both stopcocks. Deionised water (250 ml), previously equilibrated to 25°C, was added to the receptor flask; the flask was sealed with a conventional glass stopper. Each flask contained a 3.5 cm Teflon-coated magnetic stirring bar. The entire apparatus was then immersed in a constant-temperature water bath (TD Lauda) held at 25°C, under which were placed single speed synchronous motors at 500 r.p.m. (Griffin). Samples of 5 ml were withdrawn at 30-minute intervals from the receptor flask and replaced with 5 ml deionised water (equilibrated to 25°C). The concentration of drug appearing in the receptor flask was determined as described in Section 3.2.10 and corrected for the volume replacement factor.

All drug solutions were run in triplicate, except when a very high drug solubility deemed that large quantities of solid were required to investigate a saturated solution; in such cases, runs were carried out in duplicate. Linear plots for time (hours) vs. total amount of drug transported (mmol) were obtained for samples run up to 4 hours. The slopes of these lines were obtained using linear regression analysis (Microsoft® Excel 97). The average slope for the three runs of a particular concentration was calculated to be the rate of transport through the membrane (mmol/hr).

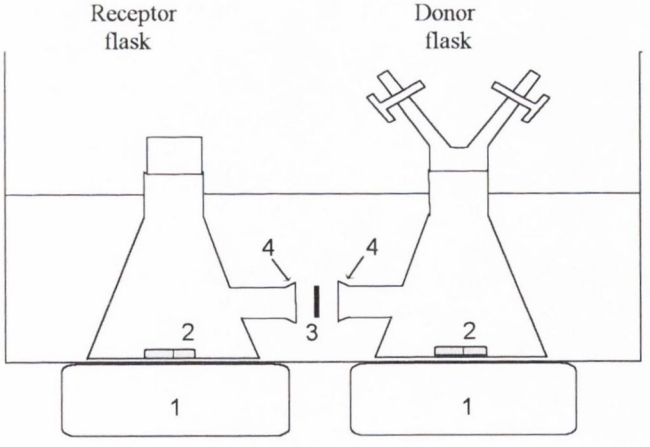

1. synchronous motor
2. magnetic stirrer bar (3.5 cm)
3. Visking® membrane (2.5 cm diameter)
4. ground-glass end

Figure 3. 1 Diagrammatic representation of the diffusion cell used in membrane transport studies

3.2.17. Surface tension measurements

Surface tension measurements of drug solutions in deionised water were carried out at 25°C on a Lauda Tensiometer TD1 using the ring accessory. The solution being investigated was contained

in a water-jacketed vessel linked to a temperature-controlled water bath (TD Lauda). Measurements were carried out in triplicate. To exclude the weight force resulting from the lamella drawn up with the ring, readings obtained were multiplied by the correction factor, f (Lauda Operating Instructions). This correction factor depends on the density of the test liquid, the ring diameter, the gravitational constant and the wire diameter. Its value for the particular ring used was calculated as follows:

$$f = 0.8759 + \left(\frac{0.0009188 \ OS_{Ruk}}{\rho} \right) \qquad \textbf{Equation 3. 1}$$

where OS_{Ruk} is the uncorrected surface tension in mN/m and ρ is the density of the test liquid in g/cm^3.

For each system examined, surface tension values (mN/m) were plotted against concentration (log scale). CAC (critical association concentration, Kriwet and Müller-Goymann, 1993) or CMC (critical micellar concentration) values were determined from a change in the concentration dependence of surface tension.

3.2.18. Solubilisation studies

A modification of the technique employed by Brito and Vaz (1986) was used to study the solubilisation behaviour of the salts examined. A range of aqueous solutions with varying drug concentration was prepared. The water insoluble fluorescent compound *N*-phenyl-1-naphthylamine (NPN) was added to the solutions (~1 mg/10 ml), which were agitated at 25°C for 24 hours in a temperature controlled shaker waterbath (Precision Scientific). A 5 ml aliquot of the solution was withdrawn and filtered through a 0.45 μm filter (Gelman Sciences) to remove excess solid NPN. The solutions were subsequently analysed for fluorescence of NPN using a Perkin-Elmer LS50B Luminescence Spectrometer (excitation λ, 356 nm; emission λ, 410 nm; minimum slit width). For each salt, relative fluorescence intensity was plotted against concentration. This plot was used to determine the CMC of the salt.

3.2.19. *Molecular modelling*

Estimations for the volume ($Å^3$) and surface area ($Å^2$) of diclofenac acid and of each of the bases were obtained using Spartan® Version 5.0 software (Wavefunction, Inc.). The minimum energy conformation *in vacuo* was simulated for each molecule. The solvation treatment model in Macromodel® (Schrodinger, Inc.) was used to simulate the minimum energy conformation in water for each molecule. This conformation was then imported into Spartan® Version 5.0 software for estimation of volume ($Å^3$) and surface area ($Å^2$).

3.2.20. *Dissolution studies on mixed discs*

Dissolution studies were performed using the USP 24 paddle method *(United States Pharmacopeia*, 2000). Powders of particle size <63 μm were obtained using a laboratory test sieve (Endecotts Ltd.). The powders, in the required ratios (w/w), were mixed in a glass vial for 3 minutes using a Turbula® T2C shaker-mixer (Glen Creston Ltd.). Discs were compressed and mounted in stainless steel disc holders and dissolution runs were carried out in a Sotax AT7 dissolution bath at 25°C, using the procedures outlined for diclofenac salts in Section 3.2.13.1. The dissolution rate was derived from the linear portion of each dissolution profile, i.e. before depletion of the disc and alteration of the disc surface area.

For each system examined, the time taken to reach steady state, t, was calculated from Equation 1.43. For systems described by Case A of the two component non-interacting model of Higuchi et al. (1965b), where A forms the surface layer:

$$S_2 = \frac{A_A \, h \, C_{SB}}{\tau \, \rho_B \, C_{SA}} \qquad \textbf{Equation 3. 2}$$

where ρ_B is the density of B; the other variables are described in Section 1.4.3.

A value of 1 g/cm^3 was used as an estimate for the density of B in cases where a value was not available in the literature. A τ value of 3 was used in the calculations; this value was deemed reasonable by Higuchi et al. (1965b). A value for ϵ, the porosity of the phase A layer, was calculated from:

$$\in = \frac{A_B}{\rho_B}$$ **Equation 3. 3**

The same equations are used, with the A and B subscripts exchanged in all terms, for systems described by case B of the two component non-interacting model.

For each system investigated, XRD analysis was performed on:

(a) the corresponding mechanical mix

(b) the disc before dissolution and

(c) the disc after dissolution.

For examination of the systems after dissolution, the discs were removed from the dissolution medium and blotted dry with tissue paper to remove excess moisture. The discs were then allowed to dry at ambient conditions overnight before analysis by XRD. The XRD patterns for the mechanical mixes and the discs before and after dissolution were compared to identify any new forms precipitating on the surface of the disc during dissolution.

3.2.21. Mathematical modelling

Experimental dissolution data was fitted to mathematical models using the non-linear curve fitting program Micromath® Scientist™ for Windows™ Version 1.05 (Micromath® Scientific software). The models applied are given in Appendix VII. The coefficient of determination (CD) and model selection criterion (MSC) were used as measures of goodness of fit for evaluating the suitability of a model.

The CD is a measure of the fraction of the total variance accounted for by the model (Scientist Handbook, 1995). It is defined by the formula:

$$CD = \frac{\sum_{i=1}^{n} w_i \left(Y_{obs_i} - \overline{Y}_{obs} \right)^2 - \sum_{i=1}^{n} w_i \left(Y_{obs_i} - Y_{cal_i} \right)^2}{\sum_{i=1}^{n} w_i \left(Y_{obs_i} - \overline{Y}_{obs} \right)^2}$$ **Equation 3. 4**

where n is the number of points, w_i is the weight applied to each point and $Yobs_i$, $\overline{Y}_{obs}$ and $Ycal_i$ are the observed data points, the weighted mean of the observed data and the model predicted data points, respectively.

The MSC is a modified Akaike Information Criterion (AIC), defined by the formula (Scientist Handbook, 1995):

$$MSC = \ln\left(\frac{\sum_{i=1}^{n} w_i \,(Y_{obs_i} - \overline{Y}_{obs})^2}{\sum_{i=1}^{n} w_i \,(Y_{obs_i} - Y_{cal_i})^2}\right) - \frac{2p}{n} \qquad \textbf{Equation 3. 5}$$

where p is the number of parameters estimated. In contrast to the AIC, the MSC has been normalised so that it is independent of the magnitude of the data points. The most appropriate model is that with the largest MSC value.

RESULTS AND DISCUSSION

Chapter 4

Physicochemical characterisation of diclofenac *N*-(2-hydroxyethyl)pyrrolidine and diclofenac diethylamine

4.1. INTRODUCTION

Bioavailability problems encountered with drugs of low aqueous solubility were discussed in Chapter 1. Improvement of the dissolution rate of these drugs is a common approach to optimising their bioavailability. As outlined in Section 2.2.1, salt formation is a commonly employed method for enhancing the solubility and dissolution rate of poorly water soluble weak electrolyte drugs. Diclofenac, 2-[(2,6-dichlorophenyl)amino]benzeneacetic acid (Figure 4. 1), is a potent non-steroidal anti-inflammatory drug, therapeutically used in inflammatory and painful conditions of rheumatic and non-rheumatic origin. It is an acidic compound (pK_a 3.80 at 25°C) with very low aqueous solubility (6 x 10^{-5} M at 25°C) in the unionised form (Chiarini et al., 1984). Many studies have been carried out on the modification of the solubility and dissolution rate of diclofenac by the preparation of salts from a variety of inorganic and organic bases (Fini et al., 1991a, 1991b, 1993a, 1993b, 1994a, 1995a and 1996).

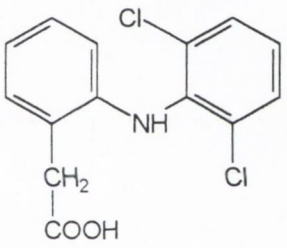

Figure 4. 1 Chemical structure of diclofenac acid

Salts of diclofenac available in pharmaceutical products include diclofenac *N*-(2-hydroxyethyl)pyrrolidine (Flector® EP plaster, gel, granules and tablets, IBSA) and diclofenac diethylamine (Voltarol® Emulgel®, Geigy). The chemical structures of the two basic counterions are shown in Figure 4. 2. Examination of the properties of these two salts has previously been reported (Ledwidge et al., 1996; Fini et al., 1995a).

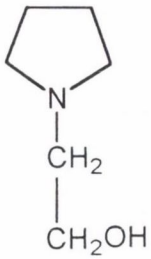

N-(2-hydroxyethyl)pyrrolidine

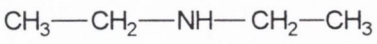

diethylamine

Figure 4. 2 Chemical structures of bases used in commercially available diclofenac salts

4.1.1. General physicochemical properties of the salts studied

In preliminary investigations, diclofenac *N*-(2-hydroxyethyl)pyrrolidine (DHEP) demonstrated an aqueous solubility of 46 mM at 25°C, higher than that of the sodium salt (30 mM) (Fini et al., 1991a). It demonstrated the highest solubility in water among a series of salts prepared with a large variety of metal hydroxide and organic bases (Fini et al., 1993a). Subsequently, a number of publications have explored the physicochemical characteristics and aqueous behaviour of DHEP (Fini et al., 1991b, 1993b, 1994b, 1994c and 1995b; Holgado et al., 1995; Ledwidge et al., 1996; Ledwidge and Corrigan, 1998). Despite extensive investigations on DHEP in the literature, anomalous behaviour of apparently similar samples continues to occur in practice. For example, unexplained precipitation of some batches from aqueous solutions has been observed.

Conflicting values for the aqueous solubility of diclofenac diethylamine (DDEA) are reported in the literature: 11 mM at 25°C (Fini et al., 1995a) and 35 mM at 20°C (Kriwet and Müller-Goymann, 1993). Information on the physicochemical characteristics of DDEA is not as extensively reported in the literature as the findings on DHEP and its properties.

4.1.2. Polymorphic / pseudopolymorphic forms of the salts studied

Only one form of DDEA has been reported in the limited published data on the salt. In contrast, four forms of DHEP have been identified: DHEP anhydrate (Fini et al., 1993b), DHEP dihydrate (Ledwidge et al., 1996), D_2HEP anhydrate (consisting of two molecules of diclofenac to each molecule of HEP), and D_2HEP monohydrate. The latter two forms were isolated following the addition of HEP to a saturated solution of diclofenac acid (DCFA) in order to study the pH-solubility profile of DHEP (Ledwidge, 1997).

DHEP dihydrate (DHEP-DH) is prepared by dissolving the anhydrous form (DHEP-A) in distilled water at 40°C, followed by slow evaporation at room temperature. The dihydrate form was shown to precipitate from solutions of DHEP-A in water, thus limiting the aqueous solubility of DHEP-A to that of the dihydrate form, 273 mM (Ledwidge, 1997).

The DSC scan obtained for DHEP-A shows a sharp melting endotherm at 102°C, followed by a broad endotherm at ~170°C which can be attributed to the volatility of the molten drug and / or decomposition (Ledwidge et al., 1996). A broad endotherm at ~60°C is observed in the DSC scan for DHEP-DH; this corresponds to elimination of water from the sample and melting of the dihydrate. The TG trace for DHEP-DH shows an increase in the rate of weight loss up to ~45°C as water of crystallisation is lost from the sample (Ledwidge et al., 1996).

In this chapter, investigation of the characteristics of DHEP and DDEA, together with hydrated forms of the salts, was carried out.

4.2. CHARACTERISATION OF SIX COMMERCIAL SAMPLES OF DHEP

The physicochemical characteristics of six commercially prepared DHEP batches (B.N.I – B.N.VI) were investigated. The batches were prepared using different preparation methods. The objective of the study was to account for a precipitation phenomenon observed for random batches (from a 20 %w/v solution in water). The samples were examined by powder X-ray diffraction, thermal analysis, Karl Fischer titration and elemental analysis. Their properties were compared with those of DHEP-A.

4.2.1. Powder X-ray diffraction analysis

The XRD trace for each sample is presented in Figure 4. 3.

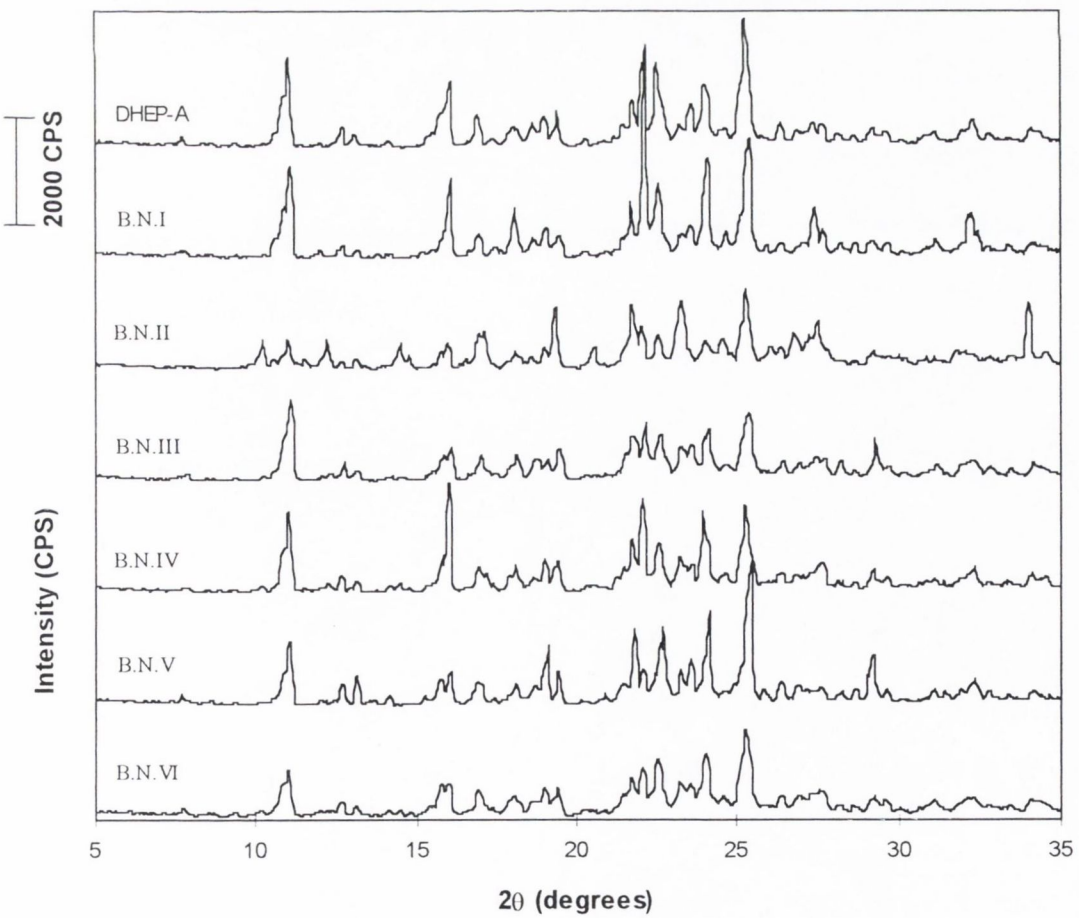

Figure 4. 3 XRD traces of DHEP-A and commercial DHEP batches

When examined in the range 2θ = 5 – 20°, the XRD trace of B.N.II was found to contain all the peaks characteristic of DHEP-A plus additional peaks at 2θ values of 10.20°, 12.25°, 14.50° and 14.80°, as indicated by the arrows in Figure 4. 4. The traces for the other DHEP samples closely resembled that of DHEP-A; small peaks corresponding to the additional peaks in the B.N.II trace were observed for B.N.IV, B.N.VI and B.N.III (Figure 4. 4). The peak height values are listed in Table 4. 1. Each peak examined was observed to decrease in height from B.N.II to B.N.III in the order in which the traces are presented in Figure 4. 4.

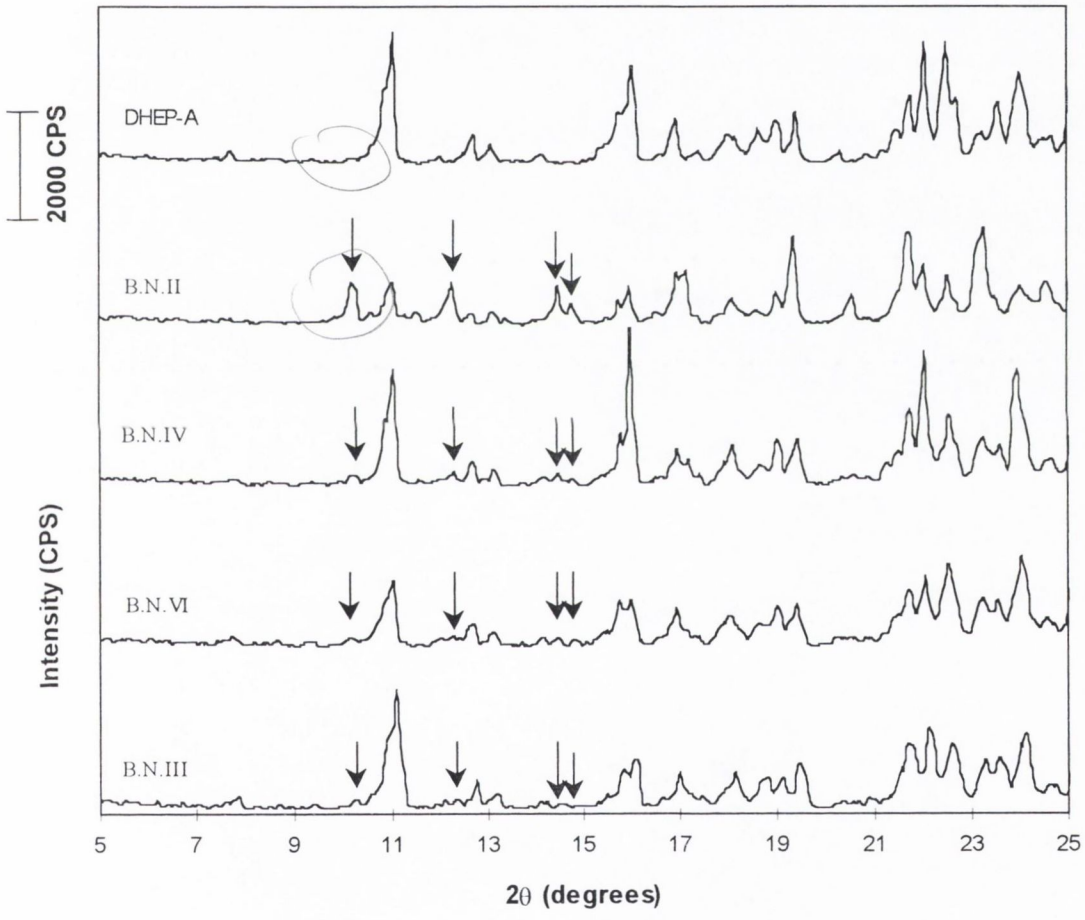

Figure 4. 4 XRD traces of DHEP batches showing peaks not evident in the XRD trace of DHEP-A

The additional peaks detected in the XRD traces may suggest the presence of an impurity in the DHEP samples, which was present in significant quantities in B.N.II and in varying amounts in the other samples. This "impurity" may consist of a polymorphic or pseudopolymorphic form of the salt.

Table 4. 1 Comparison of X-ray diffraction (XRD), differential scanning calorimetry (DSC), Karl Fischer titration (KFT) and elemental analysis results for commercial DHEP batches

B.N.	XRD *peak height** *(CPS)*				DSC *endotherm at ~65°C*	KFT *water content*	Elemental analysis *% of theoretical value*		
	peak1	*peak2*	*peak3*	*peak4*	*ΔH (J/g)*	*%w/w*	C	H	N
II	489	487	438	228	29.9	2.26 ± 0.00	97.86	103.14	98.24
IV	117	157	143	73	6.0	0.90 ± 0.01	99.61	101.19	99.85
VI	101	111	103	73	2.0	0.54 ± 0.11	99.62	101.19	99.41
III	79	99	43	9	1.1	0.37 ± 0.05	99.66	102.37	99.85
V	—	—	—	—	0.23	0.23 ± 0.04	99.97	101.86	100.74
I	—	—	—	—	—	**	99.76	99.83	99.41

*Peak height: Difference (CPS) between the peak intensity and the background intensity ($2\theta = 9.00°$)

peak 1: $2\theta = 10.20°$

peak 2: $2\theta = 12.25°$

peak 3: $2\theta = 14.50°$

peak 4: $2\theta = 14.80°$

**An accurate result could not be determined for B.N.I; due to its very low %w/w water, very large samples were required.

4.2.2. Thermal analysis

The open pan DSC scans of the samples are presented in Figure 4. 5. The DSC scan for DHEP-A is presented for comparative purposes. As reported by Ledwidge et al. (1996), it shows a sharp melting endotherm at 102°C.

Two endotherms were observed in the DSC scan of B.N.II, with onset temperatures of 64.6°C and 96.5°C. The higher temperature endotherm corresponded to the melting of DHEP-A; the broadness of the peak and the lower onset temperature (96.5°C compared to 102°C for the anhydrate) could be attributed to the presence of an "impurity". The lower temperature peak (64.6°C) also appeared in the DSC scans of B.N.IV, B.N.VI, B.N.III and B.N.V. The enthalpy changes (ΔH) for these endotherms are listed in Table 4. 1; the ΔH value was found to decrease in the same rank order as the decrease in the values for the height of the additional peaks in the XRD

traces. This was consistent with the postulated presence in the DHEP samples of an "impurity" which was present in significant quantities in B.N.II, in decreasing concentrations in the other samples and was absent from B.N.I.

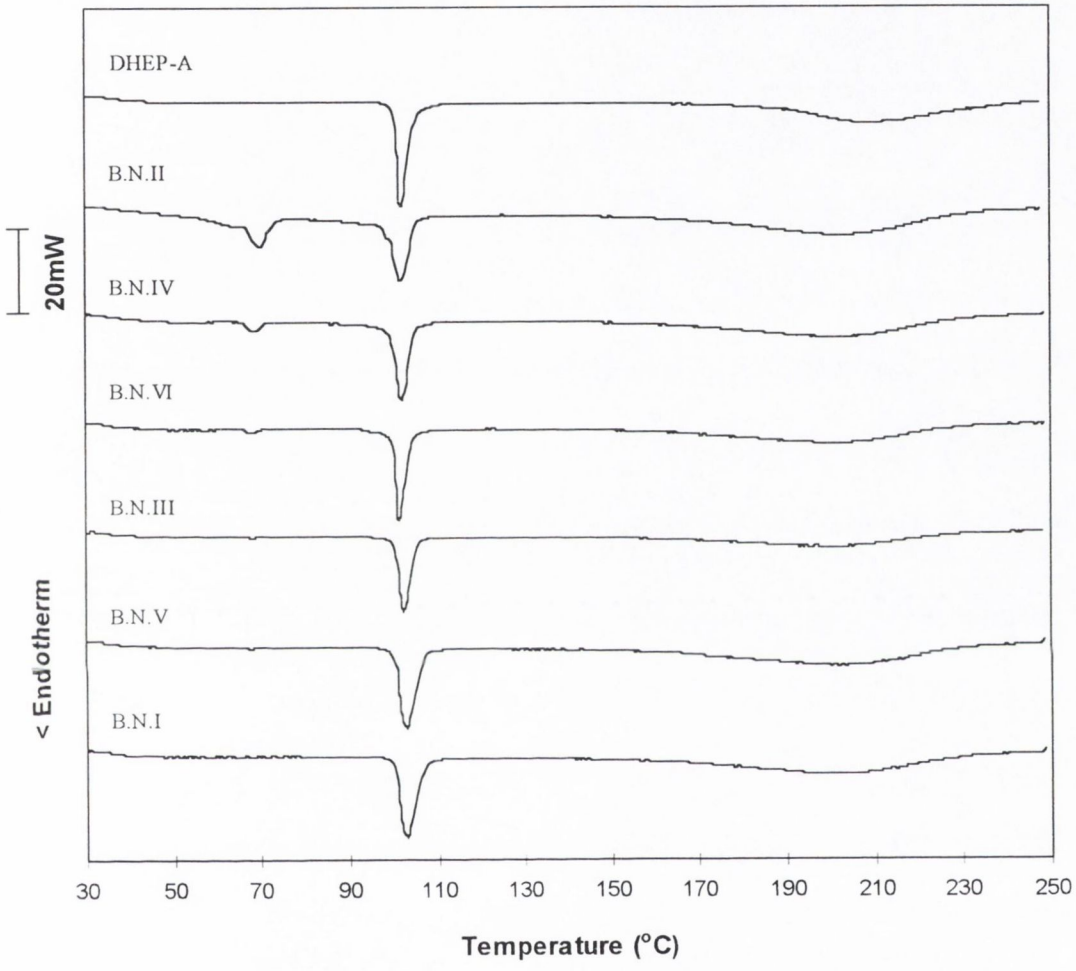

Figure 4. 5 DSC scans of DHEP-A and commercial DHEP samples

Thermal microscopy of a sample of B.N.II in air revealed melting of a certain proportion of the sample at ~70°C, a temperature that corresponded to the lower temperature endotherm in its DSC scan. This ruled out the possibility of the endotherm resulting from a solid-solid transition from one polymorphic form of DHEP-A to another.

The TG trace for B.N.II is compared with that for DHEP-A in Figure 4. 6. The first derivative curve for B.N.II showed a distinct step in the temperature range 35 – 70°C, which was absent from the DHEP-A trace. The temperature at which this weight loss occurred was consistent with the lower temperature endotherm of the DSC scan for B.N.II. The weight loss over this temperature

range was calculated to be 2.30 ± 0.10 %w/w (n = 3). There was no discernible increase in the rate of weight loss over this temperature range in the TG traces for the other commercial batches.

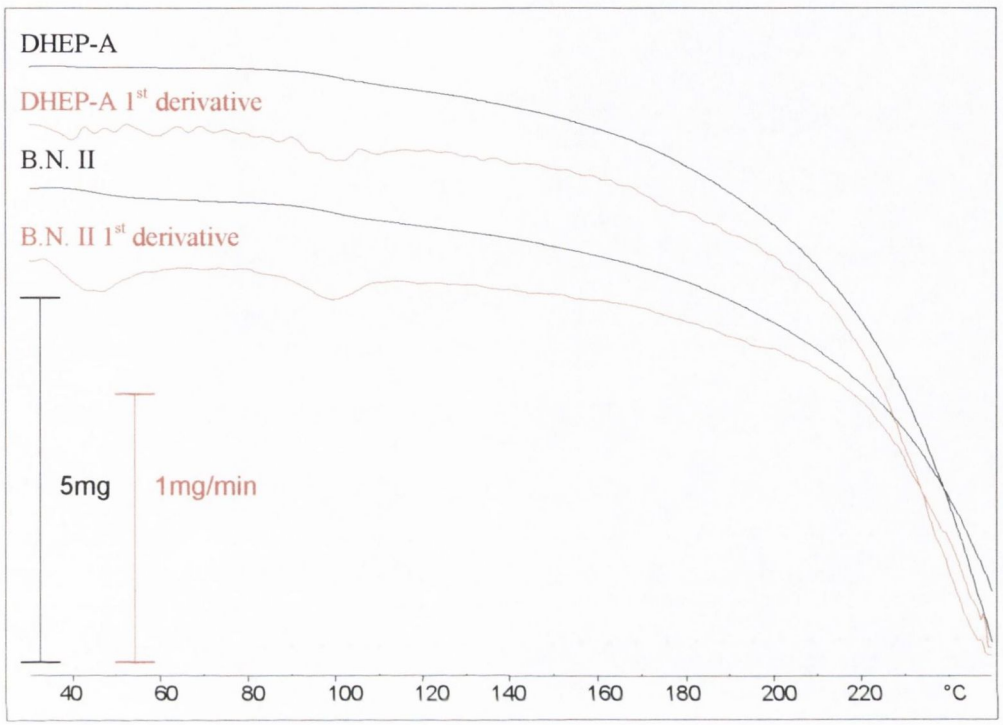

Figure 4. 6 TG traces for DHEP-A and B.N.II, including the first derivative curves

In an attempt to explain the presence of the endotherm at 64.6°C, a sample of B.N.II was heated to 75°C for 15 minutes and allowed to cool to room temperature. The sample was immediately characterised by XRD and DSC. The XRD trace obtained was identical to that of DHEP-A. The DSC scan revealed that the endotherm previously observed at ~65°C was no longer present; a single melting endotherm was observed with an onset temperature of 97.1°C and a peak temperature corresponding to that of the melting endotherm for DHEP-A. A DSC scan of the sample was obtained five days after heating. An endotherm with a sharper onset (98.9°C) was obtained which may suggest some recrystallisation into DHEP-A after sufficient time had elapsed. These results showed that the additional form present in B.N.II was converted to DHEP-A after heating to 75°C and cooling. This behaviour was consistent with that of a polymorph or solvate of the salt.

4.2.3. Elemental analysis and Karl Fischer titration

Elemental analysis was carried out on the samples of DHEP supplied. The results are listed in Table 4. 1, as percentages of the expected values for DHEP-A. Whereas the results for B.N.II showed a decrease in the percentage carbon (C) and nitrogen (N) and an increase in the percentage hydrogen (H), the results obtained for the other five samples were closer to the theoretical values for DHEP-A.

The deviations from DHEP-A observed in the elemental analysis results for B.N.II (high % H, low % C and % N) could be attributed to water molecules being present in the sample. The additional peaks in the XRD traces, together with the distinct step in the TG trace generated from the loss of volatile product, suggested that the water was present as water of crystallisation. To investigate this possibility, Karl Fischer titrations were carried out to determine the water content of the samples; the results are listed in Table 4. 1. The value decreased for all samples in the same order as the decrease in XRD peak heights and ΔH values from DSC analysis, which indicated that the presence of a hydrate could be responsible for the additional XRD peaks and the endotherm at ~65°C in the DSC scans.

The DSC evidence above, coupled with the evidence from TG, suggested the presence of a pseudopolymorphic form of DHEP-A. The KFT results provided further evidence that the pseudopolymorph was a hydrate.

4.3. IDENTIFICATION AND CHARACTERISATION OF A NOVEL HYDRATE OF DHEP

If the "impurity" present in B.N.II was a hydrate, this hydrate would be expected to seed further crystallisation of the same hydrate form from the sample in the presence of water, thus converting some or all of the DHEP-A present in the sample to the hydrate form.

A sample of B.N.II was dissolved in water at ~40°C and recrystallised by slow evaporation of the water at room temperature, the same procedure as that used for the conversion of DHEP-A to the dihydrate (Ledwidge et al., 1996). The recrystallised product was characterised by XRD, DSC, TG and KFT. The characteristics of B.N.II which distinguish it from the anhydrate form are quantified in Table 4. 2 and compared with the values obtained for the recrystallised product.

Table 4. 2 Comparison of B.N.II and the product obtained by recrystallising B.N.II from water

Sample	XRD *Peak height** *(CPS)*				DSC *endotherm at ~65°C*	TG *weight loss from 35–70°C*	KFT *water content*
	peak 1	*peak 2*	*peak 3*	*peak 4*	*ΔH (J/g)*	*%w/w*	*%w/w*
B.N.II	489	487	438	228	29.9	2.30	2.26 ± 0.00
B.N.II recrystallised from water	2977	1278	414	376	109.48	4.03	4.48 ± 0.24

*Peak height: Difference (CPS) between the peak intensity and the background intensity (2θ = 9.00°)

peak 1: 2θ = 10.20°

peak 2: 2θ = 12.25°

peak 3: 2θ = 14.50°

peak 4: 2θ = 14.80°

4.3.1. Powder X-ray diffraction analysis

The XRD trace of the product recrystallised from water is compared with that of B.N.II in Figure 4. 7; the arrows in the trace for B.N.II indicate the additional peaks relative to DHEP-A, at 2θ values of 10.20°, 12.25°, 14.50° and 14.80°. The intensities of three of these peaks were higher in the trace for B.N.II recrystallised from water than in the trace for B.N.II. The peak heights are compared in Table 4. 2.

Furthermore, peaks which are characteristic of the XRD trace for DHEP-A (2θ values of 11.00°, 15.95° and 25.30°, indicated by *) were absent from that of the recrystallised B.N.II, which would suggest that all of the DHEP-A was hydrated.

It can also be seen from Figure 4. 7 that the XRD trace obtained for the recrystallised product did not correspond to the XRD pattern of the dihydrate form (DHEP-DH).

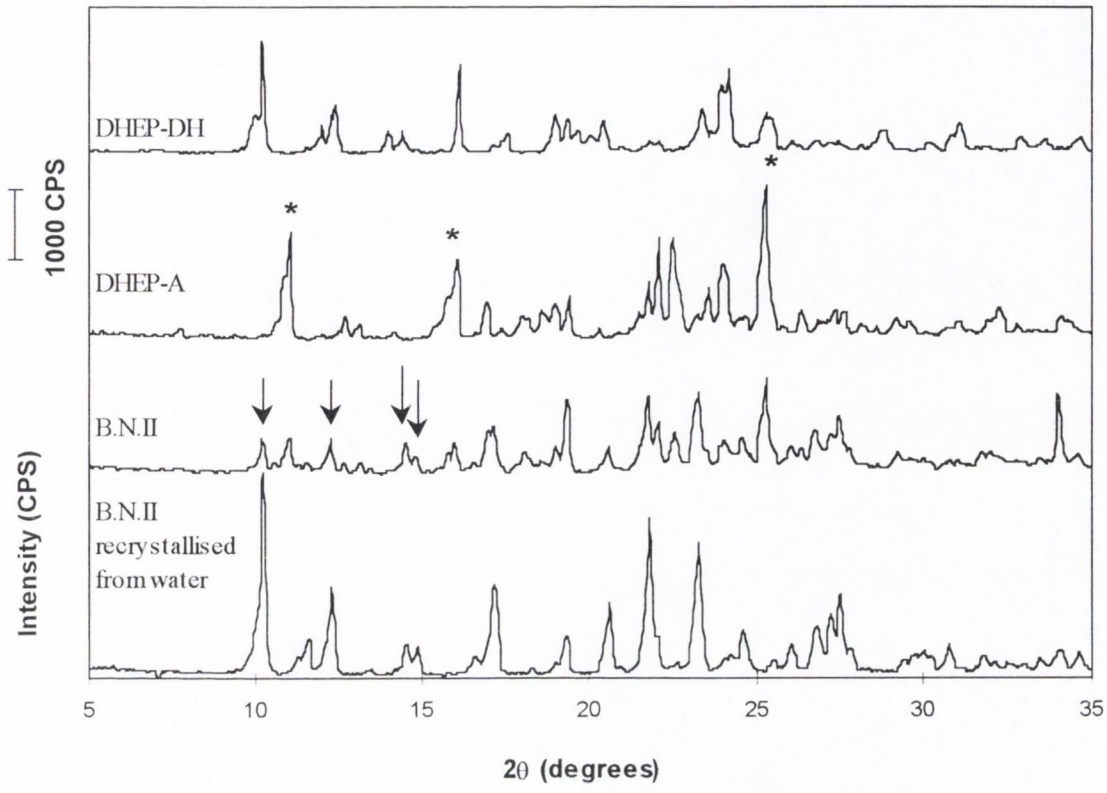

Figure 4. 7 X-ray diffraction trace of B.N.II recrystallised from water, compared with the traces for DHEP-DH, DHEP-A and B.N.II

4.3.2. Thermal analysis

The DSC scan for the recrystallised product is presented in Figure 4. 8. The main endotherm in the scan (peak temperature, 72°C) corresponded to the first of the two endotherms observed in the DSC scan for B.N.II. The endotherm for the recrystallised product had a greater peak area than that for B.N.II (Table 4. 2). This endotherm was thought to correspond to the elimination of water of crystallisation and melting of the hydrate. The presence of the small endotherm at 99°C in the DSC scan of the hydrate may have been due to recrystallisation of a small amount of DHEP-A from the melt following the melting of the hydrate and elimination of water from the system.

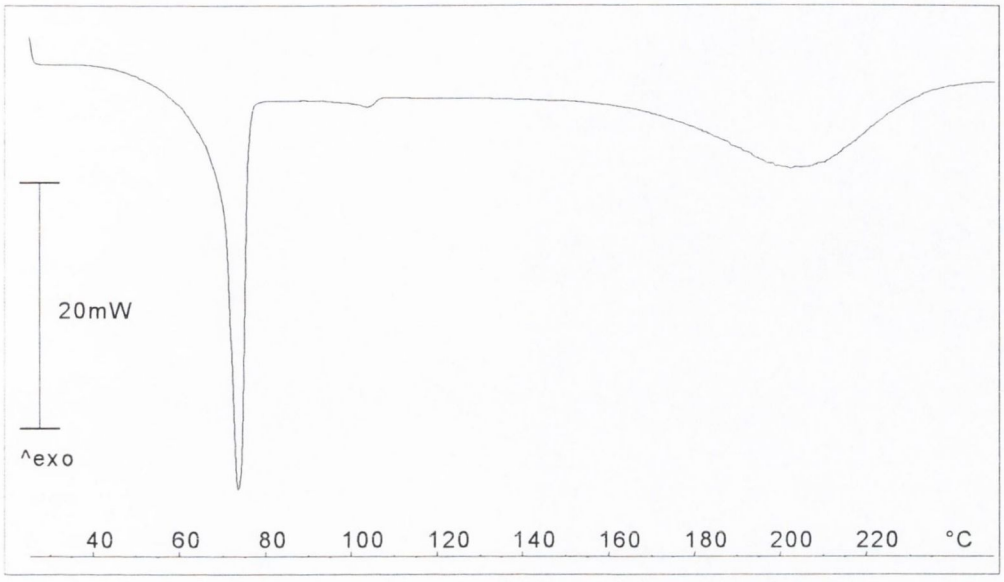

Figure 4. 8 DSC scan (10°C/min) of B.N.II recrystallised from water

DSC analysis of the hydrate carried out at a slower heating rate (2°C/min, Figure 4. 9) showed two overlapping endotherms over a temperature range corresponding to the large endotherm generated when a sample was scanned at 10°C/min (Figure 4. 8). At the slower heating rate, an initial, broader endotherm was followed by an overlapping sharp endotherm. This indicated the occurrence of two events, thought to be melting of the hydrate and loss of water of crystallisation. Subsequently, the trace showed the suggestion of a broad exotherm from ~80°C which could be attributed to recrystallisation of the anhydrate form from the melt. This was followed by an endotherm at ~100°C consistent with melting of the anhydrate. Examination of a sample of the hydrate under the hot stage microscope (heating rate ~2°C/min) confirmed melting of the solid at ~55°C, recrystallisation at ~80°C and subsequent melting of the recrystallised form.

The TG scan of the recrystallised product showed an increase in the rate of weight loss over the temperature range 35 – 70°C, as observed for B.N.II (Figure 4. 6). The inflexion in the trace for the recrystallised product corresponded to a weight loss of 4.03 ± 0.07 %w/w (n = 3).

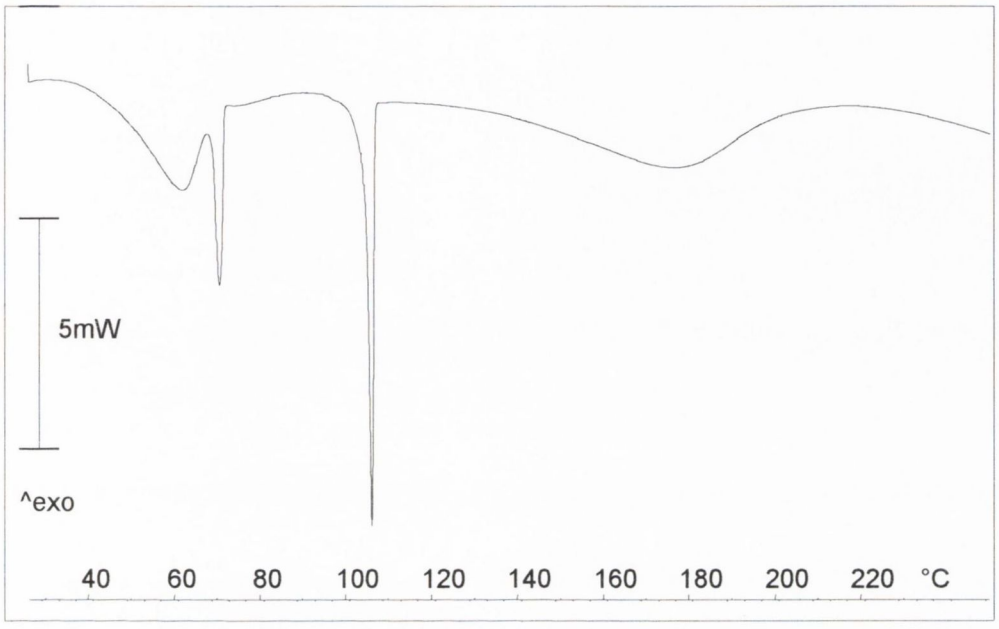

Figure 4. 9 DSC scan (2°C/min) of B.N.II recrystallised from water

4.3.3. Karl Fischer titration and elemental analysis

The recrystallised product was found, by Karl Fischer titration, to contain 4.48 ± 0.24 %w/w water (n = 3). This value corresponded to a water:drug ratio of 1:0.93. The theoretical water content of the monohydrate form of DHEP is 4.20 %w/w. The elemental analysis results for the product recrystallised from water are presented in Table 4. 3. These results conformed to the theoretical results for a possible monohydrate form of DHEP.

Table 4. 3 Elemental analysis results for B.N.II recrystallised from water

Element	*B.N.II recrystallised from water (%)*	*Theoretical values for DHEP monohydrate (%)*
C	56.04	55.94
H	6.12	6.12
N	6.36	6.53

4.3.4. FT-IR Spectroscopy

The FT-IR spectra for DHEP anhydrate, the product recrystallised from water and DHEP dihydrate are presented in Figures 2 – 4, Appendix II. When compared to the FT-IR spectrum for DHEP-A (Figure 2), broader bands of absorption were observed for the recrystallised product (Figure 3) and the dihydrate form (Figure 4) between 3600 cm^{-1} and 3100 cm^{-1}. This was consistent with the presence of water of crystallisation which generates medium intensity stretching vibrations within this frequency range (Socrates, 1994). The band of absorption in this range was slightly broader for the dihydrate form than for the recrystallised product, which was consistent with the greater number of water molecules in the dihydrate form.

4.3.5. Summary

The monohydrate form of DHEP (DHEP-MH), detected in varying quantities in commercial batches of DHEP, was prepared and characterised. The XRD pattern of the new form is presented in Figure 4. 7. Differential scanning calorimetry at 2°C/min (Figure 4. 9) revealed melting of the monohydrate with elimination of water of crystallisation, followed by recrystallisation of the anhydrate form from the melt. This thermal behaviour was characteristic of a *Type 2* pseudopolymorph according to the classification system of Giron (1995) (Section 2.5.2.1).

4.4. A STUDY OF THE SOLUBILITY AND DISSOLUTION OF DHEP MONOHYDRATE

As outlined in Section 2.4, the inclusion of a water molecule into the crystal lattice of DHEP would be expected to influence the intermolecular interactions (affecting the internal energy and enthalpy) and the crystalline disorder (entropy) and will therefore influence the free energy, thermodynamic activity, solubility, dissolution rate, stability and bioavailability (Khankari and Grant, 1995). The hydrated form of a drug is generally less soluble in water than the corresponding anhydrate due to the loss of free energy that occurs during the hydration process (Khankari and Grant, 1995). Therefore, the presence of a DHEP-MH in certain batches of DHEP may have been responsible for the precipitation observed from solutions in water.

Ledwidge (1997) examined the thermodynamic relationship between anhydrous DHEP and its dihydrate form. In our examination of the properties of DHEP, the thermodynamic relationship between the anhydrate, monohydrate and dihydrate forms of the drug was investigated.

4.4.1. Intrinsic dissolution rate study of DHEP monohydrate

An estimation of the solubility ratio between the two forms, DHEP-A and DHEP-MH, was determined using an intrinsic dissolution rate (IDR) study. Assuming the values for the diffusion layer thickness in aqueous solution for the anhydrate and monohydrate are equivalent, that the diffusion coefficients are equal and that sink conditions apply, the difference in intrinsic dissolution rate is explained by differences in saturation solubility of the drug. The relationship between IDR values and solubility is given by Equation 4.1 (Khankari and Grant, 1995):

$$\frac{\mathrm{IDR}_{\mathrm{anhydrate}}}{\mathrm{IDR}_{\mathrm{hydrate}}} = \frac{C_{\mathrm{S\,anhydrate}}}{C_{\mathrm{S\,hydrate}}} \qquad \textbf{Equation 4. 1}$$

where C_S denotes the saturation solubility.

The dissolution rate of DHEP-MH was determined in water at 25°C and compared with the dissolution rates obtained by Ledwidge (1997), under the same conditions, for DHEP-A and DHEP-DH. The dissolution profiles for the three forms are presented in Figure 4. 10.

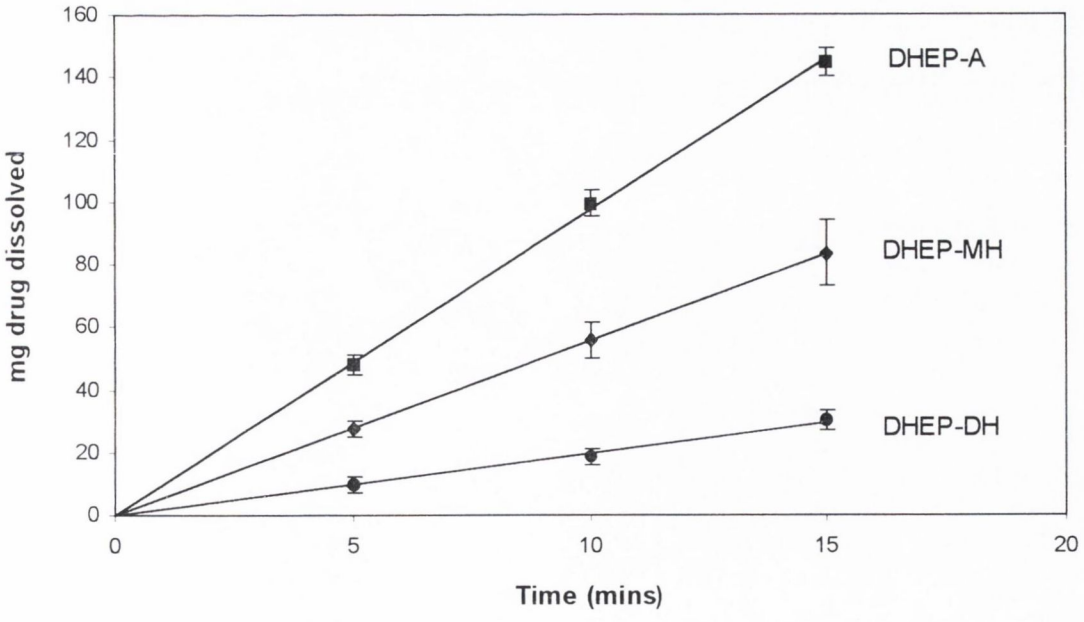

Figure 4. 10 Dissolution profiles for DHEP-A (Ledwidge, 1997), DHEP-MH and DHEP-DH (Ledwidge, 1997) in water at 25°C

The IDR value obtained for DHEP-MH at 25°C, as derived from the initial linear portion (0 – 15 min) of the dissolution plot, was 4.19 ± 0.15 mg/min/cm^2. This value lies between the intrinsic dissolution rates of the anhydrate and dihydrate forms of DHEP, 7.31 mg/min/cm^2 and 1.49 mg/min/cm^2, respectively (Ledwidge, 1997). From these intrinsic dissolution rate values, the monohydrate was estimated to be approximately 1.7 times less soluble than the anhydrate and 2.8 times more soluble than the dihydrate.

4.4.2. The thermodynamic relationship between DHEP-A, DHEP-MH and DHEP-DH

As discussed in Section 2.5.2.4, each crystalline form of a compound will have a characteristic heat of solution (Giron, 1995). The heat of solution (ΔH_{soln}) value gives information about the solution process, the relative effects of temperature on solubility and the heat of hydration (ΔH_h) between related solid forms. The ΔH_h value for a particular drug may be calculated from the ΔH_{soln} values for the hydrate and anhydrate forms, Equation 2.6 (Giron, 1995).

The integral heat of solution (ΔH_{soln}) for the monohydrate form of DHEP was determined, using the method described in Section 3.2.14, as 26.9 ± 0.6 kJ/mol. Ledwidge (1997) reported values of 22.6 ± 1.0 kJ/mol and 34.0 ± 0.6 kJ/mol for the heats of solution of DHEP-A and DHEP-DH, respectively. The enthalpy change for the hydration of DHEP-A to the monohydrate form (ΔH_h), calculated from Equation 2.6, is –4.3 kJ/mol. At constant temperature and pressure the free energy of hydration, ΔG_h, for DHEP may be calculated from the ratios of the solubilities of the hydrous and anhydrous forms according to Equation 4. 2 (Shefter and Higuchi, 1963):

$$\Delta G_h = RT \ln \left(\frac{C_{S\,\text{hydrate}}}{C_{S\,\text{anhydrate}}} \right) \qquad \textbf{Equation 4. 2}$$

Substituting the ratio of the intrinsic dissolution rates instead of that of the solubilities (Equation 4.1) yields the following equation:

$$\Delta G_h = RT \ln \left(\frac{\text{IDR}_{\text{hydrate}}}{\text{IDR}_{\text{anhydrate}}} \right) \qquad \textbf{Equation 4. 3}$$

The free energy lost on crystal dissolution and further interaction with water is less for the hydrate than for the anhydrate. This occurs because the hydrate has already interacted intimately with the water (Khankari and Grant, 1995) and means that, with respect to an aqueous environment, the hydration process is accompanied by a free energy decrease. The ΔG_h value at 25°C, calculated from Equation 4.3, is –1.38 kJ/mol. The entropy change (ΔS_h) that accompanies the conversion of DHEP-A to its monohydrate can be calculated from Equation 4.4 (Shefter and Higuchi, 1963):

$$\Delta S_h = \left(\frac{\Delta H_h - \Delta G_h}{T} \right) \qquad \textbf{Equation 4. 4}$$

The ΔS_h value calculated is –9.80 J/mol/K. Dunitz (1994) states that the entropic cost of transferring a water molecule from liquid water into the crystalline structure of biomolecules can range from 0 to ~29 J/mol/K per molecule of water. The upper limit will only apply to molecules of water that are firmly bound within the crystalline structure. The relatively low value calculated for the conversion of DHEP to its monohydrate form suggests that the water of crystallisation present in the molecule is loosely bound.

4.5. CHARACTERISATION OF A COMMERCIAL SAMPLE OF DDEA

As outlined in Section 4.1.2, only one form of DDEA, with a melting point of 157-159°C, has previously been reported (Fini et al., 1995a). DDEA is listed as the active in a commercially available aqueous gel formulation, Voltarol® Emulgel® (Data Sheet, Geigy Pharmaceuticals). The salt is reported by Fini et al. (1995a) to have a solubility in water (25°C) of 4.1 mg/ml, or 11.1 mM.

A commercial sample of DDEA was obtained, which was prepared from organic solvents. This sample was characterised by elemental analysis, FT-IR spectroscopy, X-ray diffraction and thermal analysis.

Since the FT-IR spectrum and XRD and DSC scans for DDEA have not previously been published, it was necessary to compare the information obtained with that obtained for the parent compound, diclofenac acid (DCFA). The FT-IR spectrum and XRD trace for diclofenac acid are presented in Figure 1, Appendix II and in Figure 4. 11, respectively. The XRD trace is identical to that obtained by Gubbins (1996). The DSC scan is presented in Figure 4. 12. The onset value of the endotherm was determined as 179°C. The melting point of diclofenac is reported in the literature as 156-

158°C (*Merck Index*, 1996) or 171.5°C (Maitani et al., 1993a). Gubbins (1996) obtained a similar DSC scan to that displayed in Figure 4. 12, i.e. a single endotherm with an onset value of 177°C.

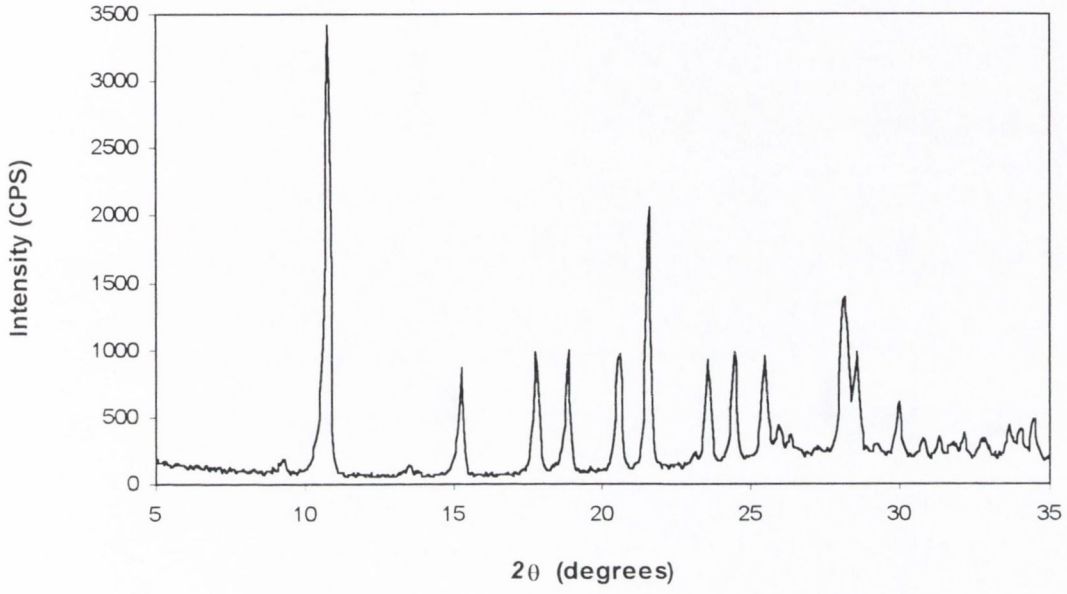

Figure 4. 11 XRD trace for diclofenac acid

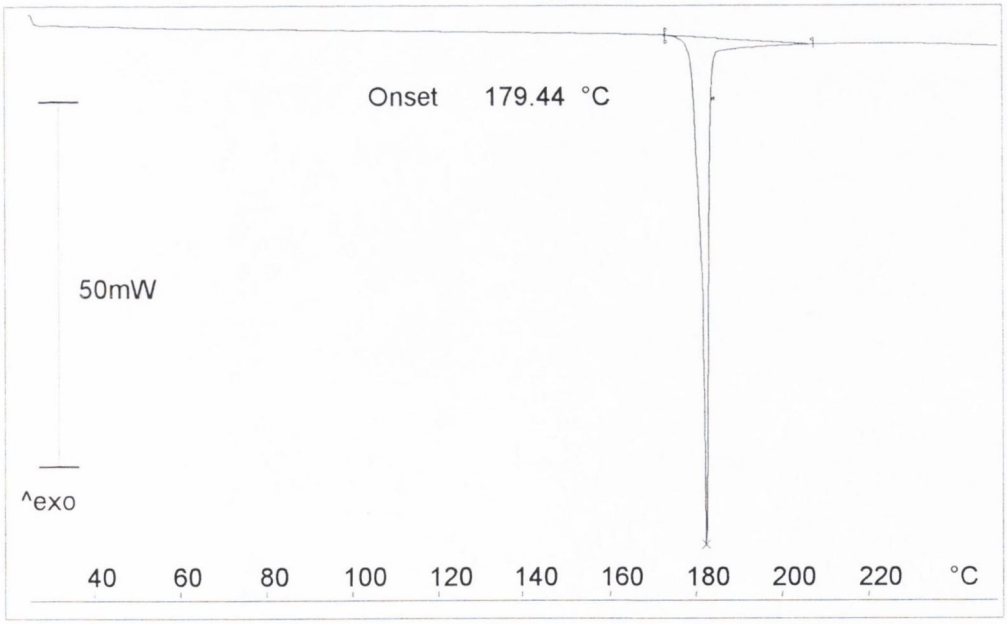

Figure 4. 12 DSC scan for diclofenac acid

4.5.1. Elemental analysis

The results of the elemental analysis of the commercial DDEA sample are listed in Table 4. 4. The results complied with the theoretical values for diclofenac diethylamine.

Table 4. 4 Elemental analysis results for the commercial DDEA sample

Element	*DDEA* *Theoretical %*	*Commercial DDEA* *Actual %*
C	58.5	58.4
H	6.0	6.1
N	7.6	7.6

4.5.2. FT-IR spectroscopy

The FT-IR spectrum for the commercial sample of DDEA (Figure 5, Appendix II) was consistent with that of a salt of diclofenac acid and diethylamine.

4.5.3. Powder X-ray diffraction analysis

The XRD trace for the commercial DDEA sample is presented in Figure 4. 13. DDEA was shown to be strongly crystalline in nature. The positions of the main diffraction peaks in the range $2\theta = 5 - 20°$ were $2\theta = 8.20°$, 12.80°, 15.25° and 17.95°.

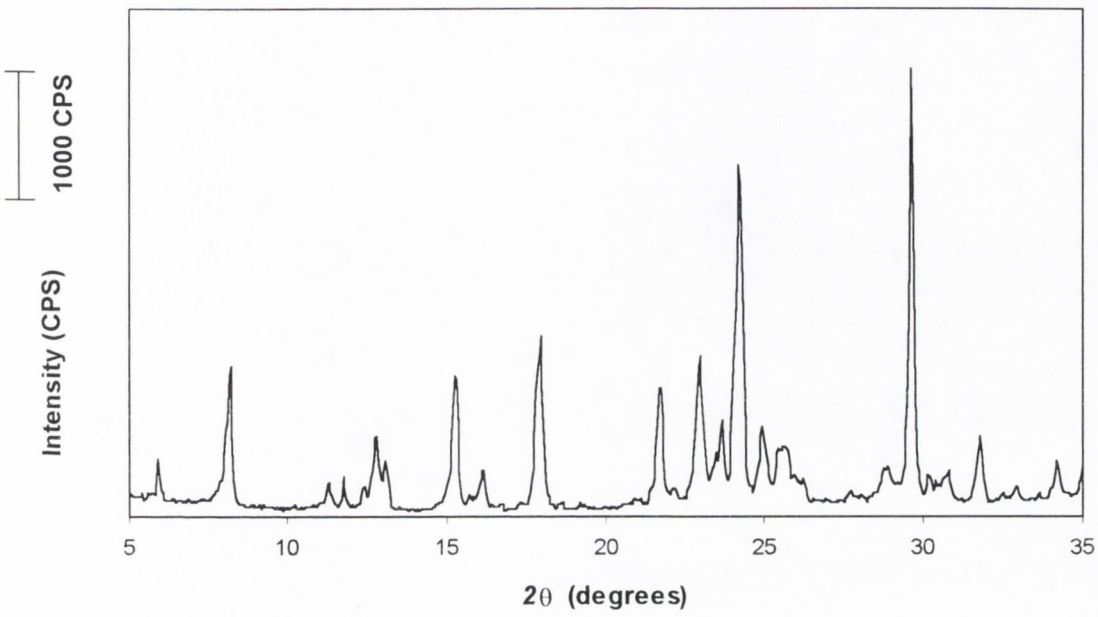

Figure 4. 13 XRD trace for the commercial sample of DDEA

4.5.4. Thermal analysis

The DSC and TG scans for the commercial DDEA sample are presented in Figure 4. 14. The DSC scan revealed two overlapping endotherms with onset temperatures of 125°C and ~135°C, lower than the reported melting point of 157-159°C (Fini et al., 1995a). The broad endotherm from ~160°C, similar to that observed in DHEP-A scans (Section 4.2.2), could be attributed to the volatility of the molten drug and / or decomposition. The TG scan showed an increase in the rate of weight loss at ~130°C, corresponding to the second of the two overlapping endotherms in the DSC scan. The sharp increase in the rate of weight loss above ~200°C corresponded to the broad peak in the DSC scan, attributed to the volatile nature of the melt and / or the occurrence of decomposition.

The sample was examined by thermal microscopy. Prior to heating, the sample was present as prismatic crystals displaying birefringence. The events observed on heating are listed in Table 4. 5. The recrystallisation from the melt of a different crystal form and subsequent re-melting explained the presence of two endothermic peaks in the open pan DSC scan (Figure 4. 14).

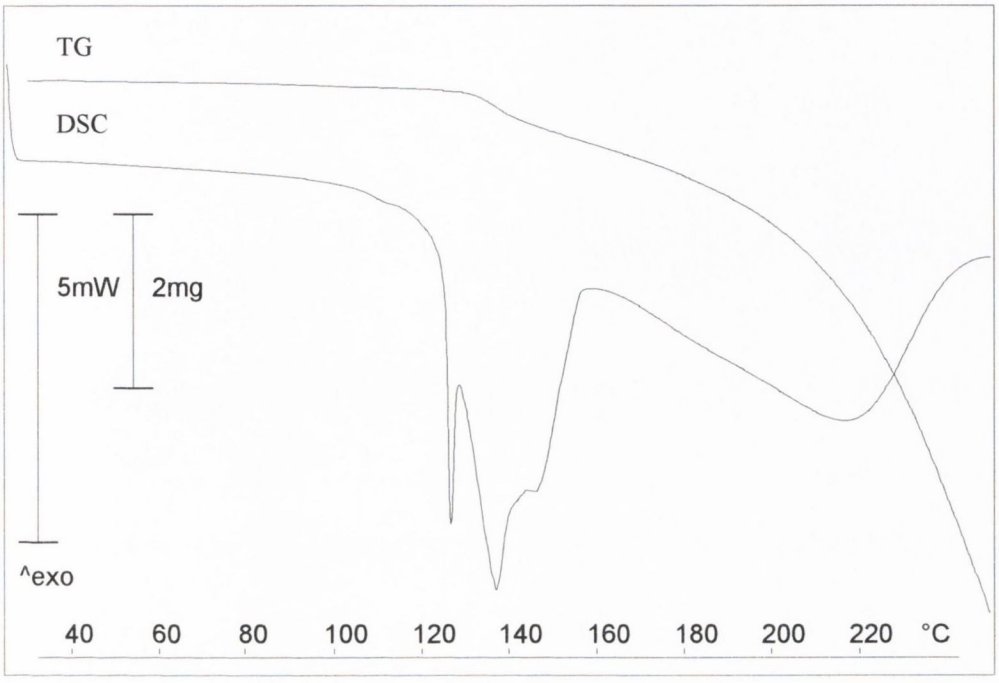

Figure 4. 14 DSC and TG scans for the commercial sample of DDEA

Table 4. 5 Thermal microscopy of the commercial sample of DDEA

Temperature range	*Thermal events observed*
115 – 130°C	melting
130 – 140°C	recrystallisation into acicular crystals displaying birefringence
145 – 160°C	melting

To investigate the nature of the thermal events, a sample was heated to 128°C (past the first endotherm), allowed to cool, then re-heated to 250°C (Figure 4. 15). An exotherm, thought to be due to recrystallisation of the lower melting crystal form, was observed on the cooling run. The trace obtained on re-heating was similar to that of the original sample (Figure 4. 14). An XRD trace obtained after heating a sample to 128°C and cooling to room temperature was identical to that of the original sample.

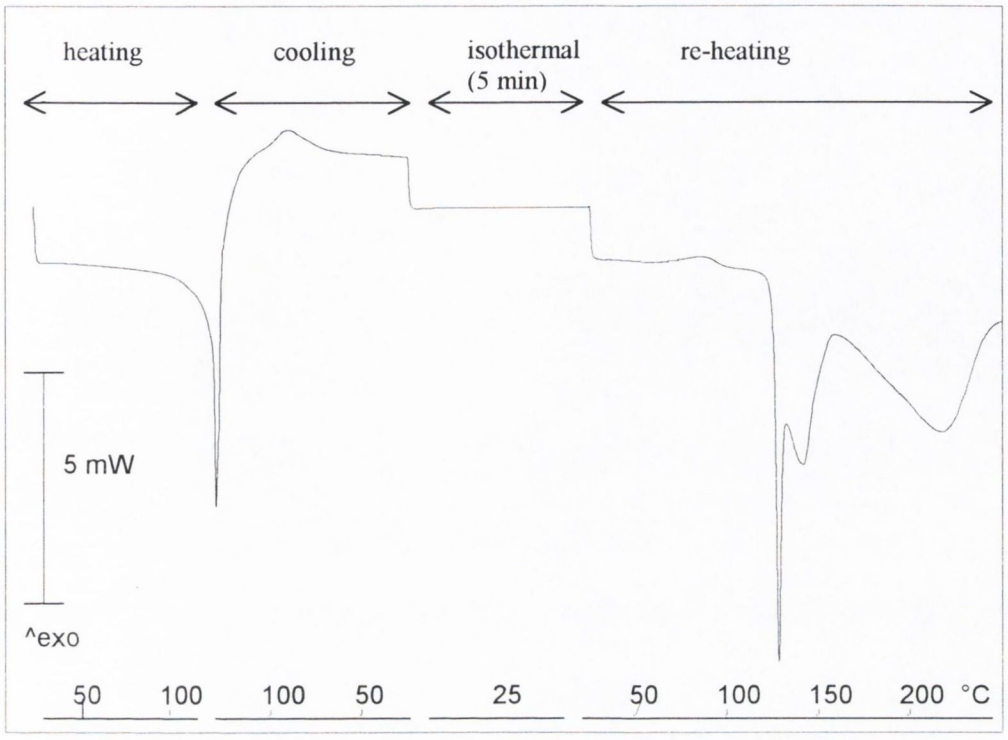

Figure 4. 15 DSC scan obtained when the commercial sample of DDEA is heated to 128°C, cooled to 25°C and re-heated to 250°C

A *Type 2* polymorphic transition was identified for DDEA, according to the classification of Giron (1995). After melting of the crystal form with the lower melting point, crystals of another polymorphic form grow from the melt. This new crystal form then melts, giving rise to a second endothermic peak. The absence of any recrystallisation exotherm in the DSC scan of DDEA may be due to the onset of melting of the higher melting form, resulting in overlap between the two endotherms and masking of any exothermic event.

4.6. PREPARATION OF DDEA FROM ACETONE

A sample of DDEA was prepared by precipitation from acetone (DDEA-A). This product was shown by XRD to be identical to the commercial sample of DDEA (Figure 4. 16). Results from thermal analysis and elemental analysis were also consistent with the results obtained for the commercial sample of DDEA (Section 4.5).

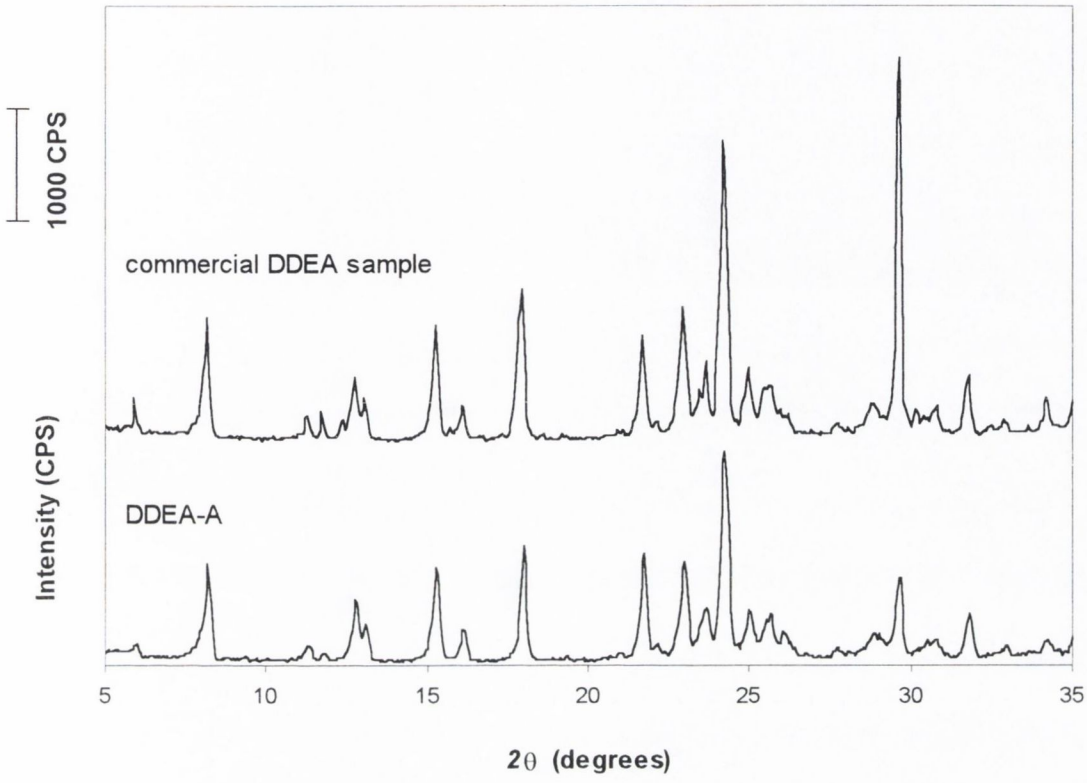

Figure 4. 16 XRD traces of the commercial sample of DDEA and DDEA-A

4.7. IDENTIFICATION AND CHARACTERISATION OF A NOVEL FORM OF DDEA

A new form of diclofenac diethylamine (DDEA-X) was isolated in two ways: (a) preparation of DDEA in water, or (b) recrystallisation following slow evaporation at room temperature of a saturated solution of DDEA in water. This new form of the salt, not previously identified, was prepared and characterised by powder X-ray diffraction, thermal analysis, Karl Fischer titration and elemental analysis. Its properties were compared with those of DDEA prepared from acetone (DDEA-A).

4.7.1. Powder X-ray diffraction analysis

The XRD traces for DDEA-A and for DDEA-X are presented in Figure 4. 17.

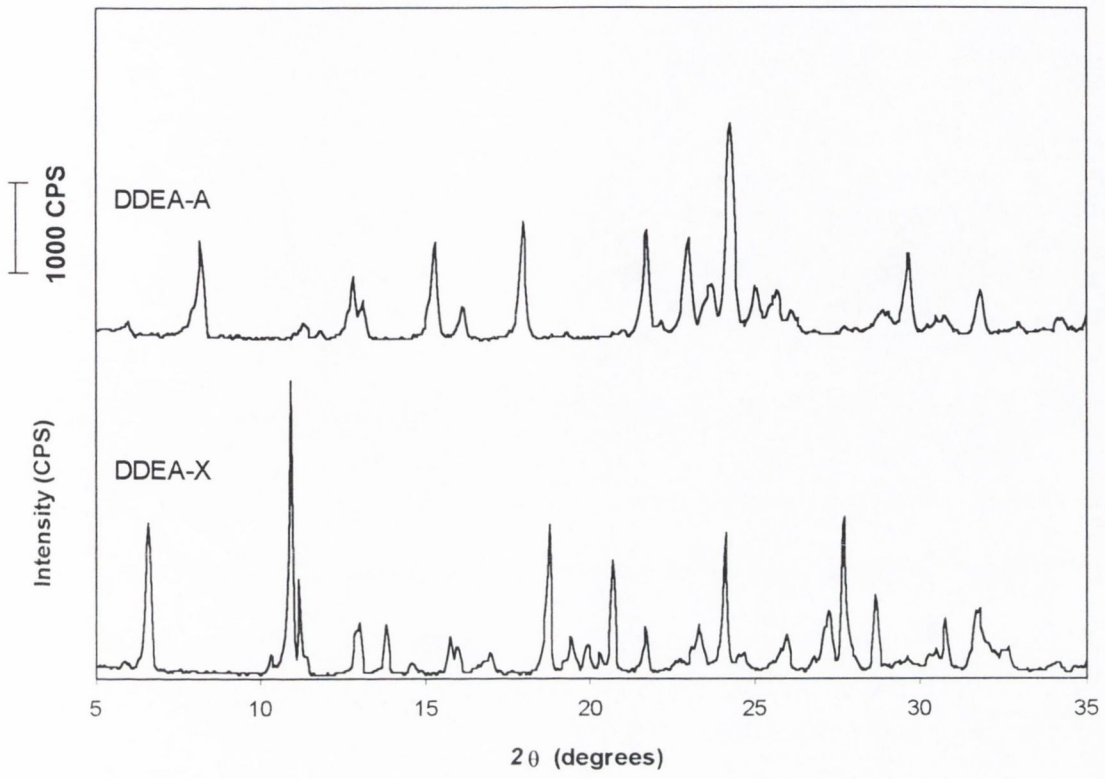

Figure 4. 17 XRD traces for DDEA-A and DDEA-X

The XRD patterns differed significantly from each other. The positions of the main diffraction peaks in the 2θ range 5 – 20° for DDEA-A and DDEA-X were 2θ = 8.20°, 12.80°, 15.25° and 17.95° and 2θ = 6.50°, 10.85°, 12.85°, 13.70°, 15.90° and 18.60°, respectively.

4.7.2. Thermal analysis

The open pan DSC scan for DDEA-X is presented in Figure 4. 18. In addition to the overlapping peaks (onset, ~120°C) which are characteristic of DDEA-A (Figure 4. 14), an additional endotherm was observed (onset, ~54°C).

In order to determine if this lower temperature thermal event was reversible, a sample of DDEA-X was held at 100°C for 30 minutes and allowed to cool to room temperature. An open pan DSC was carried out immediately and again after the sample was left at room temperature overnight. The endotherm of onset temperature ~54°C was absent from the resultant scans, resulting in scans characteristic of DDEA-A. XRD analysis of the sample after cooling to room temperature confirmed that the sample had converted to DDEA-A.

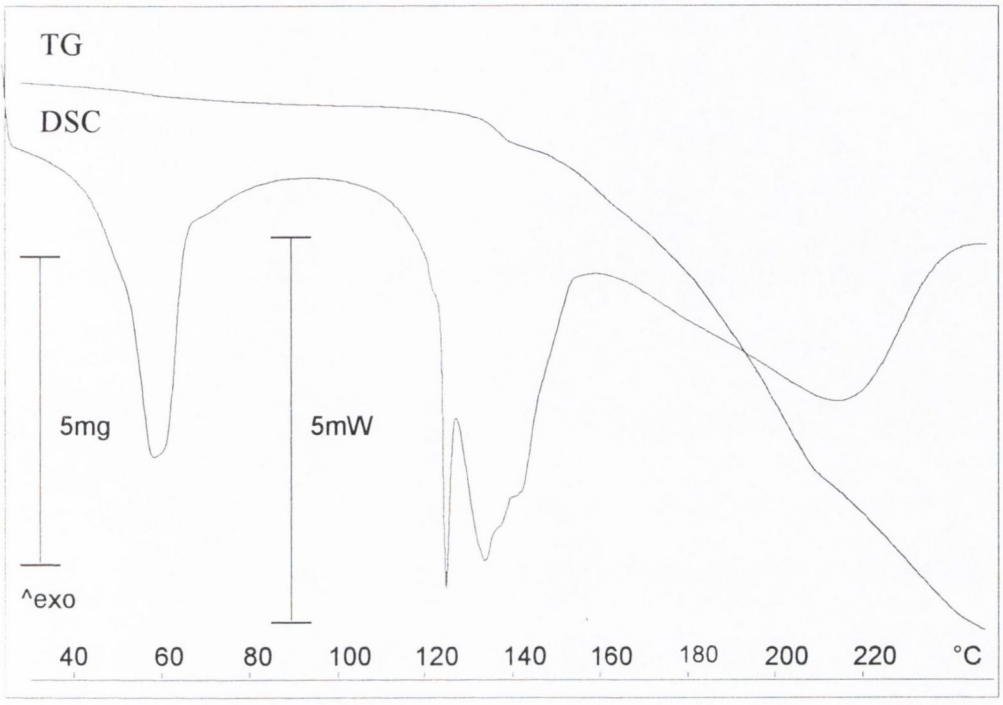

Figure 4. 18 DSC and TG scans for DDEA-X

The TG trace for DDEA-X (2.0°C/min) is presented in Figure 4. 18. As with the TG scan for DDEA-A (Figure 4. 14), an inflexion in the trace occurred at ~150°C, corresponding to an increase in the rate of weight loss. However, in contrast to DDEA-A, a weight loss of 4.32 ± 0.17 %w/w occurred for the DDEA-X samples (n = 3) over the temperature range corresponding to the first endotherm in the DSC scan.

A sample of DDEA-X mounted in air was examined under the hot stage microscope. The events observed corresponded to those events observed on heating a sample of DDEA-A (Figure 4. 14). However, the evolution of vapour on heating above ~50°C, suggested by the weight loss displayed in the TG trace, was confirmed by observation of a sample mounted in silicone oil.

4.7.3. Karl Fischer titration and elemental analysis

Karl Fischer titrations were carried out in triplicate on two batches of DDEA-X. A water content of 4.63 ± 0.16 %w/w was determined. The differences between the XRD traces for DDEA-A and DDEA-X indicated that the water present in DDEA-X consisted of water of crystallisation. The

value of 4.63 %w/w for the water content of DDEA-X represents a water:drug ratio of 1:1, suggesting that the new form identified is a monohydrate.

Elemental analysis was carried out on three batches of DDEA-X. The results obtained (expressed as the mean ± SD) compared well with those values expected for the monohydrate form of diclofenac diethylamine (Table 4. 6).

Table 4. 6 Elemental analysis results for DDEA-X batches

Element	*DDEA-X batches (n = 3) %*	*Theoretical values for DDEA monohydrate %*
C	56.00 ± 0.12	55.81
H	6.12 ± 0.05	6.26
N	7.16 ± 0.01	7.23

4.7.4. FT-IR spectroscopy

The FT-IR spectrum for DDEA-X is presented in Figure 6, Appendix II. A broadening of the absorption band between 3600 cm^{-1} and 3100 cm^{-1} was observed for DDEA-X relative to anhydrous DDEA (Figure 5, Appendix II). This was consistent with the presence of water of crystallisation which generates medium intensity stretching vibrations within this frequency range (Socrates, 1994).

4.7.5. Conclusion

The new form of DDEA isolated in this study (DDEA-X) was identified as a monohydrate form of DDEA. This monohydrate form (DDEA-MH), not previously reported, was characterised by XRD, thermal analysis and FT-IR. The additional endotherm (onset, ~54°C) in the scan for the monohydrate, and corresponding weight loss in the TG scan, was consistent with the evolution of water of crystallisation. The monohydrate converts to the anhydrate form, which then generates the endotherm characteristic of DDEA-A (onset, ~122°C). This behaviour is characteristic of a *Type 1* pseudopolymorph according to the classification of Giron (1995) (Section 2.5.2.1).

4.8. A STUDY OF THE SOLUBILITY AND DISSOLUTION OF DDEA: ANHYDRATE AND MONOHYDRATE FORMS

The monohydrate form of DDEA (DDEA-MH) was identified and characterised in Section 4.7. As described in Section 4.4, the inclusion of a water molecule into the crystal lattice of a compound will alter the thermodynamic activity of the solid, resulting in changes in properties such as solubility and dissolution rate.

In our examination of the properties of DDEA, the thermodynamic relationship between the anhydrate and monohydrate forms of the drug was investigated.

4.8.1. Solubility study of DDEA-A

A dynamic solubility study was carried out on DDEA-A at 25°C, using the paddle solubility method (Section 3.2.12.2). The solubility profile is plotted in Figure 4. 19. The solubility was observed to decrease from an initial value of ~40 – 45 mM to achieve equilibrium solubility at a value of 33.3 mM (12.3 mg/ml). It was thought that during the dissolution of the anhydrate, the solution became saturated with respect to the hydrated form (Khankari and Grant, 1995), which precipitated out of solution until the concentration reached the solubility of the monohydrate crystal form, 33.3 mM. The solid phase recovered by filtration of the saturated solution used in the solubility study (after 48 hours) was examined by XRD and was found to consist of DDEA-MH. This value of 33.3 mM was notably higher than the value of 4.1 mg/ml (11.1 mM) previously reported for the solubility of DDEA in water at 25°C (Fini et al., 1995a). The lower solubility value reported by Fini et al. (1995a) was consistent with the higher melting point of the salt form identified in their study. A salt form with a melting point of 157-9°C, the value quoted by Fini et al., was not isolated in the current study. The value obtained for the solubility of DDEA (33.3 mM) was closer in value to the reported solubility of DDEA at 20°C (35 mM, Kriwet and Müller-Goymann, 1993).

An equilibrium solubility study of DDEA-A and DDEA-MH was carried out at 25°C, using the ampoule solubility method (Section 3.2.12.1). The solubility of DDEA-A was determined as 34.96 ± 0.65 mM, which was consistent with the result obtained from the dynamic solubility study. As observed in the dynamic solubility study, the solid phase in equilibrium with the solution was shown by XRD to consist of DDEA-MH, indicating that the less soluble monohydrate precipitated from solution. The result from an equilibrium solubility study carried out using DDEA-MH as the

starting material was consistent with the value obtained for the equilibrium solubility of the anhydrate form (32.77 ± 1.15 mM after 24 hours).

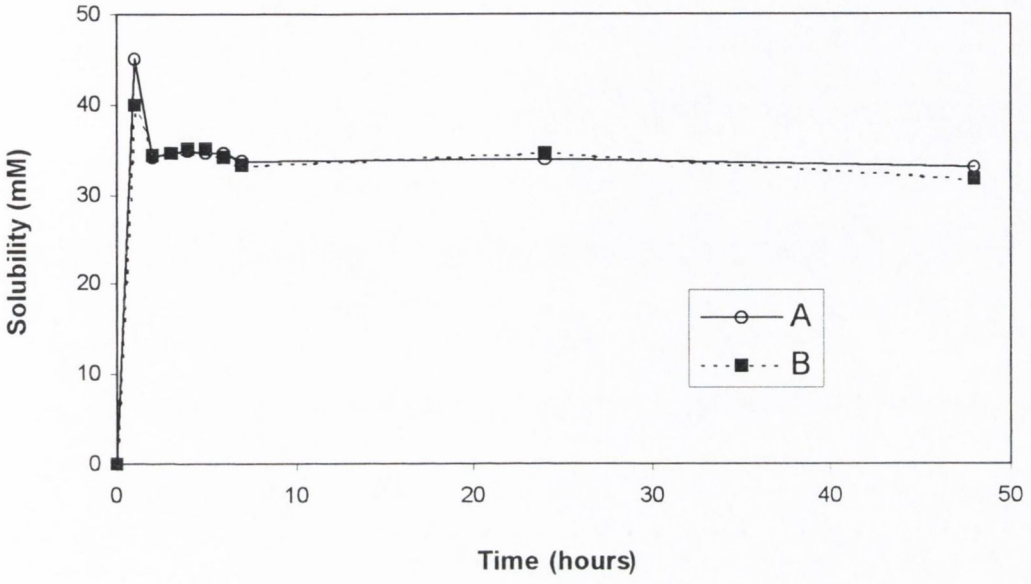

Figure 4. 19 Dynamic solubility study of DDEA-A at 25°C (duplicate runs, A and B)

4.8.2. Intrinsic dissolution rate study of DDEA anhydrate and DDEA monohydrate

An estimation of the solubility ratio between the two forms, DDEA-A and DDEA-MH, was determined using an intrinsic dissolution rate (IDR) study.

The IDR values in water at 25°C, as derived from the initial linear portion (0 – 15 min) of the dissolution plot (Figure 4. 20), were 1.15 ± 0.02 mg/min/cm^2 and 0.69 ± 0.01 mg/min/cm^2 for the anhydrate and monohydrate forms of DDEA, respectively. This indicates that the anhydrate is approximately 1.7 times more soluble than the monohydrate.

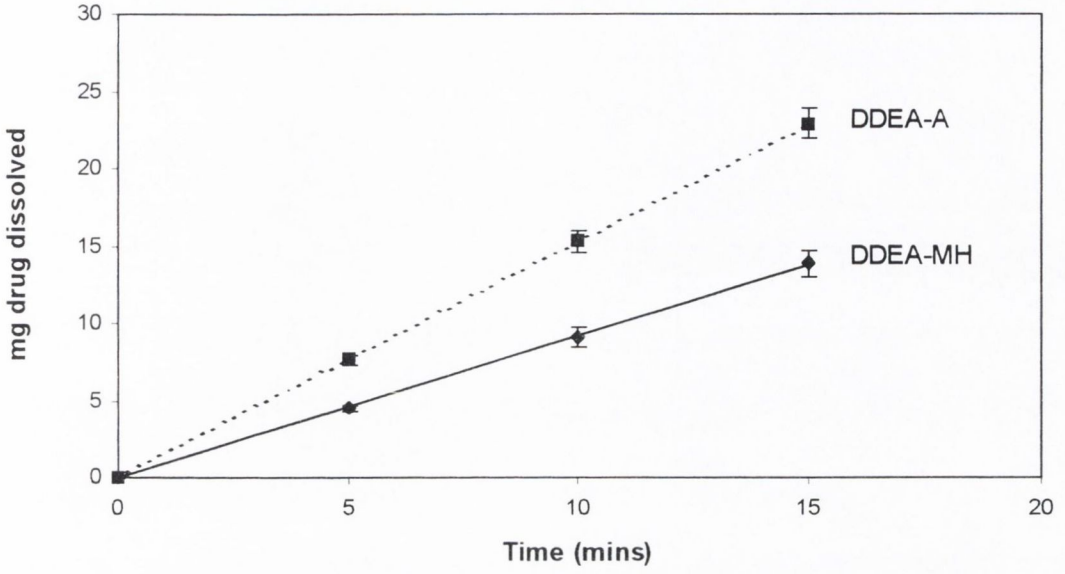

Figure 4. 20 Linear portions of the dissolution plots for DDEA-A and DDEA-MH, used to derive the intrinsic dissolution rates

4.8.3. The thermodynamic relationship between the anhydrate and monohydrate forms of DDEA

The integral heats of solution (ΔH_{soln}) for the anhydrate and monohydrate forms of DDEA were determined, using the method described in Section 3.2.14, as 26.3 ± 0.2 kJ/mol and 28.8 ± 0.6 kJ/mol, respectively. The ΔH_h value for DDEA monohydrate, calculated from Equation 2.6, is -2.57 kJ/mol. The ΔG_h value at 25°C, calculated using the intrinsic dissolution rates for the two forms (Equation 4.3) is –1.27 kJ/mol. Using the ΔH_h and ΔG_h values, the entropy of hydration value (ΔS_h) was calculated as –4.37 J/mol/K. The relatively low value calculated for the conversion of DDEA to its monohydrate form suggests that the water of crystallisation present in the molecule is loosely bound (Dunitz, 1994).

Chapter 5

Comparison of the sodium, *N*-(2-hydroxyethyl)pyrrolidine and diethylamine salts of diclofenac

5.1. INTRODUCTION

In addition to the *N*-(2-hydroxyethyl)pyrrolidine and diethylamine salts of diclofenac (characterised in Chapter 4), diclofenac sodium is another salt of diclofenac contained in pharmaceutical products (Voltarol® tablets).

A recent study by Ledwidge and Corrigan (1998) on pharmaceutically relevant properties of diclofenac *N*-(2-hydroxyethyl)pyrrolidine (DHEP) and diclofenac sodium (DNa) included investigation of the pH-solubility behaviour and the surface activity of the salts. In the current study, diclofenac diethylamine (DDEA) was compared with DHEP and DNa in terms of its pH-solubility behaviour and its tendency to self-associate in solution. In addition, a study was carried out on the transport of the three salts across a porous membrane.

5.2. pH-SOLUBILITY STUDY OF DICLOFENAC DIETHYLAMINE

A supersaturated solution is defined as a solution that contains more of the dissolved solute than it would normally contain at a given temperature (Martin, 1993). Several studies have involved the investigation of the pH-solubility profiles of drug-salt systems and reported the existence of significant areas of supersaturation and deviation from the theoretical profiles at the pH_{max} (Roseman and Yalkowsky, 1973; Bogardus and Blackwood, 1979; Serajuddin and Rosoff, 1984; Serajuddin and Jarowski, 1985a and 1985b; Serajuddin and Mufson, 1985; Serajuddin and Jarowski, 1993; Shah and Maniar, 1993).

The pH-solubility profile for DHEP showed supersaturation at the pH_{max}, with an increase in the solubility of diclofenac acid on addition of *N*-(2-hydroxyethyl)pyrrolidine to above 800 mM at pH 8.06 (Ledwidge and Corrigan, 1998). The *apparent supersaturation* was defined as the solubility achieved at the pH_{max} relative to a saturated solution. According to this definition the level of supersaturation observed in the DHEP system was greater than 3. However, supersaturation began significantly below the pH_{max} and the actual supersaturation achieved, relative to the theoretical profile, was greater than 18. On the other hand, the pH-solubility profile for DNa was found not to deviate appreciably from the theoretical profile in the pH_{max} region. The apparent supersaturation value determined was ~1.03 (Ledwidge and Corrigan, 1998).

In the present study, the pH-solubility profile of DDEA was investigated using the method described in Section 3.2.15. The profile is presented in Figure 5. 1.

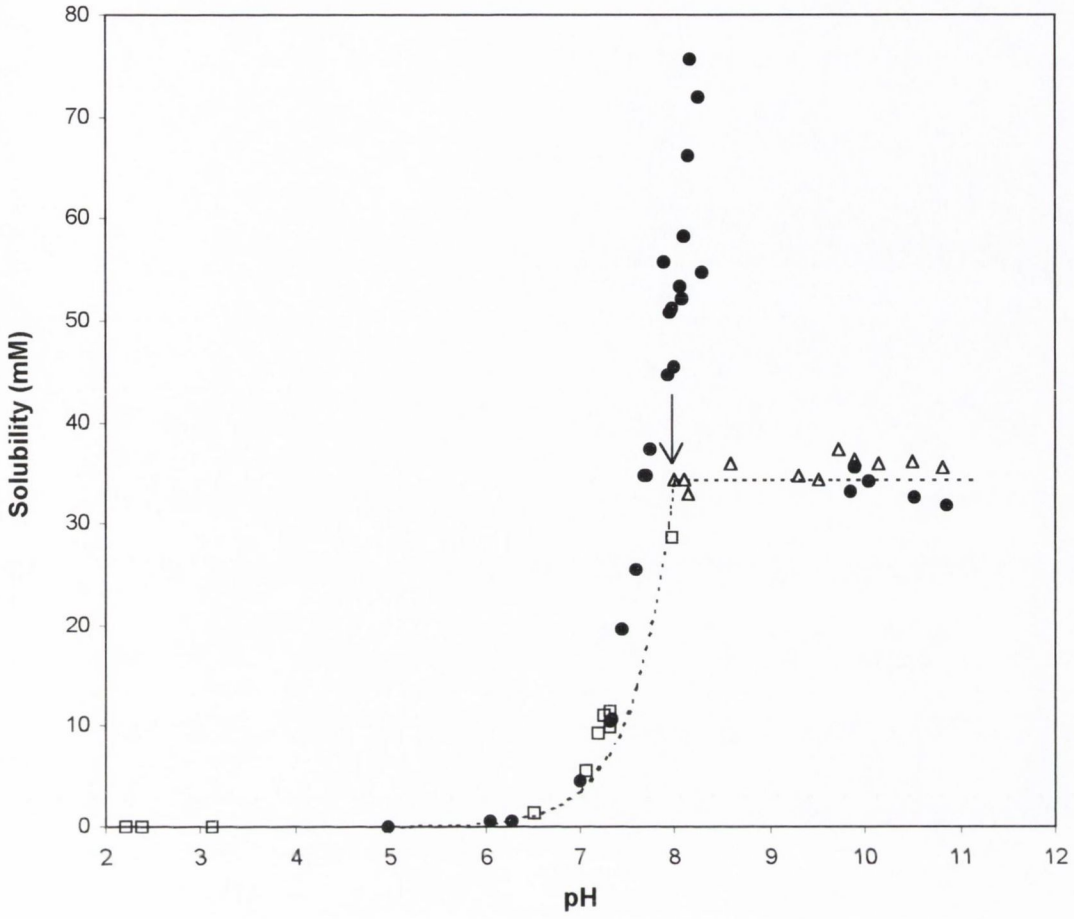

Figure 5. 1 pH-solubility profile for DDEA: addition of DEA to diclofenac acid (•), addition of HCl to DDEA (□) and addition of DEA to DDEA (Δ). The arrow indicates the data point representing a saturated solution of DDEA.

The solubility of the salt in water at 25°C was found to be 34 mM at pH 8 (indicated by the arrow in Figure 5. 1). This value was consistent with the solubility determined in the dynamic solubility study (33.3 mM, Section 4.8.1). As shown in Figure 5. 1, lowering the pH of a saturated solution of the salt with HCl resulted in a drop in the solubility and precipitation of the free acid. Addition of DEA to a saturated solution of DDEA did not cause a change in the solubility. The solubility above pH 8 remained constant at ~34 mM.

The addition of diethylamine to the solution of diclofenac acid (DCFA) caused a sharp increase in the solubility of diclofenac acid to a maximum of 76 mM at pH 8.15. As with DHEP (Ledwidge and Corrigan, 1998), a supersaturation phenomena was observed at the pH of maximum solubility. The supersaturated solution had a concentration considerably higher than the aqueous solubility of DDEA (33.3 mM). The apparent supersaturation level achieved was 2.3.

Further addition of diethylamine caused a lowering of the solubility of the solution to ~34 mM at pH ~10. The solubility remained at ~34 mM on further addition of DEA, at pH values >10. This behaviour was consistent with the solubility value of 34 mM obtained when DDEA was used as the starting material.

Estimates for pK_a' (5.02) and the intrinsic solubility of diclofenac acid ([HA], 0.037 mM) previously reported (Ledwidge and Corrigan, 1998) are used in plotting, from Equations 1.14 and 1.15 (Chowhan, 1978), the theoretical pH-solubility profile, indicated by the broken line in Figure 5. 1.

The solubility data for pH values < pH_{max} was fitted to Equation 1.14 for weak organic acids. Using 0.037 mM as the estimate of intrinsic solubility (Ledwidge and Corrigan, 1998), a value of 4.87 was obtained for the pK_a' at 25°C.

5.3. SURFACE ACTIVITY AND SELF-ASSOCIATION PROPERTIES

As described in Section 1.5, surface tension measurements can be carried out to examine the potential of a compound to self-associate (Martin, 1993). Micelle formation can be established by investigation of the ability of a compound to solubilise water-insoluble dyes (Brito and Vaz, 1986).

Diclofenac has the potential to self-associate in solution due to the amphiphilic nature of the molecule. The hydrophilic portion of the diclofenac molecule is made up of the carboxylic group, while the hydrophobic region consists of the two phenyl rings, one carrying two chlorine atoms in the ortho positions (Figure 4.1).

Previous studies demonstrated the ability of aqueous DHEP solutions to solubilise Orange OT, an azo dye, at concentrations of 35 mM and above (Fini et al., 1991a, 1991b, 1993b, 1994a, 1994b, 1994c, 1995c and 1996). Furthermore, solutions of DHEP were found to solubilise lecithins to an extent that suggested the formation of mixed micelles (Fini et al., 1993b and 1994c). Since lecithins are the main components of cell membranes, a DHEP/lecithin interaction could lead to a weakening of cell membranes, either if lecithins are removed from their places or if DHEP dissolves in the membrane lipid environment (Fini et al., 1993b). A CMC (critical micellar concentration) value of 35 mM for DHEP was confirmed by examining a series of physicochemical properties of DHEP solutions, such as surface tension, electrical conductivity and rhodamine 6G spectral shift (Fini et al., 1994a and 1994c).

Ledwidge and Corrigan (1998) evaluated the surface activity and self-association properties of the sodium and *N*-(2-hydroxyethyl)pyrrolidine salts of diclofenac. Using surface tension measurements, CAC (critical association concentration) values were determined for both salts, but only the HEP salt demonstrated solubilisation of a water insoluble compound, indicating micelle formation, at concentrations of 30 mM and greater. This result is consistent with the CMC value determined by Fini et al. (1991a) for DHEP (35 mM). The results for DNa suggested that the aggregation evident for this salt was non-micellar. Stepwise, non-micellar association, possibly involving vertical stacking of almost planar hydrophobic rings, has previously been reported for drug molecules (Attwood, 1976). Structural features of drug molecules that may promote non-micellar association include a rigid hydrophobic moiety and the presence of a hydrophilic group or atom on the hydrophobic portions of the molecules (Mukerjee, 1974; Attwood, 1982).

In the earlier reports it was proposed that the lack of micelle formation in the case of DNa was due to its low solubility (Fini et al., 1991a). However, Ledwidge and Corrigan (1998) obtained a value of 66 mM for the solubility of DNa and attributed the inability of DNa to form micelles to the effect of counterion change. This hypothesis was consistent with observations of several workers on the influence of the counterion on micellisation behaviour of salts (Mukerjee et al., 1967; Heard and Ashworth, 1968; Attwood and Florence, 1983). For example, the CMC decreases and the micellar size increases when organic counterions are used instead of inorganic ions (Mukerjee et al., 1967; Florence and Attwood, 1988).

In the current study, the surface activity and self-association properties of DDEA in solution were investigated using techniques identical to those used in the study of DHEP and DNa properties (Ledwidge and Corrigan, 1998). The results obtained were compared with those reported for the other two salts.

5.3.1. Surface tension measurements

Plots of concentration (mM) vs. surface tension (mN/m) for DDEA and DHEP solutions are presented in Figure 5. 2. In the case of DHEP, a change in the concentration dependence of surface activity was observed at 30 mM, the critical association concentration (CAC) for the salt. The concentration necessary to achieve self-association (30 mM, Ledwidge and Corrigan, 1998) is indicated in Figure 5. 2. As illustrated in the graph, solutions of DDEA with concentrations greater than this value were not investigated. This was because of the limited solubility of the salt (33mM). Consequently, the plot for DDEA did not reveal a change in the concentration dependence of surface tension, i.e. no CAC was detected. As discussed above, determination of

the CAC value of 20 mM (20°C) previously reported for DDEA (Kriwet and Müller-Goymann, 1993) involved investigation of the surface tension of supersaturated DDEA systems. In the current study, the preparation of supersaturated solutions was attempted by preparing solutions of >30 mM by heating, followed by cooling to 25°C. However, the solutions proved to be unstable on cooling and resulted in the precipitation of DDEA from solution.

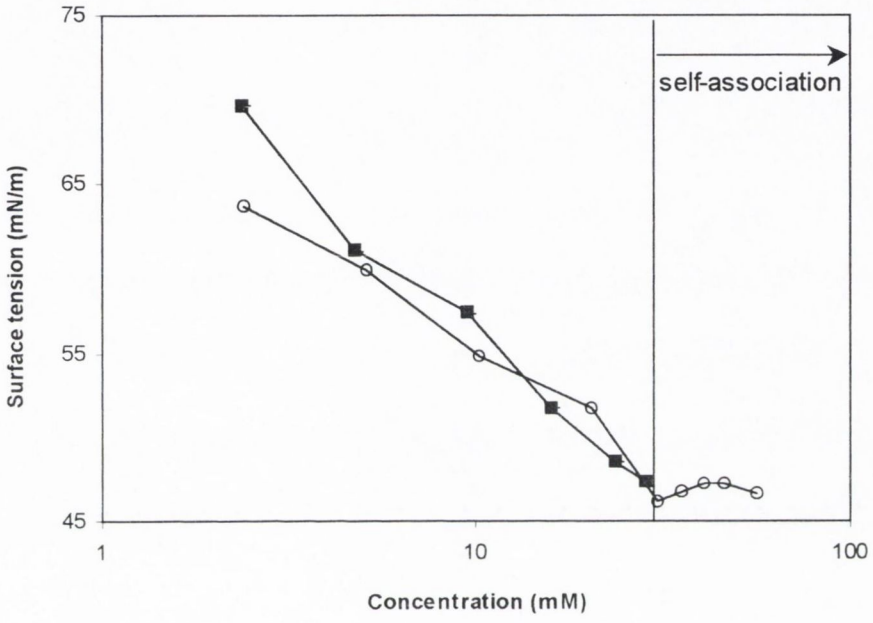

Figure 5. 2 Surface tension (mN/m) vs. concentration (mM) for DHEP (O) and DDEA (■) solutions

5.3.2. Solubilisation study

This study was carried out using the water insoluble fluorescent compound, *N*-phenyl-1-naphthylamine (NPN), as described in Section 3.2.18. The results for DDEA are presented as fluorescence intensity relative to a 40 mM DHEP solution (Figure 5. 3). Fluorescence was detected for DHEP solutions with concentrations greater than 30 mM, a value consistent with results obtained previously (Ledwidge and Corrigan, 1998). No fluorescence was observed for DDEA solutions in the concentration range examined (10 – 30 mM). This may be attributed to the solubility of DDEA (33 mM) limiting the concentrations examined to less than that necessary for micelle formation and solubilisation of NPN.

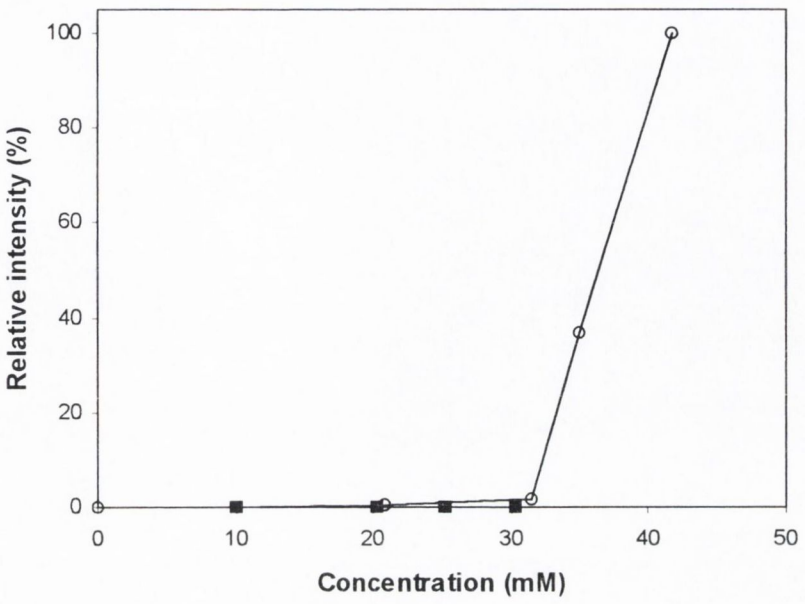

Figure 5. 3 Solubilisation study: DHEP solutions (O) and DDEA solutions(■)

Kriwet and Müller-Goymann (1993) investigated the micellar behaviour of DDEA-water systems and the transition from a micellar solution to a liquid crystalline phase via vesicle formation. A CAC value of 20 mM (20°C) was determined for the salt from the plot of surface tension versus concentration. However, whereas the solubility at 20°C was determined to be 35 mM, the surface tension measurements included solutions of DDEA with concentrations above 100 mM, i.e. supersaturated solutions. Kriwet and Müller-Goymann (1993) reported that, whereas viscosity measurements at 45°C indicated the presence of spherical micelles, a concentration-dependent increase in viscosity was observed at room temperature, indicating the formation of vesicles and lyotropic liquid crystals. Their results from transmission electron microscopy indicated that vesicles occurred only at temperatures below 32°C, the transition temperature from liquid crystals to an isotropic micellar solution. Further investigations by transmission electron microscopy showed that the region of existence of a micellar solution of DDEA at room temperature was small. A vesicle dispersion was shown to exist at a concentration as low as 2%. This was attributed to the bulky nature of the hydrophobic region of the diclofenac molecule, resulting in prevention of the packing of the hydrophobic groups into close structures such as micelles. The transition from vesicles into micelles was thought to be possible at higher temperatures due to greater flexibility of the molecule. Depending on the concentration of DDEA, the liquid crystalline phase was found to exist as a dispersion of small vesicles or large lamellar particles.

Kriwet and Müller-Goymann (1993) concluded that the liquid crystalline nature of DDEA solutions indicated a tendency for the salt to interact with the liquid crystalline structures of topical preparations and with those in living tissues, such as biomembranes. Subsequent studies demonstrated the ability of DDEA to interact with phospholipids (Kriwet and Müller-Goymann, 1994 and 1995). Molecules of DDEA were thought to align themselves with the appropriate regions of phospholipid molecules (polar and nonpolar regions), thereby participating in the microstructure of the systems (Kriwet and Müller-Goymann, 1994). In a recent study, the aqueous solubility of DDEA in the presence of pharmaceutical additives was studied (Khalil et al., 2000). Electrolytes at low concentrations exhibited a salting-in effect on DDEA, which was attributed to the association of DDEA into micelles. Addition of electrolyte causes a reduction in the thickness of the ionic atmosphere surrounding polar head groups and a consequent reduced repulsion between them, resulting in more efficient micelle formation (Attwood and Florence, 1983).

The apparent inability of DDEA to form micelles at concentrations between 10 mM and 30 mM (Figure 5. 3) can be interpreted in terms of the results obtained by Kriwet and Müller-Goymann (1993). In the previous study, viscosity measurements at 20°C of DDEA solutions in the concentration range ~30 mM to ~540 mM (supersaturated solutions) demonstrated a concentration-dependent increase in viscosity, suggesting the formation of vesicles and lyotropic liquid crystals. The authors reported that at concentrations as low as ~54 mM (2%), DDEA solutions were found by transmission electron microscopy to consist of vesicle dispersions. It was concluded that at room temperature (20°C) the concentration range at which micellar solutions of DDEA occur is limited, i.e. they occur at concentrations less than 54 mM. The results of the current study suggest that micelles were not formed in the concentration range 10 – 30 mM.

5.4. DISCUSSION

It has been proposed that self-association may be responsible for supersaturation at the pH_{max} of drug-salt systems (Roseman and Yalkowsky, 1973; Bogardus and Blackwood, 1979; Serajuddin and Rosoff, 1984; Serajuddin and Jarowski, 1985a and 1985b; Serajuddin and Mufson, 1985; Dahlan et al., 1987). Several studies have used apparent solubility product (K'_{SP}) values taken from pH-solubility data to demonstrate drug self-association in drug solutions (Bogardus and Blackwood, 1979; Serajuddin and Jarowski, 1985a; Serajuddin and Mufson, 1985; Ledwidge and Corrigan, 1998). Increasing K'_{SP} values as drug concentrations increased were explained by a lowering of the drug activity coefficient due to the possible formation of self-association complexes (Serajuddin and Mufson, 1985).

Apparent solubility product calculations for the DDEA system were carried out according to the method of Serajuddin and Mufson (1985). The solubility product, K_{SP}, of a saturated DDEA solution is expressed as:

$$K_{SP} = [DCFA^-]_S [DEA^+] \qquad \textbf{Equation 5. 1}$$

where [$DCFA^-$] and [DEA^+] are the concentrations of the diclofenac anion and protonated diethylamine, respectively, and the subscript s indicates saturation. S_T is the total solubility and is equivalent to the sum of $[DCFA^-]_S$ and the concentration of the unionised form of diclofenac acid, [DCFA]. Since [DCFA] is very low compared to $[DCFA^-]_S$, S_T is assumed equal to $[DCFA^-]_S$ and the apparent solubility product, K'_{SP}, is calculated from:

$$K'_{SP} = S_T [DEA^+] \qquad \textbf{Equation 5. 2}$$

A study was carried out by Ledwidge and Corrigan (1998) on the pH-solubility profiles of five drug-salt systems, including DNa and DHEP. The surface active characteristics of the salts were investigated and a general relationship between supersaturation at the pH_{max} and self-association of the salts was observed. The $\Delta a_{meta.het}$ value is the required activity for the formation of primary heterogenous nuclei. The presence of primary nuclei result in crystal growth and precipitation of the final solid phase from solution. It was proposed that self-association of the drug in the region of the pH_{max} reduces the activity coefficient of the drug as concentrations increase, thereby maintaining the solution activity below $\Delta a_{meta.het}$ and retarding nucleation.

The pH-solubility data, obtained on addition of DEA to saturated solutions of DCFA, is presented in Table 5. 1. An increase in the solubility product was observed within the pH range 7.93 – 8.15, i.e. around the pH_{max}, where supersaturation occurred. The elevated K'_{SP} values suggested a lowering of the activity coefficient due to self-association. This was consistent with the report that self-association occurred in the case of supersaturated DDEA solutions (Kriwet and Müller-Goymann, 1993).

Table 5. 1 K'_{SP} estimates from pH-solubility data for DDEA

pH	S_T (M)	$[DEA^+]$ (M)	K'_{SP}
7.68	3.48×10^{-2}	3.48×10^{-2}	1.21×10^{-3}
7.74	3.74×10^{-2}	3.74×10^{-2}	1.40×10^{-3}
7.93	4.46×10^{-2}	4.46×10^{-2}	1.99×10^{-3}
8.06	5.33×10^{-2}	5.33×10^{-2}	2.84×10^{-3}
8.13	6.62×10^{-2}	6.62×10^{-2}	4.38×10^{-3}
8.15	7.56×10^{-2}	7.56×10^{-2}	5.72×10^{-3}
9.84	3.32×10^{-2}	3.32×10^{-2}	1.10×10^{-3}
10.04	3.42×10^{-2}	3.44×10^{-2}	1.18×10^{-3}

Above and below this pH range, where the solubility lies between 33 and 37 mM, the solubility product values were found to remain relatively constant at $\sim 1.2 \times 10^{-3}$. Accordingly, surface tension measurements and solubilisation experiments (Section 5.3) did not detect self-association for DDEA solutions with concentrations of 30 mM and lower.

5.5. MEMBRANE TRANSPORT

The solubility of a drug represents the maximum concentration of drug available for transport across a membrane and therefore will influence the highest attainable transport rate of a drug through a membrane. Differences in solubilities between the diclofenac salts should be reflected in their maximum transport rates across a porous membrane.

5.5.1. Membrane transport of saturated and unsaturated solutions

The membrane transport of DNa, DHEP and DDEA was investigated using the diffusion cell technique described in Section 3.2.16. The porous membrane used, Visking®, has been used in a number of dialysis studies (Craig et al., 1962 and 1964), in the study of membrane transport of drug substances (Osborne, 1990; Rodríguez Bayon et al., 1993; Carr et al., 1997) and in the determination of diffusion coefficients (Tsuji et al., 1978). Previous studies have reported

Visking® to have a dry thickness of 20 μm (Bannon, 1989) and an average pore size of 2.4 nm (Corrigan et al., 1980).

5.5.1.1. Diclofenac sodium

The membrane transport of DNa solutions with concentrations in the range 12.8 – 61.4 mM was investigated. The 61.4 mM solution consisted of a saturated solution of DNa with excess undissolved solid present in the flask. The rate of mass transport (mmol/hr) was plotted against concentration (mM) in Figure 5. 4. A linear relationship was observed; the slope of the line of best fit, plotted through the origin, was calculated as 0.7800 $x10^{-3}$ mmol/hr.mM (R^2 = 0.9877).

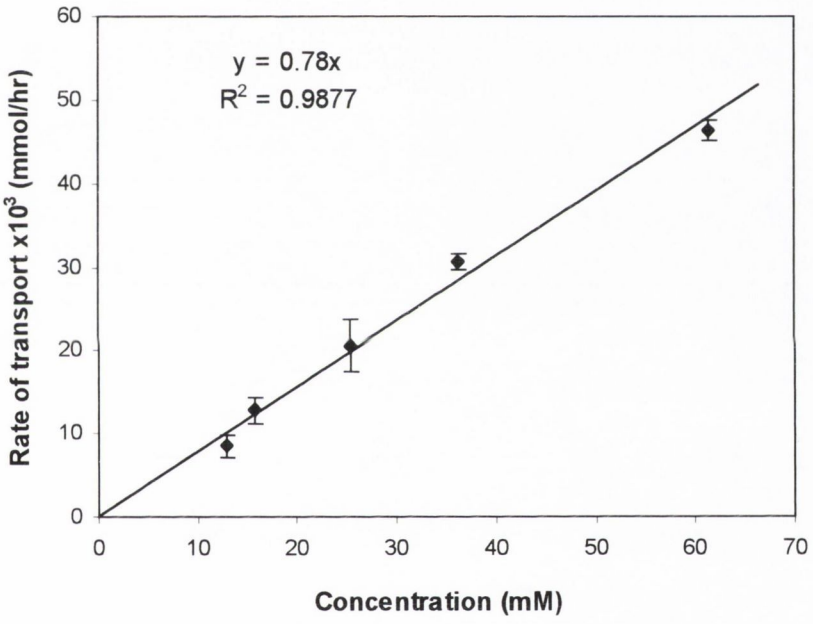

Figure 5. 4 Concentration (mM) vs. rate of transport (mmol/hr) for DNa solutions (n = 3)

5.5.1.2. Diclofenac N-(2-Hydroxyethyl)pyrrolidine

An unsaturated solution of DHEP (59.3 mM) was transported at a rate of 0.0325 ± 0.0006 mmol/hr. When plotted in Figure 5. 5, this value is found to lie below the trendline generated for DNa solutions, i.e. the rate of transport of the unsaturated solution of DHEP is found to be less than that expected for a DNa solution of equivalent concentration.

The membrane transport of saturated solutions of DHEP was investigated. A quantity of DHEP equivalent to twice its aqueous solubility (273 mM, Ledwidge, 1997) was added to deionised water and stirred at room temperature for 24 hours to allow equilibration of the solution. The solution

was filtered at room temperature and its concentration determined. It was then allowed to equilibrate to 25°C before being placed in the diffusion apparatus. This procedure was carried out in duplicate; the concentrations of the filtered solutions obtained were 239.4 mM and 254.5 mM. The variation between the concentrations of the saturated solutions was attributed to the instability of the saturated systems. Ledwidge (1997) showed that the precipitation of aqueous solutions of DHEP with time could be attributed to the salt precipitating out in the dihydrate form. The transport rates for the saturated solutions of DHEP were found to lie below the extrapolated trendline for DNa solutions (Figure 5. 5).

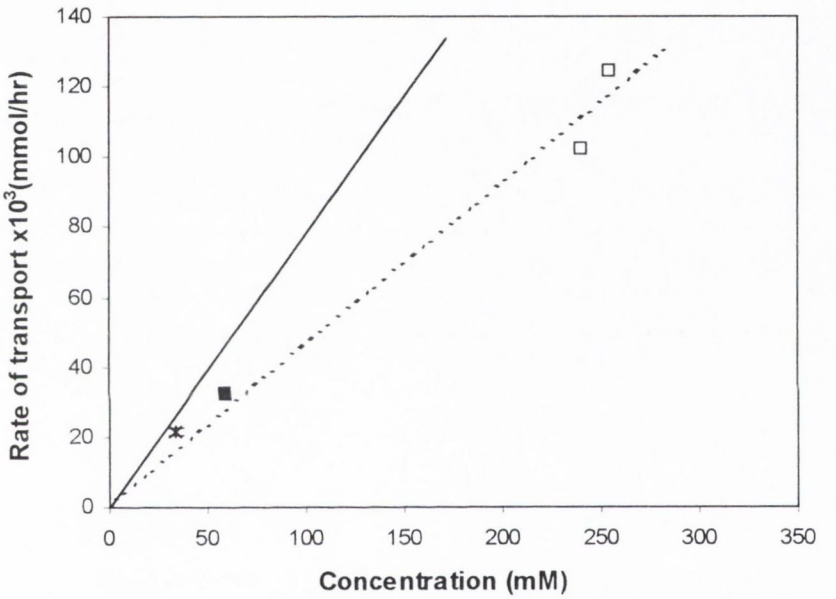

Figure 5. 5 Membrane transport of diclofenac salts: saturated DDEA solution (*), unsaturated DHEP solution (■), saturated DHEP solutions (□), trendline for DNa solutions (—) and trendline for DHEP solutions (---)

A trendline was established for the DHEP systems (dotted line, Figure 5. 5). The slope of the line, 0.4636 x10^{-3} mmol/hr.mM (R^2 = 0.9688), is lower than that generated from the DNa solutions.

5.5.1.3. Diclofenac diethylamine

The membrane transport of a saturated solution of DDEA with excess solid present in the system was investigated. A quantity of DDEA equivalent to twice the aqueous solubility (33 mM, Section 4.8.1) was added to deionised water and allowed to equilibrate at 25°C for 24 hours. The concentration was determined after 24 hours to ensure that the solution had reached equilibrium.

DDEA from the saturated solution was transported across the membrane at a rate of 0.0218 ± 0.0012 mmol/hr. By plotting this rate of transport in Figure 5. 5, it was found that the rate of transport for the DDEA solution was less than that expected for a DNa solution of equivalent concentration.

5.5.2. Maximum transport rates for diclofenac salts

The saturation solubility of DDEA, ~33 mM, is substantially lower than that of DNa, ~61 mM. Accordingly, the maximum rate of transport observed for DDEA solutions was lower than that observed for DNa solutions, as illustrated in Figure 5. 6.

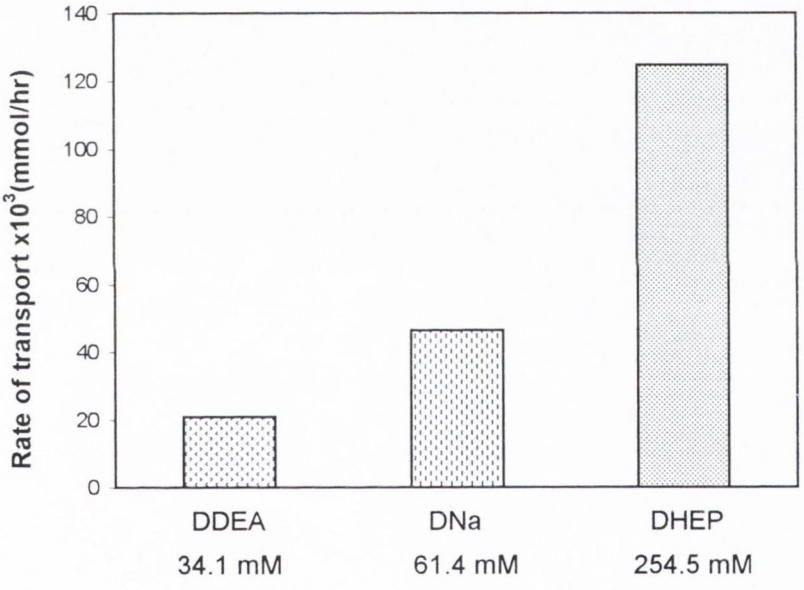

Figure 5. 6 Maximum transport rates obtained for diclofenac salts (saturated solutions)

On comparison of the rates of transport for DNa and DHEP solutions, it was noted (Figure 5. 5) that the improvement in the transport rate with the *N*-(2-hydroxyethyl)pyrrolidine salt is less than anticipated, given its superior aqueous solubility (254 mM vs. 61 mM). However, the maximum transport rate obtained for DHEP, 0.1248 mmol/hr, is almost six times higher than that obtained for DDEA, 0.0218 mmol/hr (Figure 5. 6).

5.5.3. *Effective permeability coefficients for diclofenac salts*

Transport of drug molecules through a porous polymeric membrane may occur by diffusion through the solvent-filled pores or through the polymer matrix (Martin, 1993). Accordingly, the effective permeability coefficient (P_e) for transport across a porous membrane is dependent on the aqueous permeability coefficient, P_{aq}, and the membrane permeability coefficient, P_m (Equation 1.20). The P_e value for each salt is represented by the slope of the trendline for the salt solutions in Figure 5. 5.

Using computational molecular modelling (Section 3.2.19), the volume of the diclofenac acid molecule in water was estimated to be 298.55 $Å^3$. This volume corresponds to a sphere of radius ~0.415 nm, a value consistent with previous estimates for the diclofenac anion: 0.422 nm (Lee et al., 1987), 0.473 nm (Fini et al., 1999) and 0.427 nm (Maitani et al., 1993b). Given the reported pore size for Visking® of 2.4 nm (Corrigan et al., 1980), the diclofenac anion would be considered sufficiently small for transport through the pores of the membrane.

Furthermore, previous studies have demonstrated the ability of diclofenac salts to diffuse through polymeric matrices (Lee et al., 1987; Maitani et al., 1994; Kriwet and Müller-Goymann, 1995). Maitani et al. (1994) reported that the diffusion coefficients of diclofenac salts through a silicone membrane (nonporous) were higher than that of diclofenac acid and attributed this to the permeation of diclofenac salts as ion pairs. High *n*-octanol/water partition coefficient (log P) values determined for diclofenac salts were attributed to the ability of diclofenac salts to form ion pairs in nonaqueous solution (Fini et al., 1993a, 1994b and 1999). Fini et al. (1993a) dissolved DHEP in a number of different solvents at constant concentration and observed a decrease in the electrical conductance with decreasing dielectric constant of the solvent, which they attributed to increasing ion pair association. The formation of ion pairs in the case of DNa was also studied by conductance measurements (Lee et al., 1987). Analysis of the crystal structure of the salts between diclofenac and hydroxyl bases in the solid state revealed the presence of a complex network of hydrogen bonds between the anion and cation which is thought to favour ion pair formation (Castellari and Sabatino, 1994). For those salts the structure of the ion pair may be similar to that present in the solid state, with hydrogen bonding between the hydroxyl group of the organic base and the carboxylic group of the diclofenac anion. However, Visking®, the membrane used in the current study, is a porous, non-lipid type membrane in which molecular diffusion in aqueous pores is the principal mechanism (Ho et al., 1980). The non-lipid nature of the membrane would suggest that permeation of ion pairs through the membrane did not contribute significantly to drug transport through the membrane.

Increasing counterion size may impede diffusion. The Stokes-Einstein equation describes an inverse relationship between the diffusivity of a compound and the cube root of its molar volume (Flynn et al., 1974). Ho et al. (1980) reported that the aqueous pore permeability of a cellulose membrane decreased with increasing solute size. In the case of the diclofenac salts, the volumes in water of the organic counterions were determined by computational molecular modelling (Section 3.2.19). The volume of the sodium ion was calculated from its reported ionic radius (Fini et al., 1999). A trend of decreasing effective permeability coefficient with increasing counterion volume was observed for the three salts examined (Table 5. 2).

Table 5. 2 Estimated counterion volumes and observed permeability coefficients for the diclofenac salts

Salt	*Counterion volume* $Å^3$	*Effective permeability coefficient mmol/hr.mM*
DNa	3.59	0.7800×10^{-3}
DDEA	116.05	0.6393×10^{-3}
DHEP	153.72	0.4636×10^{-3}

Self-association of a drug is another factor that may hinder diffusion. CAC values have been determined for DNa (Ledwidge and Corrigan, 1998) and DHEP (Section 5.3). The solubility of DDEA limited the concentrations examined to less than those necessary to achieve self-association. DHEP was shown to solubilise NPN (Section 5.3.2), whereas no solubilisation was detected for DNa (Ledwidge and Corrigan, 1998) or DDEA (Section 5.3.2) solutions. The lowest P_e value for transport across Visking® was observed for DHEP, the salt showing the greatest potential to self-associate and form micelles.

Chapter 6

Preparation and characterisation of a range of diclofenac salts

6.1. INTRODUCTION

It is evident from data obtained for DHEP and DDEA (Chapters 4 and 5) that substantial differences in biopharmaceutically relevant physicochemical properties exist between different diclofenac salts. Furthermore, for each salt form there exists a range of pseudopolymorphs / polymorphs. Despite a large number of studies to date, the salts have not yet been completely characterised and substantial differences in physicochemical properties for apparently similar salt forms have been reported. Therefore, in order to advance our understanding of diclofenac salts, a range of salts was examined.

Ideally, it would be useful to be able to predict salt properties from the properties of the counterion used. Several studies have described the dependence of salt properties on the nature of the counterion used (Section 2.2.3). In addition, studies have been carried out to investigate quantitative relationships between counterion characteristics and properties of the resulting salt form.

Ledwidge (1997) prepared a range of salts of a basic drug, CEL50, and determined the salt solubilities in water at 25°C. Examination of the data for salts of counter-acids with good aqueous solubility (>1 in 20) revealed good correlation ($R^2 = 0.91$, n = 7) between log salt solubility and salt melting point. Poor correlation was observed between the counter-acid melting point and salt solubility and between counter-acid pK_a and salt solubility. The relationship between final solution hydrogen ion concentration and salt solubility was found to be in accordance with pH-solubility theory; a linear relationship ($R^2 = 0.99$, n = 7) was observed for salts of the more soluble counter-acids. Two of the salts prepared, CEL50 glycolate and CEL50 adipate, had similar melting points and final solution pH values. However, there was a large difference in the aqueous solubilities of the respective counter-acids (>1 in 10 and 1 in 69 for glycolic acid and adipic acid, respectively) which may explain the difference between the aqueous solubilities of the salts. The lower solubility of adipic acid relative to glycolic acid may be attributed to the lower hydrophilicity of adipic acid due to its four-carbon alkyl chain.

Rubino (1989) determined the solubilities in water of a number of sodium salts of weakly acidic drugs. Multivariate analysis of the data indicated that the logarithms of the molar solubilities were inversely related to both the salt melting points and the stoichiometric amounts of water in the crystal hydrates. The following equation ($R^2 = 0.93$, n = 11) was derived:

$$\log C = -0.004\,\text{m.p.} - 0.100\,N + 1.691 \qquad \textbf{Equation 6. 1}$$

where C is the molar solubility, m.p. is the melting point (°C) and N is the stoichiometric number of water molecules in the crystal lattice.

A study by Anderson and Conradi (1985) investigated predictive relationships between counterion characteristics and salt solubility for a series of ammonium salts of flurbiprofen. A multiple linear regression analysis was carried out to investigate potential relationships between the log K_{SP} of six amine salts and their melting points and cation hydrophilicities. The solubility product values were found to be highly correlated with the melting points of the salts, illustrating the importance of crystal lattice forces. Higher melting points and lower K_{SP} values were observed for the more symmetric counterions. There was not significant correlation with the counterion hydrophilicity, as estimated from octanol-water partition coefficient fragment constants. The apparent lack of strong dependence of solubility on ammonium counterion hydrophilicity was illustrated by comparing a series of salts that vary in the number of hydroxyl groups. The order of hydrophilicity within this series was tris(hydroxymethyl)aminomethane (TRIS) > 2-amino-2-methyl-1,3-propanediol (AMPD) > 2-amino-2-methylpropanol (AMP) > *tert*-butylamine (tBA), whereas the rank order of salt solubilities was AMPD > TRIS ≅ AMP > tBA. The TRIS salt was not the most soluble among the tertiary amine salts despite having the most hydrophilic cation. This was attributed to the symmetry of the counterion, resulting in stronger crystalline forces and a higher melting point (Anderson and Flora, 1996).

Examination by Gould (1986) of the data published by Agharkar et al. (1976) on a series of salts of a basic antimalarial drug revealed a linear relationship between solubility (log scale) and the inverse of the melting point ($R^2 = 0.9325$, n = 4). Gould (1986) also reported strong correlation between conjugate acid melting point and salt melting point for a series of salts of an experimental drug candidate (UK47880) with a pK_a of 8 ($R^2 = 0.9385$, n = 7). Salts prepared from planar, high melting aromatic sulphonic or hydroxycarboxylic acids resulted in crystalline salts with high melting points, whereas flexible aliphatic strong acids yielded oils. Gould concluded that the comparative planar symmetry of the conjugate acid appears important for the maintenance of high crystal lattice forces. Alternatively, a strong hydrogen bonding potential of the conjugate acid or base should result in higher crystal lattice forces of the salt.

Thomas and Rubino (1996) reported an inverse linear relationship between log solubility and melting point for a series of hydrochloride salts of secondary amines. However, a study comparing the tris(hydroxymethyl)aminomethane salts of four anti-inflammatory agents with the sodium salts and the free acids reported the absence of a simple relationship between salt solubility and melting point (Gu and Strickley, 1987).

The aim of this study is to investigate the influence of salt formation on the physicochemical characteristics of the parent compound. Relationships between properties of a salt-forming agent and those of the resulting salt form, useful in the prediction of salt properties, were investigated.

6.1.1. Bases selected for the preparation of salts with diclofenac

Six basic organic compounds were selected for salt formation with diclofenac; these are listed, with the abbreviations used, in Table 6. 1.

Table 6. 1 Bases selected for the preparation of diclofenac salts

Name	*Abbreviation*
2-amino-2-methylpropanol	AMP
2-amino-2-methyl-1,3-propanediol	AMPD
benzylamine	BA
tert-butylamine	tBA
2-(dimethylamino)ethanol *or* deanol	DNL
tris(hydroxymethyl)aminomethane	TRIS

The study included four primary amines, each having four carbons and zero, one, two or three hydroxyl group(s), respectively: *tert*-butylamine, 2-amino-2-methylpropanol, 2-amino-2-methyl-1,3-propanediol and tris(hydroxymethyl)aminomethane. The structures of these bases are presented in Figure 6. 1.

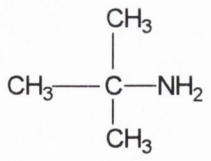

tert-butylamine

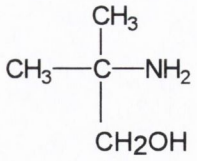

2-amino-2-methylpropanol

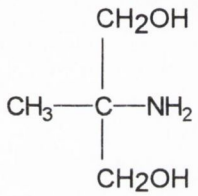

2-amino-2-methyl-1,3-propanediol

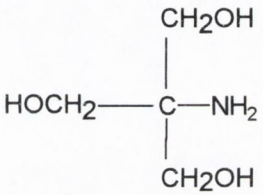

tris(hydroxymethyl)aminomethane

Figure 6. 1 Chemical structures of the four-carbon primary amines used to form salts with diclofenac

In addition, salts of the four-carbon, tertiary amine, deanol, and the aromatic primary amine, benzylamine, were included in the study (Figure 6. 2).

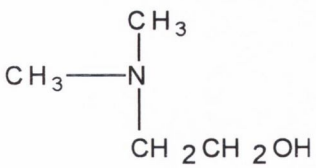

2-(dimethylamino)ethanol
or deanol

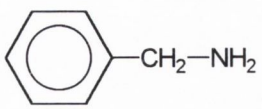

benzylamine

Figure 6. 2 Chemical structures of bases used to form salts with diclofenac

Tris(hydroxymethyl)aminomethane (TRIS) is used as an alkalising agent in the treatment of metabolic acidosis (Martindale, 1999). It is a commonly used base in the preparation of salts (Roseman and Yalkowsky, 1973; Gu and Strickley, 1987; Wang and Chowhan, 1990; Gabr and Borg, 1999), including some commercially marketed salts (Berge et al., 1977). It has previously been used to prepare a salt with diclofenac (Fini et al., 1996). As described in Section 6.1, the four-carbon primary amines selected (tBA, AMP, AMPD and TRIS) were used by Anderson and Conradi (1985) in a study involving the preparation of a series of salts of the non-steroidal anti-inflammatory drug, flurbiprofen. The study investigated possible relationships between the solubilities of the salts and their melting points and cation hydrophilicities. Deanol and benzylamine were previously used by Hirsch et al. (1978) to form salts with fenoprofen in an attempt to increase the stability of the drug.

Some of the physical properties of the six bases selected are outlined in Table 6. 2. Salts were prepared by the method described in Section 3.2.7; the solvents used are listed in Table 3.1. The products were characterised by DSC, TG, HSM, XRD, FT-IR and elemental analysis. The XRD trace for diclofenac acid (DCFA) is presented in Figure 4.11. All of the bases studied exist in a liquid form at room temperature, except AMPD and TRIS. These solids were characterised by thermal analysis and XRD.

Table 6. 2 Properties of bases selected for the preparation of diclofenac salts

Base	*Molecular weight*	*pK_a*	*Melting point*	*Boiling point*	*Solubility / miscibility* [d]
AMP	89.14	9.69 [a]	25.5°C [e]	165.5°C [e]	miscible with water soluble in alcohols
AMPD	105.14	8.80 [a]	109-111°C [d]	151-2°C [d]	250g dissolve in 100ml water at 20°C; soluble in alcohols
BA	107.2	9.35 [a]	10°C [a]	185°C [e]	miscible with water, alcohol, ether
tBA	73.14	10.69 [a]	-66.9°C [e]	44°C [e]	miscible with alcohol
DEA	73.14	10.84 [b]	-49.8°C [e]	55.5°C [e]	miscible with water, alcohol
DNL	89.14	9.26 [a]	-59°C [e]	134°C [e]	miscible with water, alcohol, ether
HEP	115.18	9.72 [c]	< -60°C [f]	79-81°C [g]	---
TRIS	121.14	8.30 [d]	171.5°C [e]	219-220°C [e]	solubility in water: 550mg/ml at 25°C; soluble in alcohol, acetone, methanol

[a] Dean, 1987

[b] Albert and Serjeant, 1984

[c] Fini et al., 1994a

[d] *Merck Index*, 1996

[e] *CRC Handbook of Chemistry and Physics*, 1995

[f] information obtained by DSC: temperature reduced to –60°C (2°C/min), no thermal events observed

[g] supplier's catalogue

6.2. DICLOFENAC *TERT*-BUTYLAMINE (DtBA)

6.2.1. Physicochemical characterisation of DtBA by XRD, thermal analysis, FT-IR spectroscopy and elemental analysis

The salt preparation procedure was carried out as described in Section 3.2.7. Elemental analysis results of the product complied with the results expected for a DCFA 1:1 salt (Table 6. 3). The FT-IR spectrum obtained was consistent with salt formation (Figure 7, Appendix II).

Table 6. 3 Elemental analysis results for the DtBA product

Element	*DtBA Theoretical %*	*DtBA product Actual %*
C	58.54	58.43
H	6.02	5.96
N	7.59	7.48

The XRD trace for DtBA is presented in Figure 6. 3.

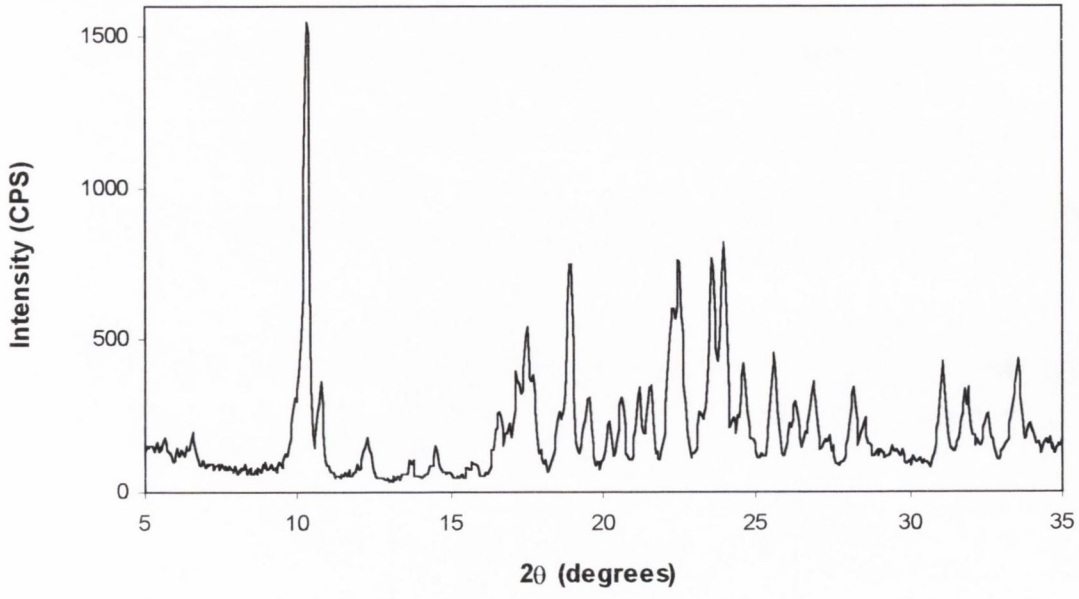

Figure 6. 3 XRD trace for DtBA

The DSC scan for the product (Figure 6. 4) displayed an endothermic peak with an onset temperature of 153°C, followed by a larger endothermic peak over the temperature range 160-200°C. The TG trace (Figure 6. 4) showed a marked increase in the rate of weight loss at a temperature corresponding to the onset of the second endotherm. Examination of the sample by HSM revealed complete melting of the sample in the temperature range 145-155°C, corresponding to the first endotherm in the DSC scan. No further events were observed.

The jagged nature of the trace for the second endotherm and the sharp increase in the rate of weight loss suggested the occurrence of degradation at that temperature. Therefore, the overlapping endotherms in the DSC scan (onset temperatures, 153°C and ~160°C) were thought to be due to melting of the salt, followed by degradation. The onset value, 153°C, was thought to be the melting point of DtBA.

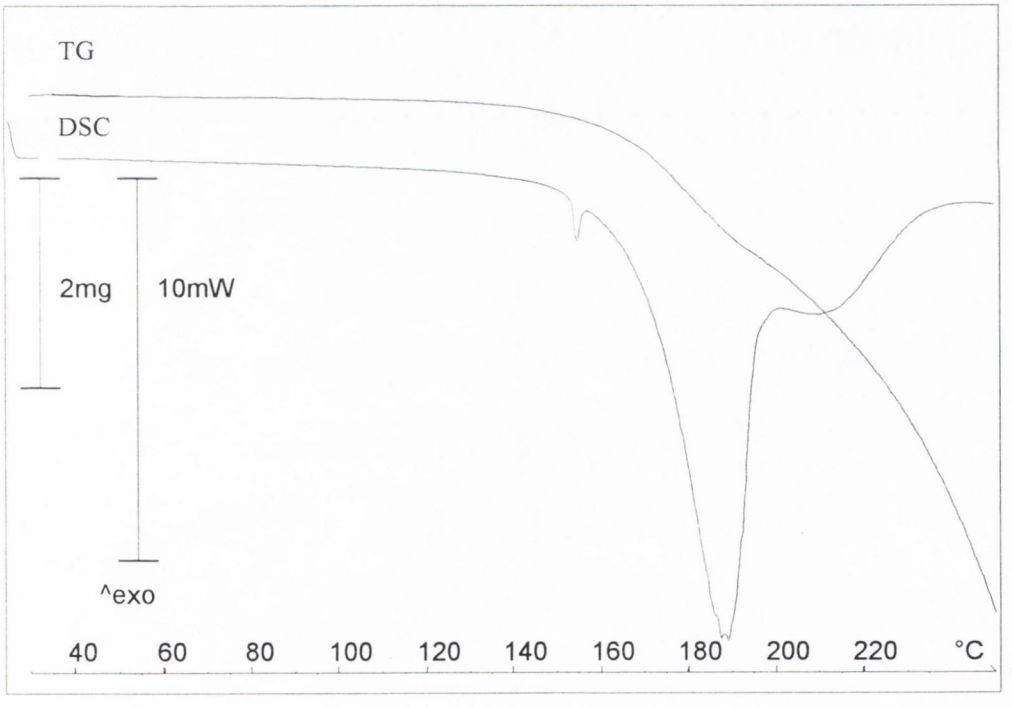

Figure 6. 4 DSC and TG traces for DtBA

6.2.2. *Solubility and intrinsic dissolution rate determination for DtBA*

The solubility of DtBA in water at 25°C was determined as 5.46 ± 0.05 mM. This was significantly lower than the solubility of the diclofenac salts studied in Chapters 4 and 5: DDEA (33 mM), DNa (66 mM) and DHEP (273 mM). The intrinsic dissolution rate of DtBA in water at 25°C was found to be $3.86 \times 10^{-4} \pm 0.09 \times 10^{-4}$ mmol/min/cm^2.

6.3. DICLOFENAC 2-AMINO-2-METHYLPROPANOL (DAMP)

6.3.1. *Physicochemical characterisation of DAMP by XRD, thermal analysis, FT-IR spectroscopy and elemental analysis*

When the salt preparation procedure (Section 3.2.7) was carried out using AMP as the basic counterion, two different products were identified, DAMP-I and DAMP-II. The methods of preparation for the two forms differed in the quantities of solvent used. The XRD traces of the two products are presented in Figure 6. 5; the crystal patterns were found to differ in peak position and relative intensities.

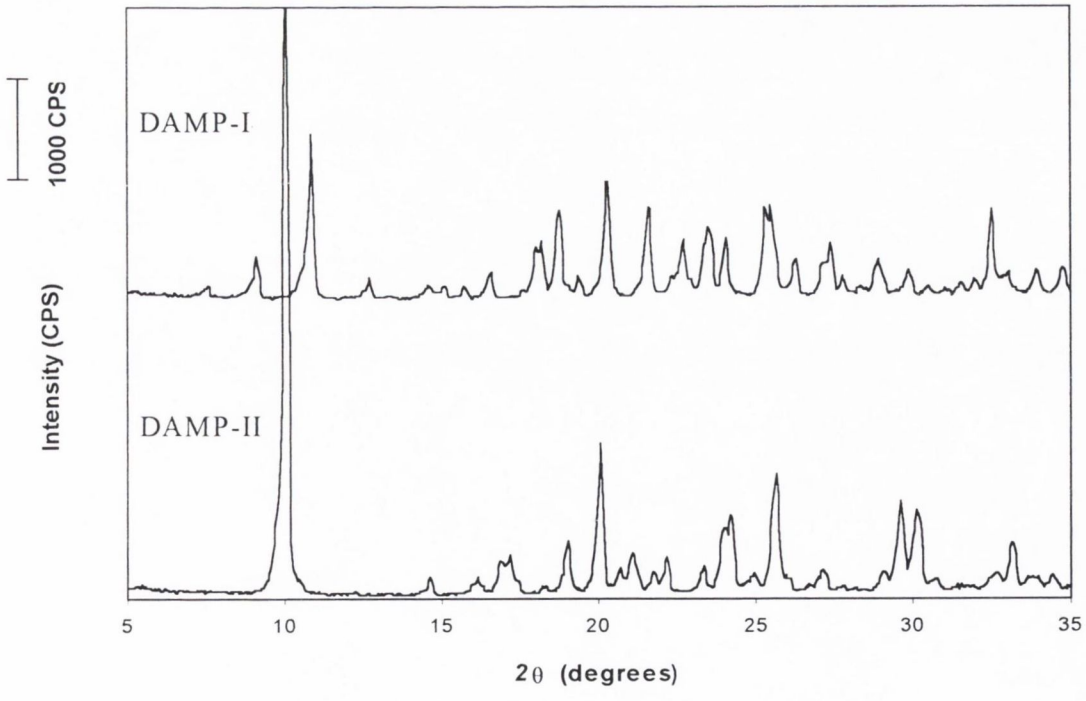

Figure 6. 5 XRD traces for DAMP-I and DAMP-II

Elemental analysis of both products gave results identical to those expected for the 1:1 salt (Table 6. 4). The FT-IR spectra for the two forms were consistent with salt formation (Figures 8 and 9, Appendix II). There were only slight differences between the FT-IR spectra of the two forms. There was a peak present at 1422 cm^{-1} in the DAMP-I spectrum, which was not present in that of DAMP-II. Previous studies on polymorphic systems have reported only slight differences between the FT-IR spectra of different polymorphs of the same compound (e.g. Lowes et al., 1987; Qiu et al., 1993; Jasti et al., 1995; Hiramatsu et al., 1996).

Table 6. 4 Elemental analysis results for DAMP products

Element	*DAMP* *Theoretical %*	*DAMP-I* *Actual %*	*DAMP-II* *Actual %*
C	56.10	56.07	55.89
H	5.77	5.72	5.71
N	7.27	7.16	7.22

The DSC trace for DAMP-I (Figure 6. 6) showed a melting peak with an onset value of 182°C, followed by the broad volatilisation/decomposition peak characteristic of diclofenac salts. The TG trace revealed an increase in the rate of weight loss from ~180°C.

The DSC scan for DAMP-II (Figure 6. 7) differed from that of DAMP-I by the presence of a shoulder on the endothermic peak. The peak temperature of the endotherm was identical to that of the endotherm in the DAMP-I DSC scan (188°C). The onset value of 161°C was considerably lower than that for DAMP-I due to the presence of the shoulder on the peak.

Figure 6. 6 DSC and TG traces for DAMP-I

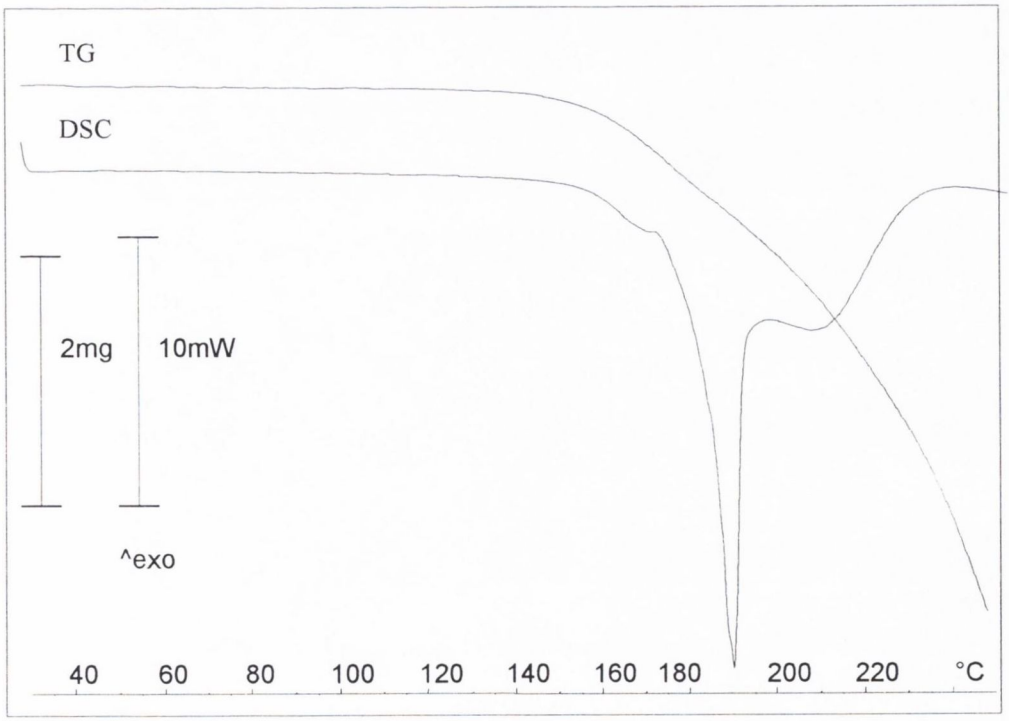

Figure 6. 7 DSC and TG traces for DAMP-II

Further investigation of the thermal properties of DAMP-II was required to explain the presence of what appears to be two overlapping peaks. DSC analysis was carried out (a) on a smaller sample size (b) at a slower heating rate (1°C/min); however, no greater resolution between the two peaks was achieved. A sample, when observed under the hot stage microscope, displayed melting at a temperature corresponding to the onset of the endotherm in the DSC scan, followed by recrystallisation and subsequent re-melting. Further investigation by DSC involved heating a sample to 170°C (just past the shoulder on the peak), cooling the sample to 25°C and re-heating the sample to 250°C (a) after 10 minutes and (b) after 4 days. In each case, the DSC and XRD traces obtained were identical to those of DAMP-I. This suggests the existence of two forms of DAMP: DAMP-I, which melts at 182°C, and DAMP-II, which converts on heating to DAMP-I. The conversion process (melting and recrystallisation) is consistent with *Type 2* polymorphism as classified by Giron (1995). The process was irreversible under the conditions studied (i.e. when the sample was stored for 4 days).

6.3.2. Solubility and intrinsic dissolution rate determination for DAMP

Of the two forms of DAMP, DAMP-I was selected for investigation of solubility and dissolution rate because of (a) its single melting endotherm in the DSC scan and (b) its ease of preparation relative to DAMP-II. The solubility of DAMP-I in water at 25°C was determined as 21.76 ± 0.25 mM. This was considerably higher than the solubility of DtBA (5.46 mM). The intrinsic dissolution rate of DAMP-I in water at 25°C was determined as $1.38 \times 10^{-3} \pm 0.03 \times 10^{-3}$ mmol/min/cm^2.

6.4. DICLOFENAC 2-AMINO-2-METHYL-1,3-PROPANDIOL (DAMPD)

6.4.1. Characterisation of AMPD by XRD and thermal analysis

The XRD trace for AMPD is presented in Figure 6. 8.

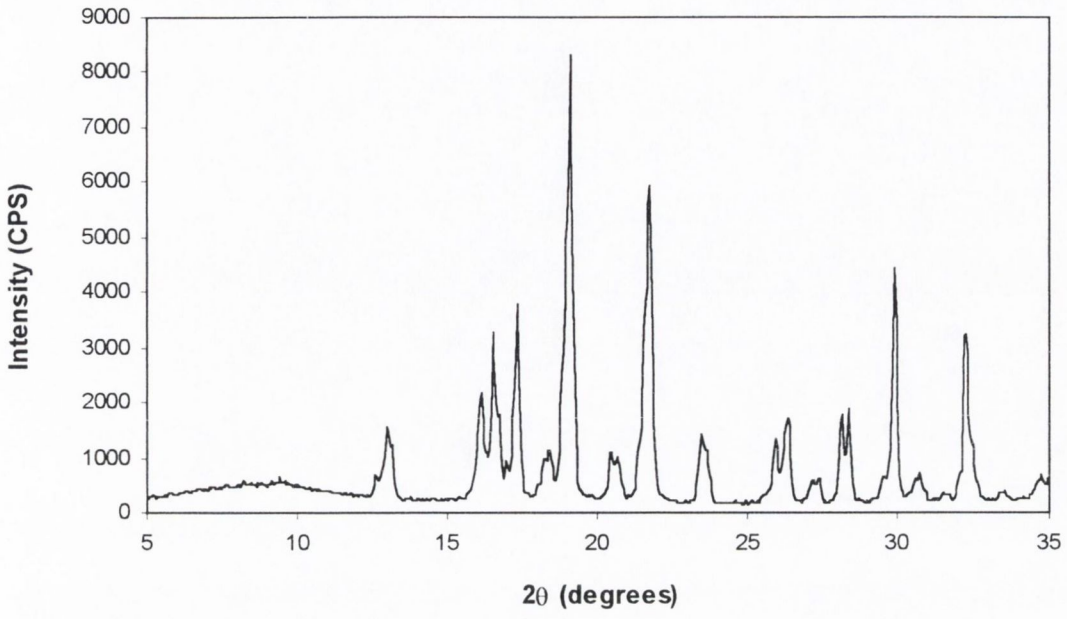

Figure 6. 8 XRD trace for AMPD

The literature value for the melting point of AMPD is 109-111°C (*Merck Index*, 1996). The DSC scan for AMPD (Figure 6. 9) showed endothermic events with onset values of 80°C and 103°C. Investigation of these events by HSM revealed a change in the appearance of the crystals at a temperature corresponding to the first endotherm, possibly due to a phase transition. Melting of the sample was observed from ~100°C, corresponding to the second endotherm. AMPD is reported to have a boiling point of 151-152°C at 10 mmHg (*Merck Index*, 1996). The broad endotherm observed from ~120°C in Figure 6. 9 was thought to correspond to evaporation of the sample, as suggested by the weight loss detected in the TG trace.

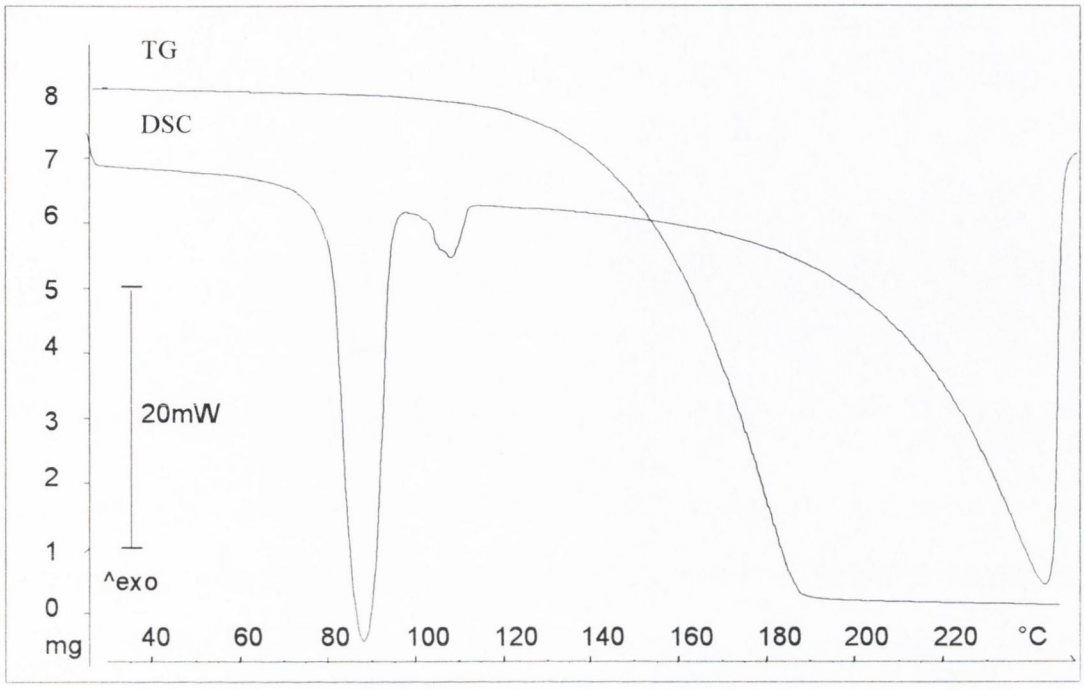

Figure 6. 9 DSC and TG scans of AMPD

6.4.2. Physicochemical characterisation of DAMPD by XRD, thermal analysis, FT-IR spectroscopy and elemental analysis

Products obtained by the salt preparation procedure (Section 3.2.7) using methanol were shown by elemental analysis to have the same elemental composition as a 1:1 DCFA:AMPD salt (Table 6. 5). The FT-IR spectrum obtained was consistent with salt formation (Figure 10, Appendix II). The XRD trace for the product (DAMPD) is presented in Figure 6. 10. Figure 6. 11 shows the DSC scan for DAMPD. Examination of a sample by HSM confirmed that the sharp endotherm with an onset value of 180°C was attributable to melting of the salt form. The broad endotherm from ~185°C in the DSC scan was thought to result from decomposition or volatilisation of the molten drug (weight loss is observed in the TG trace from that temperature, Figure 6. 11).

Table 6. 5 Elemental analysis results for DAMPD products

Element	*DAMPD* *Theoretical %*	*DAMPD product* *Actual %*	*Product A* *Actual %*
C	53.87	53.67	51.97
H	5.54	5.50	5.68
N	6.98	6.86	6.70

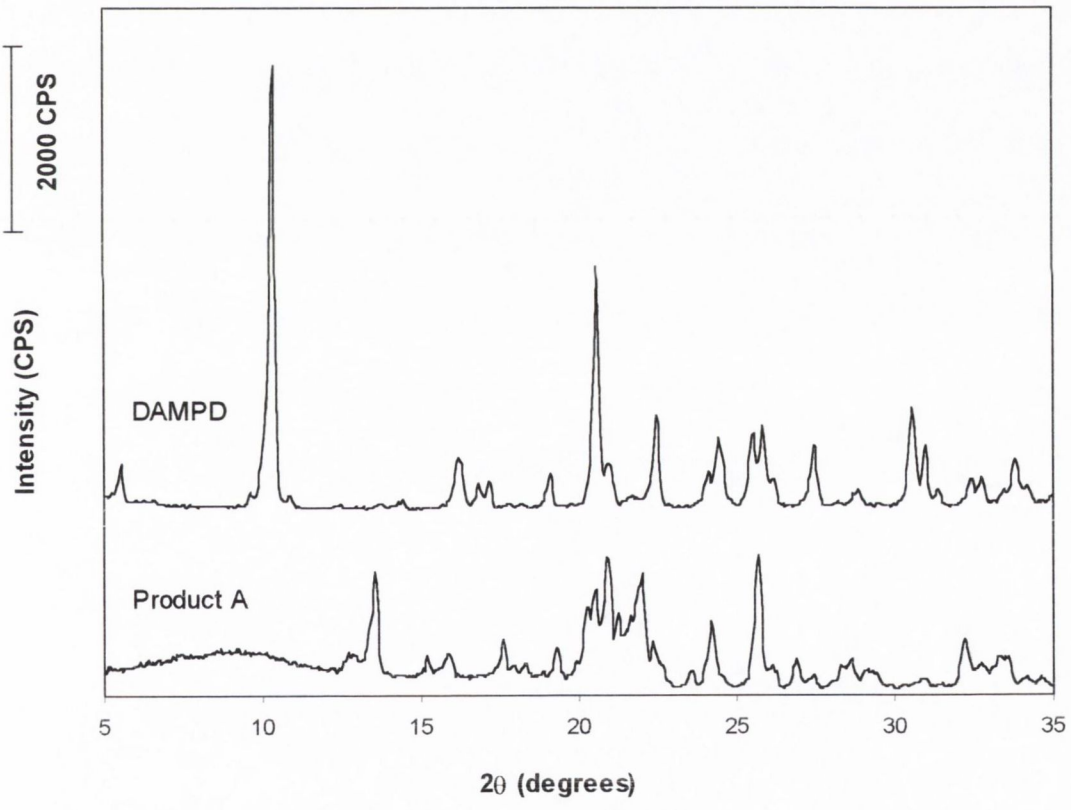

Figure 6. 10 XRD traces of DAMPD products

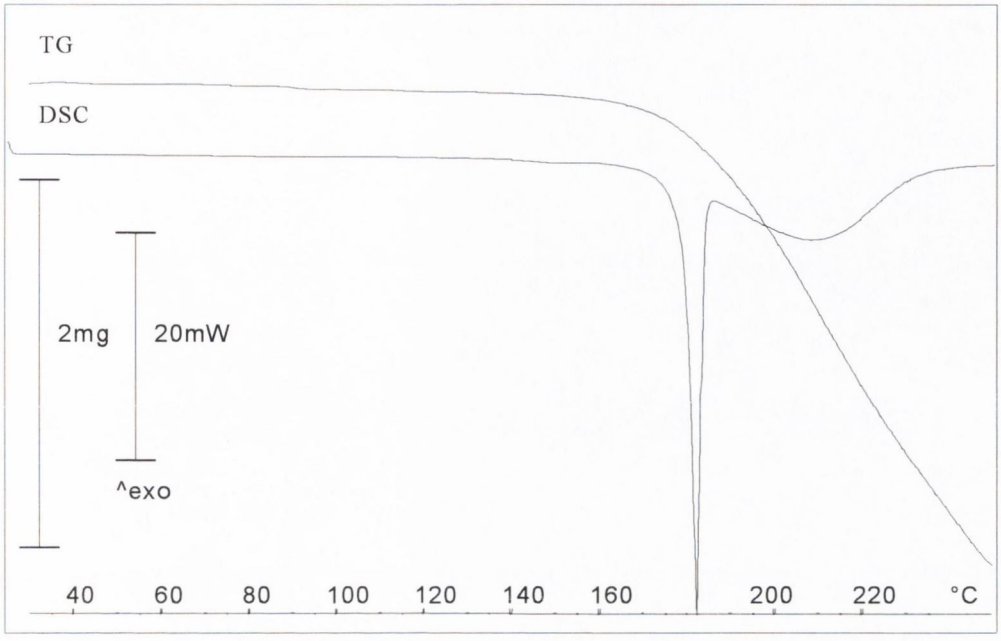

Figure 6. 11 DSC and TG traces for DAMPD

6.4.3. Identification and characterisation of the monohydrate form of DAMPD

Other products obtained by precipitation from methanol and from acetone were found to differ from the 1:1 salt (Products A – C). The XRD traces for these products (each displaying similar peak patterns) were different to the trace for DAMPD. The XRD trace for Product A is presented in Figure 6. 10. DSC analysis of Products A – C revealed an additional endotherm in the temperature range 70 – 110°C. This endotherm was found to vary in magnitude (ΔH value) between Products A – C (Table 6. 6). The DSC scan for Product A is presented in Figure 6. 12.

TG analysis of Products A – C revealed an increase in the rate of weight loss at a temperature corresponding to the additional endotherm in the DSC scans. The TG scan for Product A is presented in Figure 6. 12. The magnitude of this "step" was found to decrease in the same rank order as the magnitude of the endotherm at 70 – 110°C in the DSC scans (Table 6. 6). HSM of a sample mounted in silicone revealed the evolution of fluid from ~85 – 90°C. Elemental analysis results for Product A (Table 6. 5) deviated from the results for DAMPD. Deviation from the expected results (low % C and % N, high % H) could be attributed to the presence of water. Analysis of water content by KFT indicated that the endotherm at 70 – 110°C and the corresponding step in the TG trace could be attributed to water in the samples (Table 6. 6). The effect of the presence of water on the XRD pattern generated would suggest that the water was

present as water of crystallisation. A hydrated form of the salt may have been present in varying amounts in the different products.

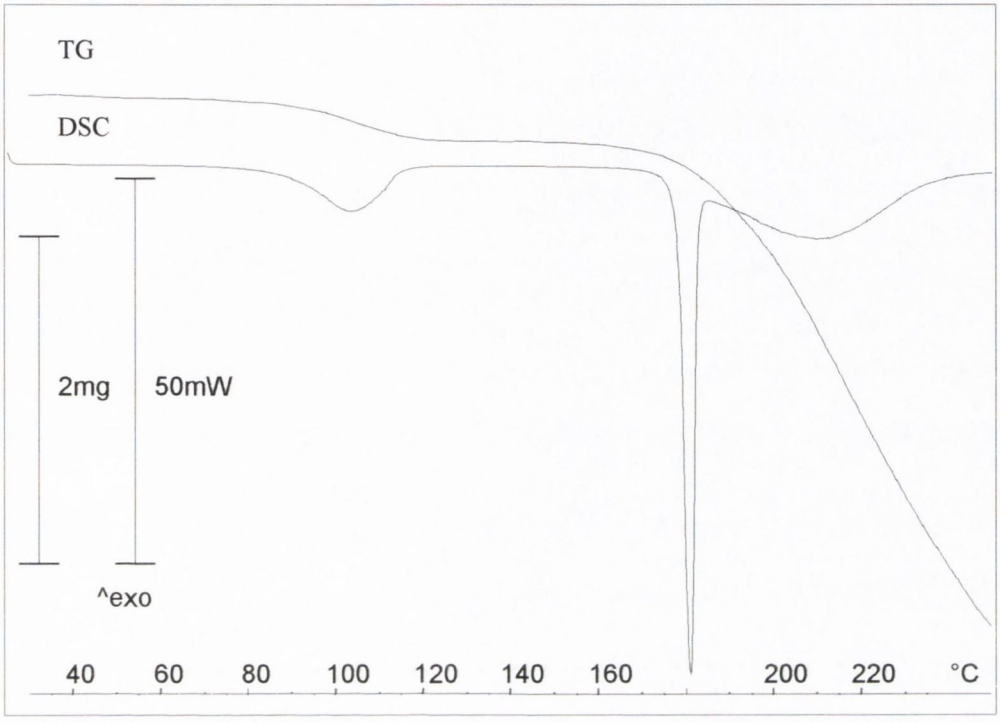

Figure 6. 12 DSC and TG traces for Product A

Table 6. 6 Examination of the DAMPD products that differed from the 1:1 salt

Product	*DSC endotherm 70 – 110°C ΔH (J/g)*	*TG step 70 – 110°C %w/w*	*KFT water content %w/w*
A	98.30	3.79	3.91 ± 0.01
B	86.87	3.35	2.94 ± 0.10
C	71.42	2.66	2.67 ± 0.32

A sample of Product C was heated to 130°C (past the first endotherm) for 10 minutes and subsequently examined by DSC, TG, XRD and elemental analysis. The endotherm at 70 – 110°C in the DSC scan and the corresponding step in the TG scan were no longer detected. The XRD

trace of the sample was found to differ from that of the sample before the heating process (Figure 6. 13), concordant with loss of water of crystallisation. The XRD trace also differed from that of DAMPD (Figure 6. 10), suggesting that the dehydrated hydrate was different in crystal structure to the anhydrous form of the salt. Elemental analysis results of the sample after heating corresponded to those for DAMPD.

To investigate further the existence of a hydrated form of the salt, Products A – C were precipitated from water using the method described in Section 3.2.8. The recrystallised products (n = 3) were examined by DSC, TG, KFT, XRD, FT-IR and elemental analysis. The results obtained for each sample were similar. The XRD traces for the recrystallised products were found to be similar to those of Products A – C. The trace for Product C recrystallised from water is presented in Figure 6. 13.

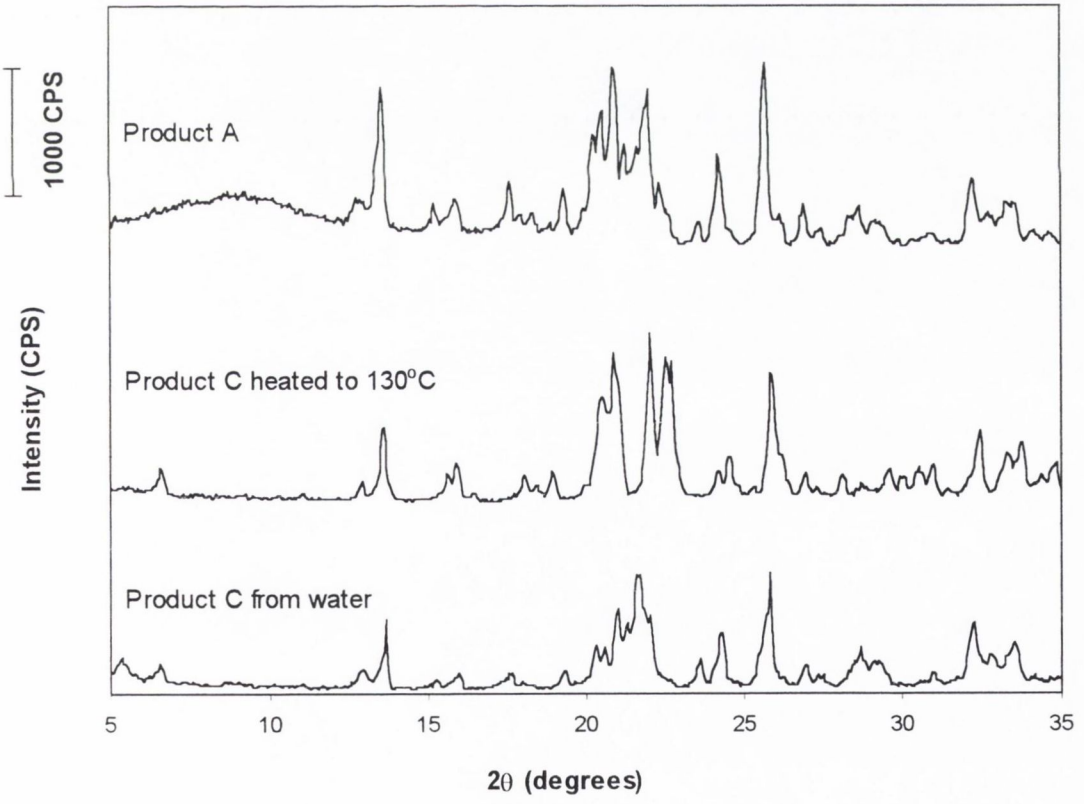

Figure 6. 13 XRD traces of DAMPD products: Product A, Product C after heating to 130°C and Product C following recrystallisation from water

The DSC scan for each product recrystallised from water revealed an endotherm at 111°C (ΔH = 116.82 ± 3.94 J/g, n = 3). The DSC scan for Product C recrystallised from water is presented in Figure 6. 14. The steps in the TG traces of the recrystallised products corresponded to a decrease in weight of 4.39 ± 0.10 %w/w (n = 3). The TG scan for Product C is presented in Figure 6. 14. The water content of the recrystallised products was determined by Karl Fischer titration as 4.24 ± 0.06 %w/w (n = 3). The theoretical water content of a monohydrate form of the salt is 4.30 %w/w.

Elemental analysis results of the recrystallised products complied with the results expected for a monohydrate form of the salt. The FT-IR spectrum for Product C recrystallised from water (Figure 11, Appendix II) was similar to that for DAMPD with increased absorbance between 3100 cm^{-1} and 3600 cm^{-1} which can be attributed to water of crystallisation.

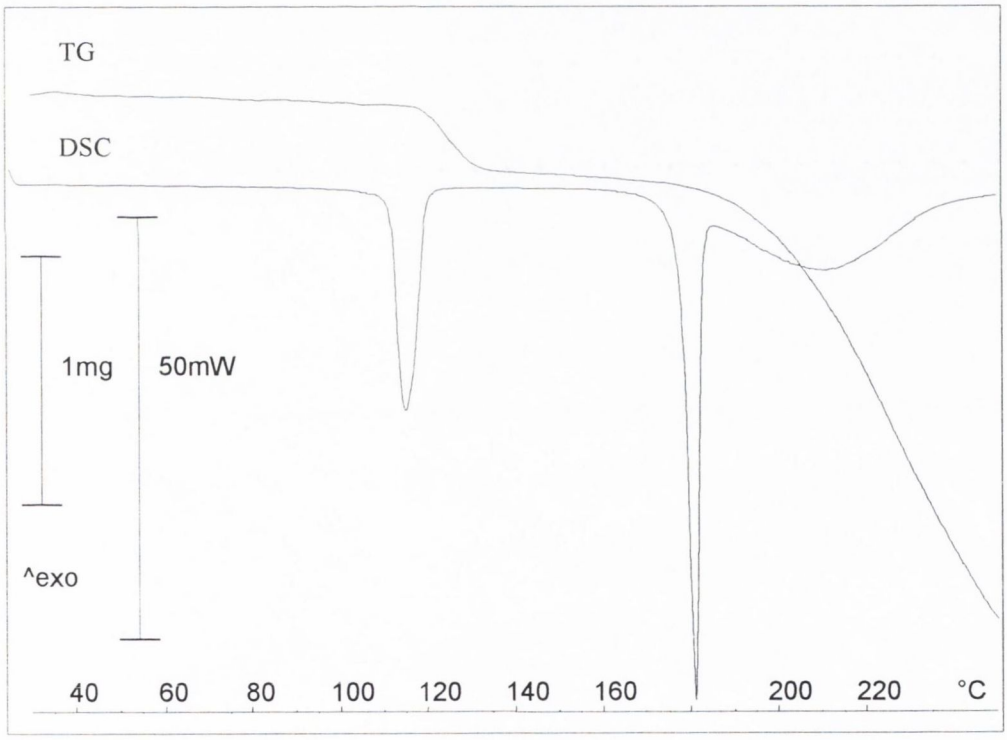

Figure 6. 14 DSC and TG traces for Product C recrystallised from water

In conclusion, the monohydrate form of DAMPD was identified. It is thought that certain crystallisation conditions yield products, such as Products A – C, that consist of either a mixture of DAMPD and its monohydrate form or partially dehydrated DAMPD monohydrate.

6.4.4. Solubility and intrinsic dissolution rate determination for DAMPD

An ampoule solubility study in water at 25°C using anhydrous DAMPD as the starting material yielded a solubility value of 6.77 ± 0.03 mM. The XRD trace of the solid in equilibrium with the saturated solution after 24 hours (the first sampling time) was consistent with that of the monohydrate form of the salt. Therefore, the solubility of the salt is limited to that of its monohydrate form which precipitates from a solution of the anhydrate. The intrinsic dissolution rate of the salt in water at 25°C was determined as $4.51 \times 10^{-4} \pm 0.07 \times 10^{-4}$ mmol/min/cm^2. XRD analysis of a disc after 5 minutes dissolution generated a trace consistent with the monohydrate form of the salt, indicating that conversion of the anhydrate to the monohydrate had occurred. The intrinsic dissolution rate determined therefore related to DAMPD monohydrate. Instantaneous hydration of the solid on the surface of discs upon immersion in water has previously been reported. Rubino (1989) reported no differences in the dissolution rates determined for the anhydrous, sesquihydrate and 4.6 hydrated forms of sodium sulfathiazole due to hydration of the anhydrate and sesquihydrate forms to the most hydrated form.

6.5. DICLOFENAC BENZYLAMINE (DBA)

6.5.1. Physicochemical characterisation of DBA by XRD, thermal analysis, FT-IR spectroscopy and elemental analysis

Attempts to prepare a salt from diclofenac acid and benzylamine by precipitation from acetone according to the salt preparation procedure described in Section 3.2.7 were unsuccessful. Two products have been identified following combination of solutions of diclofenac acid and benzylamine in ethyl acetate: DBA-I and DBA-II (the different products may have resulted from slight changes in preparation conditions). The procedure was also carried out in methanol, resulting in the formation of DBA-II.

The XRD traces of the two forms are presented in Figure 6. 15. The crystal patterns were found to differ in peak position and relative intensities.

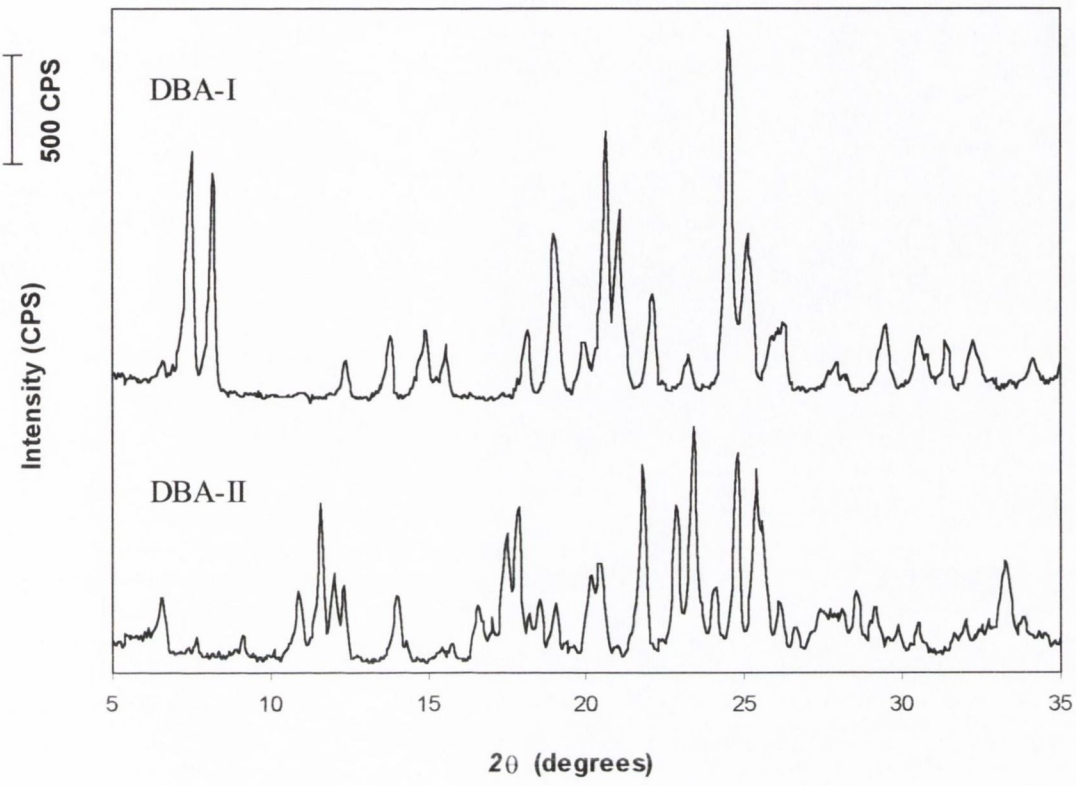

Figure 6. 15 XRD traces of DBA-I and DBA-II

Elemental analysis results for the two forms complied with those expected for a DCFA:BA 1:1 salt (Table 6. 7). Their FT-IR spectra (Figures 12 and 13, Appendix II) were consistent with salt formation. As observed for the two polymorphs of DAMP, the FT-IR spectra of DBA-I and DBA-II were found to be only slightly different. Differences observed included the presence of a peak at 1534 cm^{-1} in the spectrum of DBA-I and a peak at 1549 cm-1 in the DBA-II spectrum.

Table 6. 7 Elemental analysis results for DBA-I and DBA-II

Element	*DBA* *Theoretical %*	*DBA-I* *Actual %*	*DBA-II* *Actual %*
C	62.53	62.49	62.37
H	5.01	5.06	4.96
N	6.95	6.92	6.85

The DSC trace for DBA-I (Figure 6. 16) showed an endothermic peak with an onset value of 157°C, followed by the broad volatilisation/decomposition peak characteristic of diclofenac salts. HSM confirmed that the endotherm at 157°C was due to melting of the salt. The TG trace (Figure 6. 16) revealed an increase in the rate of weight loss from a temperature corresponding to the onset of the endothermic event in the DSC scan. This may be attributed to volatilisation of the sample as it melted.

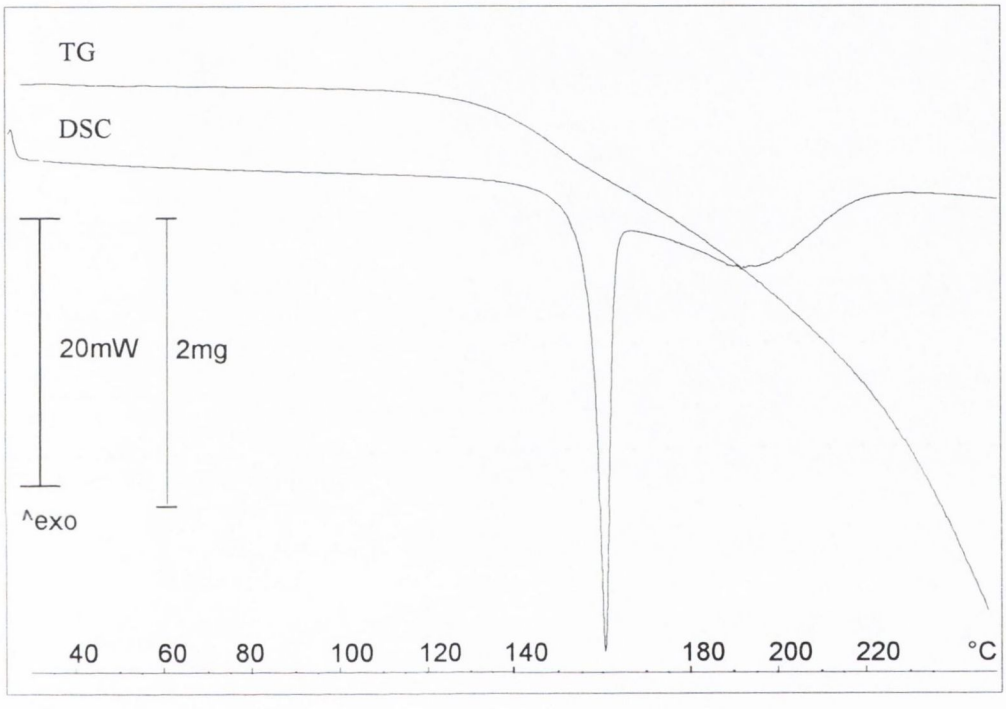

Figure 6. 16 DSC and TG traces for DBA-I

The DSC scan for DBA-II (Figure 6. 17) differed from that of DBA-I by the presence of second endothermic peak with an onset value of 137°C. The TG trace obtained (Figure 6. 17) was similar to that for DBA-I (Figure 6. 16). Further investigation of the thermal properties of DBA-II was carried out to explain the presence of two endotherms prior to degradation. A sample, when observed under the hot stage microscope, displayed melting at a temperature corresponding to the onset of the first endotherm in the DSC scan, followed by recrystallisation into acicular crystals. These crystals melted at ~160°C, a temperature corresponding to the onset of the second endotherm in the DSC scan.

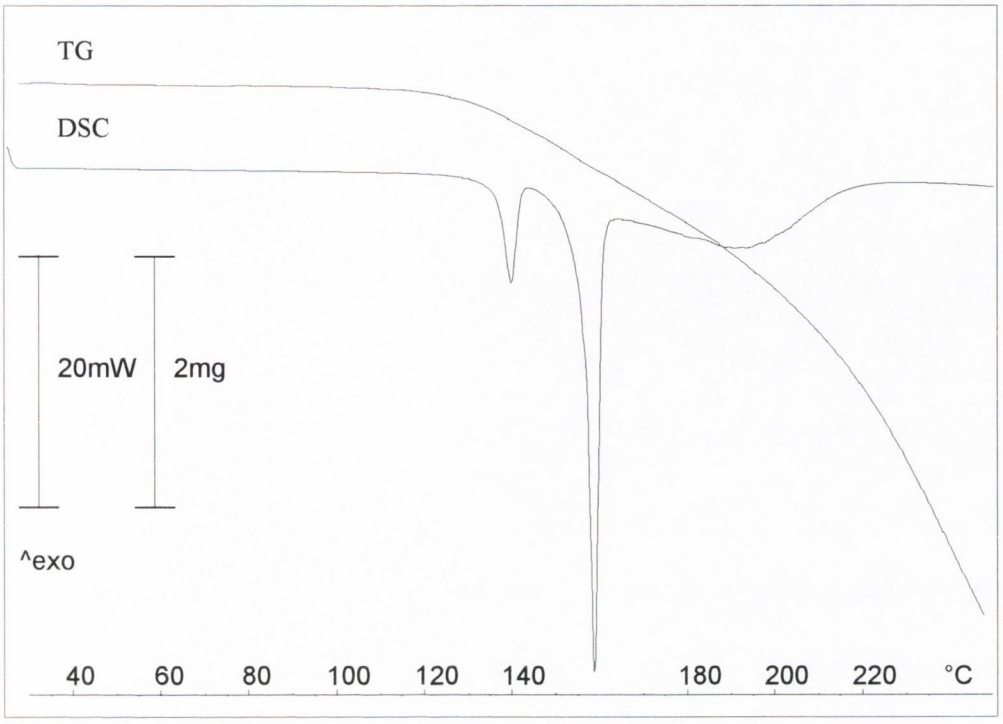

Figure 6. 17 DSC and TG traces for DBA-II

Further investigation by DSC involved heating a sample to 143°C (past the first endotherm), cooling to 25°C and re-heating the sample to 250°C (a) after 10 minutes and (b) after 2 days. In each case, the DSC and XRD traces obtained were identical to those of DBA-I. This suggests the existence of two forms of DBA: DBA-I, which melts at 157°C and DBA-II, which converts on heating to DBA-I. This thermal behaviour is consistent with a *Type 2* polymorphic transition (Giron, 1995). The conversion from DBA-II to DBA-I was irreversible under the conditions studied (i.e. when the sample was stored for 2 days).

6.5.2. Solubility and intrinsic dissolution rate determination for DBA

Of the two forms of DBA, DBA-I was selected for investigation of the solubility and dissolution rate for the same reasons DAMP-I was selected over DAMP-II, namely: (a) a single melting endotherm in the DSC scan and (b) the ease of preparation of DBA-I relative to DBA-II. The solubility of DBA-I was determined as 4.16 ± 0.04 mM.

As described in the procedure for determination of intrinsic dissolution rate (Section 3.2.13.1), XRD analysis was carried out on discs of each of the salts before dissolution to ensure that compression of the powder into a disc did not result in any change in the crystal structure of the compound. The diffraction pattern obtained from the surface of a disc of DBA, compressed at 8 tonnes for 5 minutes, differed from that of the original powder (Figure 6. 18). The alteration in the baseline of the trace was thought to be an effect of the method of mounting the disc in the sample holder and did not reflect a change in the crystal form of the drug; this phenomenon was observed for all the discs analysed. However, an extra peak was observed at $2\theta = 9.45°$ in the XRD trace for the disc (indicated by the arrow in Figure 6. 18). This extra peak suggested a change in the solid state form of the salt due to the compression procedure.

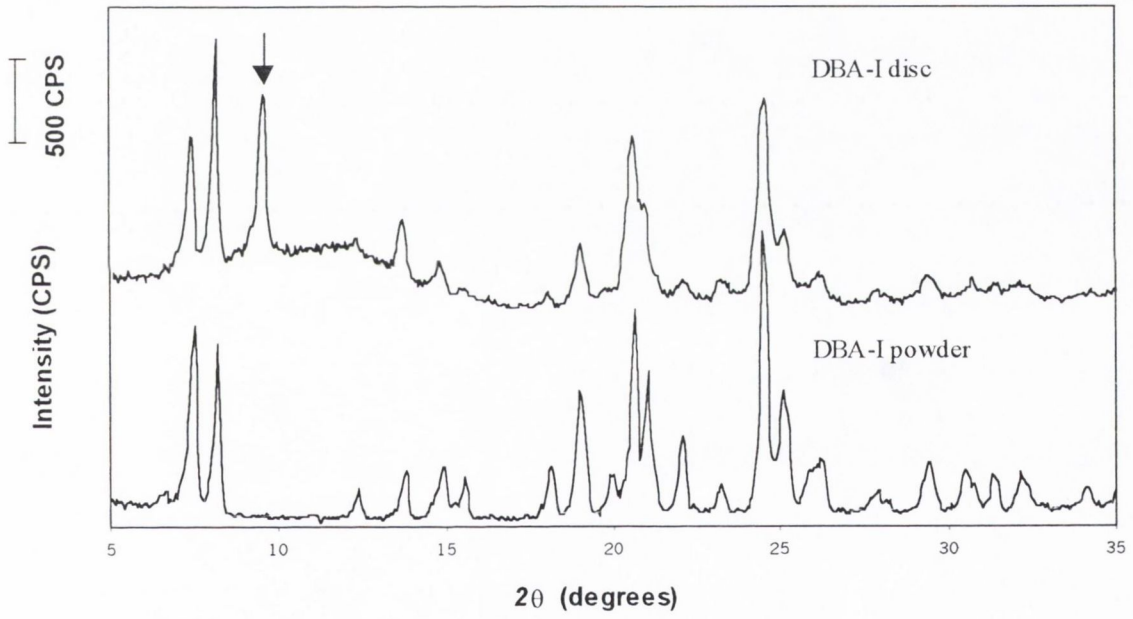

Figure 6. 18 XRD trace for a DBA-I disc, compressed at 8 tonnes for 5 minutes, compared with the XRD trace for DBA-I powder before compression

Despite the existence of an additional peak in the XRD trace, DSC analysis of disc reground after compression at 8 tonnes for 5 minutes did not reveal any change in the thermal behaviour of the salt (Figure 6. 19). However, when the compression time was increased to 10 minutes, an additional endotherm was observed at ~110°C in the DSC scan of the reground disc. This endotherm was observed to increase in magnitude with increasing compression time, e.g. the ΔH values for the endotherms after 10 minutes compression and 12 hours compression were 5.51 J/g and 10.37 J/g, respectively (Figure 6. 19).

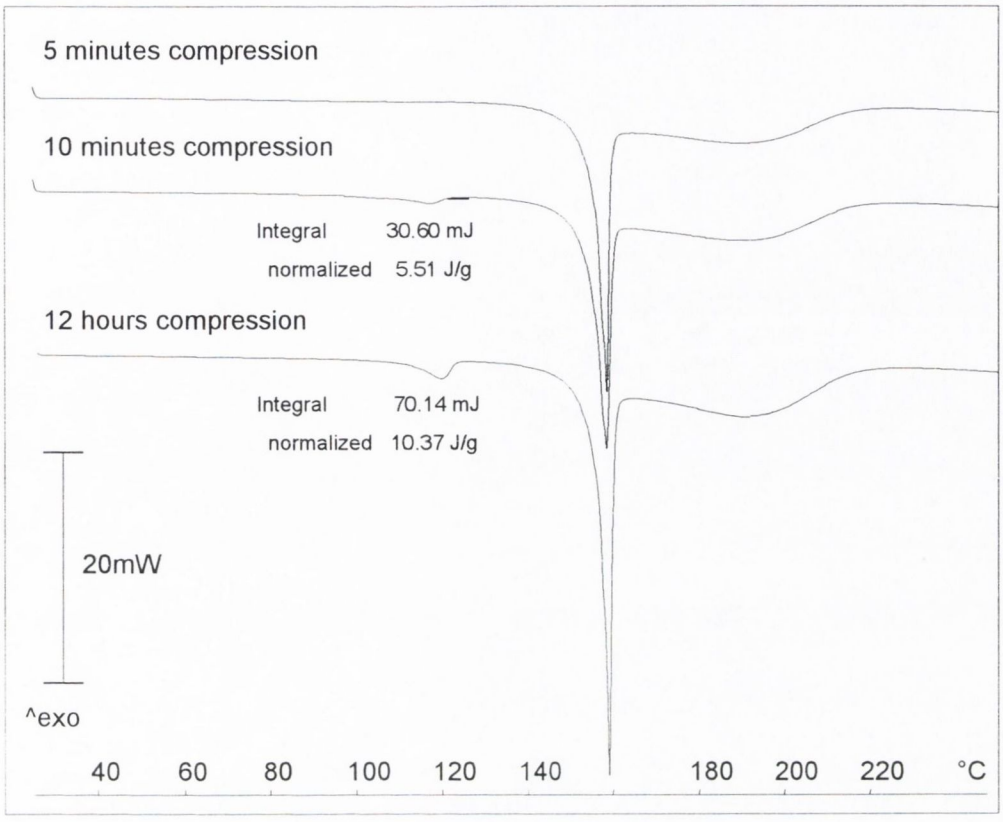

Figure 6. 19 DSC scans of powder from reground DBA discs; the discs were compressed at 8 tonnes for 5 mins, 10 mins and 12 hours

The changes in the solid state properties of DBA-I following compression could not be accounted for by conversion to DBA-II. The additional peak in the XRD trace following compression did not correspond to a peak characteristic of DBA-II. The extra endotherm in the DSC scan for the reground discs occurred at a temperature (onset 110°C) lower than that of the first endotherm in the DSC scan for DBA-II, which had an onset value of 137°C.

Due to the effect of compression, the intrinsic dissolution rate study performed on discs prepared from DBA-I yielded a result ($4.57 \times 10^{-4} \pm 0.15 \times 10^{-4}$ mmol/min/cm^2) which did not relate to the salt in its original solid state.

Previous studies have reported compaction-induced phase transformation for various drugs, such as phenylbutazone (Ibrahim et al., 1977), carbamazepine (Lefebvre et al., 1986), chlorpropamide (Otsuka et al., 1989) and piroxicam (Ghan and Lalla, 1992). These solid phase changes have been attributed to the influence of dislocational strain which is induced in a crystal during plastic flow (Summers et al., 1976). Polymorphic transitions in the solid state occur through a mechanism of

nucleation and growth of a second phase within the first (Cahn, 1950). Dislocations act as preferential nucleation sites because they possess higher free energy, resulting in a reduction in the energy necessary for transition.

Chan and Doelker (1985) investigated relationships between the extent of transformation and the energy of compression for three model drugs: caffeine, sulfabenzamide and maprotiline. The degree of polymorphic transformation, calculated using ΔH values measured by DSC, was found to increase at higher compression energy values. This observation was in agreement with the results obtained by XRD and DSC for DBA discs (Figure 6. 18 and Figure 6. 19). In the case of all three compounds studied by Chan and Doelker, a transition occurred from a lower melting point metastable form to a higher melting point stable form, a trend consistent with the results of other studies (Nogami et al., 1969; Ibrahim et al., 1977; Pirttimäki et al., 1993). The authors attributed this to lower intermolecular attractive forces and lower yield stress values of the lower melting form. On the other hand, the results of a study on the effect of compression on a stable form (A) and a metastable form (C) of chlorpropamide (Otsuka et al., 1989) suggested that each form was transformed into the other by mechanical energy. Summers et al. (1976) reported changes in the solid state of sulphathiazole Form II following compression. The DSC scan for sulphathiazole Form II showed a single melting endotherm at 201°C. However, compacts prepared from Form II displayed two endotherms in the DSC scan, at 129°C and 200°C. The presence of the additional endotherm at 129°C was attributed to transition of Form II to Form I due to compression. Similarly, the DSC results for DBA revealed an additional endotherm at a temperature lower than the melting point of the original form (Figure 6. 19), suggesting phase transformation from DBA-I into another form of the salt.

6.6. DICLOFENAC TRIS(HYDROXYMETHYL)AMINOMETHANE (DTRIS)

6.6.1. Characterisation of TRIS by XRD and thermal analysis

The XRD trace for TRIS is presented in Figure 6. 20. The crystalline pattern was consistent with that obtained by McGloughlin (1989).

The DSC and TG scans for TRIS are presented in Figure 6. 21. The DSC scan displayed two endotherms with onset temperatures of 134.5°C and 172.0°C. Examination by hot stage microscopy confirmed that the sample melted at a temperature corresponding to the higher temperature endotherm (onset temperature, 172.0°C). This correlated with the literature value for the melting point of TRIS, 171.5°C (*CRC Handbook of Chemistry and Physics*, 1989). The lower

temperature endotherm, which represented an event which was not detectable by HSM or by TG, was possibly indicative of a solid phase transition.

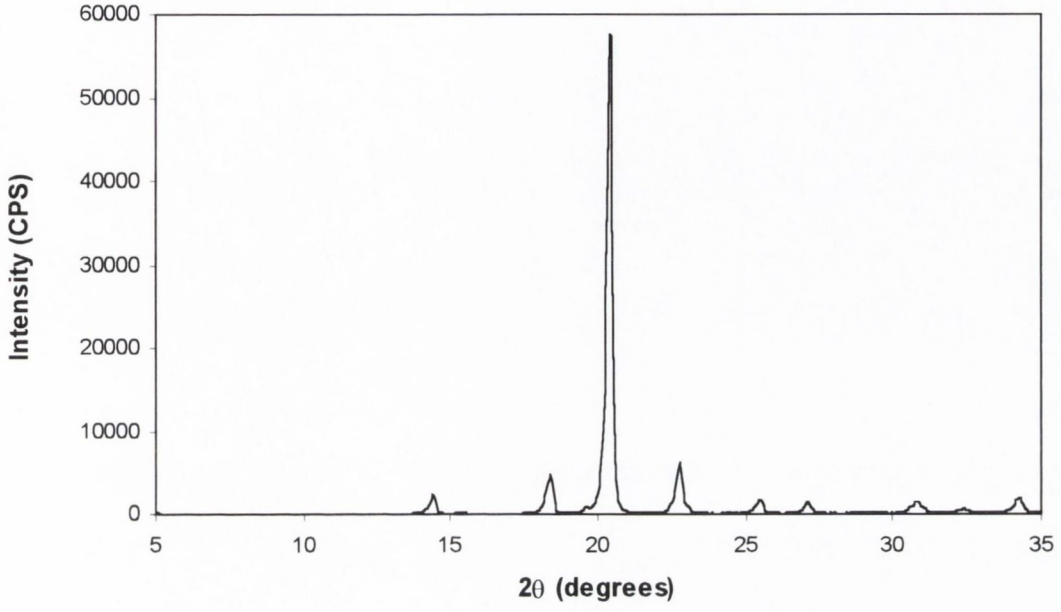

Figure 6. 20 XRD trace for TRIS

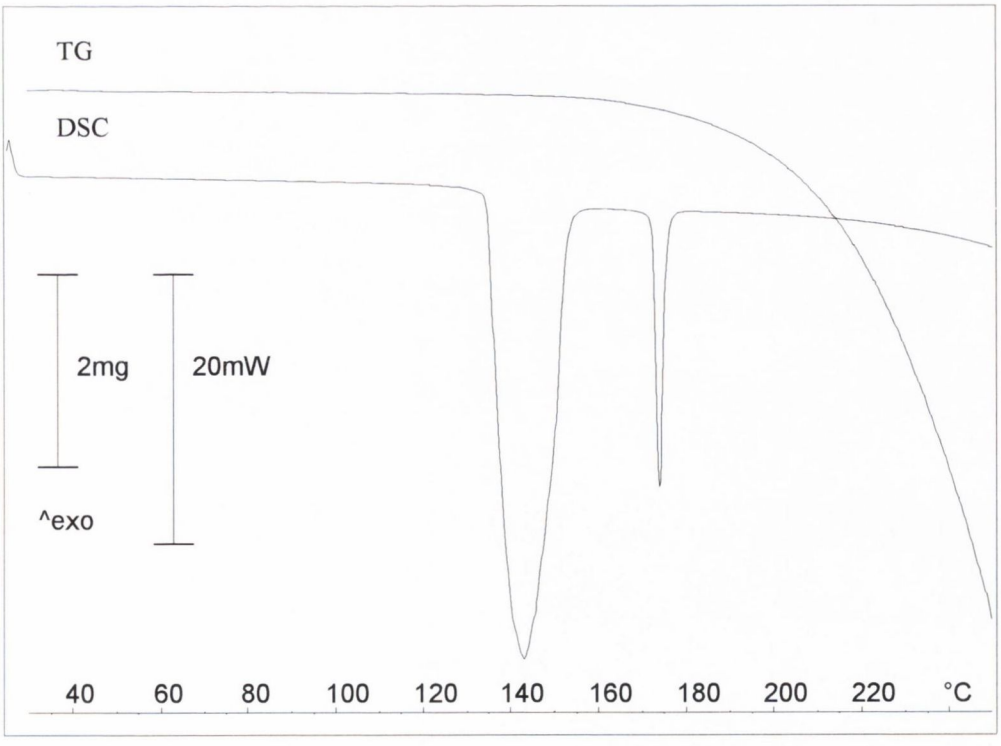

Figure 6. 21 DSC and TG scans for TRIS

6.6.2. Physicochemical characterisation of DTRIS by XRD, thermal analysis, FT-IR spectroscopy and elemental analysis

TRIS was used by Fini and co-workers (1996) in the preparation of a salt with diclofenac. The salt, prepared in methanol, was reported to have a melting point of 194-196°C and a solubility in water at 25°C of 1.67 mg/ml (4.00 mM).

In this study, the salt preparation procedure was carried out as described in Section 3.2.7. Elemental analysis results for the product complied with the expected results for a 1:1 DCFA:TRIS salt (Table 6. 8). The FT-IR spectrum obtained (Figure 14, Appendix II) was consistent with salt formation.

Table 6. 8 Elemental analysis results for the DTRIS product

Element	*DTRIS* *Theoretical %*	*DTRIS product* *Actual %*
C	51.80	51.70
H	5.33	5.32
N	6.71	6.53

The XRD of the product obtained is presented in Figure 6. 22. The DSC and TG scans are presented in Figure 6. 23. Examination of the product by HSM confirmed that the endotherm with an onset value of 209°C was attributable to melting of the product. This value differed from the melting point of 194-196°C previously published (Fini et al., 1996).

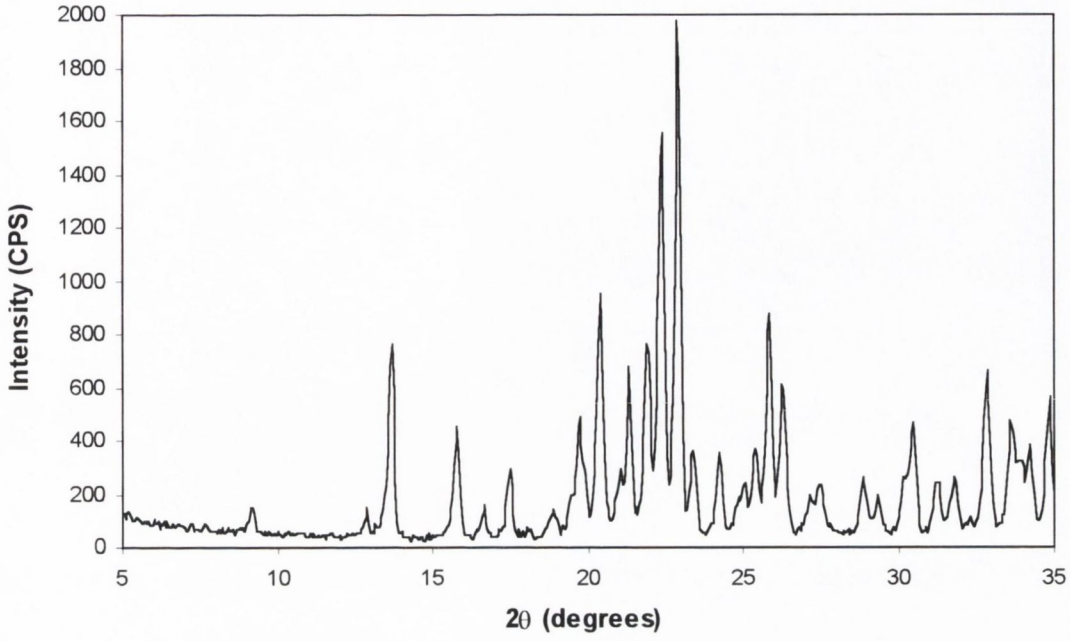

Figure 6. 22 XRD trace for DTRIS

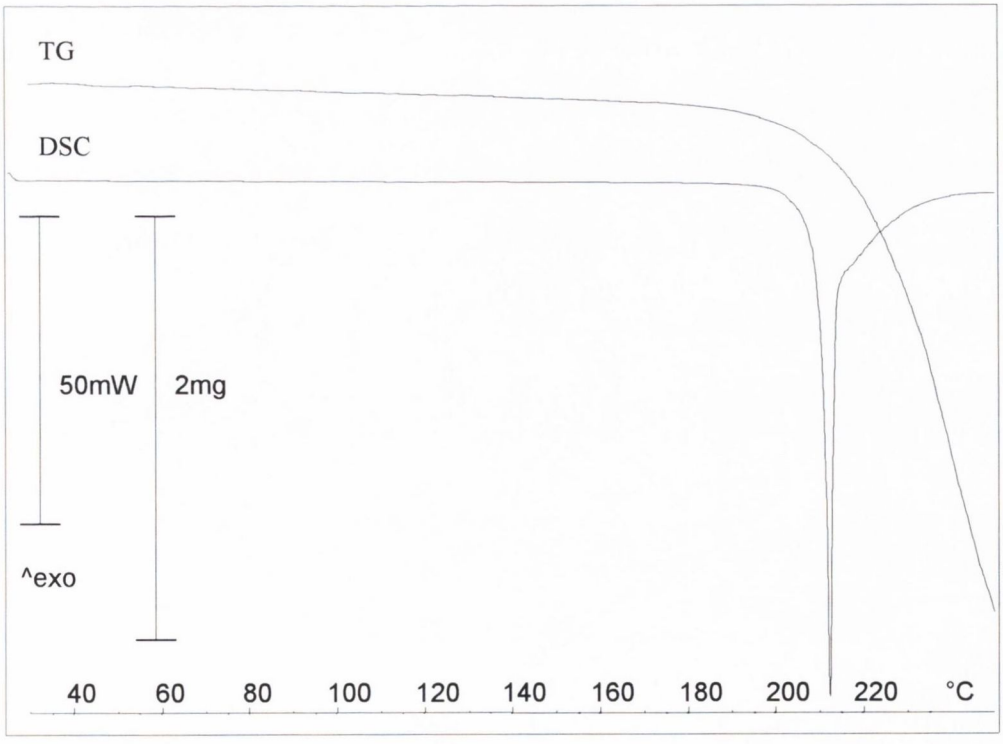

Figure 6. 23 DSC and TG scans for DTRIS

6.6.3. *Solubility and intrinsic dissolution rate determination for DTRIS*

The solubility of DTRIS in water at 25°C was determined as 3.89 ± 0.06 mM. This compared well with the value of 4.00 mM reported by Fini et al. (1996). The intrinsic dissolution rate for DTRIS in water at 25°C was found to be $2.45 \times 10^{-4} \pm 0.06 \times 10^{-4}$ mmol/min/cm^2.

6.6.4. *pH-solubility study of DTRIS*

Supersaturation was detected at the pH_{max} of the pH-solubility profiles for diclofenac salts with solubilities of 273 mM (DHEP, Ledwidge and Corrigan, 1998) and 33 mM (DDEA, Section 5.2). To investigate if the potential to form supersaturated solutions extended to diclofenac salts at the lower end of the solubility range, the pH-solubility profile of DTRIS was examined using the method described in Section 3.2.15. DTRIS had the lowest solubility (3.95 mM) within the range of salts examined.

The pH-solubility profile for DTRIS is presented in Figure 6. 24. The addition of a 0.1 N / 1.0 N TRIS to the solution of diclofenac acid caused an increase in the solubility of diclofenac to a maximum of 5.91 mM at pH 7.35. As with DDEA (Section 5.2), a supersaturation phenomenon was observed at the pH of maximum solubility. The most supersaturated solution detected had a concentration considerably higher than the value for the aqueous solubility of DTRIS obtained from the ampoule solubility method (3.95 mM, Section 6.6.3). This represented a supersaturation level of 1.49. This illustrated that it is possible for salts of diclofenac at the lower end of the solubility range to form supersaturated solutions.

Further addition of TRIS caused a lowering of the solubility to 4.76 mM at pH 7.5. A plateau existed in the profile from pH 7.5 to pH 8.7. The concentration within this pH range (~4.7 mM) was higher than the solubility of DTRIS in water (3.95mM). Further addition of TRIS beyond pH 8.7 resulted in a decrease in the solubility of diclofenac acid. This drop in solubility could be attributed to the common ion effect.

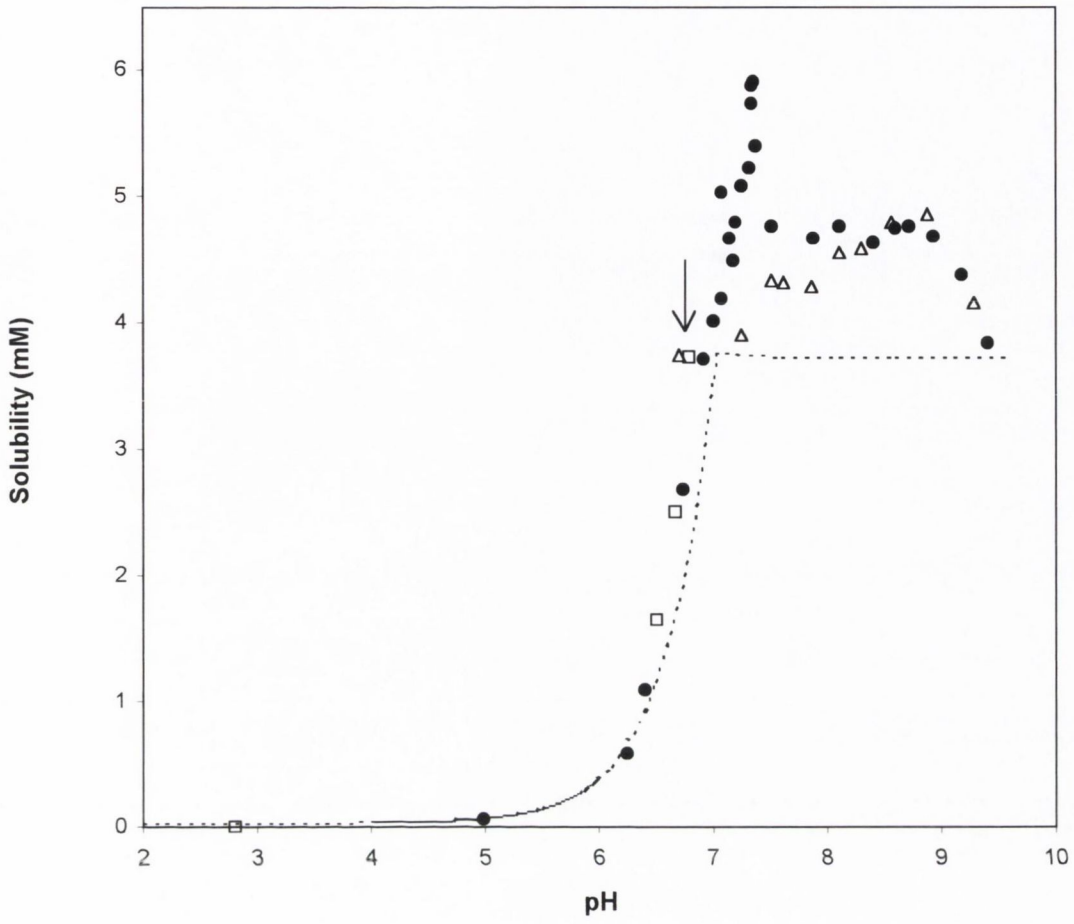

Figure 6. 24 pH-solubility profile of DTRIS: addition of TRIS to diclofenac acid (•), addition of HCl to DTRIS (□) and addition of TRIS to DTRIS (Δ). The arrow indicates the data point representing a saturated solution of DTRIS.

The solubility of DTRIS in water at 25°C was found to be 3.73 mM at pH 6.79 (indicated by the arrow in Figure 6. 24). This value was comparable to the value obtained for the aqueous solubility of DTRIS using the ampoule solubility technique (3.95 mM). As shown in Figure 6. 24, lowering the pH of a saturated solution of the salt with HCl caused a drop in the solubility and precipitation of the free acid. Addition of 0.1 N / 1.0 N TRIS to a saturated solution of DTRIS resulted in an increase in the solubility to a maximum of 4.86 mM at pH 8.9, a solubility which corresponds to the plateau in the profile generated by the addition of TRIS to diclofenac acid. Above this pH, there was a decrease in solubility following further addition of TRIS, thought to be due to the common ion effect.

The theoretical pH-solubility profile for DTRIS, indicated by the broken line in Figure 6. 24, was plotted as described for DDEA (Section 5.2).

6.7. DICLOFENAC 2-(DIMETHYLAMINO)ETHANOL (DDNL)

6.7.1. Physicochemical characterisation of DDNL by XRD, thermal analysis, FT-IR spectroscopy and elemental analysis

Elemental analysis results of the product prepared from diclofenac acid and DNL complied with the theoretical values for a 1:1 salt (Table 6. 9). The FT-IR spectrum of the product was consistent with the formation of a salt from the two components (Figure 15, Appendix II).

Table 6. 9 Elemental analysis results for the DDNL product

Element	*DDNL Theoretical %*	*DDNL product Actual %*
C	56.10	56.08
H	5.77	5.73
N	7.27	7.18

The XRD trace for the product (DDNL) is presented in Figure 6. 25.

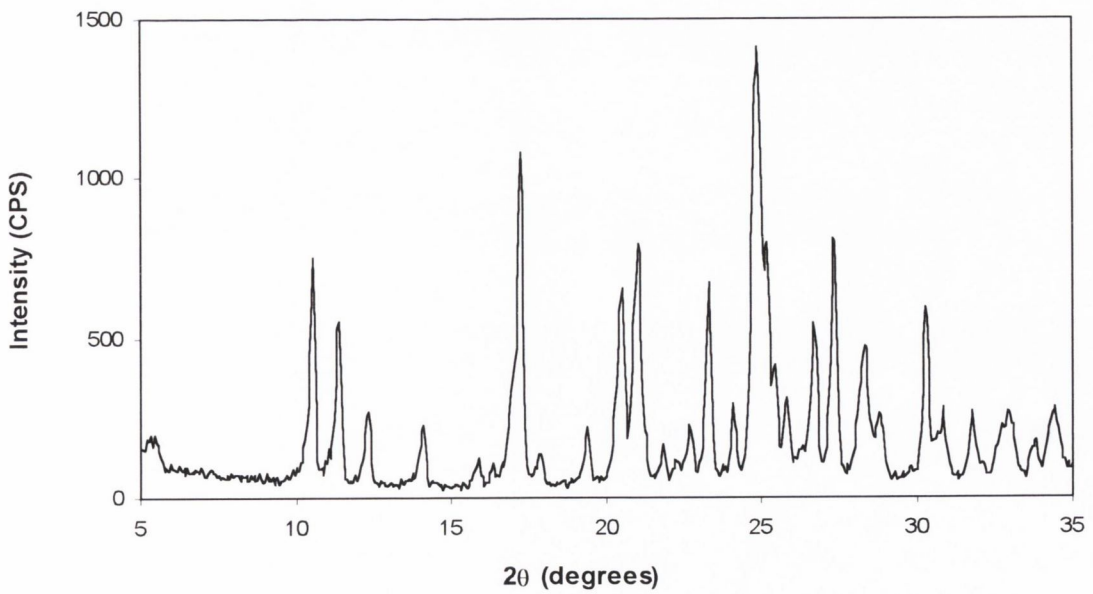

Figure 6. 25 XRD trace for DDNL

The DSC scan for the product (Figure 6. 26) showed two overlapping endotherms before the broad endotherm from ~160°C. The onset temperature of the first endotherm was 105°C. Thermal microscopy revealed melting from ~105°C, followed by crystallisation of crystals from the melt and subsequent re-melting. This crystallisation and melting of the newly formed crystals explained the presence of the second endotherm (peak temperature, 120°C) in the DSC scan. A possible exothermic recrystallisation peak may have been masked because of the occurrence of the two melting endotherms close together. The TG trace (Figure 6. 26) showed an increase in the rate of weight loss from 110°C, resulting in a step corresponding to a weight loss of ~6 %w/w. Analysis by KFT excluded the possibility of water being present in the sample. The weight loss may have corresponded to volatilisation of deanol (b.p. 135°C) from the melt.

In an attempt to isolate the higher melting form, a sample was heated to 113°C (just past the first endotherm) and cooled to room temperature. The XRD and DSC traces of the product after this heating process were found to be identical to the traces shown in Figures 6.25 and 6.26, thus establishing that the melting endotherm at 105°C was reversible. In conclusion, two forms of DDNL were thought to exist; one converted to the other on heating.

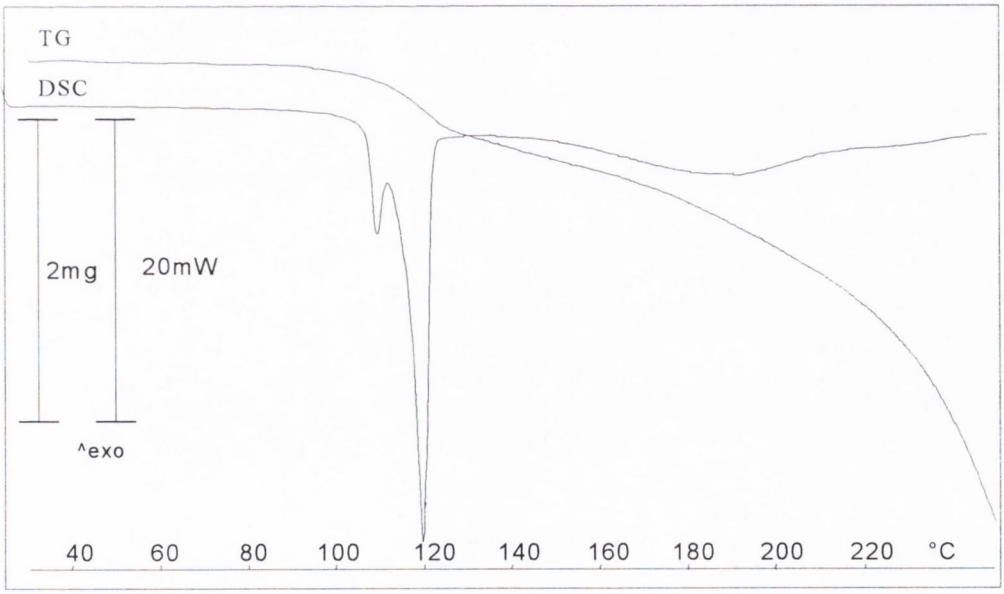

Figure 6. 26 DSC and TG traces for DDNL

6.7.2. *Solubility and intrinsic dissolution rate determination for DDNL*

The solubility of DDNL in water at 25°C was determined as 446.65 ± 14.97 mM. This solubility value was considerably higher than the solubilities determined for the other salts examined. This salt also showed a superior aqueous solubility to DHEP, the most soluble salt form of diclofenac available in pharmaceutical products (273 mM, Ledwidge, 1997). For this reason, the properties of DDNL in solution were investigated further. Its pH-solubility profile and its surface activity were investigated. The membrane transport from a saturated solution of the salt could not be examined; due to the high viscosity of the solution, adequate stirring could not be achieved using the diffusion cell apparatus employed for investigating the membrane transport of DNa, DDEA and DHEP.

The intrinsic dissolution rate of DDNL in water at 25°C was found to be $1.67 \times 10^{-2} \pm 0.03 \times 10^{-2}$ mmol/min/cm^2.

6.7.3. *pH-solubility study of DDNL*

The pH-solubility profile of DDNL was investigated using the method described for DDEA (Section 5.2). The profile is presented in Figure 6. 27. The addition of deanol to a solution of diclofenac acid caused a sharp increase in the solubility of diclofenac acid, resulting in supersaturation relative to the equilibrium solubility of DDNL (447 mM). The supersaturated systems obtained could not be filtered due to their viscous nature. For each supersaturated system analysed, the concentration determination was carried out on the supernatant obtained following centrifugation of the sample as described in Section 3.2.12.1. The maximum point indicated on the graph (pH 9.23) represents a clear gel-like system with no excess solid present. This suggests that the concentration determined (883 mM) was lower than the maximum solubility that could be achieved at the pH_{max}. The supersaturated solution generated had a concentration which was approximately twice that of the aqueous solubility of DDNL determined using the ampoule technique (447 mM) and is comparable to the value obtained by Ledwidge (1997) for the supersaturated solution generated on the addition of *N*-(2-hydroxyethyl)pyrrolidine to diclofenac acid (>800 mM). The addition of diclofenac acid in an attempt to further saturate the solution resulted in viscous, paste-like system; centrifugation of this system did not result in the formation of a supernatant layer.

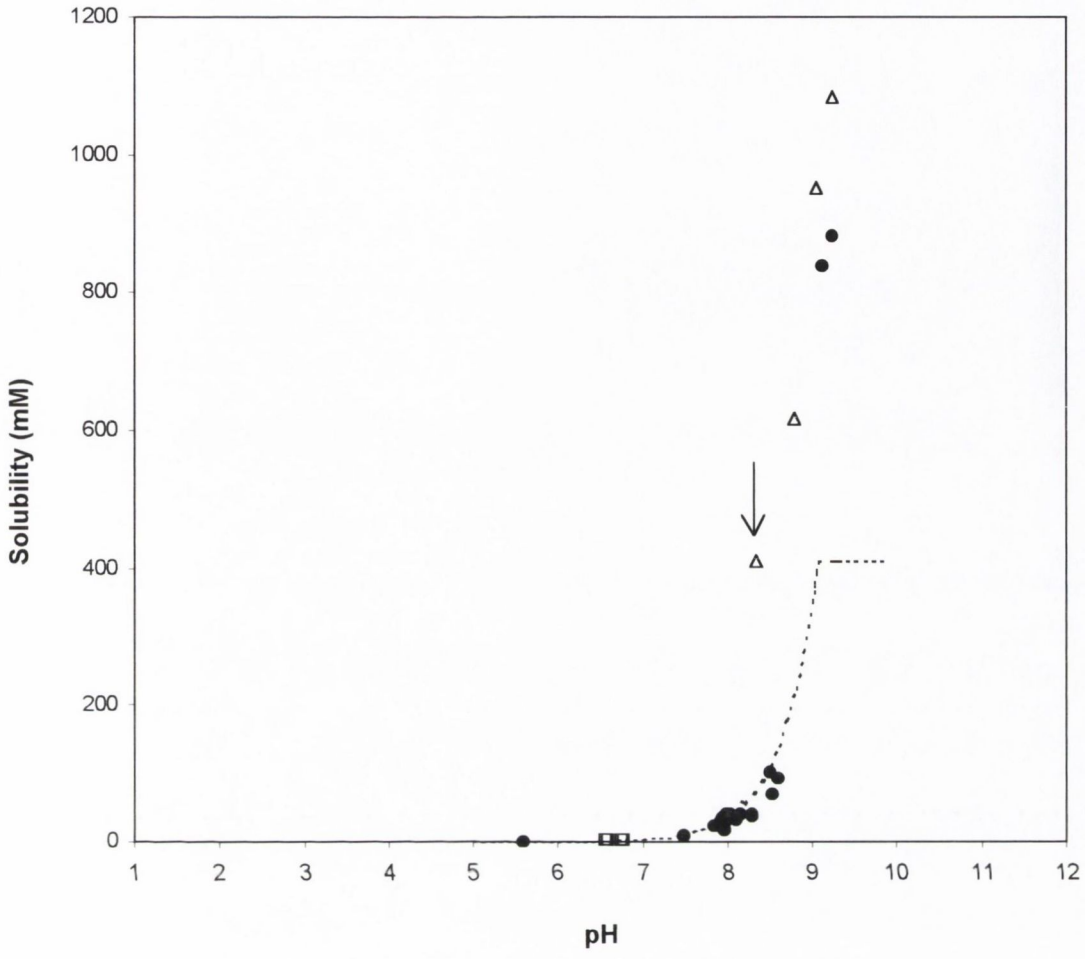

Figure 6. 27 pH-solubility profile for DDNL: addition of DNL to diclofenac acid (•), addition of HCl to DDNL (□) and addition of DNL to DDNL (Δ). The arrow indicates the data point representing a saturated solution of DDNL.

The solubility of DDNL in water at 25°C was found to be 412 mM at pH 8.33 (indicated by the arrow in Figure 6. 27). This value was comparable to the equilibrium solubility determined by the ampoule method (447 mM). As shown in Figure 6. 27, lowering the pH of a saturated solution of the salt with HCl caused a drop in the solubility and precipitation of the free acid. Addition of DNL to a saturated solution of DDNL resulted in a dramatic increase in the solubility with increasing pH. The maximum point shown on the graph (pH 9.23) represents a gel-like system with no excess solid present. The concentration, considered to be lower than the maximum solubility obtainable at this pH, was determined to be 1084 mM. Any further addition of solid resulted in the formation of paste-like systems that could not be centrifuged into two layers.

The theoretical pH-solubility profile, indicated by the broken line in Figure 6. 27, was plotted as described in Section 5.2.

6.7.4. Surface activity and self-association properties of DDNL

Investigation of the surface activity of DDNL involved surface tension measurements of solutions in the concentration range 2.8 to 66.4 mM, as described in Section 3.2.17. The plot of concentration (mM) vs. surface tension (mN/m) for these solutions is plotted in Figure 6. 28; the graph also shows the corresponding plot for DHEP.

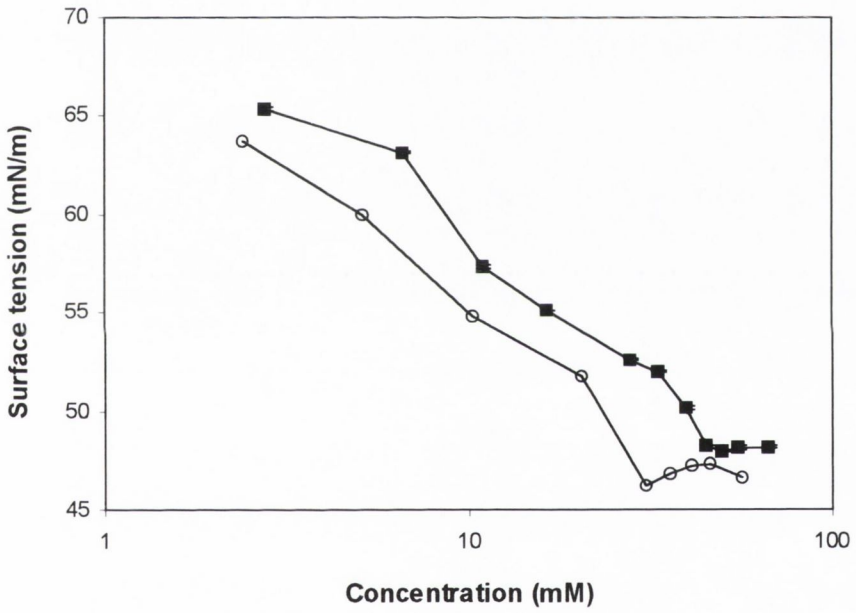

Figure 6. 28 Surface tension (mN/m) vs. concentration (mM) for DDNL (■) and DHEP (O) solutions

A decrease in the surface tension of the DDNL solutions was observed with increasing concentration. At concentrations above 45 mM, the surface tension was independent of concentration, thus indicating a CAC value for the salt of 45 mM.

The results of the solubilisation study, carried out using the water insoluble fluorescent compound *N*-phenyl-1-naphthylamine (NPN), are presented in Figure 6. 29 as fluorescence intensity relative to a 40 mM DHEP solution. Solubilisation of NPN was observed for DDNL solutions at concentrations of 45 mM and higher. This result compares quite well with the CAC value of 45 mM obtained from the surface tension measurements.

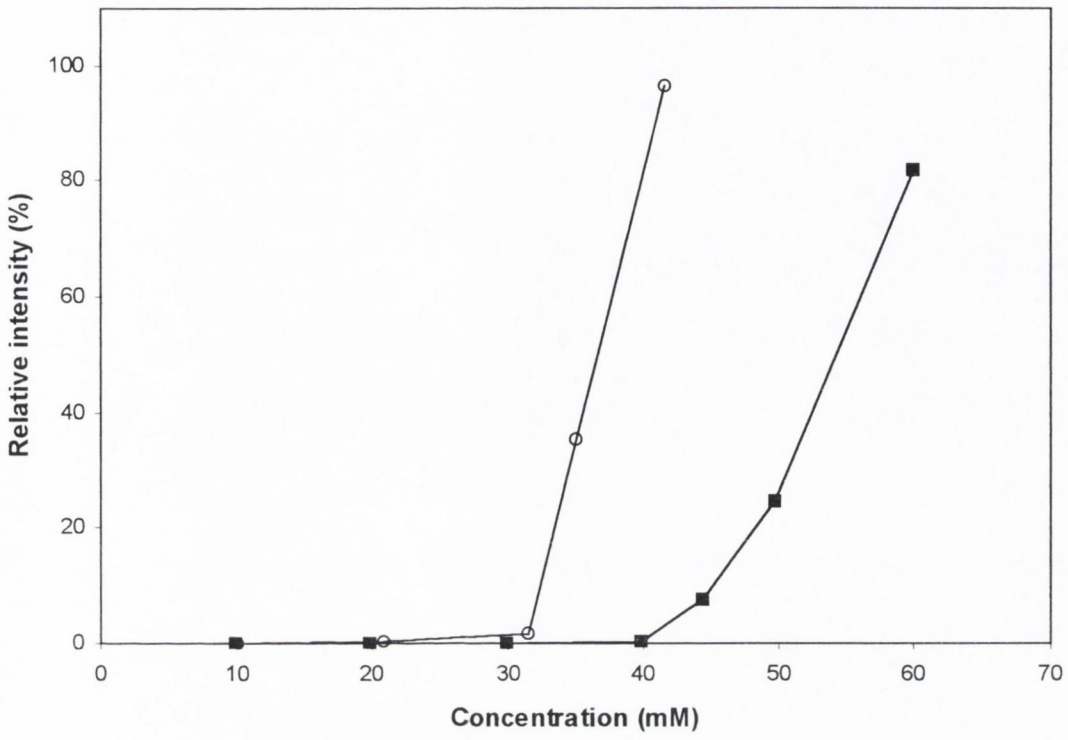

Figure 6. 29 Solubilisation study: DHEP solutions (o) and DDNL solutions (■)

6.8. RELATIONSHIP BETWEEN SOLUBILITY AND INTRINSIC DISSOLUTION RATE FOR THE DICLOFENAC SALTS STUDIED

Several studies have reported a direct relationship between solubilities and intrinsic dissolution rates for a large variety of substances (Parrott et al., 1955; Hamlin et al., 1965; Higuchi et al., 1965a; Nelson and Shah, 1975; Shah and Nelson, 1975; Tsuji et al., 1978; Nicklasson et al., 1981; Nicklasson et al., 1982; Sjökvist Saers and Craig, 1992; Forbes et al., 1995). These solubility-dissolution rate relationships can be used to estimate solubilities where limited amounts of material were available (Nicklasson and Nyqvist, 1983) and to aid salt selection (Forbes et al., 1995).

The solubility, saturated solution pH, apparent solubility product and intrinsic dissolution rate values (in water at 25°C) for the diclofenac salts studied, including DDEA, are summarised in Table 6. 10. Apparent solubility product calculations were carried out as outlined in Section 5.4 (Serajuddin and Mufson, 1985).

Table 6. 10 Solubility and intrinsic dissolution rate data for diclofenac salts in water at 25°C

Salt	*Solubility (mM)*	*pH of saturated solution*	K'_{SP}	*Intrinsic dissolution rate (mmol/min/cm²)*
DAMPD	6.77 ± 0.03	7.24	4.58×10^{-5}	$4.51 \times 10^{-4} \pm 0.07 \times 10^{-4}$
DAMP	21.76 ± 0.25	7.62	4.74×10^{-4}	$1.38 \times 10^{-3} \pm 0.03 \times 10^{-3}$
DBA	4.16 ± 0.04	7.21	1.73×10^{-5}	$4.57 \times 10^{-4} \pm 0.15 \times 10^{-4}$*
DtBA	5.46 ± 0.05	7.45	2.98×10^{-5}	$3.86 \times 10^{-4} \pm 0.09 \times 10^{-4}$
DDEA	34.96 ± 0.65	8.19	1.22×10^{-3}	$1.87 \times 10^{-3} \pm 0.04 \times 10^{-3}$
DDNL	446.65 ± 14.97	8.57	1.99×10^{-1}	$1.67 \times 10^{-2} \pm 0.03 \times 10^{-2}$
DTRIS	3.95 ± 0.04	7.13	1.56×10^{-5}	$2.45 \times 10^{-4} \pm 0.06 \times 10^{-4}$

*this value does not relate to the original solid form of the salt

The plot of solubility against intrinsic dissolution rate is presented in Figure 6. 30. According to the Noyes-Whitney equation (Equation 1.21), under sink conditions the following relationship should apply:

$$G = K C_S \qquad \textbf{Equation 6. 2}$$

where G is the intrinsic dissolution rate, C_S is the solubility and K is the dissolution rate constant. In the current study, the line of best fit through the data (R^2 = 0.9963, n = 7) was found to pass through the origin, in accordance with Equation 6.2 and with previously reported trends (Hamlin et al., 1965; Tsuji et al., 1978). According to the Nernst-Brunner film theory, the slope of the line, K, is equal to D/h, where D is the diffusion coefficient of the solute and h is the diffusion layer thickness. The value obtained for K was $3.76 \times 10^{-2} \pm 0.08 \times 10^{-2}$ cm.min^{-1}.

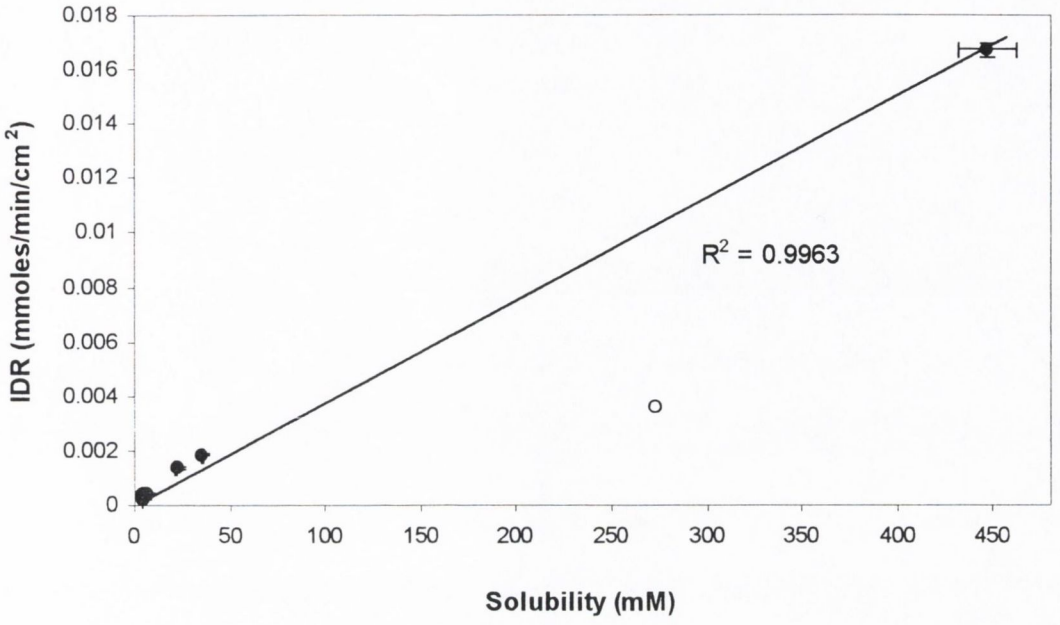

Figure 6. 30 Plot of solubility (mM) versus intrinsic dissolution rate (mmoles/min/cm^2) for the diclofenac salts studied (●). The plot also shows the data point for DHEP (○) (Ledwidge, 1997).

The data reported by Ledwidge (1997) for DHEP (solubility, 273 mM; IDR, 3.62 x 10^{-3} mmol/min/cm^2) was investigated in relation to the solubility-intrinsic dissolution rate plot for the other salts (Figure 6. 30). The data point for DHEP (as indicated by the circle in Figure 6. 30) was found to deviate notably from the trendline for the other diclofenac salts.

When the solubilities are plotted against the intrinsic dissolution rates on a log-log scale, a linear relationship with a slope of 1.0 is expected, in accordance with the following derivation of the Noyes-Whitney equation:

$$\log G = \log K + \log C_s \qquad \textbf{Equation 6. 3}$$

Previous studies have reported linear relationships between log solubility and log dissolution rate, with slopes of unity or close to unity: 1.02 ± 0.04 (Nicklasson et al., 1981), 1.00 ± 0.06 (Nicklasson et al., 1982) and 1.06 (Forbes et al., 1995). Nelson and Shah (1975) and Shah and Nelson (1975) reported slopes of 0.939 and 0.978, respectively, for a plot of log C_S versus log G for a series of alkyl esters of *p*-aminobenzoic acid. The authors proposed that a small change in diffusivity over the ester series might have contributed to the reduced slope.

The log-log plot of solubility against intrinsic dissolution rate for the diclofenac salts is presented in Figure 6. 31. The line of best fit ($R^2 = 0.9854$, n = 7) was found to have a slope of 0.84 ± 0.05. Deviation from the theoretical line with a slope of unity (indicated by the dashed line in Figure 6. 31) indicates lower dissolution rates than expected for the salts with higher solubilities. This may be due to high viscosities of solutions of the higher solubility salts, resulting in a reduction in their diffusion coefficients. According to the Stokes-Einstein equation (Flynn et al., 1974), the diffusion coefficient is inversely related to the viscosity of the medium. The influence of the viscosity of a salt solution on diffusion through the aqueous boundary layer has previously been reported (Nelson, 1957; Morozowich et al., 1962; Serajuddin and Jarowski, 1985b).

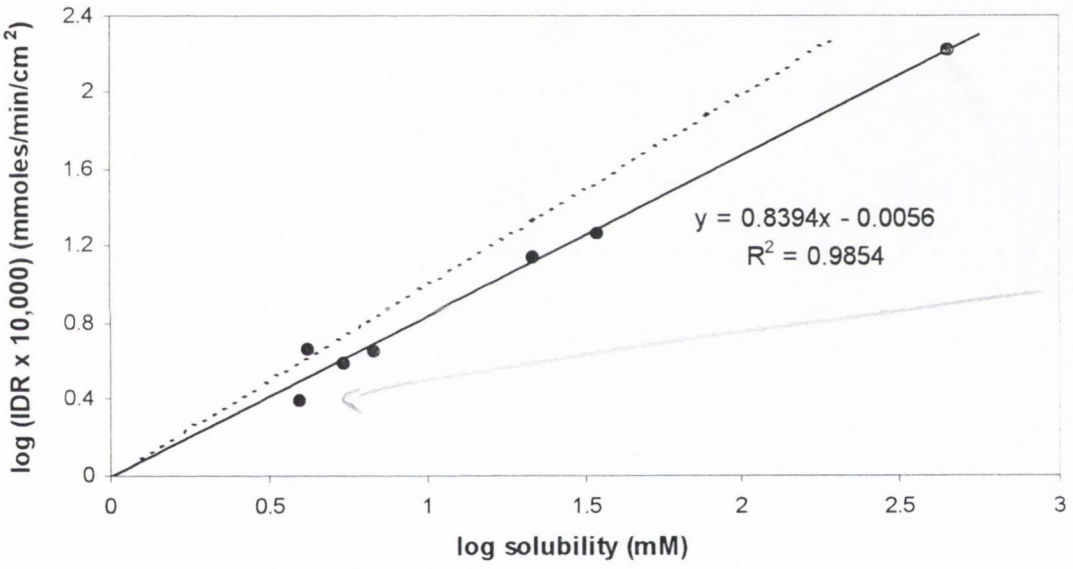

Figure 6. 31 Plot of log solubility (mM) versus log (intrinsic dissolution rate x 10,000) (mmoles/min/cm^2) for the diclofenac salts studied. The dashed line represents the theoretical relationship of slope unity.

6.9. RELATIONSHIPS BETWEEN SALT MELTING POINT / ENTHALPY OF FUSION AND SOLUBILITY FOR THE DICLOFENAC SALTS STUDIED

Thomas and Rubino (1996) reported an inverse linear relationship between salt melting point and the logarithm of salt solubility for a series of secondary amine hydrochloride salts. Ledwidge (1997) reported an identical relationship for a series of CEL50 salts. Gould (1986), on examination of data obtained from a range of salts of a basic antimalarial drug (Agharkar et al.,

1976), reported a direct relationship between the inverse of the melting point and the logarithm of the solubility. Anderson and Conradi (1985) reported a nonlinear relationship between salt melting point and log K_{SP} for a series of flurbiprofen salts. Conversely, Gu and Strickley (1987) concluded that no simple solubility-melting point relationship could be established for tris(hydroxymethyl)aminomethane salts of four anti-inflammatory drugs.

The melting point and enthalpy of fusion values for the diclofenac salts studied, including DDEA and DHEP, are listed in Table 6. 11.

Table 6. 11 Melting point and enthalpy of fusion values (n = 3) for diclofenac salts

Salt	*Melting point* °C	*Enthalpy of fusion (ΔH_f)* J/g
DAMP-I	183.21 ± 2.14	215.55 ± 3.85
DAMPD	179.19 ± 0.70	171.61 ± 8.64
DBA-I	156.25 ± 0.58	125.90 ± 1.69
DtBA	152.37 ± 0.29	10.69 ± 0.33
DDEA	124.65 ± 0.35	28.95 ± 2.98
DDNL	108.46 ± 0.35	21.72 ± 5.63
DHEP	101.95 ± 0.07	94.77 ± 1.45
DTRIS	208.92 ± 0.10	469.43 ± 11.22

Reasonable correlation was found between salt melting point and the logarithm of the solubility (R^2 = 0.6651, n = 8) and between the inverse of the melting point and the logarithm of the solubility (R^2 = 0.7780, n = 8). The correlation was poor between the enthalpy of fusion of the salt and the solubility (R^2 = 0.1489, n = 8) or the logarithm of the solubility (R^2 = 0.2145, n = 8).

6.10. EXPLORATION OF RELATIONSHIPS BETWEEN PROPERTIES OF THE SALT-FORMING AGENT AND THOSE OF THE RESULTING SALT FORM

In accordance with the linear relationship between conjugate acid melting point and salt melting point reported for a series of salts of UK47880 (Gould, 1986), examination of the data for the diclofenac salts revealed reasonable correlation (R^2 = 0.7518, n = 7) between base melting point

and salt melting point (Figure 6. 32). However, poor correlation ($R^2 = 0.1695$, n = 7) was observed between base melting point and salt solubility. This lack of correlation is in accordance with the results obtained by Ledwidge (1997) for a series of CEL50 salts.

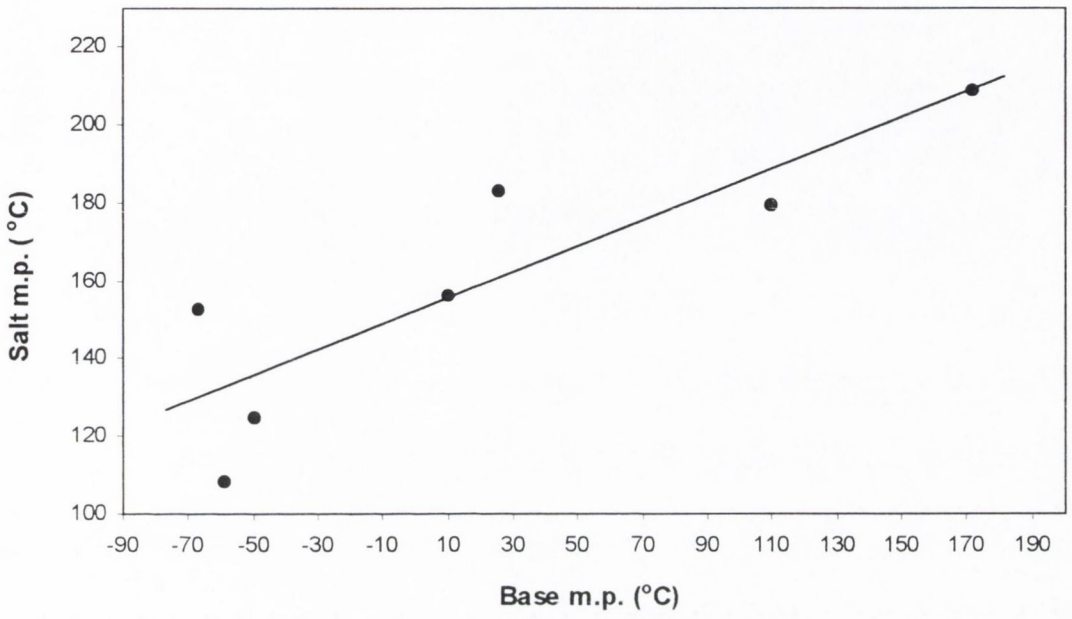

Figure 6. 32 Base melting point versus salt melting point for the diclofenac salts studied

Ledwidge (1997) reported poor correlation between counter-acid pK_a and salt solubility for a series of CEL50 salts. Accordingly, no correlation was found ($R^2 = 0.0040$, n = 8) for the relationship between base pK_a and salt solubility for the diclofenac salts.

The study by Ledwidge (1997) revealed a linear relationship between final solution hydrogen ion concentration, $[H^+]$, and salt solubility. Examination of the data obtained for the diclofenac salts revealed a linear log-log relationship between $[H^+]$ and salt solubility ($R^2 = 0.8957$, n = 8). The pH of the saturated solution is plotted against the logarithm of salt concentration in Figure 6. 33.

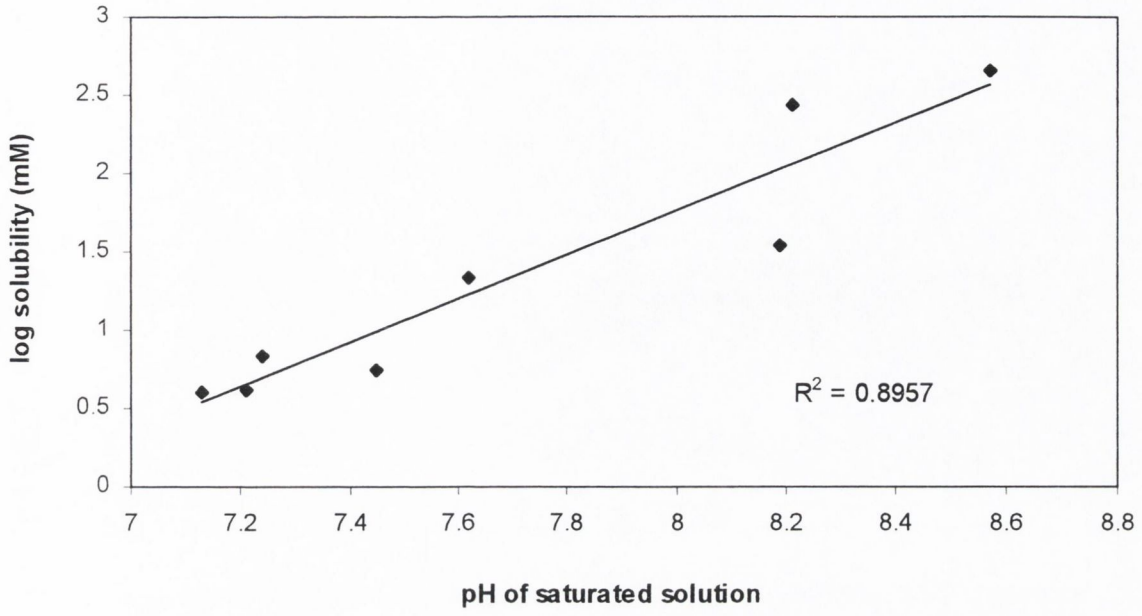

Figure 6. 33 pH of the saturated solution versus solubility of the salt for the diclofenac salts studied

The solubility and saturated solution pH values obtained for each of the salts is plotted in relation to the theoretical pH-solubility curves in Figure 6. 34. The theoretical curves were derived from Equation 1.14, using values of 0.037 mM and 5.02 for intrinsic solubility and pK_a', respectively (Ledwidge, 1997).

Whereas the data points for most of the salts are consistent with the expected pH-solubility relationship, the solubility values for DDNL and DHEP are considerably higher than expected given the pH of their saturated solutions. Similar deviations from their theoretical pH-solubility profiles have been reported for the salts of acidic (Roseman and Yalkowsky, 1973; Chowhan, 1978; Serajuddin and Jarowsky, 1985b) and basic (Serajuddin and Rosoff, 1984; Serajuddin and Jarowski, 1985a; Serajuddin and Mufson, 1985) compounds. As a result of these deviations, estimation of the apparent pK_a from the pH-solubility data would result in a lower (in the case of an acidic compound) or higher (for a basic compound) value than the theoretical value for the pK_a of the acid or base.

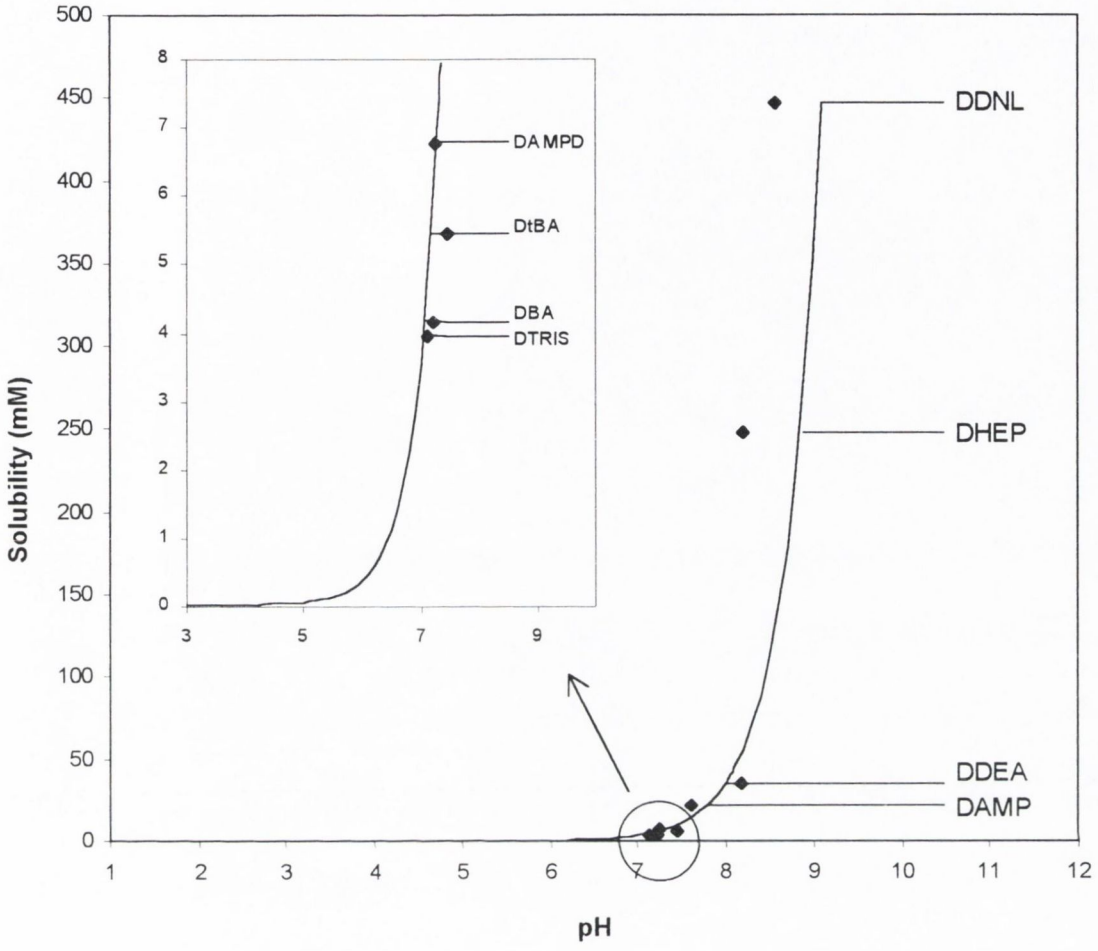

Figure 6. 34 pH of the saturated solution versus solubility for each of the diclofenac salts. The lines represent the theoretical pH-solubility profiles.

In line with previous findings, deviation of the data points for DHEP and DDNL from the theoretical line (Figure 6. 34) indicated an apparent $pK_a^{'}$ value lower than 5.02. Equation 1.14 was used to fit a pH-solubility curve to the DDNL and DHEP data. The value for intrinsic solubility was fixed at 0.037 mM (Ledwidge, 1997); a value of 4.47 ± 0.04 was obtained for the $pK_a^{'}$. The theoretical curve obtained using this lower $pK_a^{'}$ is plotted in relation to the theoretical curve plotted using a $pK_a^{'}$ value of 5.02 (Figure 6. 35).

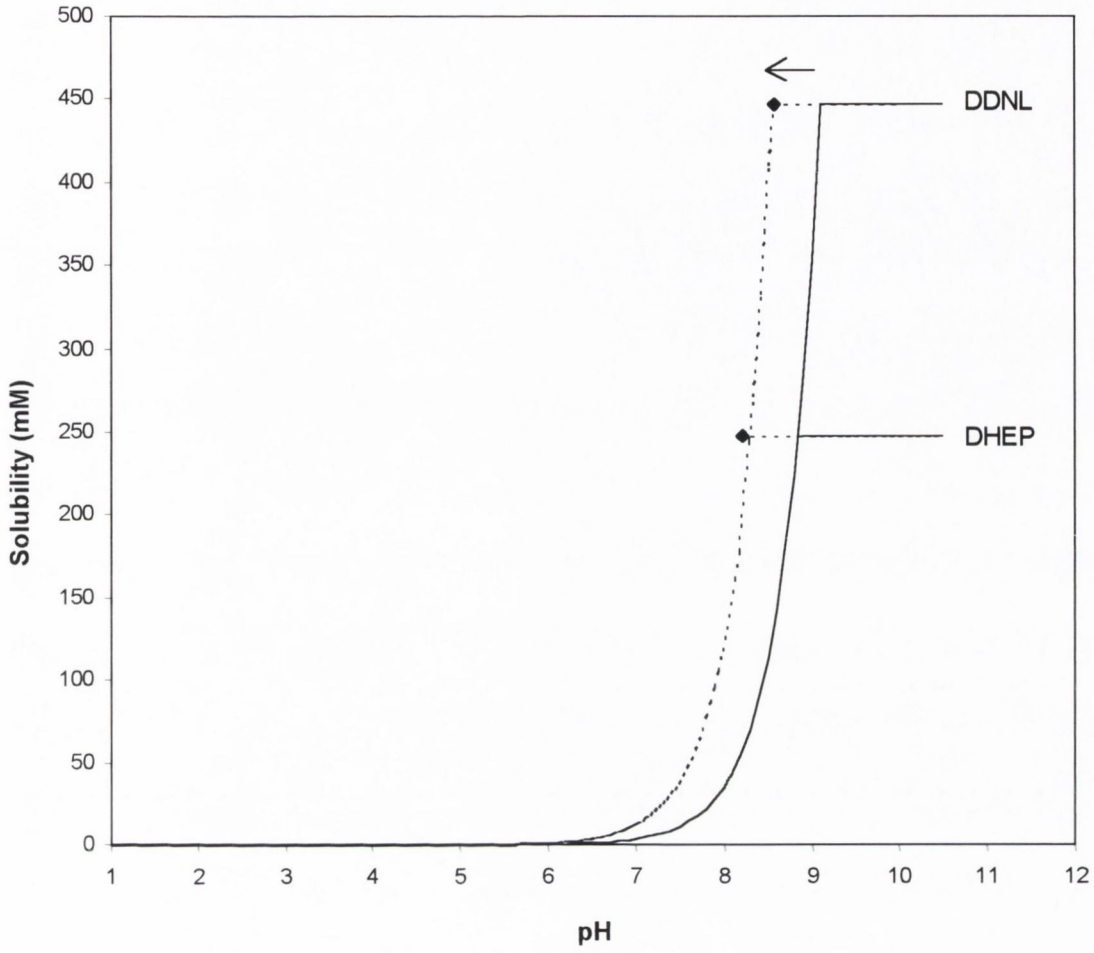

Figure 6. 35 Saturated solution pH versus solubility for DHEP and DDNL, in relation to theoretical pH-solubility profiles derived using pK_a' values of 5.02 (—) and 4.47 (·····)

Roseman and Yalkowsky (1973) investigated the pH-solubility behaviour of the tromethamine salt of prostaglandin $F_{2\alpha}$ ($PGF_{2\alpha}$) and observed that at pH values above 5, there was a marked increase in solubility, significantly greater than would be expected from the ionisation constant of the acid. This behaviour was attributed to the formation of micelles that solubilise the drug once critical concentration and pH values are reached. Using potentiometric titration, they determined the pK_a of $PGF_{2\alpha}$ in aqueous media to be 4.90. Above the CMC, the potentiometrically-determined pK_a increased as a function of concentration to a maximum value of 5.6. These findings were consistent with the behaviour of other surfactant systems, such as bile acids (Ekwall, 1957a and 1957b; Small, 1986) and carnithine (Yalkowsky and Zografi, 1970). Roseman and Yalkowsky (1973) plotted concentration versus observed pK_a and showed that the point at which the pK_a deviated from the value of 4.90 was in agreement with the CMC determined by the drop volume

technique. They postulated that the higher pK_a of the micellar $PGF_{2\alpha}$ compared to the monomer was due to the negative carboxyl groups in the micelle being closer to one another than they are in free solution. They reasoned that the accumulation of negative charges on the micellar surface placed each individual carboxylate in a negatively charged environment, resulting in more protons in the vicinity of each carboxyl group. Therefore, deprotonation of each group was inhibited and the observed pK_a increased.

The phenomenon of higher observed pK_a values above the CMC could also be considered in terms of the experimental method and the equilibrium involved:

$$HA + H_2O \longleftrightarrow A^- + H_3O^+ \qquad \textbf{Equation 6. 4}$$

where HA is the free acid and A^- is the ionised form. Potentiometric titration (Roseman and Yalkowsky, 1973) involved the gradual addition of 1.0 N HCl to aqueous solutions of different concentrations of the salt form and measurement of the resulting pH. At concentrations above the CMC, association of the ionised molecules, A^-, into micelles resulted in the solubilisation of the protonated acid, HA. Thus, HA was effectively removed from the aqueous system, causing a shift of the equilibrium (Equation 6.4) to the left. This resulted in a reduction in $[H_3O^+]$ and an increase in the measured pH. Therefore, plots of fraction of total titrant (β) versus pH were shifted upwards on the pH axis (Roseman and Yalkowsky, 1973) and the observed pK_a was higher than that measured at concentrations below the CMC.

In the current study and previous studies (Roseman and Yalkowsky, 1973; Chowhan, 1978; Serajuddin and Jarowsky, 1985b), the apparent reduction in the pK_a' value observed in the pH-solubility profiles can be attributed to the technique used in estimating the pK_a' and consideration of the equilibrium involved (Equation 6.4). The apparent dissociation constant, K_a', is given by:

$$K_a' = \frac{[H_3O^+][A^-]}{[HA]} \qquad \textbf{Equation 6. 5}$$

where [X] denotes the concentration of species X. The association of the ionised molecules, A^-, into micelles resulted in the solubilisation of the protonated acid, HA, causing an increase in the effective concentration of HA. The method used in this study to estimate pK_a' involved application of Equation 1.14, which describes the pH-solubility relationship for a weak acid at pH

values less than the pH_{max}. This equation assumes that the solubility of the free acid is limiting and that the increase in solubility with increasing pH is due to increasing $[A^-]$. Solubilisation of HA due to micelle formation resulted in an overestimation of the contribution of $[A^-]$ to the total solubility, C_S, and an exaggerated value for the ratio of ionised to unionised forms of the acid, $[A^-]/[HA]$, was obtained. From Equation 6.5, it can be seen that the calculated $K_a^{'}$ value is therefore an overestimation, resulting in an observed $pK_a^{'}$ value lower than the true value.

The octanol-water partition coefficient (log P) of each base, an indicator of base hydrophilicity, was estimated using fragment constants (Hansch and Leo, 1979) and is listed in Table 6. 12. No significant correlation was found between diclofenac salt solubility and counterion hydrophilicity (R^2 = 0.0127, n = 8). This is in accordance with results of the study by Anderson and Conradi (1985) on a series of flurbiprofen salts.

The volume and surface area values (*in vacuo* and in water) for the bases used in the preparation of diclofenac salts, determined using molecular modelling (Section 3.2.19), are listed in Table 6. 12. No correlation between counterion volume or surface area values and solubility was found.

Table 6. 12 Volume and surface area (*in vacuo* and in water) and log P values estimated for the basic counterions used to prepare diclofenac salts

Compound	*Volume ($Å^3$)*		*Surface area ($Å^2$)*		*log P*
	In vacuo	*In water*	*In vacuo*	*In water*	
AMP	124.87	125.31	148.52	149.66	1.04
AMPD	135.45	136.04	156.86	159.70	0.89
BA	141.72	142.21	161.56	162.86	1.69
DEA	114.76	116.05	144.22	144.00	1.17
DNL	125.68	127.43	151.24	155.74	0.92
HEP	131.53	153.72	151.81	176.35	1.33
tBA	113.94	115.12	139.20	141.38	1.19
TRIS	146.08	146.10	166.51	168.27	0.74

The data for the salts prepared from the series of four-carbon primary amines, tBA, AMP, AMPD and TRIS (Figure 6. 1), is summarised in Table 6. 13. As can be observed from the data, no

general trends exist between counterion properties, hydrophilicity, melting point and pK_a, and salt solubility.

The rank order of solubilities was found to be DAMP > DAMPD > DtBA > DTRIS. Anderson and Conradi (1985) prepared flurbiprofen salts using the same series of bases and reported a rank order of AMPD > TRIS ≅ AMP > tBA for their solubilities.

Table 6. 13 Counterion and salt properties for the series of four-carbon primary amines

Base	*No. of hydroxyl groups*	*Base pK_a*	*Base m.p. (°C)*	*Salt m.p. (°C)*	*pH of saturated solution**	*Salt solubility* (mM)*
tBA	0	10.69	-66.9	152.37	7.45	5.46
AMP	1	9.69	25.5	183.21	7.62	21.76
AMPD	2	8.80	110	179.19	7.24	6.77
TRIS	3	8.30	171.5	208.92	7.13	3.95

* in water at 25°C

The most hydrophilic counterion within the series, TRIS, resulted in the salt of lowest solubility. This is contrary to the expected trend of an increase in water solubility with increasing hydroxylation, or hydrophilicity, of the base. However, the hypothesis that greater hydrophilicity of the counterion results in greater water solubility of the resulting salt neglects the possibility of stronger interactions in the crystal due to increased polarity of the counterion. DTRIS has the highest melting point (209°C) within the series. Therefore, its low water solubility can be attributed to its strong crystal lattice. The strength of the crystal lattice can be attributed to the symmetry of the counterion (Gould, 1986; Anderson and Flora, 1996) and hydrogen bonding within the crystal. Fini et al (1995a) studied the solubility of a range of diclofenac salts, including salts prepared using monoethanolamine, diethanolamine, triethanolamine and TRIS. They reported that the presence of hydroxyl groups in the ethanolamine cations did not result in an improvement in salt solubility. Furthermore, the increase in hydroxyl group number within the group was not reflected in an increase in solubility. TRIS, with three hydroxyl groups, resulted in the salt of lowest solubility within the group. These observations were attributed to intermolecular hydrogen bond interactions existing in the solid state. Also, in the case of diclofenac salts, the influence of intramolecular hydrogen bonding needs to be considered (Fini et al., 1996). In a previous study,

Dhanaraj and Vijayan (1987) examined the crystal structure of the meclofenamic acid:ethanolamine 1:1 salt in the solid state and reported that the hydroxyl group of the cation interacted via a hydrogen bond with the carboxylate group of the anion. Since meclofenamic acid closely resembles diclofenac acid in molecular structure, it was not surprising that this type of hydrogen bond was found to exist in salts of diclofenac containing cations carrying the hydroxyethyl moiety (Castellari and Sabatino, 1994). Therefore, the overall hydrophilicity of the salts was masked by internal interactions and their affinity for polar solvents was reduced.

The salt displaying the highest water solubility within the series (21.76 mM) is that of AMP, the base with one hydroxyl group. The melting point determined for DAMP (183°C) is the second highest of the four salts. Therefore, the high aqueous solubility of the salt cannot be attributed to either the hydrophilicity of the base or weak crystal lattice forces in the salt.

The pK_a of TRIS (8.30) is the lowest in the series and the pH of a saturated solution of DTRIS (7.13) is lower than the values obtained for the other salts in the series. The low solubility of DTRIS is therefore consistent with the linear relationship between pH of the saturated solution and the logarithm of the solubility of the salt (Figure 6. 33). In accordance with this trend, the pH of a saturated solution of DAMP, the most soluble salt, is higher than the pH of the solutions of the other salts in the series, despite the pK_a of AMP being one unit lower than that of tBA.

In summary, the solubility of the salts of diclofenac and the four-carbon primary amines has not been shown to be dependent on any one parameter, but on a combination of factors such as salt crystal lattice strength and the pH of the saturated salt solution.

Chapter 7

The effect of basic organic compounds on the dissolution of diclofenac salts

7.1. INTRODUCTION

Excipients may play an active part in altering the effectiveness of formulations (Kalinkova, 1999). As outlined in Chapter 1, several studies have investigated the mechanism of dissolution from acidic drug:acidic excipient physical mixes, in water (Shah and Parrott, 1976), in phosphate buffer (Ramtoola, 1988; Healy, 1995) and in an acidic medium (Higuchi et al., 1965b). Studies on the influence of basic excipients (Levy et al., 1965; McGloughlin, 1989) or buffering agents (Javaid and Cadwallader, 1972; Doherty and York, 1989; Tirkonnen et al., 1995; Chakrabarti and Southard, 1997; Preechagoon et al., 2000) on the dissolution of acidic drugs have been reported. The effect of acidic excipients on the dissolution of salts of basic drugs has also been investigated (Ventouras et al., 1977; Ventouras and Buri, 1978; Gruber et al., 1980; Cleary, 1987; McNamara, 1988; Thoma and Zimmer, 1990; Kohri, 1991; van der Veen et al., 1991a and 1991b; Gabr, 1992; Thoma and Ziegler, 1998; Streubel et al., 2000).

The objective of this study was to investigate the effect of a basic excipient on the dissolution of a salt of a weakly acidic drug. The dissolution behaviour in water of diclofenac salt:basic excipient compressed discs was studied.

7.1.1. Properties of the diclofenac salts and solid organic bases employed in the study

Two diclofenac salts, diclofenac deanol (DDNL) and diclofenac *tert*-butylamine (DtBA), were selected for the study. The salt of deanol (DNL), a tertiary four-carbon amine (Figure 6.2), has the highest intrinsic dissolution rate (in water at 25°C) of all the salts investigated (Section 6.7.2). DtBA, prepared from a primary four-carbon amine (Figure 6.1), has one of lowest dissolution rates of the salts studied (Section 6.2.2). The solubility and intrinsic dissolution rate values and the calculated diffusion coefficient values for these two salts are summarised in Table 7. 1. The diffusion coefficient calculated for DDNL (2.49×10^{-4} cm^2/min) was notably lower than that calculated for DtBA (4.70×10^{-4} cm^2/min). The diffusion coefficient of a solute has been shown to be inversely proportional to the cube root of its molar volume (Equation 1.72). The difference in diffusion coefficient values between DDNL and DtBA could not accounted for by the difference in the volumes of the two counterions in water: 127.43 Å^3 and 115.12 Å^3 for DNL and tBA, respectively (estimated as described in Section 3.2.19). In Chapter 6, the solubility-dissolution rate relationship for a range of diclofenac salts was investigated (Section 6.8). In the case of salts with solubilities at the higher end of the range, lower dissolution rates than expected, given their solubility values, were reported. This was attributed to the high viscosities of the salt solutions, resulting in a reduction in their diffusion coefficients. Accordingly, the lower diffusion coefficient

value for DDNL is thought to be due to the high viscosity of a saturated DDNL solution, resulting in hindered diffusion within the boundary layer.

Table 7. 1 Solubility (C_S), intrinsic dissolution rate (G) and diffusion coefficient (D) values (25°C) for the diclofenac salts used in the study

Salt	C_S		*G*	*D**
	mg/ml	*mM*	*mmoles/min/cm²*	*cm²/min*
DtBA	2.02 ± 0.02	5.46 ± 0.05	$3.86 \times 10^{-4} \pm 0.09 \times 10^{-4}$	4.70×10^{-4}
DDNL	172.09 ± 5.77	446.65 ± 14.97	$1.67 \times 10^{-2} \pm 0.03 \times 10^{-2}$	2.49×10^{-4}

*calculated from the Nernst-Brunner equation (Equation 1.25), using a h value of 66.46×10^{-4} cm (Appendix VI)

Of the six bases used to prepare salts with diclofenac (Chapter 6), the two that exist in the solid state at room temperature, 2-amino-2-methyl-1,3-propanediol (AMPD) and tris(hydroxymethyl)aminomethane (TRIS), were used as basic excipients in the dissolution study. The two bases are four-carbon primary amines, with two (AMPD) and three (TRIS) hydroxyl groups (Figure 6.1). Their physical properties are listed in Table 6.2.

TRIS was previously employed in a study of the dissolution from mechanical mixtures of an acidic drug and a basic excipient (McGloughlin, 1989). It was also used to modify the microenvironmental pH in hydrochlorothiazide capsule (Adesunloye and Stach, 1998) and tablet (Gabr and Borg, 1999) formulations.

7.2. SOLUBILITY AND DISSOLUTION RATE DETERMINATIONS FOR AMPD AND TRIS

The solubility (gravimetric solubility method, Section 3.2.12.3) and intrinsic dissolution rate values of AMPD and TRIS were determined in water at 25°C. The values obtained and the calculated diffusion coefficient (D) values for the bases, are listed in Table 7. 2.

The solubility of AMPD has been reported in terms of 250 g of the compound dissolving in 100 ml water at 20°C (Dean, 1987). In this study, the solubility value obtained for AMPD (726 mg/ml) corresponded to 264 g of the solid dissolving in 100 ml water.

The literature value for the solubility of TRIS in water at 25°C is 550 mg/ml (*Merck Index*, 1996). The value obtained for the solubility of TRIS in water at 25°C (481 mg/ml) was comparable with this value.

Table 7. 2 Solubility (C_S), intrinsic dissolution rate (G) and diffusion coefficient (D) values (25°C) for the solid organic bases used in the study

Base	C_S		*G*	*D**
	mg/ml	*mM*	*mmoles/min/cm²*	*cm²/min*
AMPD	725.47 ± 31.54	6900 ± 300	$2.18 \times 10^{-1} \pm 0.09 \times 10^{-1}$	2.10×10^{-4}
TRIS	480.93 ± 7.27	3970 ± 60	$1.58 \times 10^{-1} \pm 0.07 \times 10^{-1}$	2.65×10^{-4}

*calculated from the Nernst-Brunner equation (Equation 1.25), using a h value of 66.46×10^{-4} cm (Appendix VI)

7.3. DISSOLUTION OF DICLOFENAC FROM AMPD:DTBA SYSTEMS

AMPD is the more soluble of the two bases employed in the study and DtBA is a diclofenac salt of low solubility (5.46 mM). AMPD:DtBA systems with AMPD weight fractions in the range 12 – 98% were studied. The dissolution profiles are presented in Figure 7. 1. The dissolution rates calculated from these profiles are listed in Table 1, Appendix VII. Little enhancement in dissolution rate was observed for the systems prepared with 12 – 90% AMPD. Dissolution of diclofenac was fastest from the 95:5 and 98:2 systems.

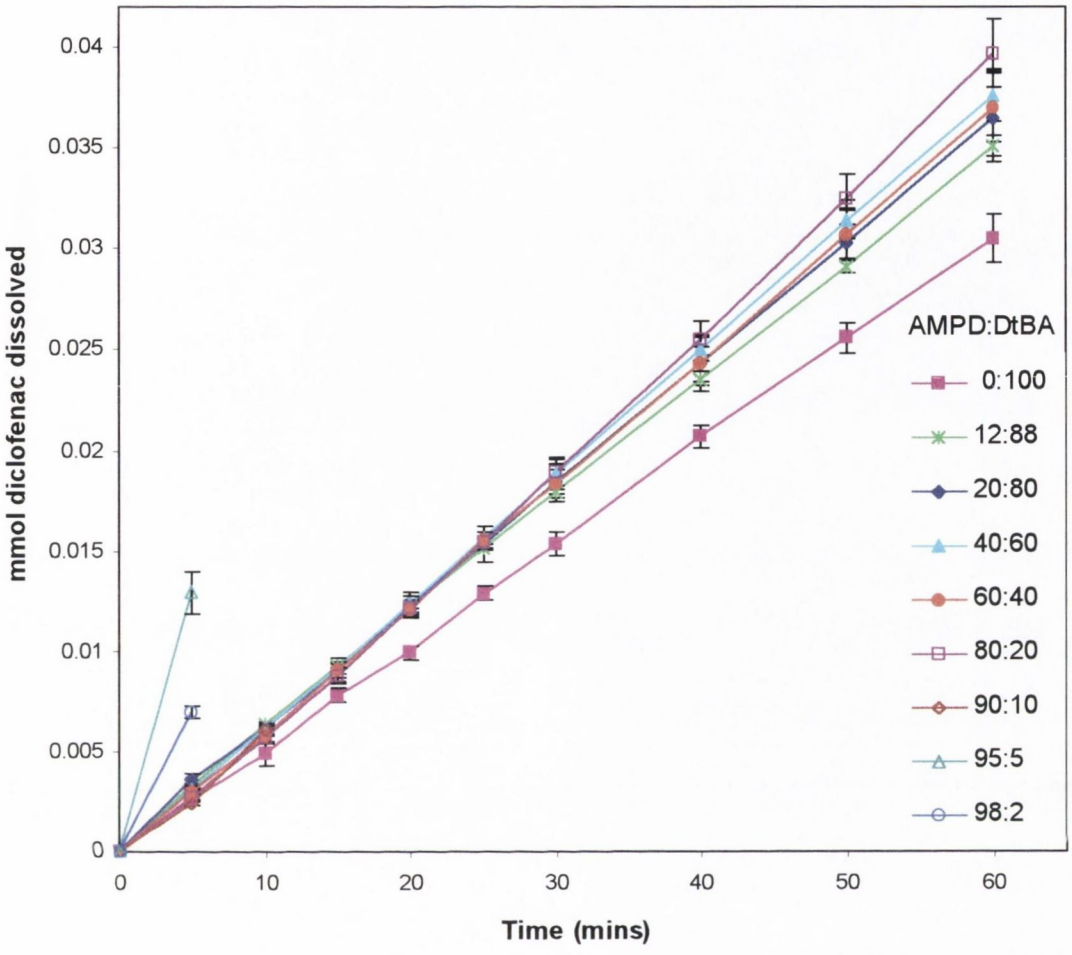

Figure 7. 1 Dissolution of diclofenac from AMPD:DtBA discs

7.3.1. XRD analysis of mechanical mixes and discs before and after dissolution

XRD analysis was carried out on (a) mechanical mixes, (b) discs before dissolution and (c) discs after dissolution for the 40:60, 60:40 and 95:5 AMPD:DtBA systems. For each system, the XRD trace for the disc before dissolution exhibited peaks at the same 2θ values as the trace for the corresponding mechanical mix. The XRD trace for each disc after dissolution was compared with the trace for the corresponding disc before dissolution (Figure 7. 2 – Figure 7. 4).

The traces for the 40:60 AMPD:DtBA discs are presented in Figure 7. 2. Additional peaks were observed in the trace for the disc after dissolution, as illustrated by the arrows in Figure 7. 2.

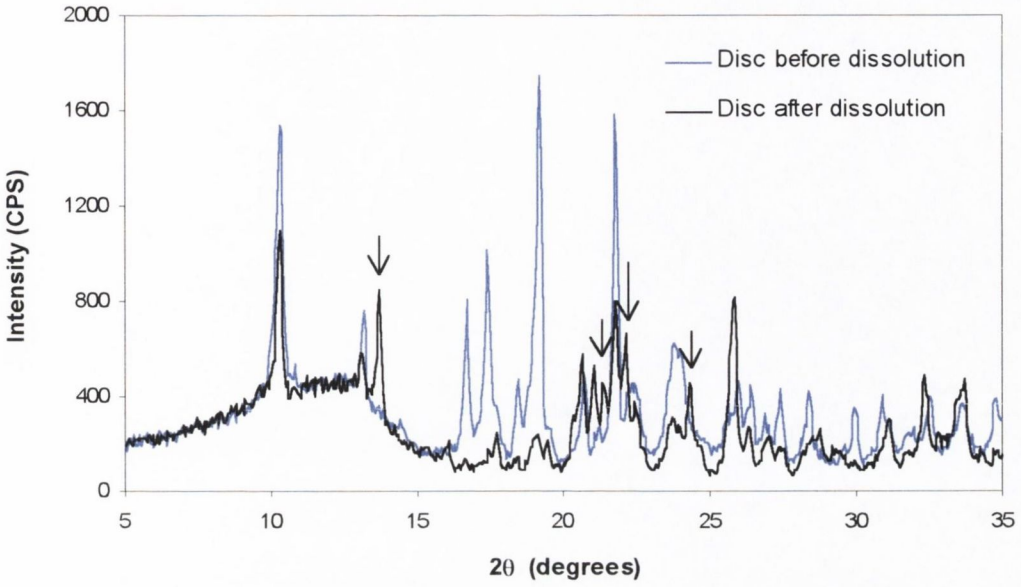

Figure 7. 2 XRD traces for AMPD:DtBA 40:60 discs before and after dissolution

The traces for the 60:40 AMPD:DtBA discs are presented in Figure 7. 3. As with the 40:60 system, additional peaks were observed in the trace for the disc after dissolution, as illustrated by the arrows in Figure 7. 3.

The traces for the 95:5 AMPD:DtBA discs are presented in Figure 7. 4. The trace for the disc after dissolution was found to have identical peaks to that of the disc before dissolution. The peak at 10.30° in the XRD trace of the disc before dissolution, which is characteristic of DtBA, was absent in that of the disc after dissolution.

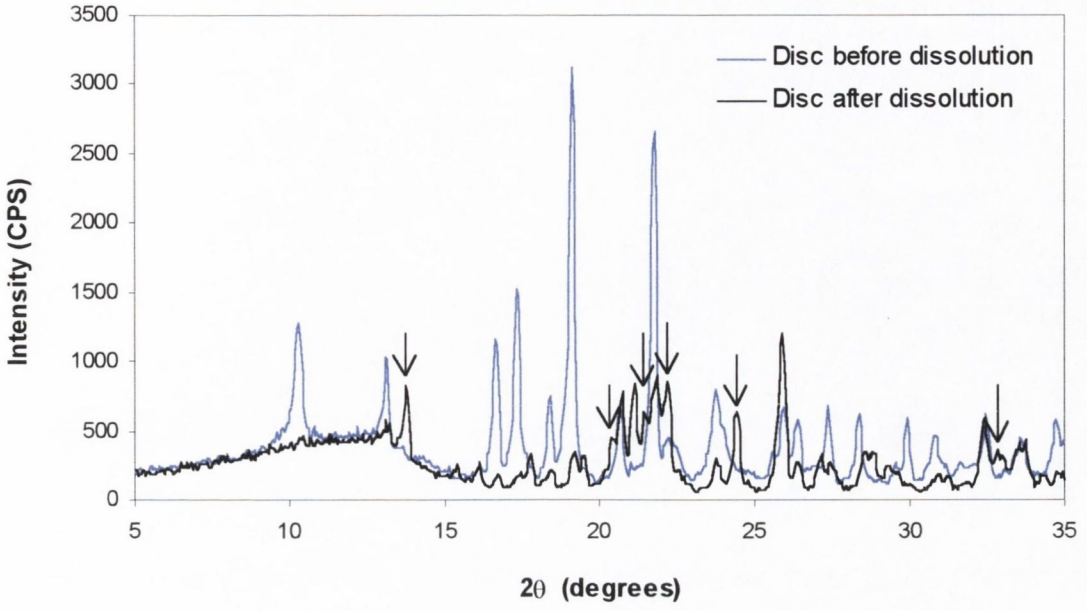

Figure 7. 3 XRD traces for AMPD:DtBA 60:40 discs before and after dissolution

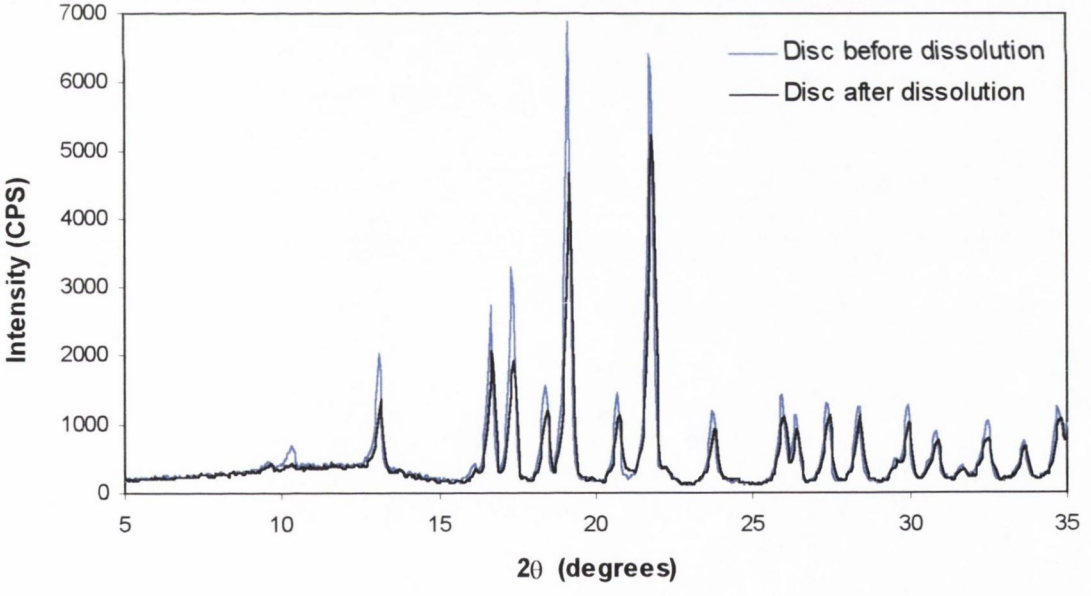

Figure 7. 4 XRD traces for AMPD:DtBA 95:5 discs before and after dissolution

The XRD traces for AMPD:DtBA 40:60 and 60:40 discs after dissolution were examined with reference to the traces for AMPD, DtBA, DAMPD anhydrate and DAMPD monohydrate (DAMPD-MH) (Figure 7. 5). The presence of the extra peaks in the traces for the 40:60 and 60:40 systems was consistent with the formation of DAMPD-MH in the disc.

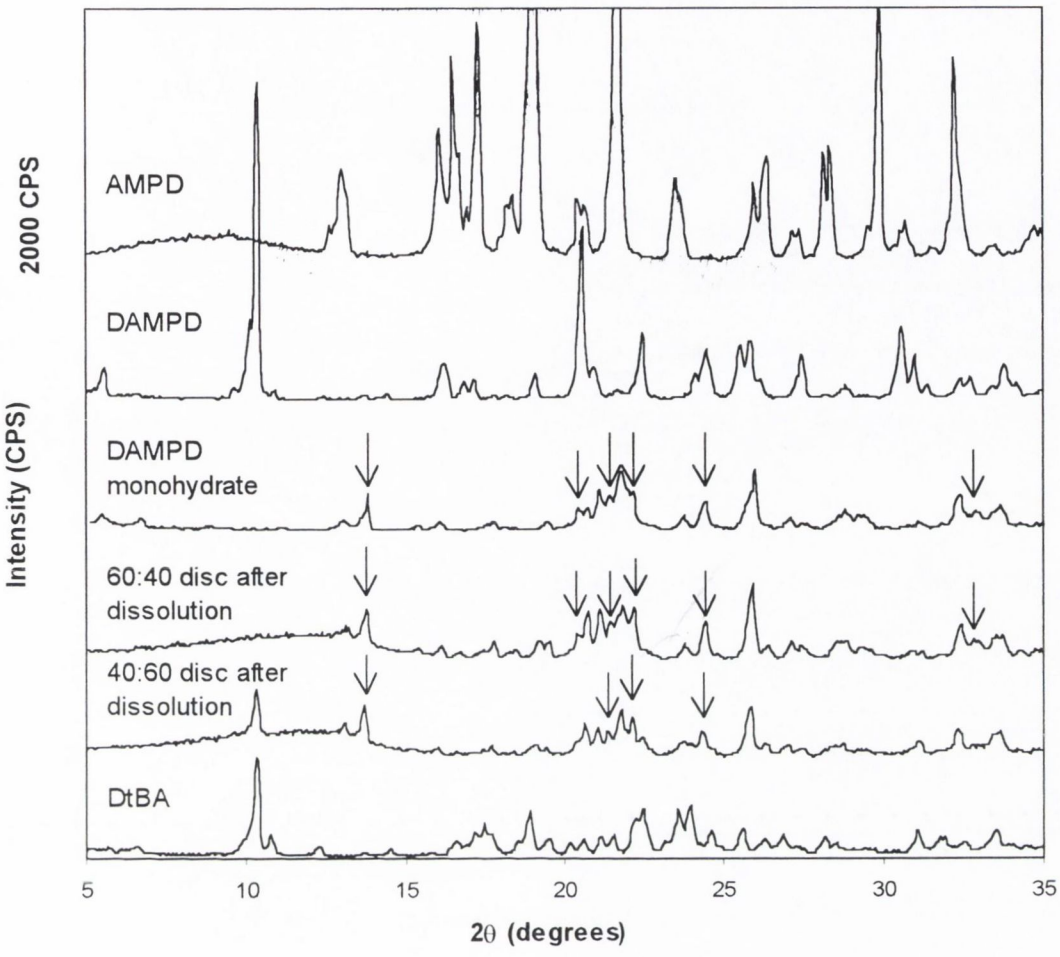

Figure 7. 5 XRD traces for the AMPD:DtBA 40:60 and 60:40 discs after dissolution compared with traces for AMPD, DtBA, DAMPD anhydrate and DAMPD-MH; the arrows indicate peaks which were not present in traces of the discs before dissolution; they correspond to peaks on the DAMPD-MH trace, as illustrated

DAMPD-MH may also have been present in the 95:5 AMPD:DtBA system. However, due to the high content of AMPD, characteristic AMPD peaks dominated the XRD trace. These peaks had very high intensity values and may have resulted in concealment of other components in the system.

7.3.2. Two component non-interacting model

The dissolution rates determined from the dissolution profiles (Figure 7. 1) are plotted against %AMPD in Figure 7. 6. The black line in Figure 7. 6 represents the rates predicted from the two

component non-interacting model of Higuchi et al. (1965b), calculated using Equations 1.35, 1.36, 1.37, 1.45 and 1.46. According to the model, the critical mixture ratio occurred at 99.8% AMPD and all the systems examined (20 – 98% AMPD) were represented by Case B of the two component non-interacting model (Section 1.4.3), i.e. DtBA was the surface layer controlling dissolution. Due to the large solubility difference between DtBA and AMPD (~1:1,300), the time taken to reach steady state conditions, estimated as described in Section 3.2.20, was not reached within the time taken to complete a dissolution run. However, the dissolution rate of DtBA, the surface layer, is predicted to be constant from the onset of dissolution and equal to the dissolution rate of the pure DtBA. On the other hand, the dissolution of AMPD would not have reached a constant steady state rate.

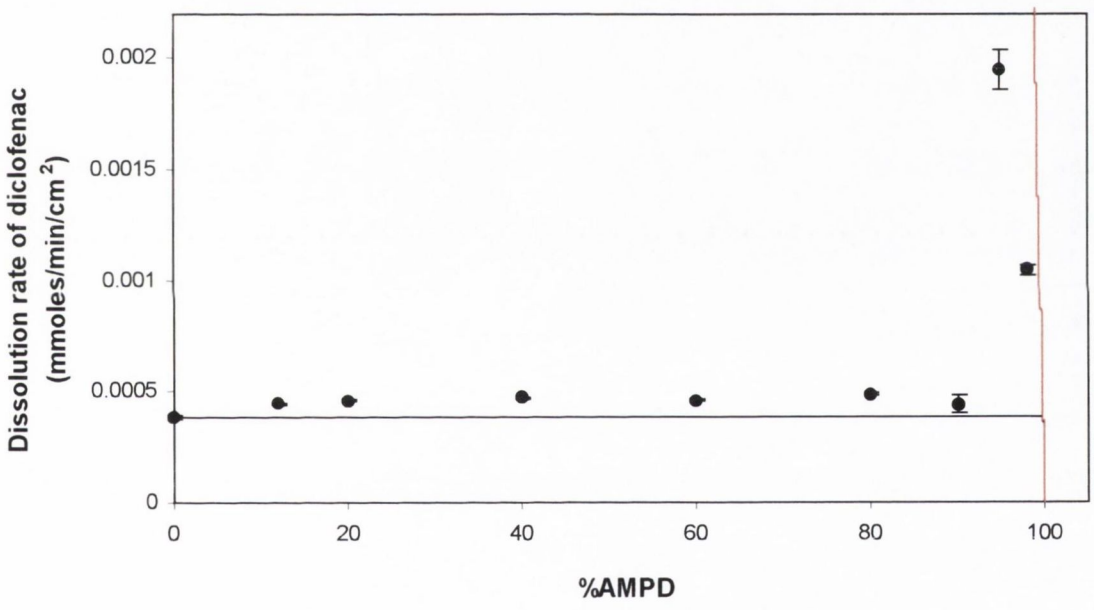

Figure 7. 6 Dissolution of diclofenac from AMPD:DtBA discs showing actual data (•) and theoretical lines for the two component non-interacting model (—) and carrier controlled dissolution (—)

Experimental rates for the 95:5 and 98:2 AMPD:DtBA systems showed considerable deviation from the two component non-interacting model. The system prepared with 95% AMPD showed a 5-fold degree of enhancement in dissolution rate, relative to the rate predicted from the model. In these systems, the two component non-interacting model predicted the existence of a controlling drug layer at the solid-liquid interface. However, formation of this layer was dependent on the presence of enough drug, with the necessary cohesive properties, to form and support a porous

surface layer. In practice, there may have been insufficient drug to maintain an intact surface. In such a situation, *carrier controlled dissolution* can occur (Corrigan, 1985). The drug can be either molecularly dispersed in the excipient or dispersed as fine particles. Dissolution of the excipient can cease to be hindered by a surface drug layer and the excipient can act as a carrier, bringing drug into the dissolution medium as it dissolves. This extension of carrier phase dissolution control to higher drug weight fractions than predicted by the two component model is thought to be a consequence of the disparate solubilities of carrier and drug (Corrigan and Stanley, 1982).

When the drug is considered to be molecularly dispersed in the carrier, drug release has been shown to be dependent on the product of the carrier dissolution rate, G_C, and the ratio of amounts of drug and carrier present, A_d / A_C (Corrigan and Stanley, 1982):

$$G_d = \frac{G_C A_d}{A_C} \qquad \textbf{Equation 7. 1}$$

Carrier controlled dissolution has also been observed for PVP:sulfathiazole coprecipitates (Simonelli et al., 1969) and PEG:hydroflumethiazide and PEG:bendrofluazide coprecipitates (Corrigan et al., 1979). In these studies, dissolution was found to be consistent with Equation 7. 1 for low drug content systems. Dubois and Ford (1985) showed that, for a range of eight drugs, the dissolution rates from drug:PEG 6000 solid dispersions at low drug content were controlled by the dissolution of PEG 6000 only and were independent of the drug they contained, thus complying with the carrier controlled dissolution theory.

Corrigan and Stanley (1982) studied release from β-cyclodextrin:drug discs prepared from mechanical mixtures and reported that observed dissolution rates were intermediate between those predicted by the interacting two component model (Section 1.4.4) and a carrier controlled model (Equation 7. 1). They postulated that if crystalline drug was dispersed in the carrier, as was the case with mechanical mix systems, particulate drug would be passively carried into the dissolution medium as the carrier dissolves, giving a dissolution rate intermediate between that predicted by the two theories. Dubois and Ford (1985) also reported deviation from carrier controlled dissolution for griseofulvin:PEG 6000 solid dispersions at low drug content and attributed this to the presence of drug crystallites in the dispersions.

Dissolution from *p*-aminobenzoate:PEG 6000 (Sjökvist Saers and Craig, 1992) and paracetamol:PEG 4000 (Lloyd et al., 1999) solid dispersions was found to be most rapid from systems with low drug loadings. Sjökvist Saers and Craig (1992) suggested that there are two possible mechanisms involved in drug release from solid dispersions with low concentrations of

drug. Firstly, the carrier may form a concentrated diffusion layer into which the drug dissolves prior to release into the bulk medium. This mechanism may lead to carrier controlled dissolution since the rate limiting step to drug release is the dissipation of the carrier diffusion layer. The second mechanism, which may apply to drugs of very low solubility, involves the release of intact drug particles into the dissolution medium, in which dissolution from a large surface area may take place.

In the case of the 95:5 and 98:2 AMPD:DtBA systems, lower dissolution rates than those predicted by Equation 7. 1 (illustrated by the red line in Figure 7. 6) were obtained. As discussed above, deviation from predicted rates has been attributed to dispersion of the drug as fine particles in the base, in contrast to the existence of a molecular dispersion. Furthermore, Equation 7.1 assumes that the dissolution rate of the base, G_C, was not affected by the presence of the drug. A lowering of the base dissolution rate due to the presence of the drug may account for observed dissolution rates lower than those predicted by Equation 7.1. In addition, the diffusivity of the drug in the aqueous boundary layer may be lowered due to the high viscosity of saturated solutions of AMPD, resulting in slower dissolution than predicted.

While the experimental data in the region 12 – 90% AMPD appeared to follow the trend predicted by the two component non-interacting model (Figure 7. 6), poor goodness of fit parameters were obtained since the observed dissolution rates were consistently higher than those predicted. However, for 40:60 and 60:40 AMPD:DtBA systems after dissolution, XRD analysis (Section 7.3.1) has revealed the presence of DAMPD-MH, which was formed from diclofenac acid and AMPD present in the discs. Peaks characteristic of DAMPD-MH were not evident in the XRD trace for the 95:5 AMPD:DtBA disc after dissolution, which was attributed to the high intensity of the AMPD peaks (Section 7.3.1). Previous studies have reported interactions between ionisable drugs and excipients in formulations, resulting in the formation a new salt forms (McGloughlin, 1989; Eerikäinen et al., 1991). McGloughlin (1989), in a study of the dissolution of acidic drug:basic excipient compressed discs, performed XRD analysis on the discs after dissolution and detected the formation of the resultant salt form. Eerikäinen et al. (1991) observed a markedly slower release of sodium indomethacin trihydrate from granules when calcium hydrogen phosphate dihydrate was included in the formulation. The authors attributed this to the formation of the calcium salt of indomethacin, which is less water-soluble than the sodium salt.

DAMPD-MH has an aqueous solubility of 6.77 mM (Section 6.4.4), higher than that of DtBA (5.46 mM). The formation of DAMPD-MH in the disc would therefore be expected to promote the dissolution of the diclofenac acid from the discs. Accordingly, observed dissolution rates for the discs prepared with 12 – 90% AMPD were, on average, 19.4% higher than the predicted rates.

This indicated that a modified model that accounted for the formation of a new salt in the discs was required.

7.3.3. Two component (salt conversion) model

A model was developed (Appendix VIII) which assumed that all the diclofenac anion present, initially in the form of DtBA (SALT1), interacted with available AMPD (BASE) to form DAMPD-MH (SALT2). For systems with proportions of AMPD less than the AMPD:DtBA 1:1 molar ratio, DtBA was present in excess and all the AMPD was assumed to convert to DAMPD-MH. The dissolution rates in this region were predicted from the two component non-interacting model with DtBA and DAMPD-MH as the two components. A consequence of salt conversion was the formation of the free base from SALT1 (tBA), in the liquid form (m.p. -66.9°C), which would be expected to diffuse from the surface of the disc. When discs were prepared with proportions of AMPD greater than the AMPD:DtBA 1:1 molar ratio, there was more than enough AMPD present to convert all the diclofenac anion to DAMPD-MH. The systems that resulted were comprised of DAMPD-MH and AMPD and were again described by the two component non-interacting model.

This model was a modification of the two component (salt formation) model developed by McGloughlin (1989) which described dissolution from discs prepared from acid and base mixtures. The salt formation reaction between the acid and the base was assumed to go to completion. Therefore, at the acid:base 1:1 molar ratio, the system was thought to consist entirely of the salt form. For 0 to 0.5 mole fraction of the base, the acid was present in excess and dissolution was represented by a two component mixture of the acid and the salt, whereas for higher mole fractions of the base, the two component non-interacting model was applied to the base:salt system. McGloughlin (1989) compared experimental dissolution rates from naproxen:procaine mixes with the rates predicted from the model. The model accurately predicted the maximum dissolution rate for naproxen and the composition range over which the maximum dissolution rates occurred.

Computer modelling (Section 3.2.21) was used to simulate expected dissolution rates for the AMPD:DtBA systems, according to the two component (salt conversion) model. The black line in Figure 7. 7 represents the theoretical dissolution rates.

Calculations (Section 3.2.20) were carried out to ensure that dissolution of the diclofenac salts had reached steady state conditions before the first sampling point in the dissolution experiment. In the case of systems with AMPD present after salt conversion (discs prepared with >22.2% AMPD), as described by a DAMPD-MH:AMPD two component model, AMPD would not be expected to have

achieved a steady state rate during the dissolution run. This is due to the large solubility difference between DAMPD-MH and AMPD (~1:1,000).

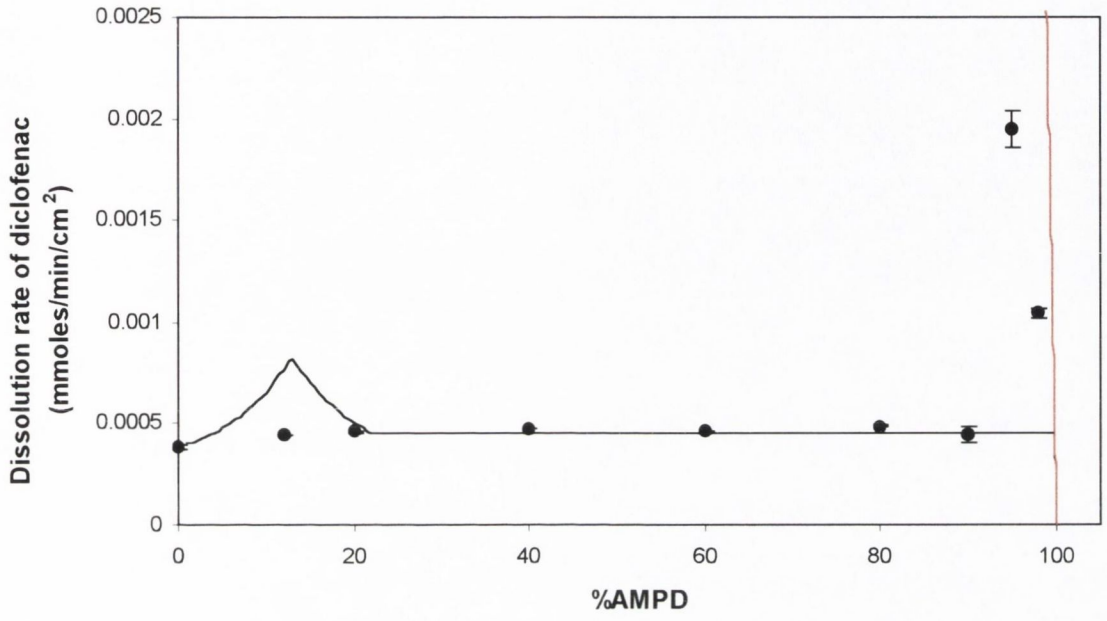

Figure 7. 7 Dissolution of diclofenac from AMPD:DtBA discs showing actual data (•) and theoretical lines for the two component (salt conversion) model (—) and carrier controlled dissolution (—)

Experimental data for the discs with 12 – 90% AMPD were a poor fit to the two component (salt conversion) model (CD = 0.40; MSC = 0.50). Excluding the data point for 12% AMPD from the goodness of fit determination yielded improved CD and MSC values. In the region 20 – 90% AMPD this model was superior to the two component non-interacting model (Figure 7. 6) for predicting dissolution from AMPD:DtBA mechanical mixes. Again, the 95:5 and 98:2 AMPD:DtBA systems were found to dissolve at considerably faster rates than predicted by the model. This was attributed to carrier controlled dissolution. The red line in Figure 7. 7 represents the theoretical rates for carrier controlled dissolution of molecularly dispersed DAMPD-MH. The lower proportion of base present, following interaction with the diclofenac anion to form DAMPD-MH, was taken into account in calculating the predicted rates. Experimental rates for the 95:5 and 98:2 systems are lower than the rates expected from carrier controlled dissolution. Possible explanations for this deviation are described in Section 7.3.2.

The enhancement in dissolution rate of diclofenac from systems prepared with 0 – 22% AMPD, as predicted by the two component (salt conversion) model (Figure 7. 7), was not observed experimentally. The model applied the DAMPD-MH:DtBA two component non-interacting model to systems with concentrations of AMPD less than the AMPD:DtBA 1:1 molar ratio and predicted that simultaneous dissolution of two diclofenac salts, DtBA and DAMPD-MH, occurred. According to the model, the dissolution rate of diclofenac from systems in this region was equal to the sum of the respective dissolution rates of the two salts. A graphical representation of the model for AMPD:DtBA systems prepared with less than 22% AMPD is shown in Figure 7. 8.

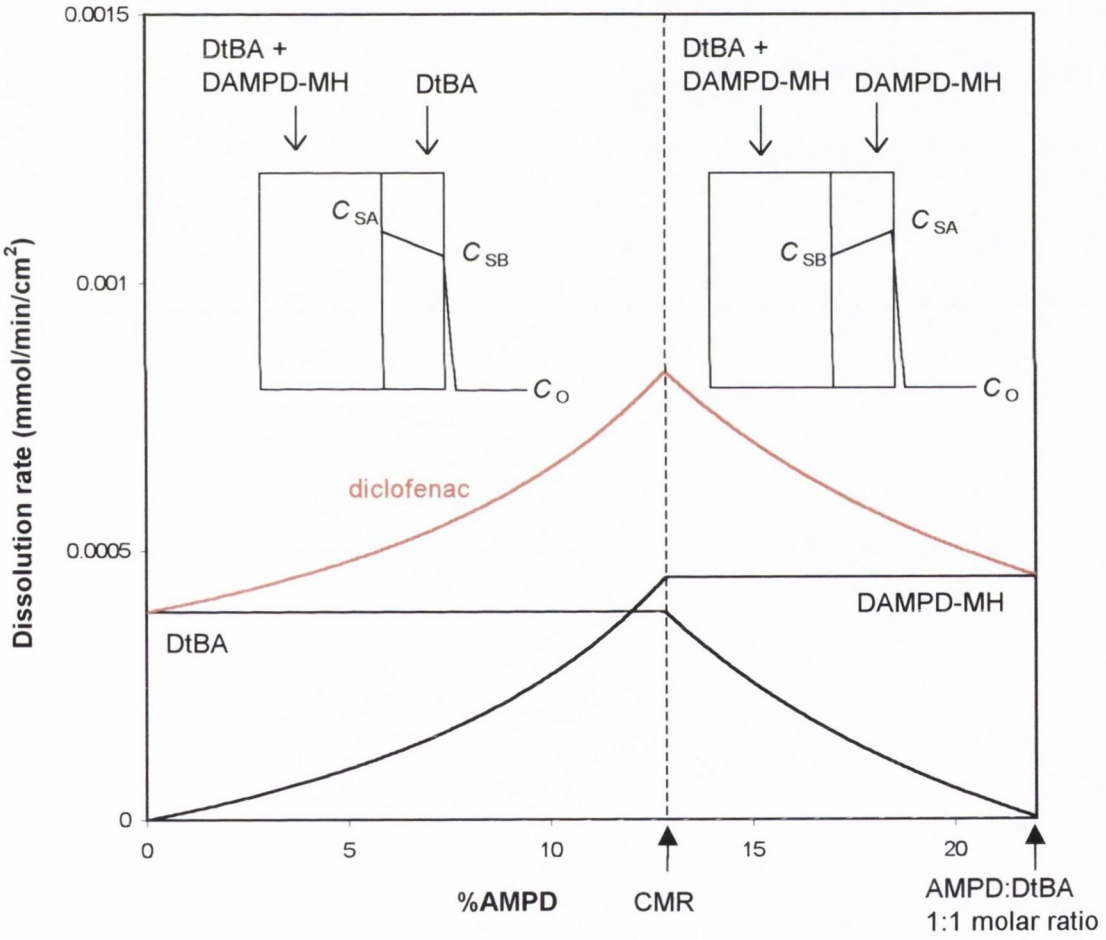

Figure 7. 8 The two component (salt conversion) model for AMPD:DtBA systems prepared with %AMPD less than the AMPD:DtBA 1:1 molar ratio, represented by a DAMPD-MH:DtBA two component non-interacting model

Consideration of the systems that result in the steady state, above and below the critical mixture ratio (CMR), as predicted by the two component non-interacting model, revealed that modification

of the model was required. For those systems in which the more soluble of the two salts (DAMPD-MH) was predicted to form the surface layer, the dissolution of diclofenac was limited to the dissolution rate of the more soluble salt. As depicted in Figure 7. 8, the driving force for the dissolution of DAMPD-MH was the concentration gradient from C_{SA}, its solubility, to C_O, its concentration in the bulk medium (assumed to be zero in sink conditions). Dissolution of the less soluble salt (DtBA) had to occur from within the disc, through the surface layer. The upward concentration gradient from the solubility of DtBA (C_{SB}) to that of DAMPD-MH in the surface layer (C_{SA}) provided a barrier to the dissolution of DtBA.

In the case of systems in which the least soluble salt (DtBA) was predicted to form the surface layer (at concentrations below the CMR in the case of the DAMPD-MH:DtBA two component non-interacting system), the dissolution of the more soluble salt (DAMPD-MH) had to occur across two boundaries, the surface layer of DtBA and the aqueous boundary layer. Its dissolution through the surface layer was thought to be severely impeded by the low concentration gradient between C_{SA} and C_{SB} and by the tortuosity (τ) of the surface layer of DtBA. The dissolution of diclofenac from these systems was therefore approximated to that of the less soluble salt, that forming the surface layer.

The two component (salt conversion) model was modified with regard to dissolution from systems with %BASE less than the BASE:SALT1 1:1 molar ratio. In this concentration range, the dissolution of diclofenac was predicted to be equal to the intrinsic dissolution rate of the salt expected to form the surface layer.

The theoretical rates calculated from the two component (salt conversion) model, modified as described above, for AMPD:DtBA mixtures are presented in Figure 7. 9. The experimental data in the range 12 – 90% AMPD was found to be a very good fit to the model (CD = 0.97; MSC = 3.49). This modified version of the two component (salt conversion) model was employed in the prediction of dissolution from the remaining base:diclofenac salt systems.

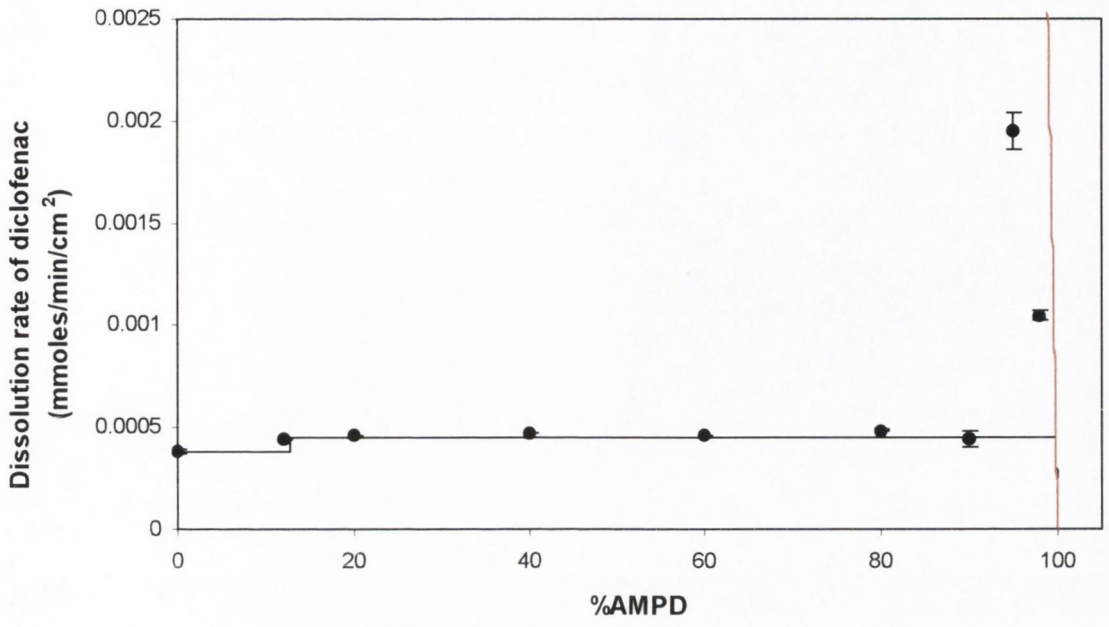

Figure 7. 9 Dissolution of diclofenac from AMPD:DtBA discs showing actual data (•) and theoretical lines for the two component (salt conversion) model, modified (—) and carrier controlled dissolution (—)

7.3.4. Three component (salt conversion) model

An assumption of the two component (salt conversion) model was complete salt conversion, i.e. that all the diclofenac acid present (as SALT1) reacted with the available BASE to form SALT2. A less simplistic model, the three component (salt conversion) model was developed (Appendix VIII) to describe a system where all the diclofenac acid present did not convert to SALT2, even when there was sufficient base present. According to the model, a fixed percentage (P) of the diclofenac acid moles present converted to SALT2, whereas (100 – P)% remained as SALT1. At initial concentrations of BASE less than the amount required to convert P% of the diclofenac acid, the systems were comprised of mixtures of SALT1 and SALT2. As in the case of the two component (salt conversion) model, the dissolution of diclofenac from these mixtures was thought to be limited to the dissolution rate of the surface layer component, as predicted by the two component non-interacting model. When the initial BASE concentration was greater than the amount required for P% conversion from SALT1 to SALT2, the system was represented by a SALT2:SALT1:BASE three component non-interacting model (Simpson and Parrott, 1983) and dissolution rates were calculated using Equations 1.53 – 1.68. In the three-component systems

where two diclofenac salts were present, one in a receding layer and one in the surface layer, the dissolution of diclofenac was thought to be equal to that of the salt present in the surface layer.

A number of factors may influence the level of conversion from SALT1 to SALT2. In order to investigate if the % conversion was influenced by the relative basicities of the counterions or the relative solubilities of the salts, P values were calculated from the ratio of DAMPD-MH and DtBA solubilities (6.77 mM : 5.46 mM) and from the ratio of AMPD and tBA K_b values (6.3×10^{-6} : 4.9×10^{-4}). The P values calculated were 55% and 1%, respectively. These P values were used in the three component (salt conversion) model and agreement between observed and predicted dissolution rates was examined (Figure 7. 10). As in the case of the two component (salt conversion) model, the 95:5 and 98:2 systems were thought to have exhibited carrier controlled dissolution. The dashed lines in Figure 7. 10 represent the theoretical dissolution rates for carrier controlled dissolution of molecularly dispersed DAMPD-MH and DtBA.

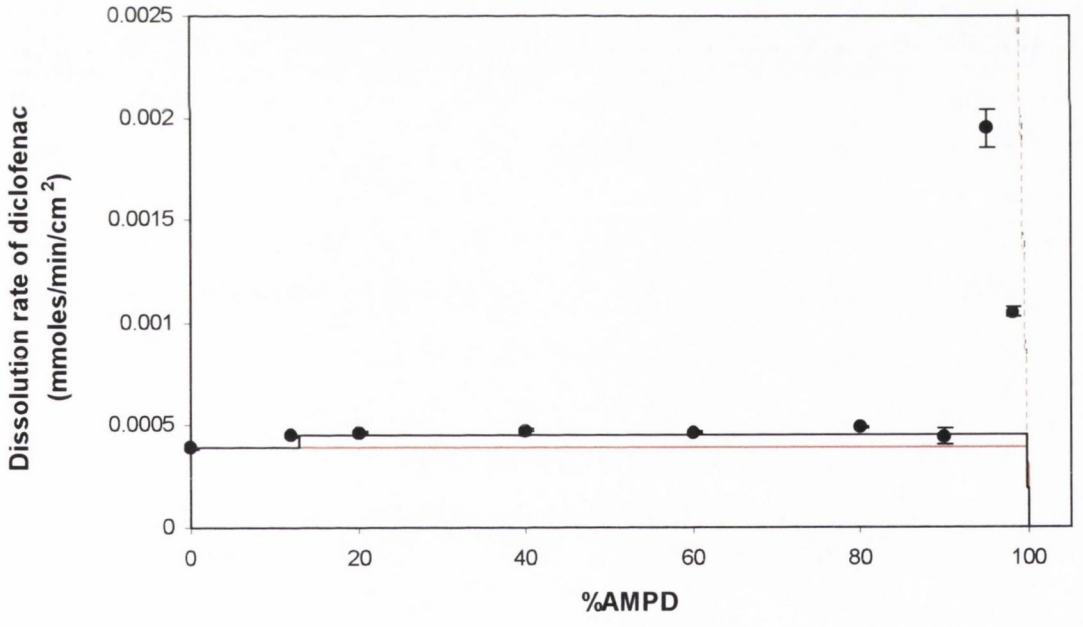

Figure 7. 10 Dissolution of diclofenac from AMPD:DtBA discs showing actual data (•), theoretical lines for the three component (salt conversion) model (—) and carrier controlled dissolution (---) when P = 55% and theoretical lines for the three component (salt conversion) model (—) and carrier controlled dissolution (---) when P = 1%

The dissolution rates predicted using a P value of 55% (calculated from the ratio of the salt solubilities) were similar to the rates predicted by the two component (salt conversion) model (Figure 7. 9), resulting in the same MSC value (3.49) for the data in the 12 – 90% AMPD region. The similarity of the results obtained by the two models can be explained in terms of their predictions regarding the surface layer. In the case of the three component (salt conversion) model, examination of the region represented by the three component model (13.6 – 100% AMPD) revealed that for the systems prepared with 13.6 – 99.5% AMPD, "Case V" (Section 1.4.5) was predicted to be the steady state situation. "Case V" represents DAMPD-MH:DtBA:AMPD discs with a surface layer of DAMPD-MH and an intermediary layer of DAMPD-MH and DtBA. The model predicted that the dissolution of diclofenac from these systems was limited to the dissolution rate of DAMPD-MH. Similarly, in the case of the two component (salt conversion) model, DAMPD-MH was predicted to form the surface layer for discs prepared with concentrations of AMPD up to 99.8%.

On the other hand, the rates predicted for the 12 – 90% AMPD systems when P = 1% (calculated from the ratio of the K_b values of tBA and AMPD) were similar to the rates predicted from the simple AMPD:DtBA two component non-interacting model (Section 7.3.2), as expected considering the low % conversion to DAMPD-MH. Both models resulted in the same goodness of fit values for the experimental data (CD = 0.81; MSC = 1.65).

By allowing the value of P to vary from 0 to 100, it was possible to determine the % conversion from DtBA to DAMPD-MH required for the three component (salt conversion) model to deviate from the two component non-interacting model and predict rates identical to those predicted by the two component (salt conversion) model (representing 100% conversion). It was calculated that when there was <51.7% conversion, the three component (salt conversion) model resembled the two component non-interacting model and when there was >51.7% conversion, the rates predicted were the same as those predicted by the two component (salt conversion) model and were therefore a better fit to the data (MSC = 3.49). This suggests that the level of conversion from DtBA to DAMPD-MH in the AMPD:DtBA discs was greater than 51.7%. This finding was consistent with the observation from XRD analysis that DAMPD-MH was formed in the discs. The limit for the detection of a diclofenac salt in diclofenac salt:base mixed discs was estimated to be ~35%.

7.4. DISSOLUTION OF DICLOFENAC FROM TRIS:DtBA SYSTEMS

TRIS is less soluble than AMPD, the base combined with DtBA in the previous section. TRIS:DtBA systems with 20 – 98% TRIS were studied. The dissolution profiles are presented in

Figure 7. 11 and the dissolution rates calculated from the profiles are listed in Table 2, Appendix VII. The results obtained were qualitatively similar to those of the AMPD:DtBA systems. Little enhancement in dissolution rate was observed, except for those systems in the region of carrier controlled dissolution, i.e. the systems containing 95% and 98% AMPD.

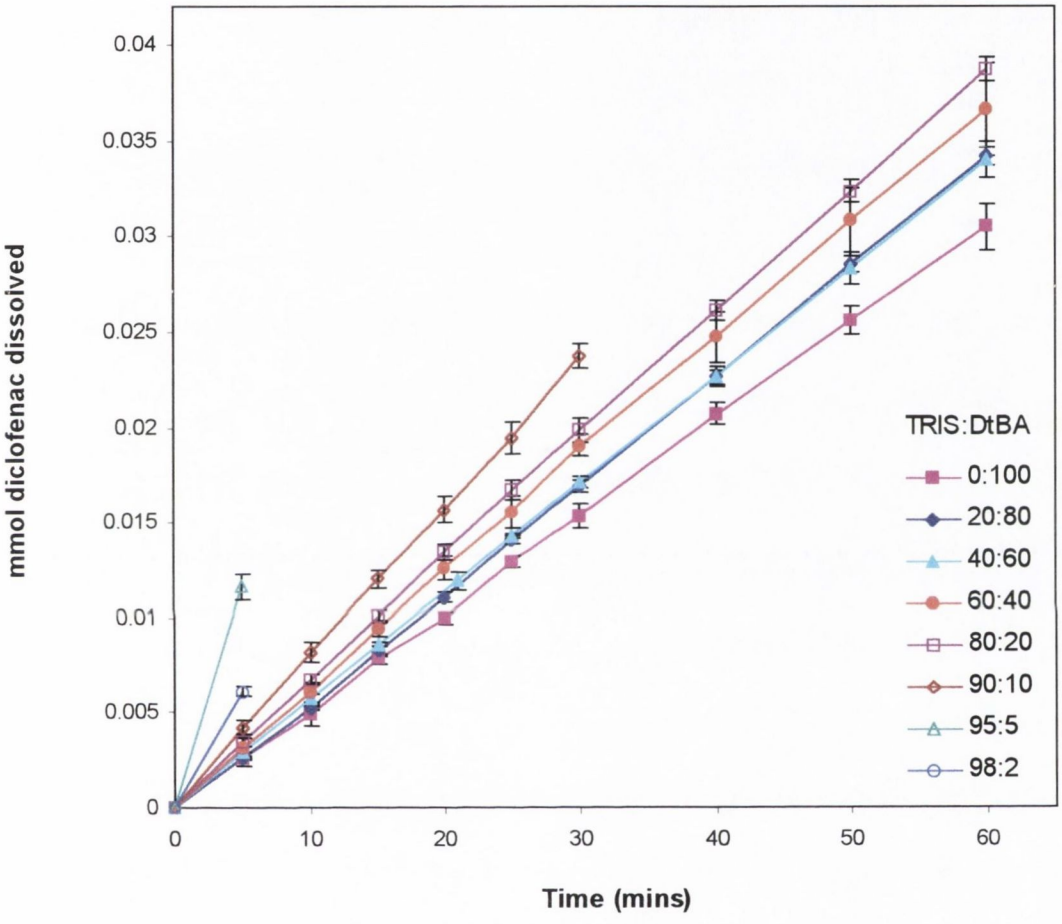

Figure 7. 11 Diclofenac dissolution from TRIS:DtBA discs

7.4.1. XRD analysis of mechanical mixes and discs before and after dissolution

XRD analysis was carried out on (a) mechanical mixes, (b) discs before dissolution and (c) discs after dissolution for the 40:60, 60:40 and 95:5 TRIS:DtBA systems. For each system, the XRD trace for the disc before dissolution exhibited peaks at the same 2θ values as the trace for the corresponding mechanical mix. The XRD trace for each disc after dissolution was compared with the trace for the corresponding disc before dissolution (Figure 7. 12 – Figure 7. 14).

Traces for the 40:60 TRIS:DtBA discs are presented in Figure 7. 12. Additional peaks were observed in the trace for the disc after dissolution, as illustrated by the arrows in Figure 7. 12.

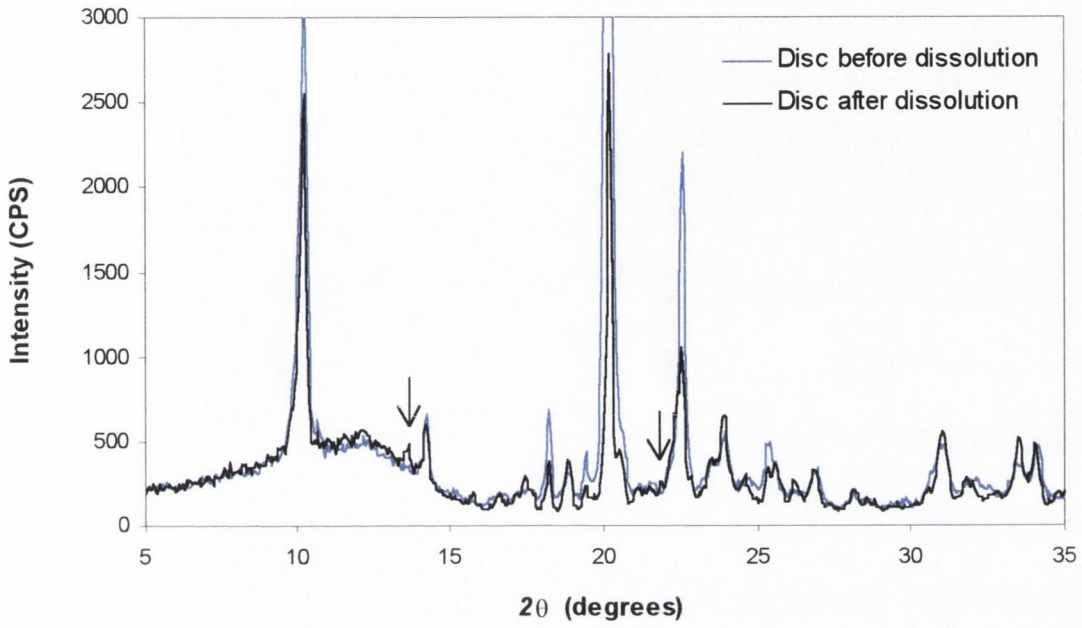

Figure 7. 12 XRD traces for TRIS:DtBA 40:60 discs before and after dissolution

The traces for the 60:40 TRIS:DtBA discs are presented in Figure 7. 13. As with the 40:60 system, additional peaks were observed in the trace for the disc after dissolution, as illustrated by the arrows in Figure 7. 13.

The trace for the TRIS:DtBA 95:5 disc after dissolution, shown in Figure 7. 14, was found to have identical peaks to the trace of the disc before dissolution. The intensity of the peak at 10.30°, which is characteristic of DtBA, was found to be lower in the XRD of the disc after dissolution.

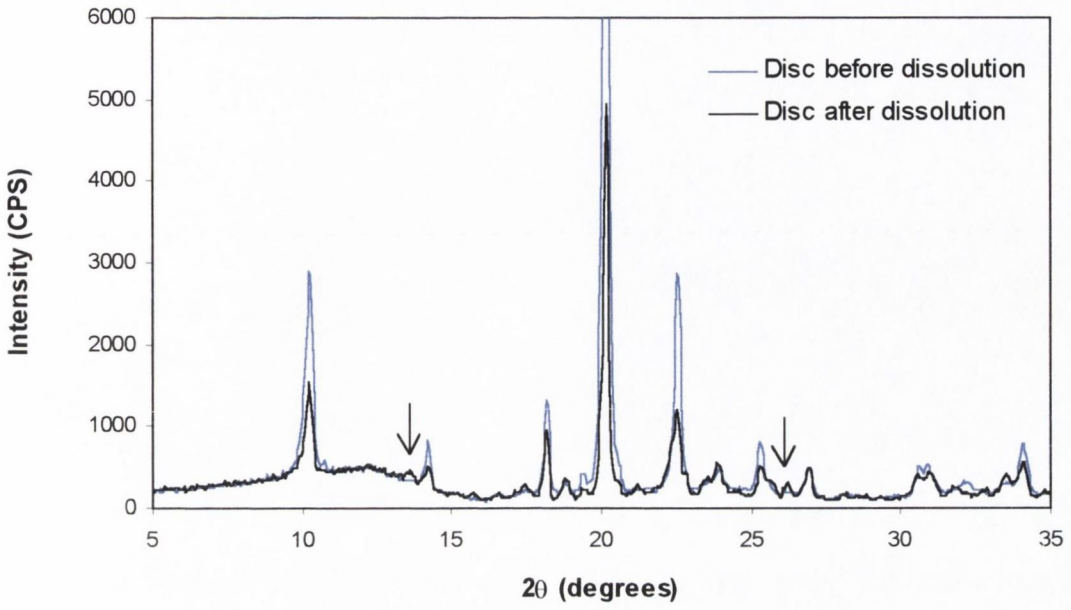

Figure 7. 13 XRD traces for TRIS:DtBA 60:40 discs before and after dissolution

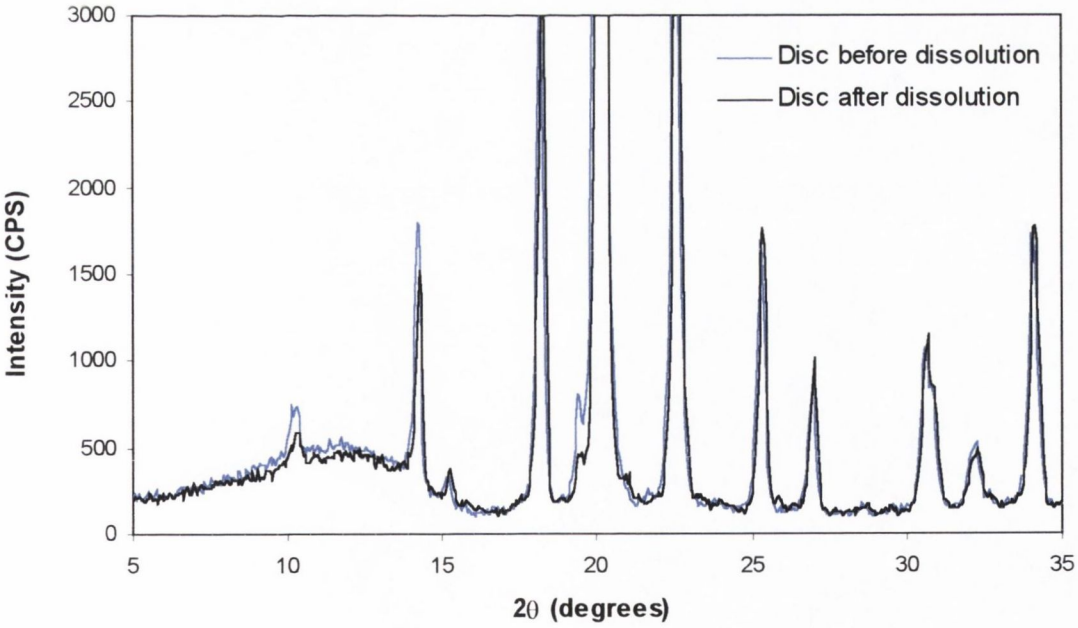

Figure 7. 14 XRD traces for TRIS:DtBA 95:5 discs before and after dissolution

The traces for TRIS:DtBA 40:60 and 60:40 discs after dissolution are examined with reference to the XRD traces for TRIS, DtBA and DTRIS (Figure 7. 15). The presence of the extra peaks in the traces for the discs was consistent with the presence of DTRIS in the disc. DTRIS may also have

been present in the 95:5 system but could not be detected by XRD because of the high proportion of TRIS, which generated peaks of very high intensity.

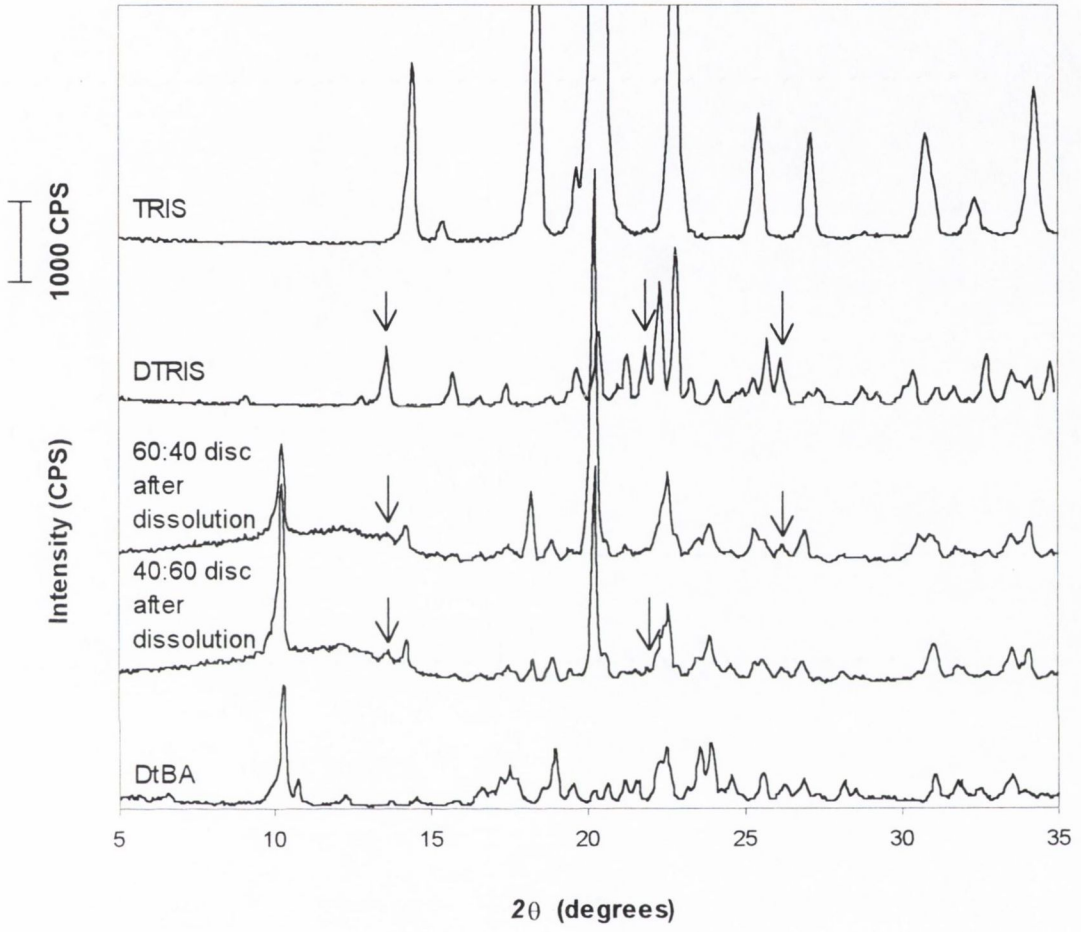

Figure 7. 15 XRD traces for the TRIS:DtBA 40:60 and 60:40 discs after dissolution compared with traces for TRIS, DtBA and DTRIS; the arrows indicate peaks which were not present in traces of the discs before dissolution; they correspond to peaks on the DTRIS trace, as illustrated

7.4.2. Two component non-interacting model

The observed dissolution rates for the TRIS:DtBA systems are plotted against %TRIS in Figure 7. 16. The black line represents the rates predicted from the two component non-interacting model. As in the case of the AMPD:DtBA systems, the model predicted that at concentrations less than the CMR (99.8% TRIS), DtBA was the surface layer controlling dissolution. Therefore, the dissolution rate of DtBA was predicted to be constant from time 0 in all the TRIS:DtBA systems

examined. TRIS, on the other hand, was estimated to have failed to reach steady state dissolution during the dissolution run.

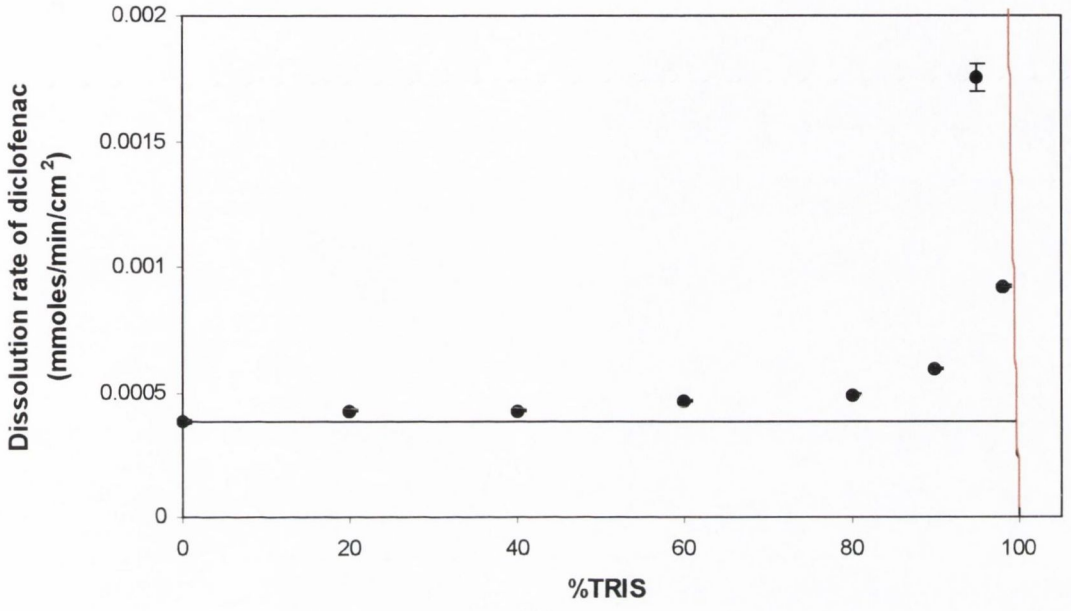

Figure 7. 16 Dissolution of diclofenac from TRIS:DtBA discs showing actual data (•) and theoretical lines for the two component non-interacting model (—) and carrier controlled dissolution (—)

Considerable levels of enhancement in dissolution rate, relative to that predicted by the two component non-interacting model, were observed for the 95:5 and 98:2 systems (~5-fold enhancement in the case of the 95:5 system). The higher dissolution rates for these two systems were attributed to the occurrence of carrier controlled dissolution. The red line in Figure 7. 16 represents carrier controlled dissolution of molecularly dispersed drug. As observed for the equivalent AMPD:DtBA systems, experimental rates for the 95:5 and 98:2 TRIS:DtBA systems were lower than the rates predicted for carrier controlled dissolution of molecularly dispersed drug. These deviations may be attributed to the factors discussed in Section 7.3.2 in relation to the 95:5 and 98:2 AMPD:DtBA systems.

Experimental rates for the systems with 20 – 90% TRIS were found to be higher than the rates predicted from the two component model. The CD and MSC values describing the fit of the experimental data to the model were low at 0.70 and 1.20, respectively.

7.4.3. Two component (salt conversion) model

XRD analysis revealed the presence of DTRIS in the 40:60 and 60:40 TRIS:DtBA systems after dissolution (Section 7.4.1). Therefore, the two component (salt conversion) model was applied to the TRIS:DtBA systems. The black line in Figure 7. 17 represents the theoretical dissolution rates according to the model. Calculations (Section 3.2.20) were carried out to ensure that dissolution of the diclofenac salts had reached steady state conditions before the first sampling point. There is a large solubility difference between DTRIS and TRIS (~1:1,000). Therefore, in the case of discs prepared with >24.7% TRIS (i.e. with mole fractions of TRIS >0.5), which result in the presence of excess TRIS after salt conversion, the dissolution of TRIS would not be expected to have achieved a steady state rate during the dissolution run.

The new salt formed in the discs (DTRIS) has a lower solubility (3.95 mM) than DtBA (5.46 mM). Therefore, the rates predicted from the two component (salt conversion) model in the region 10.7 – 100% TRIS (Figure 7. 17) were lower than those predicted from the two component non-interacting model (Figure 7. 16).

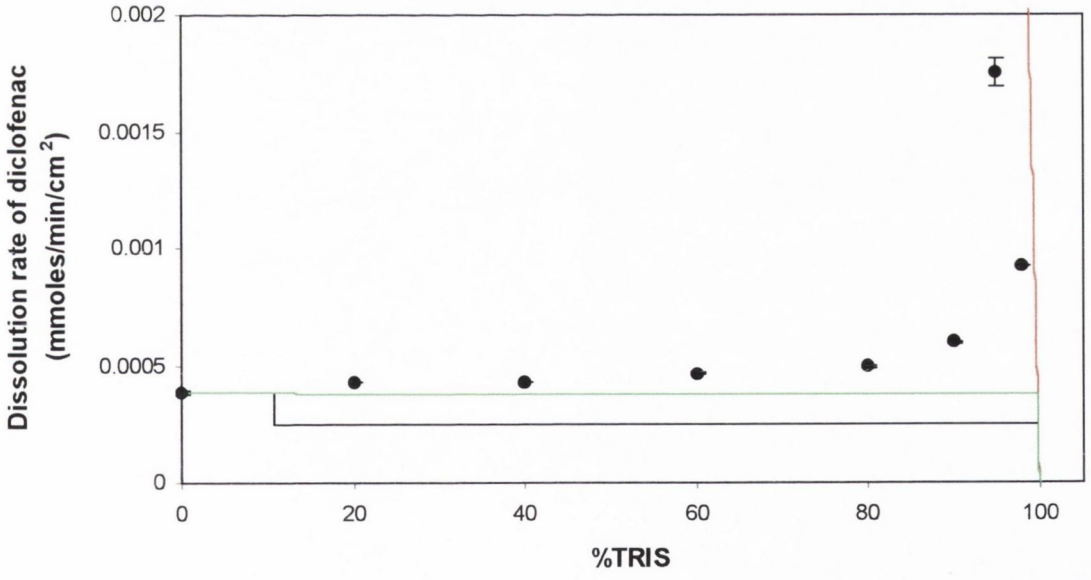

Figure 7. 17 Dissolution of diclofenac from TRIS:DtBA discs showing actual data (•) and theoretical lines for the two component (salt conversion) model, when C_S(DTRIS) = 3.95 mM (—) and when C_S(DTRIS) = 5.91 mM (—), and for carrier controlled dissolution (—)

Observed dissolution rates in the region 20 – 90% TRIS were found to be higher than the rates predicted by the two component (salt conversion) model, resulting in a poor fit to the model. The two component (salt conversion) model was less accurate than the two component non-interacting model in predicting dissolution from TRIS:DtBA mechanical mixes.

The very high dissolution rates obtained for the 95:5 and 98:2 TRIS:DtBA systems were attributed to the ability of the base to act as a carrier for DTRIS. For the prediction of dissolution rates pertaining to carrier controlled dissolution of molecularly dispersed drug (Equation 7.1), the lower % base left after the formation of DTRIS was taken into consideration. The predicted dissolution rates are illustrated by the red line in Figure 7. 17. As was the case with the two component non-interacting model, the experimental dissolution rates for the 95:5 and 98:2 TRIS:DtBA systems were lower than the predicted rates.

Whereas the two component (salt conversion) model accurately predicted dissolution rates for the AMPD:DtBA systems containing 20 – 90% AMPD, the observed dissolution rates for the TRIS:DtBA systems containing 20 – 90% TRIS were, on average, 1.9 times higher than the rates predicted by the model. The model predicted that dissolution from the TRIS:DtBA systems in this region was limited to the dissolution rate of DTRIS, which is thought to form the surface layer. The ability of DTRIS to form supersaturated solutions may contribute to deviation from the two component (salt conversion) model. Whereas the solubility of the salt measured using DTRIS as the starting material was 3.95 mM, examination of the pH-solubility profile of DTRIS (Section 6.6.4) revealed that the addition of TRIS to diclofenac resulted in a maximum solubility of 5.91 mM, representing a supersaturation level of 1.49. This suggests that the presence of TRIS in the TRIS:DtBA discs has the potential to result in concentrations of diclofenac in excess of the equilibrium solubility of DTRIS. The green line in Figure 7. 17 represents the dissolution rates predicted by the two component (salt conversion) model when the maximum solubility obtained in the pH-solubility study (5.91 mM) is used as the solubility value for DTRIS, C_S(DTRIS). It can be seen from Figure 7. 17 that using this higher solubility of DTRIS results in more accurate prediction by the model of the rate of dissolution from TRIS:DtBA systems containing 20 – 90% TRIS.

7.4.4. Three component (salt conversion) model

The three component (salt conversion) model was applied to the TRIS:DtBA systems. The P values calculated from the salt solubility and base K_b values were 42% and 0.4%, respectively. The resulting theoretical rates are presented in Figure 7. 18, together with the experimental data.

As in the case of the AMPD:DtBA mixtures, the dissolution rates predicted using a P value of 42% (calculated from the ratio of the salt solubilities) were similar to the rates predicted by the two component (salt conversion) model (Figure 7. 17). As observed for the two component (salt conversion) model, a poor fit to the model was obtained for the data in the 20 – 90% AMPD region (when 3.95 mM was used as the value for the solubility of DTRIS).

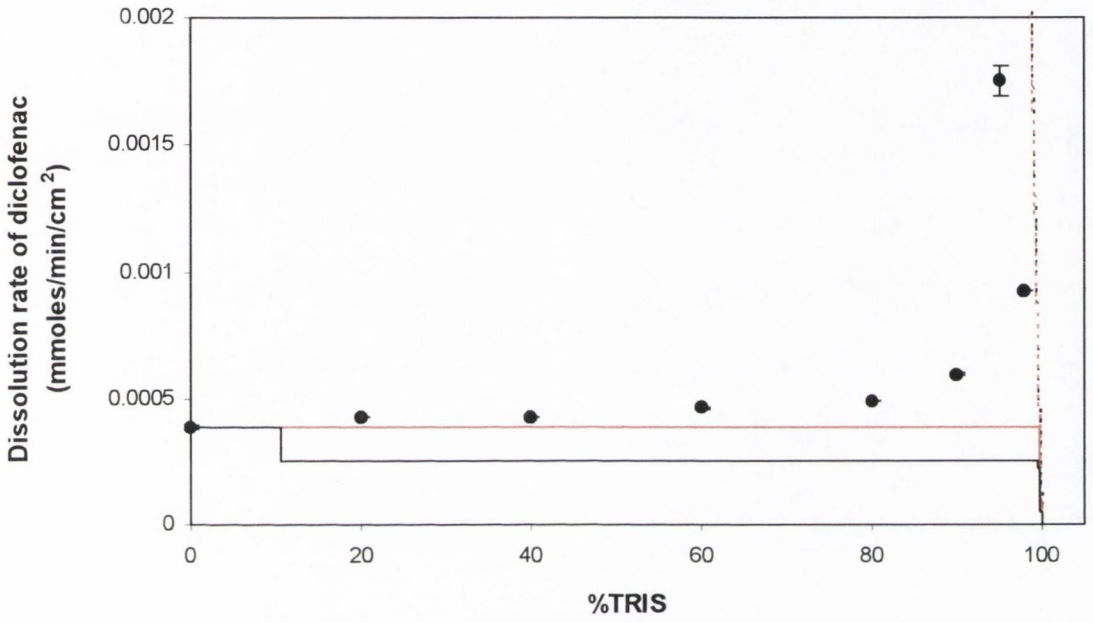

Figure 7. 18 Dissolution of diclofenac from TRIS:DtBA discs showing actual data (•), theoretical lines for the three component (salt conversion) model (—) and carrier controlled dissolution (---) when P = 42% and theoretical lines for the three component (salt conversion) model (—) and carrier controlled dissolution (---) when P = 0.4%

The rates predicted for the TRIS:DtBA systems when P = 0.4% (calculated from the ratio of the K_b values of tBA and TRIS) were identical to the rates predicted from the simple TRIS:DtBA two component non-interacting model (Section 7.4.2), as expected considering the low % conversion to DTRIS, and resulted in the same goodness of fit values for the experimental data (CD = 0.70; MSC = 1.20).

By allowing the P value to vary, it was calculated that when the P value was <36.4%, the rates predicted by the three component (salt conversion) model were identical to those predicted by the two component non-interacting model, resulting in a better fit to the experimental data (MSC = 1.20) than when P was >36.4% (two component (salt conversion) model). This suggested that the

level of conversion from DtBA to DTRIS in the TRIS:DtBA discs was <36.4%. On the other hand, the potential for DTRIS to form supersaturated solutions may be the cause of the observed deviation from the three component (salt conversion) model when P was greater than 36.4%.

7.5. DISSOLUTION OF DICLOFENAC FROM AMPD:DDNL SYSTEMS

DDNL has an aqueous solubility (446 mM) ~80 times higher than that of DtBA (5.46 mM). AMPD is the more soluble of the two bases employed in the study. AMPD:DDNL systems with AMPD weight fractions in the range 5 – 98% were studied. The dissolution profiles are presented in Figure 7. 19 and the dissolution rates calculated from the profiles are listed in Table 3, Appendix VII. These results differ from those obtained with the DtBA systems in that significant lowering in the dissolution rate of diclofenac relative to pure DDNL was observed. With the exception of the 5:95 system, incorporation of AMPD in the discs resulted in suppression of the dissolution of diclofenac.

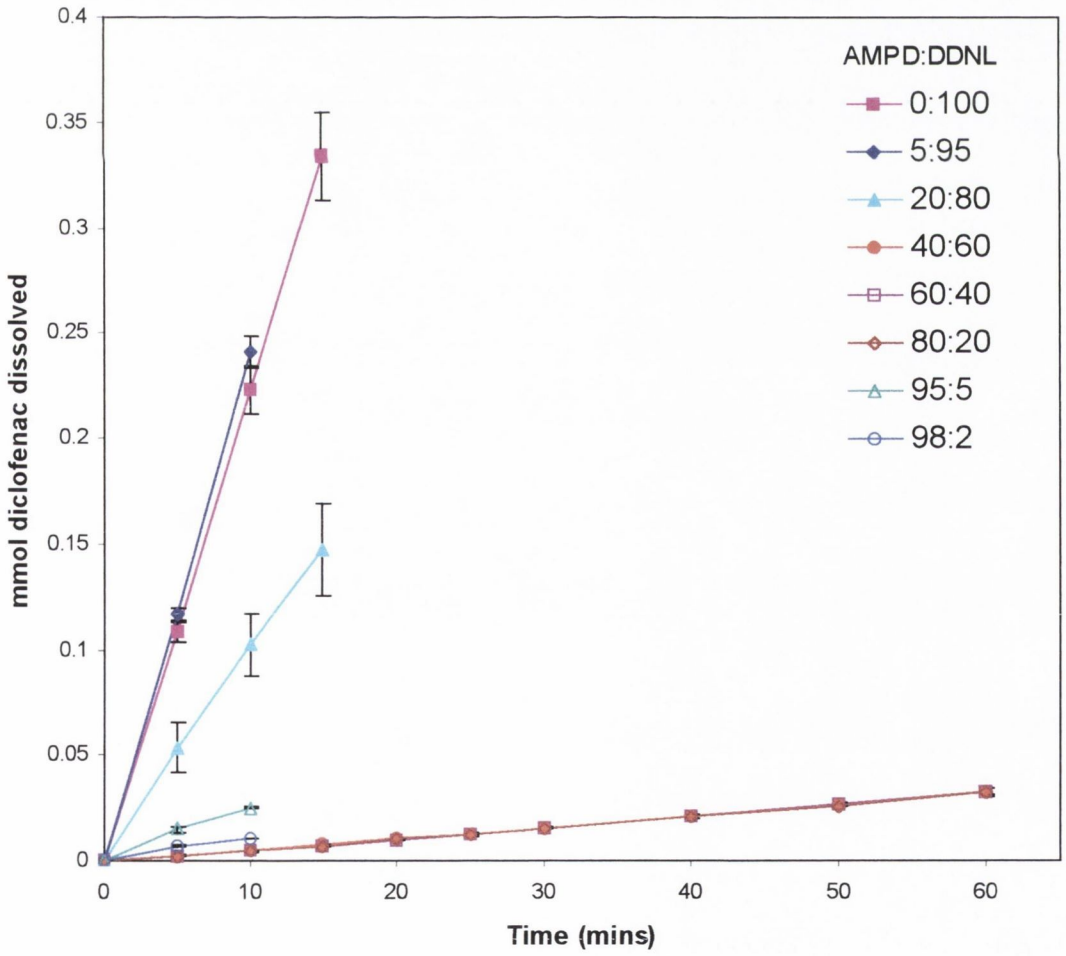

Figure 7. 19 Diclofenac dissolution from AMPD:DDNL discs

7.5.1. *XRD analysis of mechanical mixes and discs before and after dissolution*

XRD analysis was carried out on (a) mechanical mixes, (b) discs before dissolution and (c) discs after dissolution for the 40:60, 60:40 and 95:5 AMPD:DDNL systems. For each system, the XRD trace for the disc before dissolution exhibited peaks at the same 2θ values as the corresponding trace for the mechanical mix. The XRD trace for each disc after dissolution was compared with the trace for the corresponding disc before dissolution (Figure 7. 20 – Figure 7. 22).

The traces for the 40:60 AMPD:DDNL discs are presented in Figure 7. 20. Additional peaks were observed in the trace for the disc after dissolution, as illustrated by the arrows in Figure 7. 20.

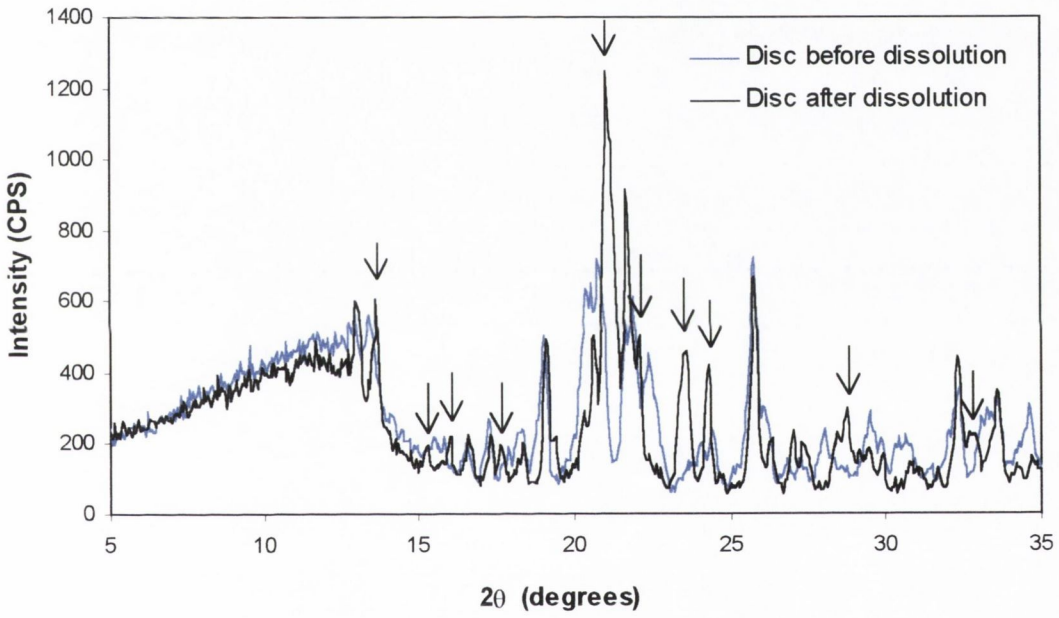

Figure 7. 20 XRD traces for AMPD:DDNL 40:60 discs before and after dissolution

The traces for the 60:40 AMPD:DDNL discs are presented in Figure 7. 21. As with the 40:60 system, additional peaks were observed in the trace for the disc after dissolution, as illustrated by the arrows in Figure 7. 21.

The traces for the AMPD:DDNL 95:5 discs before and after dissolution are presented in Figure 7. 22. Again, extra peaks were observed in the trace for the disc after dissolution when compared to that of the disc before dissolution.

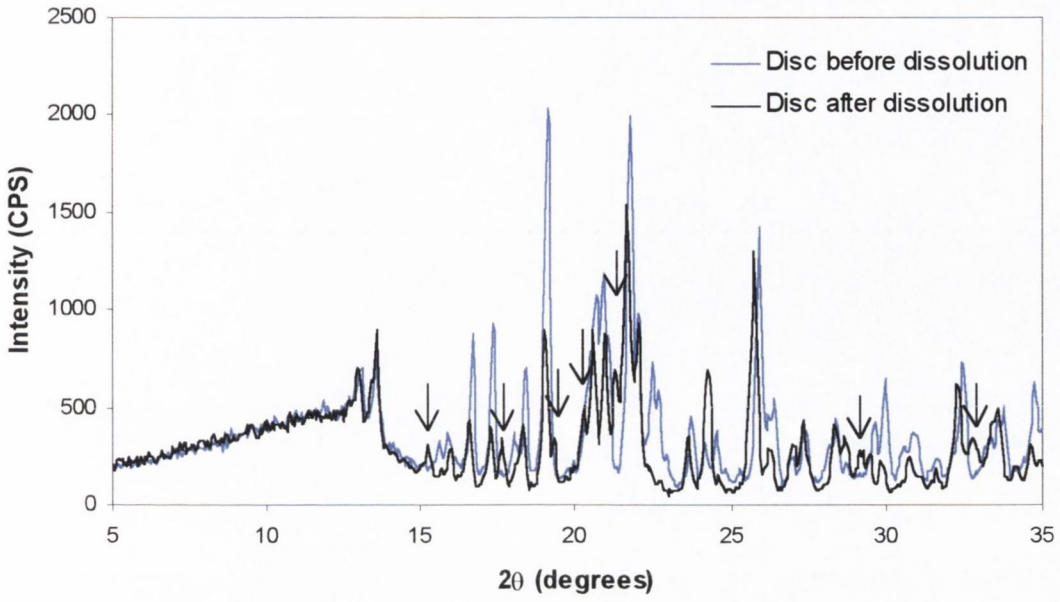

Figure 7. 21 XRD traces for AMPD:DDNL 60:40 discs before and after dissolution

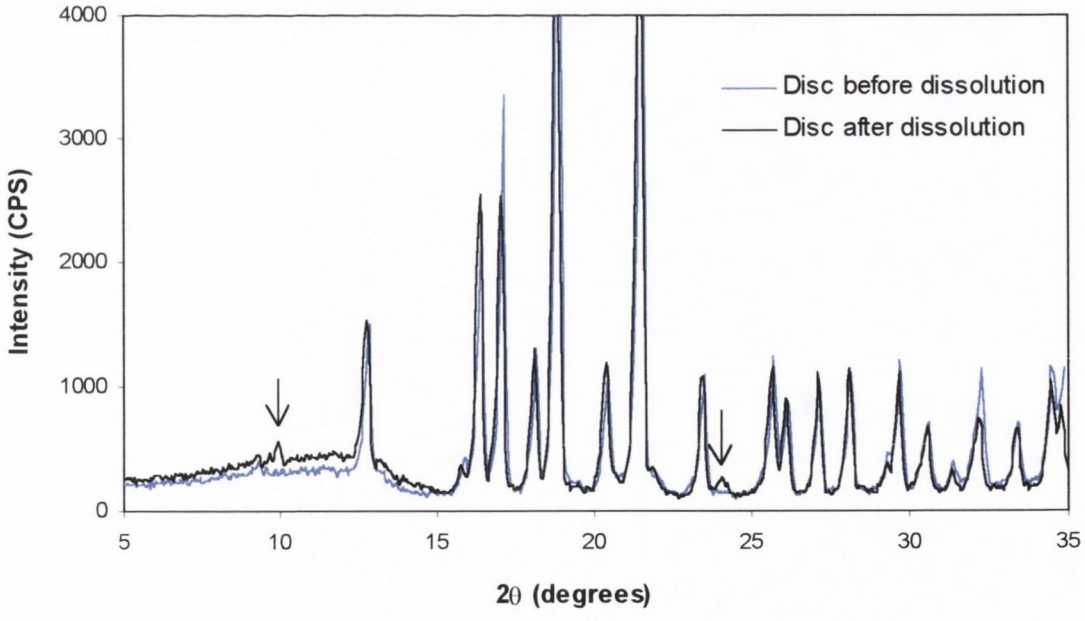

Figure 7. 22 XRD traces for AMPD:DDNL 95:5 discs before and after dissolution

The traces for AMPD:DDNL 40:60, 60:40 and 95:5 discs after dissolution are examined with reference to the XRD traces for AMPD, DDNL, DAMPD anhydrate and DAMPD-MH (Figure 7. 23).

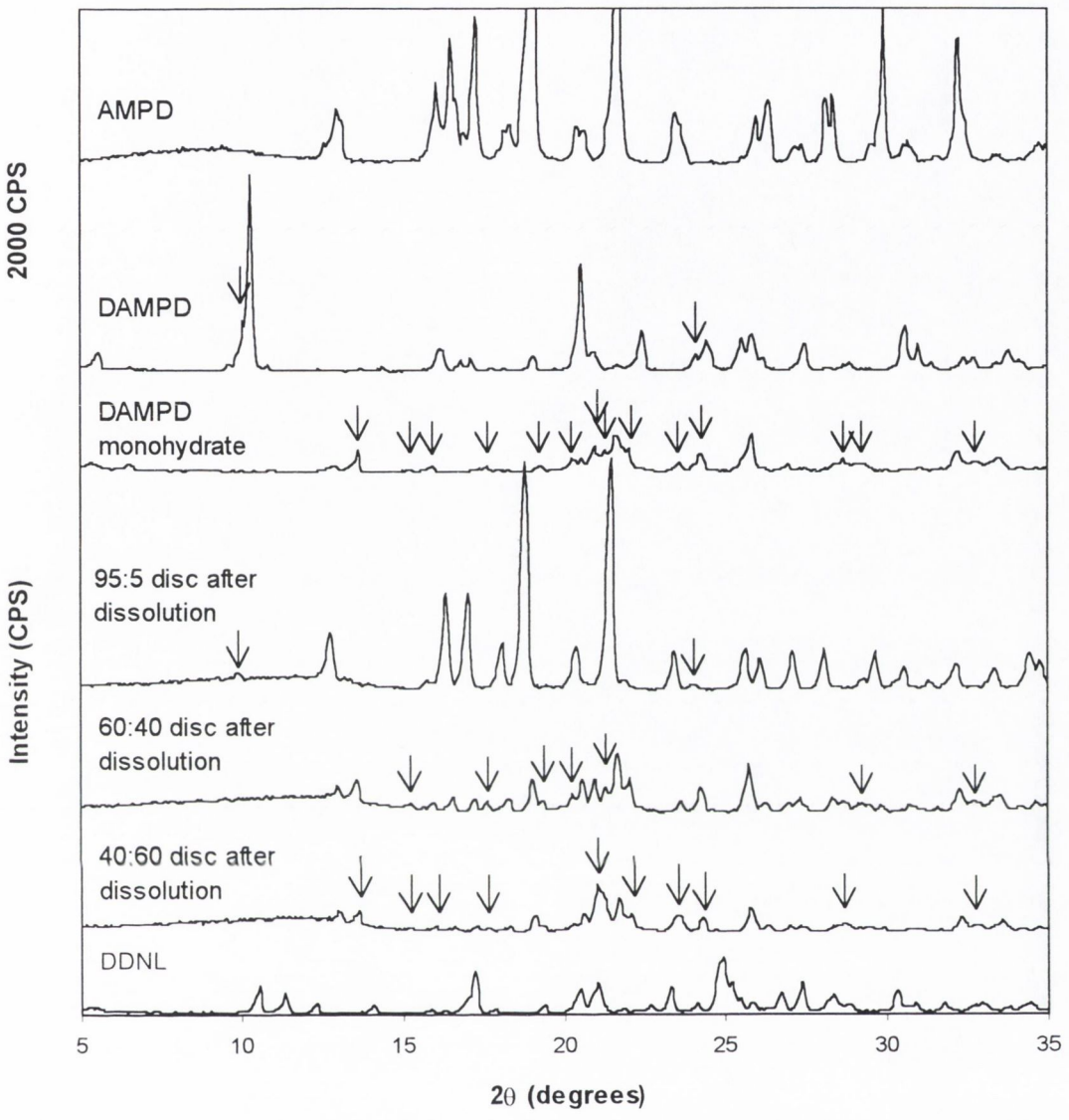

Figure 7. 23 XRD traces for the AMPD:DDNL 40:60, 60:40 and 95:5 discs after dissolution compared with traces for AMPD, DDNL, DAMPD and DAMPD-MH; the arrows indicate peaks which were not present in traces of the discs before dissolution

The presence of the extra peaks in the traces for the 40:60 and 60:40 systems were consistent with the presence of DAMPD-MH in the disc. The two additional peaks evident in the trace for the 95:5 disc after 10 minutes dissolution corresponded to peaks present in the trace for DAMPD anhydrate. XRD analysis of discs of pure AMPD anhydrate after 5 minutes dissolution indicated complete conversion to the monohydrate form (Section 6.4.4). The apparent absence of conversion of DAMPD (newly formed from diclofenac acid and AMPD) to DAMPD-MH in the 95:5 AMPD:DDNL system may have been a result of the drying process after the discs were removed

from the dissolution medium. As described in Section 3.2.20, the discs were allowed to dry in ambient conditions overnight. Dehydration from DAMPD-MH to the anhydrous form may have resulted in the 95:5 discs due to a variation in drying conditions, for example an elevated ambient temperature.

7.5.2. Two component non-interacting model

The dissolution rates determined from the dissolution profiles (Figure 7. 19) are plotted against %AMPD in Figure 7. 24. The line in Figure 7. 24 represents theoretical rates calculated from the two component non-interacting model. According to the model, the critical mixture ratio occurs at the 92.9:7.1 w/w ratio and DDNL forms the surface layer controlling dissolution in the systems prepared from 5 – 90% AMPD. Therefore, the dissolution rate of DDNL was predicted to be constant from the onset of dissolution and equal to the dissolution rate of the pure drug. The calculations outlined in Section 3.2.20 were applied to confirm that dissolution of DDNL from the 95:5 and 98:2 systems had reached steady state before the first sampling point of the dissolution run.

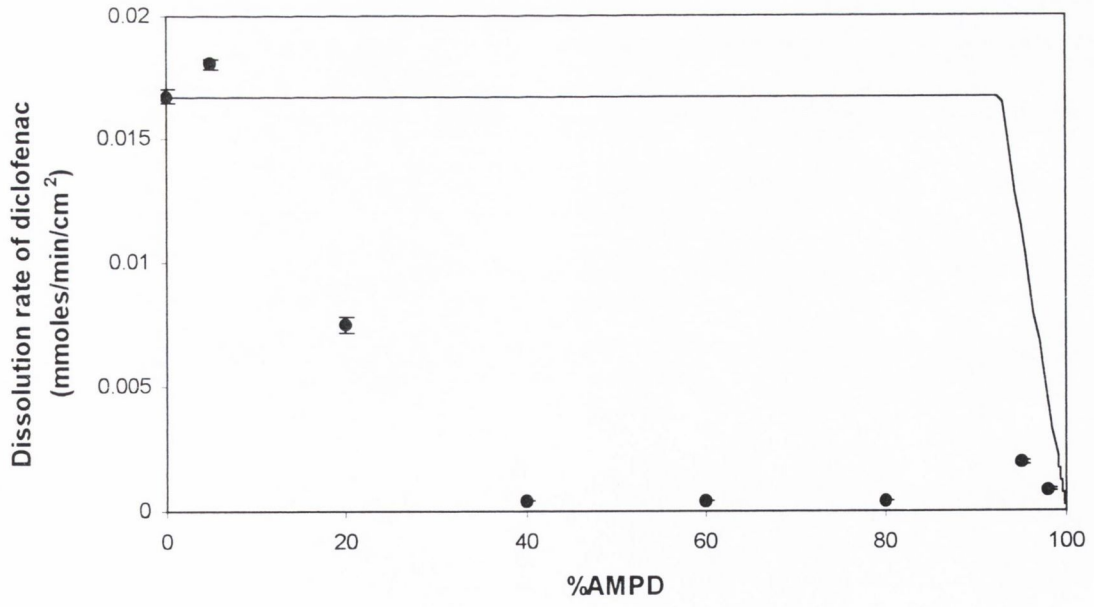

Figure 7. 24 Dissolution of diclofenac from AMPD:DDNL discs showing actual data (•) and the theoretical line for the two component non-interacting model (—)

Whereas the two component non-interacting model resulted in a reasonable fit for AMPD:DtBA and TRIS:DtBA data in the region of 20 – 90% base (MSC = 1.74 and 1.20, respectively), experimental data for the AMPD:DDNL systems was found to deviate dramatically from the model. The observed rate for the 5:95 system was higher than that predicted, whereas the rates determined for the systems with 20 – 98% AMPD were considerably lower than the theoretical rates. Deviation from the model was most apparent in the region 40 – 80% AMPD, where observed dissolution rates were ~40 times lower than those predicted.

XRD analysis of the 40:60, 60:40 and 95:5 AMPD:DDNL systems after dissolution revealed the presence of DAMPD monohydrate / anhydrate in the discs (Figure 7. 23), indicating that the diclofenac acid, initially present as DDNL, has interacted with the AMPD to form a salt. There is a ~66-fold difference in solubility between DDNL (446.7 mM) and DAMPD-MH (6.8 mM). Accordingly, the conversion from DDNL to DAMPD-MH resulted in dramatically different dissolution rates to those predicted from the two component non-interacting model (Figure 7. 24).

7.5.3. Two component (salt conversion) model

The two component (salt conversion) model was applied to the AMPD:DDNL systems; the black line in Figure 7. 25 represents the theoretical dissolution rates calculated from the model. Data obtained for the dissolution of diclofenac from the discs prepared with 40 – 80% AMPD was observed to be in very good agreement with the model. However, experimental dissolution rates for the 5:95 and 20:80 AMPD:DDNL systems were found to be higher than those predicted by the model. The two component (salt conversion) model involved the application of the DAMPD-MH:DDNL two component non-interacting model at concentrations of AMPD <21.4%. Calculation of the time required to reach steady state conditions for each of the systems examined with <21.4% AMPD (Section 3.2.20) revealed that the dissolution of DDNL from the 5:95 and 20:80 AMPD:DDNL systems would not be expected to achieve steady state before depletion of the disc. This can be attributed to the large solubility difference between DAMPD and DDNL (1:66). According to the two component model proposed by Higuchi et al. (1965b), the dissolution profile from time 0 for the receding layer (DDNL for the two systems studied) should show a downward curvature, reflecting a decrease in the dissolution rate with time. Therefore, the observed dissolution rates for the 5% and 20% AMPD systems would be expected to be higher than the steady state dissolution rates which were predicted by the two component non-interacting model.

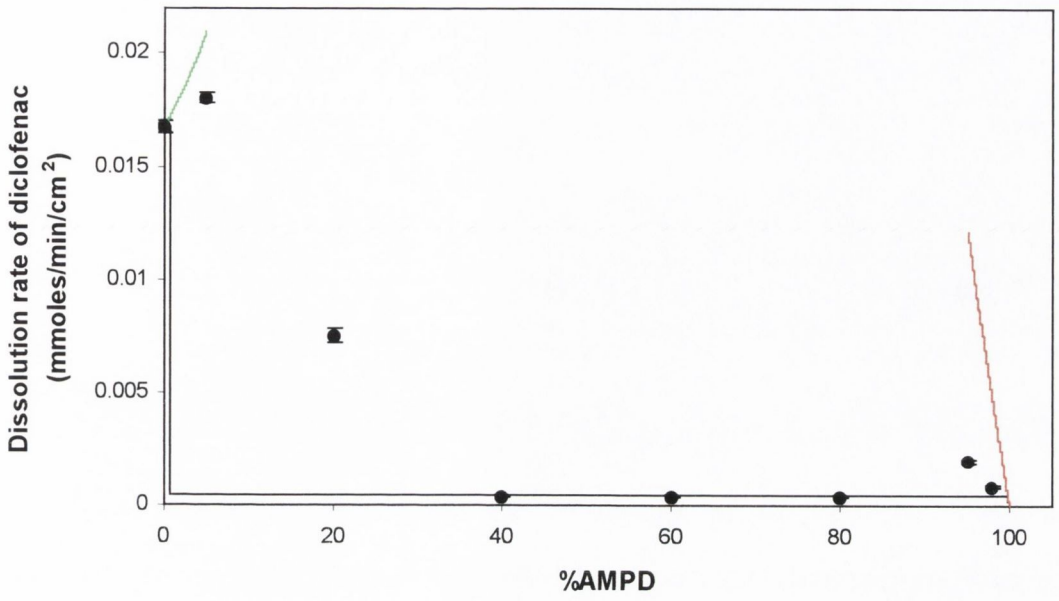

Figure 7. 25 Dissolution of diclofenac from AMPD:DDNL discs showing actual data (•) and theoretical lines for the two component (salt conversion) model (—) and carrier controlled dissolution (— and —)

However, the absence of steady state conditions would not account for a higher dissolution rate than that of pure DDNL, as observed in the case of the 5:95 system. The ability of DDNL to solubilise poorly water-soluble materials by self-association (Section 6.7.4) may contribute to the enhanced dissolution of diclofenac from the 5:95 system. Alternatively, the ~66-fold solubility difference between the two components thought to exist in the disc, DDNL and DAMPD-MH, suggests that DDNL may have the ability to act as a carrier for DAMPD-MH. This would involve an extension of the region in which dissolution is controlled by DDNL to higher weight fractions of DAMPD-MH than predicted by the two component non-interacting model. Equation 7.1, which relates to carrier controlled dissolution of molecularly dispersed drug, was used to calculate the dissolution rate of DAMPD-MH in the region corresponding to discs prepares from ≤5% AMPD. The dissolution rate of diclofenac in this region was estimated to equal the intrinsic dissolution rate of DDNL plus the dissolution rate of DAMPD-MH, as predicted from Equation 7.1, and is represented by the green line in Figure 7. 25. As observed in the case of carrier controlled dissolution from AMPD:DtBA and TRIS:DtBA discs prepared with ≥95% base, the dissolution rate of diclofenac for the 5:95 AMPD:DDNL system was lower than that predicted using Equation 7.1. This may be attributed to the drug being present as fine particles, the influence of DAMPD-

MH on the dissolution rate of DDNL or the high viscosity of a saturated solution of DDNL resulting in a lower diffusion coefficient for DAMPD-MH.

For systems with >21.4% AMPD, the model was comprised of the AMPD:DAMPD-MH two component model. All the systems examined occurred below the calculated critical mixture ratio. Therefore, according to the model, DAMPD-MH formed the surface layer and had a constant dissolution rate.

As observed for the AMPD:DtBA and TRIS:DtBA systems of equivalent w/w ratios, the observed dissolution rates for the 95:5 and 98:2 AMPD:DDNL systems were higher than those predicted from the two component (salt conversion) model. A ~4-fold degree of enhancement, relative to the predicted dissolution rate, was observed for the 95% AMPD system. This enhanced dissolution was attributed to the ability of the base to act as a carrier for DAMPD-MH. As with the AMPD:DtBA and TRIS:DtBA systems, the experimental dissolution rates for the 95:5 and 98:2 AMPD:DDNL systems were lower than the rates predicted for carrier controlled dissolution of molecularly dispersed drug (illustrated by the red line in Figure 7. 25).

The two component (salt conversion) model was found to predict dissolution rates for AMPD:DDNL systems more accurately than the two component non-interacting model (Figure 7. 24). Predictions by the two component (salt conversion) model were found to be most accurate for discs prepared with 40 – 80% AMPD.

7.5.4. Three component (salt conversion) model

The three component (salt conversion) model was applied to the AMPD:DDNL systems. The P values calculated from the salt solubility and base K_b values were 1.5% and 26%, respectively. As with the two component (salt conversion) model, the DAMPD-MH:DDNL two component non-interacting model was applied at concentrations of AMPD <21.4% and calculation of the time taken to reach steady state for the 5% and 20% AMPD systems indicated that these systems had not reached steady state during the dissolution run.

As seen in Figure 7. 26, the theoretical rates calculated when P = 1.5% are close to those predicted from the two component non-interacting model (Figure 7. 24) and are therefore in poor agreement with experimental data in the 40 – 80% AMPD systems. The dissolution rates predicted using a P value of 26% (calculated from the ratio of the K_b values) were similar to the rates predicted by the

two component (salt conversion) model (Figure 7. 25) and a good fit to the model was obtained for the data in the 40 – 80% AMPD region.

By allowing the P value to vary from 0 to 100, it was estimated that a level of conversion from DDNL to DAMPD-MH of >2.5% was required for the rates predicted from the three component (salt conversion) model to equal those predicted by the two component (non-interacting) model. This suggests that the level of conversion in the AMPD:DDNL discs was >2.5%.

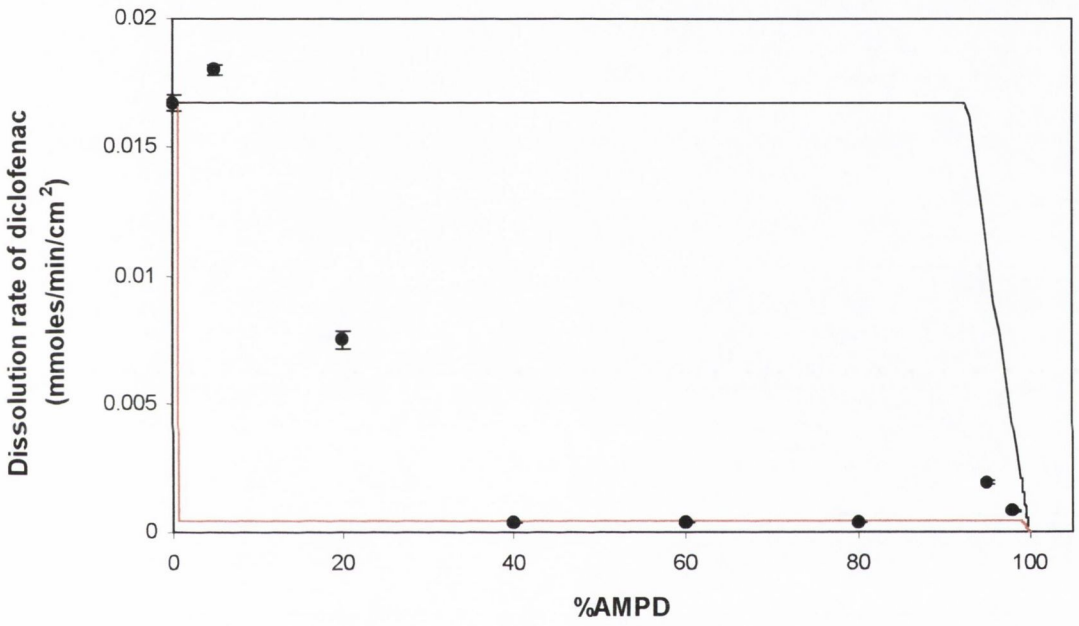

Figure 7. 26 Dissolution of diclofenac from AMPD:DDNL discs showing actual data (•) and theoretical lines for the three component (salt conversion) model when P = 1.5% (—) and when P = 26% (—)

7.6. DISSOLUTION OF DICLOFENAC FROM TRIS:DDNL SYSTEMS

Dissolution of diclofenac from discs prepared using DDNL and TRIS, a less soluble base than AMPD, was examined. The dissolution profiles for TRIS:DDNL systems with TRIS weight fractions in the range 5 – 98% are presented in Figure 7. 27. The dissolution rates calculated from the profiles are listed in Table 4, Appendix VII. As in the case of the AMPD:DDNL systems, incorporation of the base in the discs resulted in suppression of the dissolution of diclofenac, with the exception of the 5:95 system.

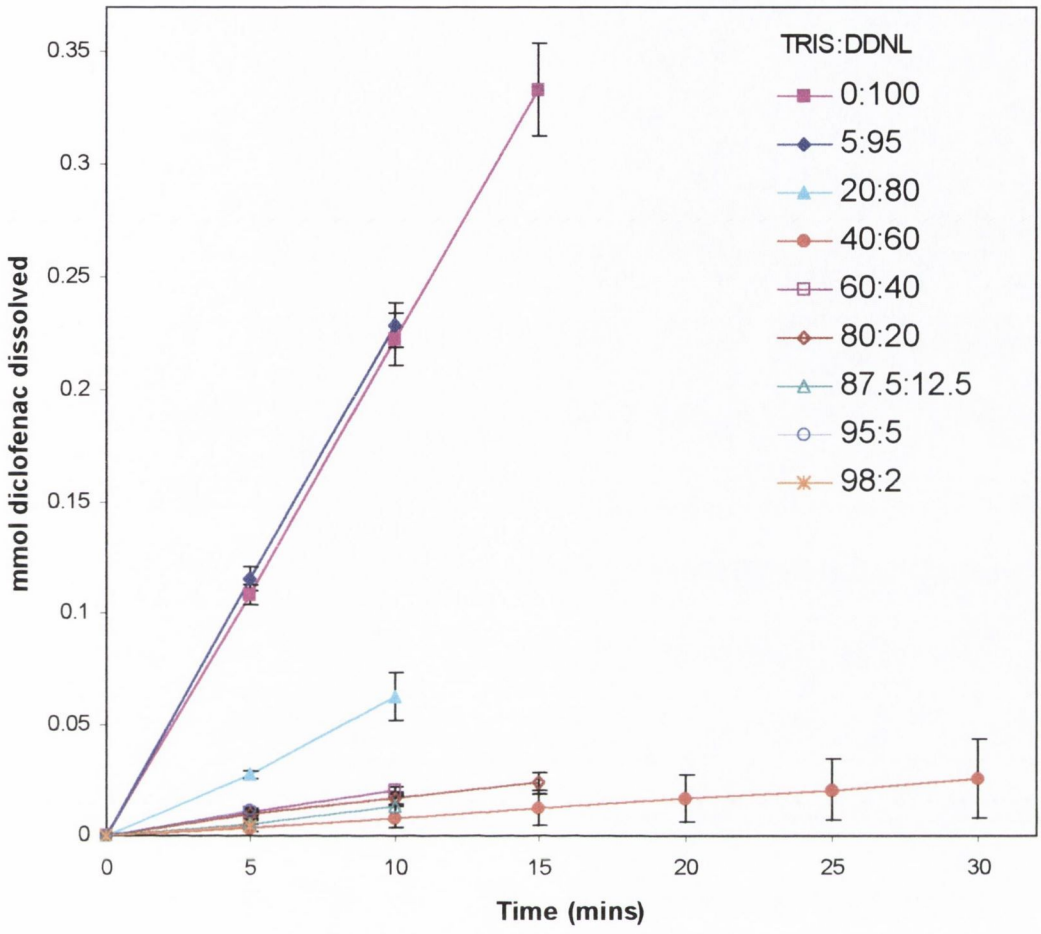

Figure 7. 27 Diclofenac dissolution from TRIS:DDNL discs

7.6.1. XRD analysis of mechanical mixes and discs before and after dissolution

XRD analysis was carried out on (a) mechanical mixes, (b) discs before dissolution and (c) discs after dissolution for the 40:60, 60:40 and 95:5 TRIS:DDNL systems. For each system, the XRD trace for the disc before dissolution exhibited peaks at the same 2θ values as the trace for the corresponding mechanical mix. The XRD trace for each disc after dissolution was compared with the trace for the corresponding disc before dissolution (Figure 7. 28 – Figure 7. 30).

The traces for the 40:60 AMPD:DDNL discs are presented in Figure 7. 28. The trace for the disc after dissolution was found to have identical peaks to that of the disc before dissolution.

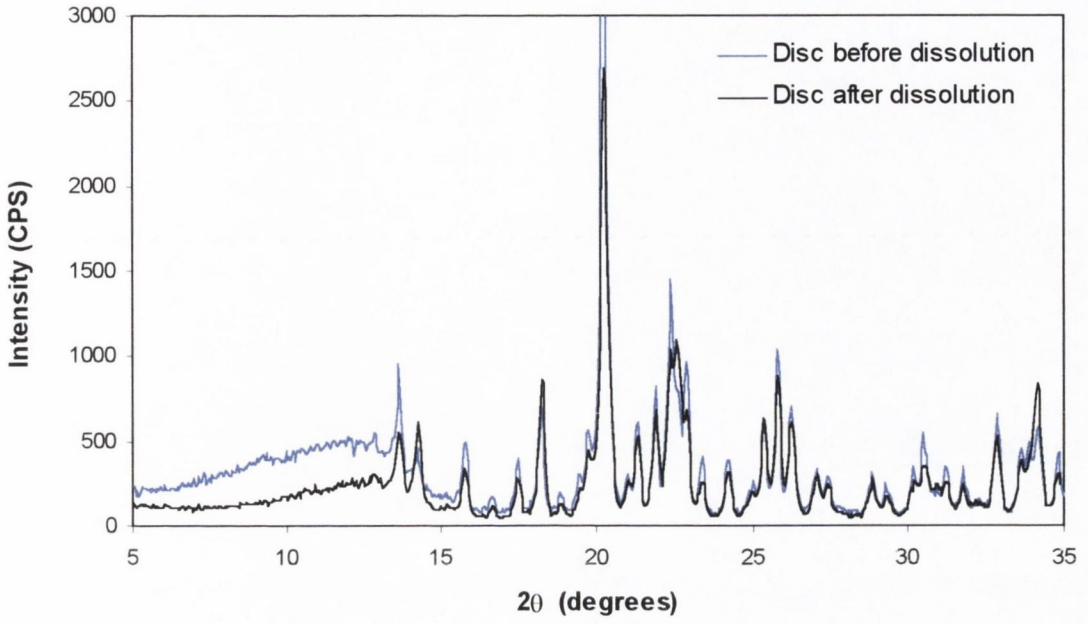

Figure 7. 28 XRD traces for TRIS:DDNL 40:60 discs before and after dissolution

The traces for the 60:40 TRIS:DDNL discs are presented in Figure 7. 29. Additional peaks were observed in the trace for the disc after dissolution, as illustrated by the arrows in Figure 7. 29.

The traces for the TRIS:DDNL 95:5 discs before and after dissolution are presented in Figure 7. 30. An extra peak was observed in the trace for the 95:5 disc after dissolution when compared to that of the disc before dissolution, as illustrated by the arrow in Figure 7. 30.

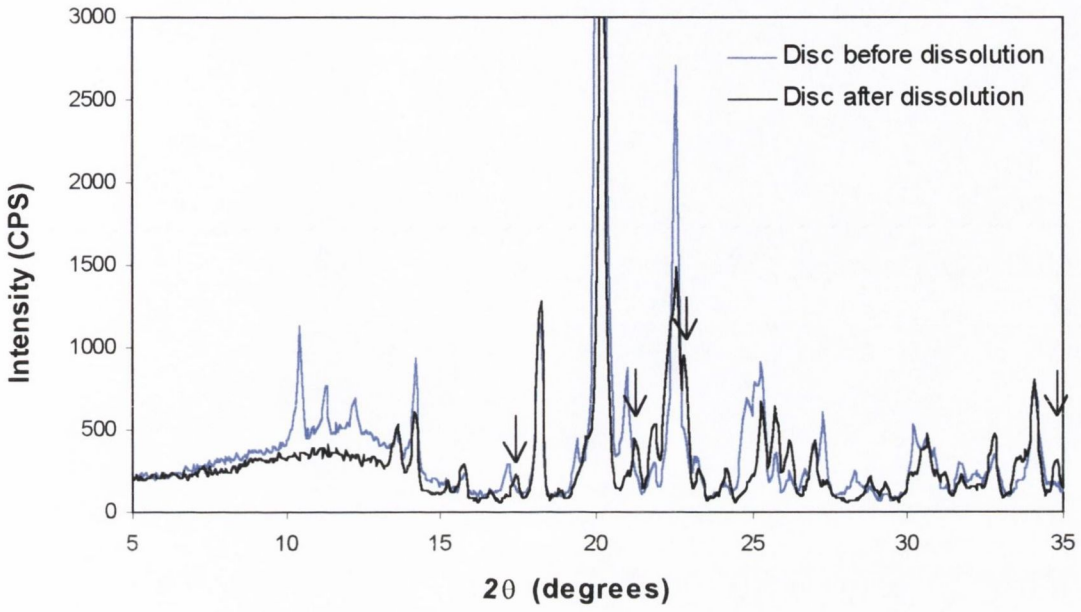

Figure 7. 29 XRD traces for TRIS:DDNL 60:40 discs before and after dissolution

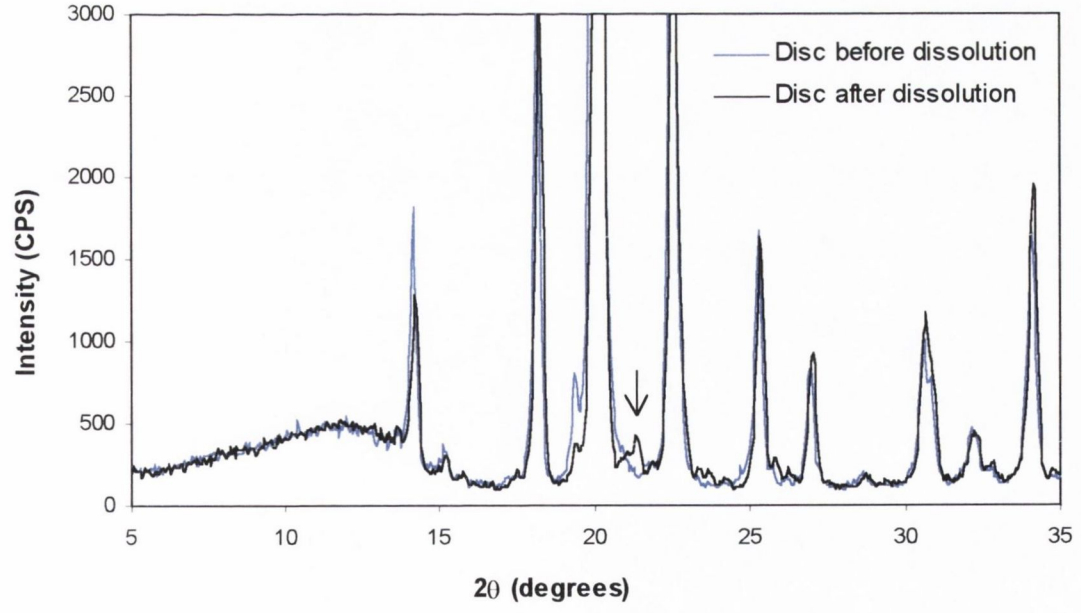

Figure 7. 30 XRD traces for TRIS:DDNL 95:5 discs before and after dissolution

The traces for TRIS:DDNL 60:40 and 95:5 discs after dissolution were examined with reference to the XRD traces for TRIS, DDNL and DTRIS (Figure 7. 31). The presence of the extra peaks in the traces for the disc systems was consistent with the presence of DTRIS in the disc.

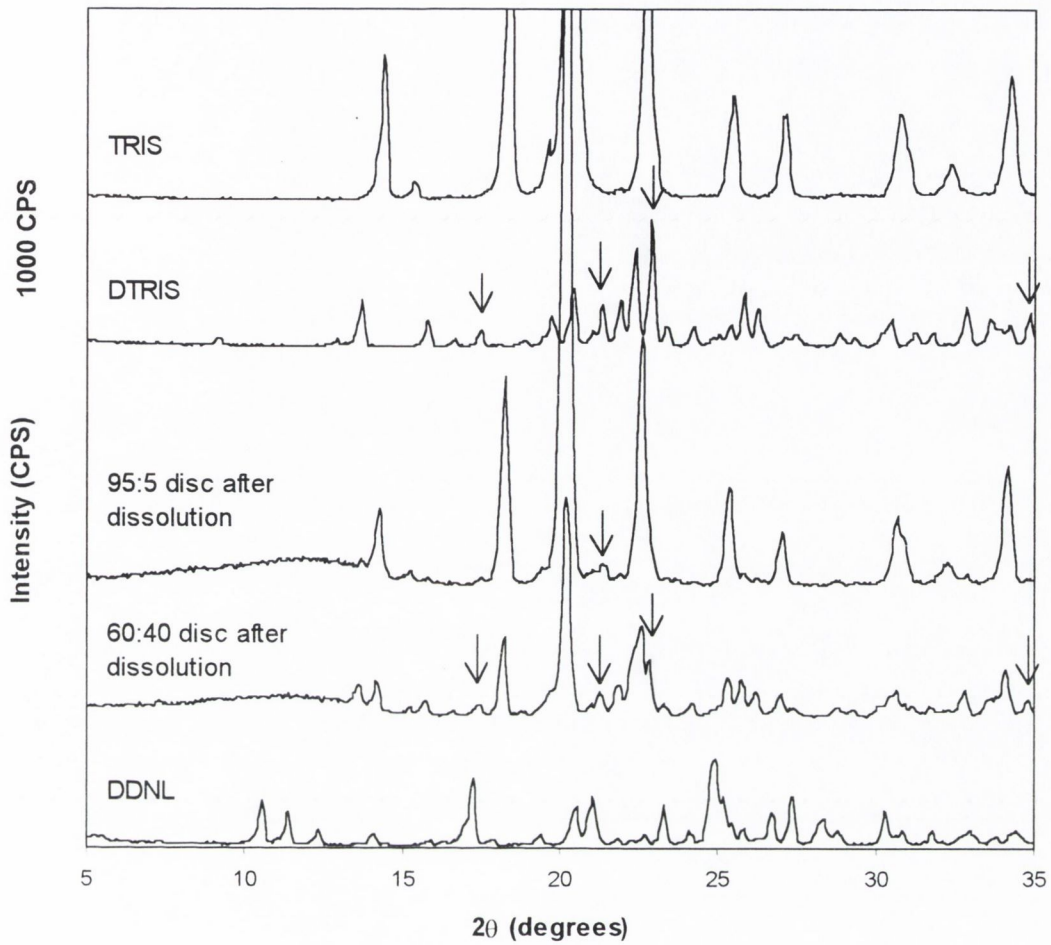

Figure 7. 31 XRD traces for the TRIS:DDNL 60:40 and 95:5 discs after dissolution compared with traces for TRIS, DDNL and DTRIS; the arrows indicate peaks which were not present in traces of the discs before dissolution; they correspond to peaks on the DTRIS trace, as illustrated

7.6.2. Two component non-interacting model

The observed dissolution rates for the TRIS:DDNL systems are plotted against %TRIS in Figure 7. 32. The line in Figure 7. 32 represents theoretical rates calculated from the two component non-interacting model. According to the model, the critical mixture ratio occurred at the 90.4:9.6 TRIS:DDNL weight fraction. Therefore, DDNL was expected to have formed the surface layer controlling dissolution in the systems prepared with 5 – 87.5% TRIS and the dissolution rate of diclofenac was predicted to be constant from the onset of dissolution and equal to the dissolution rate of pure DDNL. The calculations outlined in Section 3.2.20 were applied to confirm that

dissolution of DDNL from the 95:5 and 98:2 systems had reached steady state before the first sampling point of the dissolution run.

As in the case of the AMPD:DDNL systems, experimental data for the TRIS:DDNL discs showed considerable deviation from the model. The rates predicted for the systems with 40 – 87.5% AMPD were ~15 times higher than the experimental rates.

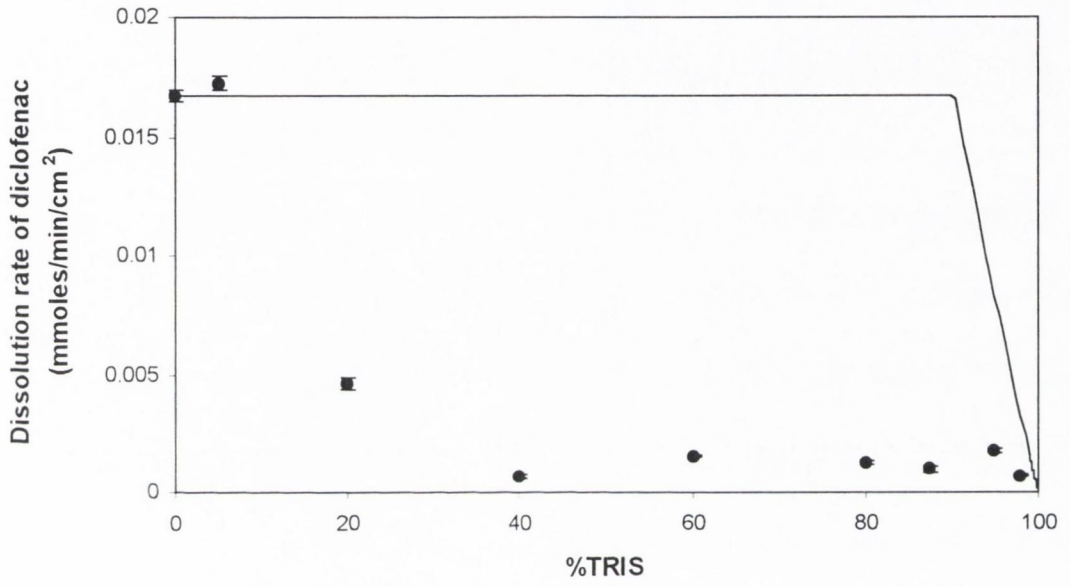

Figure 7. 32 Dissolution of diclofenac from TRIS:DDNL discs showing actual data (•) and the theoretical line for the two component non-interacting model (—)

XRD analysis of the 60:40 and 95:5 TRIS:DDNL systems after dissolution revealed the presence of DTRIS in the discs (Figure 7. 31), indicating that the diclofenac acid, initially present as DDNL, interacted with the TRIS to form a salt. DTRIS has a solubility (3.95 mM) ~110 times lower than that of DDNL (446.7 mM). Accordingly, expected dissolution rates from TRIS:DDNL systems were substantially lower than those predicted from the two component non-interacting model (Figure 7. 32).

7.6.3. Two component (salt conversion) model

The two component (salt conversion) model was thought to be a more accurate model than the simple two component non-interacting model for predicting dissolution from TRIS:DDNL

systems, as it accounts for conversion from DDNL to DTRIS. The black line in Figure 7. 33 represents the theoretical dissolution rates according to the two component (salt conversion) model. Experimental dissolution rates for all systems were found to be higher than those predicted by the model.

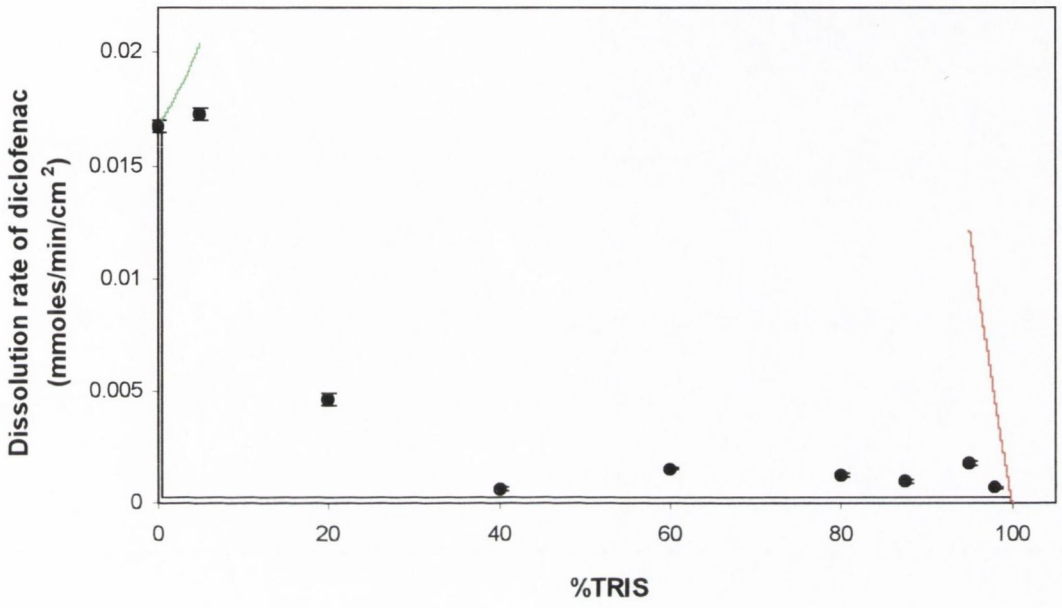

Figure 7. 33 Dissolution of diclofenac from TRIS:DDNL discs showing actual data (•) and theoretical lines for the two component (salt conversion) model (—) and carrier controlled dissolution (— and —)

The two component (salt conversion) model involved the application of the DTRIS:DDNL two component non-interacting model at concentrations of TRIS <23.9%. Calculation of the time required to reach steady state conditions for the systems in that concentration range (Section 3.2.20) revealed that the dissolution of DTRIS from the 5:95 and 20:80 TRIS:DDNL systems would not be expected to have achieved steady state before depletion of the disc. This can be attributed to the large solubility difference between DTRIS and DDNL (1:113). As seen with the 5:95 and 20:80 AMPD:DDNL systems (Section 7.5.3), downward curvature of the dissolution profile of DDNL before the steady state was reached would account for the observed rates being higher than those predicted for the steady state.

As in the case of the 5:95 AMPD:DDNL system, the dissolution rate for the 5:95 TRIS:DDNL system was higher than that of DDNL. However, in contrast to the AMPD:DDNL system, the

increase in dissolution rate relative to DDNL was not as great as that obtained for the 5:95 AMPD:DDNL system and was not found to be statistically significant. As described for the AMPD:DDNL system, an increase in dissolution rate could be attributed to the ability of DDNL to solubilise DTRIS. Alternatively, the 113-fold solubility difference between DDNL and DTRIS would suggest the tendency for carrier controlled dissolution to occur. The predicted rates for carrier controlled dissolution, calculated as described in Section 7.5.3, are illustrated by the green line in Figure 7. 33.

For systems with >23.9% TRIS, the model was comprised of the TRIS:DTRIS two component model. All the systems examined occurred below the calculated critical mixture ratio. Therefore, according to the model, DTRIS forms the surface layer and has a constant dissolution rate.

As in the case of the AMPD:DtBA, TRIS:DtBA and AMPD:DDNL systems prepared with 95% or 98% base, carrier controlled dissolution would be expected to influence dissolution from the TRIS:DDNL systems with $\geq$95% TRIS. The dissolution rates calculated from Equation 7.1, relating to carrier controlled dissolution of molecularly dispersed drug, are represented by the red line in Figure 7. 33. As previously observed for 95:5 and 98:2 base:salt systems, the experimental dissolution rates for the 95:5 and 98:2 AMPD:DDNL systems were lower than the rates predicted for carrier controlled dissolution.

The two component (salt conversion) model (Figure 7. 33) was found to predict dissolution rates for TRIS:DDNL systems more accurately than the two component non-interacting model (Figure 7. 32), particularly for systems prepared with 40 – 87.5% TRIS. However, whereas the two component (salt conversion) model was very accurate for predicting dissolution from AMPD:DDNL systems prepared with 40 – 80% AMPD (Figure 7. 25), observed dissolution rates for TRIS:DDNL systems in this region were higher than the rates predicted by the model. Similarly, higher rates than predicted by the model were observed for TRIS:DtBA systems prepared with 20 – 90% TRIS (Section 7.4.3). As discussed in the case of the TRIS:DtBA systems, the ability of DTRIS to form supersaturated solutions may contribute to deviation from the model.

7.6.4. Three component (salt conversion) model

The three component (salt conversion) model was applied to the TRIS:DDNL systems. The P values calculated from the salt solubility and base K_b values were 0.9% and 10%, respectively. The resulting theoretical rates are presented in Figure 7. 34.

As with the two component (salt conversion) model, the DTRIS:DDNL two component non-interacting model was applied at concentrations of TRIS <23.9% and calculations relating to the 5% and 20% TRIS systems indicated that these systems had not reached steady state during the dissolution run.

Theoretical rates calculated from the three component (salt conversion) model using a P value of 0.9% (calculated from the ratio of the salt solubilities) were similar to those rates predicted from the two component non-interacting model (Figure 7. 32) and therefore differed dramatically from the experimental data. The dissolution rates predicted using a P value of 10% (calculated from the ratio of the K_b values) were identical to the rates predicted by the two component (salt conversion) model (Figure 7. 33) and showed the best fit to the model in the 40 – 87.5% TRIS region.

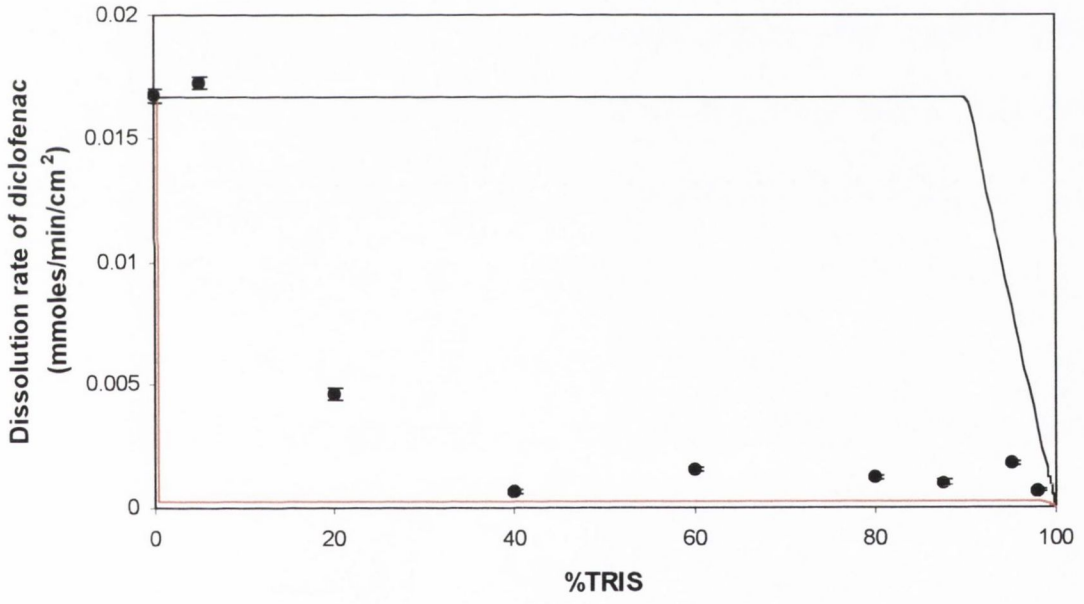

Figure 7. 34 Dissolution of diclofenac from TRIS:DDNL discs showing actual data (•) and theoretical lines for the three component (salt conversion) model when P = 0.9% (—), P = 10% (—)

By allowing the P value to vary, it was estimated that when the P value was >1.4%, the rates predicted by the three component (salt conversion) model were identical to those predicted by the two component (salt conversion) model, resulting in a better fit to the experimental data than when P was <1.4%, resulting in a prediction identical to the two component (salt conversion) model. This suggested that the level of conversion from DtBA to DTRIS in the TRIS:DtBA discs was >1.4%.

7.7. CONCLUSION

Dissolution tests on physical mixes of diclofenac salts with the organic amine bases, TRIS and AMPD, revealed that the dissolution rate of DtBA was slightly enhanced at certain weight fractions of the base. On the other hand, the dissolution rate of DDNL, the more soluble diclofenac salt, was dramatically reduced in the presence of AMPD or TRIS.

McGloughlin (1989) reported that benzoic acid:TRIS compressed discs resulted in enhanced dissolution rates of benzoic acid, of the same order as the dissolution rate of a 1:1 benzoic acid:TRIS salt. A recent study by Gabr and Borg (1999) investigated the effect of different weight fractions of TRIS on the dissolution rates of hydrochlorothiazide from hydrochlorothiazide:TRIS coprecipitates. Maximum relative enhancements of 10 and 5 were obtained in water and 0.1 N HCl, respectively. The authors deduced from results of a study of the solubility of hydrochlorothiazide in water with increasing concentrations of TRIS that a 1:1 *soluble complex* was formed. Examination of the coprecipitates by FT-IR, differential scanning calorimetry and X-ray diffraction confirmed that hydrochlorothiazide and TRIS had interacted to form a new species. The nature of the interaction between the two components was not established. On consideration of the FT-IR results, the authors suggested that there may have been an interaction between the acidic NH group of hydrochlorothiazide and the basic group of TRIS. In the case of all four diclofenac salt:base systems investigated in this study, XRD analysis of discs after dissolution revealed interaction of the diclofenac acid from the original salt form with the added base, to produce an alternative salt form.

For three of the four systems studied, AMPD:DtBA, AMPD:DDNL and TRIS:DDNL, the two component non-interacting model was less effective in predicting diclofenac dissolution from the discs than the model which took into account the salt conversion process. The lack of suitability of the two component non-interacting model is particularly notable in the case of the AMPD:DDNL and TRIS:DDNL systems, where the salts formed were considerably less soluble than DDNL. The observed rates were 66 and 15 times lower than the rates predicted by the two component non-interacting model for the AMPD:DDNL and TRIS:DDNL systems, respectively. In applying the two component (salt conversion) model, consideration was given to deviation at particular regions of the composition profile: carrier controlled dissolution theory was applied to discs with $\geq 95\%$ base and, in the case of the DDNL systems, to discs with $\leq 5\%$ base and non-steady state conditions were found to exist during the dissolution run for the DDNL discs with low proportions of base.

Higher dissolution rates than predicted by the two component (salt conversion) model were observed for TRIS:DtBA and TRIS:DDNL systems in the region where the model accurately predicted dissolution from AMPD:DtBA and AMPD:DDNL systems. Whereas TRIS is ~1.5 times less soluble than AMPD and the resulting salt with diclofenac, DTRIS, is less soluble than DAMPD-MH, the incorporation of 40 – 80% TRIS with DDNL resulted in dissolution rates on average ~2.9 higher than those of the corresponding AMPD systems. These findings may be explained by observation made during the pH-solubility study of DTRIS, i.e. that the addition of TRIS to a diclofenac acid solution resulted in supersaturation relative to the equilibrium solubility of DTRIS.

Comparison of the goodness of fit of the data to the two component non-interacting model and to the two component (salt conversion) model indicated whether each system was best represented by 0% or 100% conversion from SALT1 to SALT2. However, reaction of the diclofenac acid, present in the disc as SALT1, with the base to form SALT2 is unlikely to occur on an "all or nothing" basis. The three component (salt conversion) model predicted dissolution rates for varying degrees of conversion (P values). For values of P below a certain threshold value, the dissolution rates predicted by the three component (salt conversion) model were identical to those simulated by the two component non-interacting model. When the P value exceeded this limit, the rates predicted by the three component (salt conversion) and by the two component (salt conversion) models were the same. For each salt:base system studied, the degree of conversion from the original salt to the newly-formed salt was estimated to occur above / below a threshold value particular to that system.

To investigate if the level of conversion from SALT1 to SALT2 could be predicted, P values were calculated from the ratio of SALT1 and SALT2 solubilities and the ratio of the K_b values of the two bases. In the case of the salt:base systems in which the rates predicted by the two component (salt conversion) model showed best agreement with experimental data (AMPD:DtBA, AMPD:DDNL and TRIS:DDNL systems), no correlation was observed between the method of calculating P and the prediction of dissolution rates identical to those of the two component (salt conversion) model. For AMPD:DtBA discs, the P value calculated from the ratio of the salt solubilities resulted in rates identical to those predicted by two component (salt conversion) model. On the other hand, in the case of the AMPD:DDNL and TRIS:DDNL systems, the predicted rates were the same as those predicted by two component (salt conversion) model when the P values calculated from base K_b values were employed. This suggests that the degree of conversion from SALT1 to SALT2 was not solely dependent on either the relative solubilities of the two salts or the relative basicities of the bases.

Chapter 8

General discussion

8.1. SALT FORMATION

Salt formation is a frequently employed technique for altering the physicochemical properties of a drug substance. For example, dramatic enhancements in solubility relative to the free acid or base can be achieved through salt formation (e.g. Senior, 1973; Agharkar et al., 1976; Gu and Strickley, 1987; Forbes et al., 1995). This study involved an investigation of the properties of diclofenac salts prepared from a range of organic bases. Two of the salts, DHEP and DDEA, are available in pharmaceutical products. Another of the salts studied, DTRIS, was also prepared in a previous study (Fini et al., 1996). Five novel salts of diclofenac were prepared from the following organic bases: *tert*-butylamine (tBA), 2-amino-2-methylpropanol (AMP), 2-amino-2-methyl-1,3-propanediol (AMPD), benzylamine (BA) and deanol (DNL). In the case of DAMP and DBA, two polymorphic forms of each salt were identified. For three of the salts, novel pseudopolymorphic forms were identified.

The solubility and intrinsic dissolution rates of each the diclofenac salts were determined. The aqueous solubilities of the salts ranged from 3.95 mM (DTRIS) to 446 mM (DDNL), representing a 113-fold difference in solubility. The solubility of DDNL exceeded that of DHEP (273 mM), the most soluble salt previously identified. Its solubility (446mM) is ~7.4×10^3 times higher than the reported aqueous solubility of diclofenac acid (6×10^{-2} mM, Chiarini et al., 1984).

There are several reports in the literature of a correlation between salt melting point and salt solubility. For example, Gould (1986) reported a relationship between the inverse of the salt melting point and the logarithm of the salt solubility for a series of salts of a basic antimalarial drug ($R^2 = 0.9325$, n = 4). An inverse relationship between salt melting point and log solubility was reported by Thomas and Rubino (1996) for a series of secondary amine hydrochloride salts ($R^2 = 0.807$, n = 8) and by Ledwidge (1997) for a series of CEL50 salts ($R^2 = 0.91$, n = 7). Anderson and Conradi reported a nonlinear relationship between salt melting point and log K_{SP} for a series of flurbiprofen salts. For the series of diclofenac salts studied, a relationship between the inverse of the salt melting point and the logarithm of the salt solubility was observed ($R^2 = 0.7780$, n = 8).

Relationships between the properties of the salt forming agents and those of the resulting diclofenac salts were explored. Reasonable correlation was found between the free base melting point and the salt melting point ($R^2 = 0.7518$, n = 7). However, despite the observed relationship between salt melting point and salt solubility, correlation between the base melting point and salt solubility was poor ($R^2 = 0.1695$, n = 7). Similarly, Ledwidge (1997) reported a lack of correlation between base melting point and salt solubility for a series of CEL50 salts.

The study of diclofenac salts revealed a log-log relationship between hydrogen ion concentration in the saturated salt solution and salt solubility (R^2 = 0.8957, n = 8). This is analogous to the relationship found in the case of the salts of CEL50, a basic drug, studied by Ledwidge (1997) (R^2 = 0.90, n = 7). The plots for the two salt series of pH of the saturated solution against log solubility are presented in Figure 8. 1. As expected the solubility of the salts of the acidic drug increased as the pH of the salt solution increased, whereas the inverse applied in the case of the basic drug.

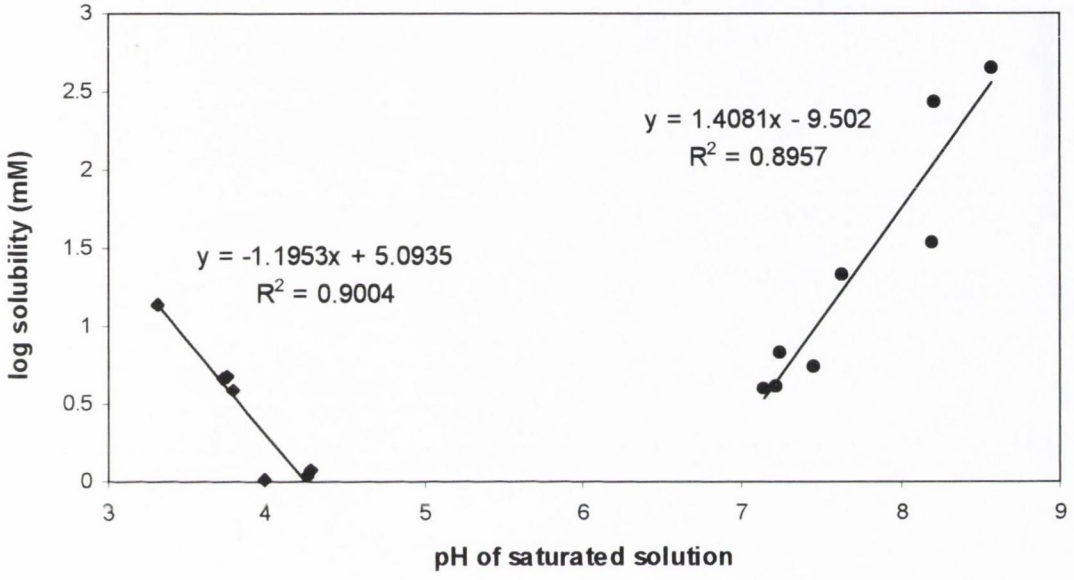

Figure 8. 1 pH of the saturated solution versus solubility of the salt for the diclofenac salts studied (•) and a series of CEL50 salts studied by Ledwidge, (1997) (♦)

The equation derived by Rubino (1989) (Equation 6.1), relating salt solubility to the salt melting point and the stoichiometric amounts of water in the hydrate forms, was used to calculate predicted solubilities for the diclofenac salts. The plot of log predicted solubility against log observed solubility is presented in Figure 8. 2. The graph also includes the data used to derive the equation (Rubino, 1989) and values relating to the CEL50 salt series investigated by Ledwidge (1997). The plot of the data obtained by Rubino (1989) has a slope of 1.04 (R^2 = 0.9329, n = 11), close to the ideal slope of unity (represented by the dashed line in Figure 8. 2).

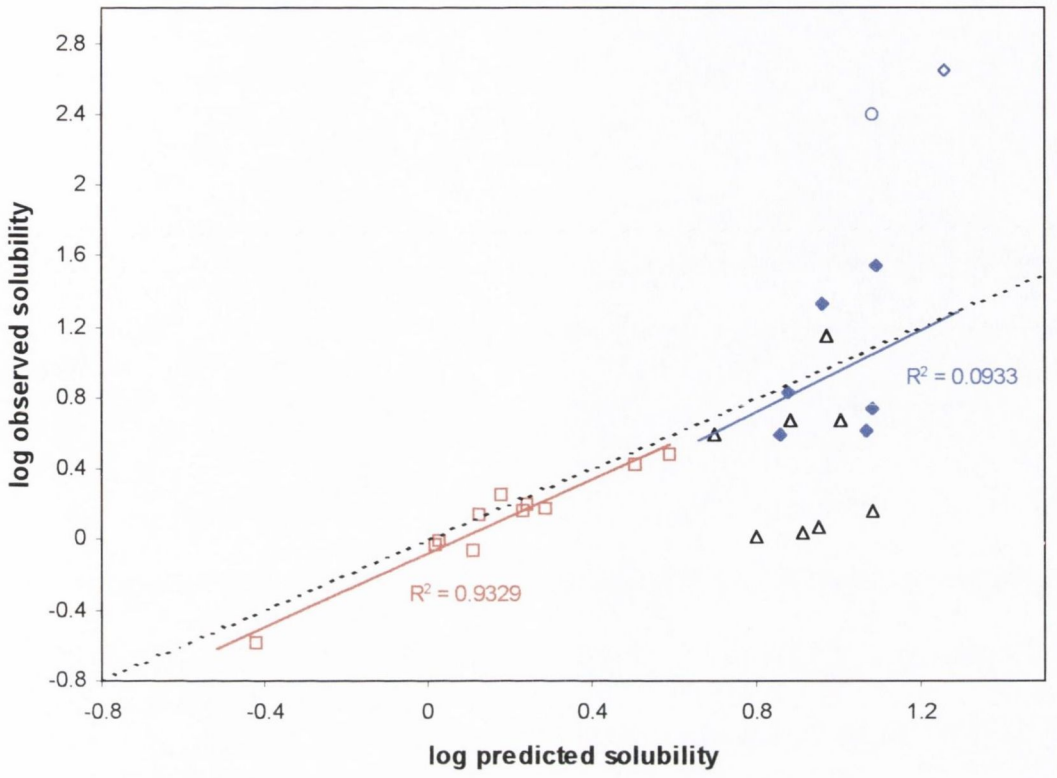

Figure 8. 2 Log predicted solubility (calculated from Equation 6.1) versus log observed solubility for a series of sodium salts (Rubino, 1989) (□), a series of CEL50 salts (Ledwidge, 1997) (△), DHEP (○), DDNL (◇) and the other diclofenac salts studied (♦). Trendlines are illustrated for the sodium salt data (—) and the diclofenac salt data (—). The dashed line represents the line of slope 1.

Predicted and observed solubilities (log scale) displayed no correlation in the case of the CEL50 salt series. When the data for all the diclofenac salts studied was fitted to a straight line, a large slope of 4.25 was obtained. The slope of the line was distorted by the inclusion of DHEP and DDNL, which showed very high observed solubility values relative to the values predicted from their melting points and hydration characteristics. This may be attributed to the ability of DHEP and DDNL to form micelles at concentrations above 30 mM and 45 mM, respectively. These two salts were therefore excluded from the series of salts and an alternative trendline was fitted, as illustrated in Figure 8. 2. This line has a slope of 1.14. However, there is a high degree of scatter around the line, indicating a lack of correlation between the predicted and observed solubilities.

8.2. HYDRATE FORMATION

In a previous study (Ledwidge et al., 1996) reported the identification of a dihydrate form of DHEP. In the current study, a monohydrate form of DHEP was also identified following its detection in commercial batches of the salt. In addition, hydrate forms of DDEA (monohydrate) and DAMPD (monohydrate) were identified. As discussed in Section 2.4, the existence of hydrate forms of a drug will influence pharmaceutically relevant properties, such as solubility, and will therefore have implications in terms of formulation and bioavailability. The hydrate of a compound is always less soluble in water than the corresponding anhydrous form which crystallised from water at the same temperature (Khankari and Grant, 1995). Therefore, the presence of the monohydrate form of DHEP in commercial batches of anhydrous DHEP may be responsible for the precipitation from aqueous solutions of certain batches of the salt.

A systematic analysis of the tendency of diclofenac salts to form solvates during salt preparation (Fini et al., 1995a) revealed that such behaviour was common to salts containing a hydroxyl cation crystallised from protic solvents. The authors attributed this to participation of molecules of protic solvent in the inter- or intra-molecular hydrogen bonding. Examination of the crystal structure of salts of meclofenamic acid with choline and ethanolamine in the solid state indicated that the hydroxyl group of the cation interacts via hydrogen bonding with the carboxylate group of the anion (Dhanaraj and Vijayan, 1987). Since meclofenamic acid is structurally related to diclofenac, it was not surprising that the salt of diclofenac and HEP, a hydroxyl base, was found to exist as ion pairs in the solid state (Castellari and Sabatino, 1994). In these structures, besides the electrostatic interactions, cation and anion are bound by hydrogen bonds involving the carboxylate group of the diclofenac anion and the OH group of the cation. In the current study, hydrates were identified for two salts prepared from bases with hydroxyl groups, DHEP and DAMPD. In addition, despite the absence of a hydroxyl group in the DEA molecule, a monohydrate form of DDEA was identified. This suggests that the formation of a hydrate of a diclofenac salt is not dependent on the presence of a hydroxyl group on the cation of the salt.

DHEP and DDEA are both commercially available in pharmaceutical products. Novel hydrates of both salts have been identified in this study. The behaviour in solution of the novel hydrates of DHEP (DHEP-MH) and DDEA (DDEA-MH) was investigated. The results for DHEP-MH are summarised in Table 8. 1, together with the data previously obtained for the anhydrate and dihydrate forms of DHEP (Ledwidge, 1997).

Table 8. 1 Intrinsic dissolution rate, solubility and heat of solution values (water, 25°C) for the anhydrate, monohydrate and dihydrate forms of DHEP

DHEP crystalline form	*Intrinsic dissolution rate (mmol/min/cm²)*	*Solubility (mM)*	*Heat of solution (kJ/mol)*
DHEP-A	0.0178*	1350**	22.6 ± 1.0*
DHEP-MH	0.0102	774**	26.9 ± 0.6
DHEP-DH	0.0036*	273	34.0 ± 0.6*

* Ledwidge (1997)

** estimated from intrinsic dissolution rate

The intrinsic dissolution rate of DHEP-MH in water at 25°C was found to be ~2.8 times higher than that of the dihydrate form and ~1.7 times lower than that of the anhydrate. Substitution of the intrinsic dissolution rate values for the monohydrate and dihydrate forms and the equilibrium solubility of the dihydrate form into Equation 4.1 resulted in an estimation of 774 mM for the solubility of the monohydrate form. The heat of solution of DHEP-MH (water, 25°C) was determined to be 26.9 ± 0.6 kJ/mol, a value which lies between the heat of solution values determined for the anhydrate and dihydrate values (Ledwidge, 1997).

The intrinsic dissolution rate, solubility and heat of solution values for the anhydrous and monohydrate forms of DDEA are summarised in Table 8. 2. The intrinsic dissolution rate of DDEA-A was found to be ~1.7 times greater than that of DDEA-MH. Since the monohydrate form precipitates from aqueous solutions of the anhydrous form, the solubility of DDEA-A was estimated from the ratio of the intrinsic dissolution rates of the two forms (Equation 4.1). This resulted in an estimate of 57 mM for the aqueous solubility of DDEA-A.

The heats of solution for the DHEP forms were determined in water. However, water:methanol 50:50 v/v was used for measurement of DDEA-A and DDEA-MH heats of solution in order to fulfil the requirement for rapid dissolution (Section 3.2.14). Whereas the heat of solution depends on the solvent, the difference between the heats of solution of two forms of the same compound (equal to heat of hydration in the case of hydrate and anhydrate forms) is independent of the solvent (Giron, 1995).

Table 8. 2 Intrinsic dissolution rate and solubility values (water, 25°C) and heat of solution values (water:methanol 50:50 v/v, 25°C) for the anhydrate and monohydrate forms of DDEA

DDEA crystalline form	*Intrinsic dissolution rate (mmol/min/cm²)*	*Solubility (mM)*	*Heat of solution (kJ/mol)*
DDEA-A	0.0031	57*	26.3 ± 0.2
DDEA-MH	0.0019	35	28.8 ± 0.6

* estimated from intrinsic dissolution rate

A 24-fold difference was observed between the estimated solubility values for the anhydrous forms of DHEP and DDEA. On the other hand, an 8-fold difference was observed between DHEP-DH and DDEA-MH, the hydrate forms that precipitate from aqueous solutions of DHEP-A and DDEA-A, respectively.

8.3. SUPERSATURATION AT THE pH_{max}

The pH-solubility profiles of three diclofenac salts, DDEA, DDNL and DTRIS, were studied. In each system, the addition of the appropriate base to diclofenac acid resulted in supersaturation at the pH_{max}. Several studies have used apparent solubility product (K'_{SP}) values taken from pH-solubility data to demonstrate drug self-association in drug solutions (Bogardus and Blackwood, 1979; Serajuddin and Jarowski, 1985a; Serajuddin and Mufson, 1985). Increasing K'_{SP} values as drug concentrations increased were explained by a lowering of the drug activity coefficient due to the possible formation of self-association complexes (Serajuddin and Mufson, 1985). Ledwidge and Corrigan (1998) investigated the pH-solubility profile of DHEP and reported an increase in K'_{SP} values in the pH region in which supersaturation occurred. This finding was attributed to the ability of DHEP to self-associate. The self-association behaviour of the salt was confirmed by demonstrating its ability to solubilise NPN, a water-insoluble dye (Ledwidge and Corrigan, 1998).

The apparent supersaturation levels achieved for the DTRIS, DDEA and DDNL systems were 1.5, 2.3 and >2.4, respectively. These levels were lower than the value of >3 reported for the DHEP pH-solubility profile (Ledwidge and Corrigan, 1998). The level of supersaturation determined for

all four diclofenac salts are in the same range as the values previously reported for the pH-solubility profiles of papaverine (~3, Serajuddin and Mufson, 1985), theophylline (~4.5, Serajuddin and Jarowski, 1985b), salicylic acid (~1.4, Serajuddin and Jarowski, 1985b), trimethoprim (~1.4, Dahlan et al., 1987), phenytoin (~1.3, Serajuddin and Jarowski, 1993) and bupivacaine (~1.4, Shah and Maniar, 1993).

The apparent solubility product (K'_{SP}) values taken from the pH-solubility data for DDEA, DDNL and DTRIS are presented in Table 5.1, Table 8. 3 and Table 8. 4, respectively. For each salt system, there was an increase in the calculated solubility product around the pH_{max}, the region where supersaturation was observed. The most dramatic increase in K'_{SP} was observed for DDNL solutions at pH 9.11 and pH 9.23, relative to the solutions at lower pH values. Accordingly, of the three salts studied, the greatest degree of supersaturation (>2.4) was observed for DDNL. The observation of increased K'_{SP} values at the pH_{max} was in accordance with the results obtained in previous studies (Bogardus and Blackwood, 1979; Serajuddin and Jarowski, 1985a; Serajuddin and Mufson, 1985; Ledwidge and Corrigan, 1998) and suggested the occurrence of self-association.

Surface tension measurements and solubilisation studies did not detect self-association for unsaturated DDEA solutions (<33 mM). However, the formation of vesicles and lyotropic liquid crystals in supersaturated solutions of DDEA has been reported (Kriwet and Müller-Goymann, 1993). The ability of DDNL to self-associate in solution was demonstrated by surface tension measurements and solubilisation of NPN. A CAC value of 45 mM was obtained (Section 6.7.4).

Table 8. 3 K'_{SP} estimates from pH-solubility data for DDNL

pH	S_T (M)	$[DNL^+]$ (M)	K'_{SP}
7.94	3.44×10^{-2}	3.44×10^{-2}	1.19×10^{-3}
8.15	3.94×10^{-2}	3.94×10^{-2}	1.55×10^{-3}
8.29	4.09×10^{-2}	4.09×10^{-2}	1.67×10^{-3}
8.52	6.99×10^{-2}	6.99×10^{-2}	4.89×10^{-3}
9.11	8.39×10^{-1}	8.39×10^{-1}	7.04×10^{-1}
9.23	8.83×10^{-1}	8.83×10^{-1}	7.80×10^{-1}

Table 8. 4 K'_{SP} **estimates from pH-solubility data for DTRIS**

pH	S_T (M)	[$TRIS^+$] (M)	K'_{SP}
7.14	4.67×10^{-3}	4.67×10^{-3}	2.18×10^{-5}
7.17	4.50×10^{-3}	4.50×10^{-3}	2.02×10^{-5}
7.31	5.23×10^{-3}	5.23×10^{-3}	2.73×10^{-5}
7.35	5.91×10^{-3}	5.91×10^{-3}	3.49×10^{-5}
7.88	4.67×10^{-3}	4.68×10^{-3}	2.18×10^{-5}
8.6	4.75×10^{-3}	4.75×10^{-3}	2.26×10^{-5}
8.93	4.68×10^{-3}	4.69×10^{-3}	2.20×10^{-5}

The tendency for some diclofenac salts to self associate may affect their diffusivity. Self-association of solutes in solution leads to the formation of larger molecules, which generally diffuse more slowly in solution (Grant and Higuchi, 1990). A reduction in diffusivity affects transport across membranes (e.g., Nagadome et al., 1995; Mikkelson et al., 1980). Accordingly, DHEP demonstrated a lower effective permeability for transport across a porous membrane than DDEA or DNa. Whereas micelle formation was detected for DHEP from concentrations of 30 mM, DDEA and DNa solutions do not display self association at concentrations below their saturated aqueous solubilities.

8.4. EFFECT OF AN IONISABLE EXCIPIENT ON THE DISSOLUTION OF DICLOFENAC SALTS

Soluble excipients, such as polyethylene glycols, polyvinylpyrrolidine, cyclodextrins and sugars (e.g. mannitol, lactose), have been widely used to improve the dissolution rate of drugs (e.g., Simonelli et al., 1969; Corrigan et al., 1979; Corrigan and Stanley, 1982). In addition, ionisable excipients, which have the potential to interact with acidic or basic drugs, have been used to enhance dissolution. For example, improved dissolution of acidic drugs through the use of basic excipients (Levy et al., 1965; Javaid and Cadwallader, 1972; McGloughlin, 1989) or buffering agents (Doherty and York, 1989; Tirkonnen et al., 1985) has been reported.

McGloughlin (1989) developed two models to predict dissolution from acidic drug:basic excipient mixtures, the two component (linear solubility) model and the two component (salt formation) model. Both models predicted a plateau in the dissolution rate:composition profile, corresponding

to the solubility of the salt of the acid and base. Similarly, the solubility of the drug:excipient salt would be expected to strongly influence dissolution from mixtures of a salt of an acidic drug and a basic excipient or mixtures of a salt of a basic drug and an acidic excipient. Of the mechanical mixes studied by Cleary (1987), consisting of a salt of a basic drug and an acidic excipient, the greatest degree of enhancement in dissolution rate was observed for the quinidine sulphate:succinic acid system (14-fold increase in dissolution rate for discs containing 35 %w/w succinic acid). In a subsequent study, McNamara (1988) prepared the 2:1 quinidine succinate salt and reported that the initial dissolution rate of this salt was similar to the dissolution of quinidine from quinidine sulphate:succinic acid and quinidine:succinic acid mechanical mixes. The author concluded that the solubility product of a salt formed between quinidine and the acidic excipient, if greater than that of quinidine sulphate, is likely to govern the solubility of the drug and hence its dissolution rate in the presence of that acid.

The importance of the solubility of the drug:excipient salt was also recognised by Thoma and Zimmer (1990) in a study of the release of noscapine, a weakly basic drug, from dosage forms containing noscapine hydrochloride and an organic acid excipient: succinic, adipic, tartaric, citric, ascorbic or fumaric acid. The authors concluded that the ability to improve the dissolution of a weakly basic drug using an organic acid was dependent on various factors, including the solubility of the salt formed with the drug.

Acidic excipients have been widely used to improve the dissolution of salts of weak bases (Ventouras et al., 1977; Ventouras and Buri, 1978; Gruber et al., 1980; Thoma and Zimmer, 1990; Kohri et al., 1991; van der Veen et al., 1991a and 1991b; Gabr, 1992; Thoma and Ziegler, 1998; Streubel et al., 2000). Such enhancements in drug dissolution rate in the presence of an acidic excipient would suggest that, in each case, the drug:excipient salt was more soluble than the original salt incorporated in the formulation. However, the studies did not involve preparation of the possible salt forms and assessment of their solubilities. For many systems studied, drug dissolution rate was shown to increase with increasing excipient content to a maximum and thereafter decrease with increasing excipient content (Cleary, 1987; McNamara, 1988; Ventouras and Buri, 1978). It is likely that the maximum dissolution rate obtained was strongly influenced by the solubility of the drug:excipient salt, as well as by the solubility of the original salt form.

In the current study, the effect of combining soluble basic excipients with salts of diclofenac, an acidic drug, was investigated. The observed dissolution rates of diclofenac from the AMPD:DtBA and TRIS:DtBA systems studied are presented in Figure 8. 3.

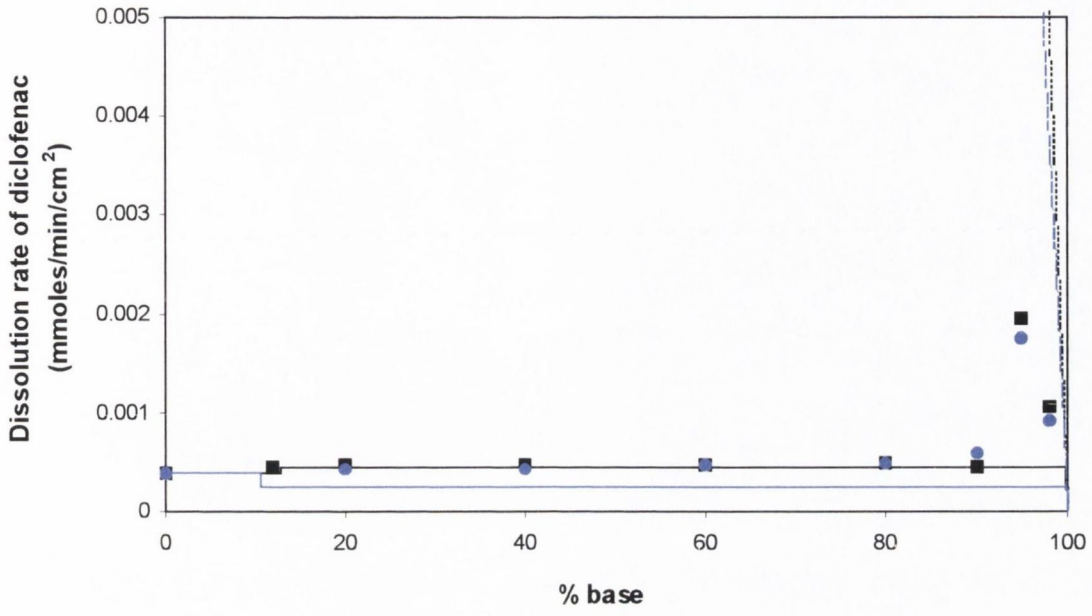

Figure 8. 3 Composition versus dissolution profiles for AMPD:DtBA (■) and TRIS:DtBA (●) systems. For each base:salt system, the line of the corresponding colour represents the rates calculated from the two component (salt conversion) model. The rates predicted for carrier dissolution in the systems containing ≥ 95% base are represented by the dashed lines.

In the presence of 12 – 90% base the dissolution rate of DtBA, a diclofenac salt of low solubility (5.46 mM), was slightly enhanced. In the case of AMPD:DtBA systems, the average dissolution rate of diclofenac from discs prepared with 12 – 90% AMPD was 1.2 times higher than the dissolution rate of DtBA on its own. This enhanced dissolution was attributed to the conversion from DtBA to DAMPD-MH, which has an aqueous solubility of 6.77 mM. The average degree of enhancement of dissolution from the TRIS:DtBA systems prepared with 20 – 90% TRIS was 1.3. In contrast to the AMPD:DtBA systems, the dissolution rates were closer in value to the intrinsic dissolution rate of DtBA than to the dissolution rate of the alternative salt form, DTRIS. However, the enhanced dissolution rate may result from the ability of DTRIS to form supersaturated solutions.

The observed dissolution rates of diclofenac from the AMPD:DDNL and TRIS:DDNL systems are presented in Figure 8. 4. The dissolution rate of the more soluble diclofenac salt, DDNL (446 mM), was dramatically reduced in the presence of AMPD or TRIS. In the composition range 40 – 80% base the dissolution rates were, on average, 43 and 15 times lower than the intrinsic

dissolution rate of DDNL for the AMPD:DDNL and TRIS:DDNL systems, respectively. This suppression in dissolution rate was attributed to the formation of a salt of lower solubility in the discs, DAMPD-MH (6.77 mM) or DTRIS (3.95 mM).

As discussed above, McNamara (1988) postulated that the dissolution of drug from a salt:excipient mixture is governed by the solubility product of the drug:excipient salt if its solubility product is higher than that of the original salt. The results from the AMPD:DDNL and TRIS:DDNL systems in this study suggest that it is possible for the solubility of the drug:excipient salt to have a dramatic effect on the dissolution of the drug when its solubility is lower than the solubility of the original salt.

The lines in Figure 8. 3 and Figure 8. 4 illustrate the rates predicted from the two component (salt conversion) model for each system. The two component (salt conversion) model was found to predict dissolution rates more accurately than the two component non-interacting model for the AMPD:DtBA, AMPD:DDNL and TRIS:DDNL systems.

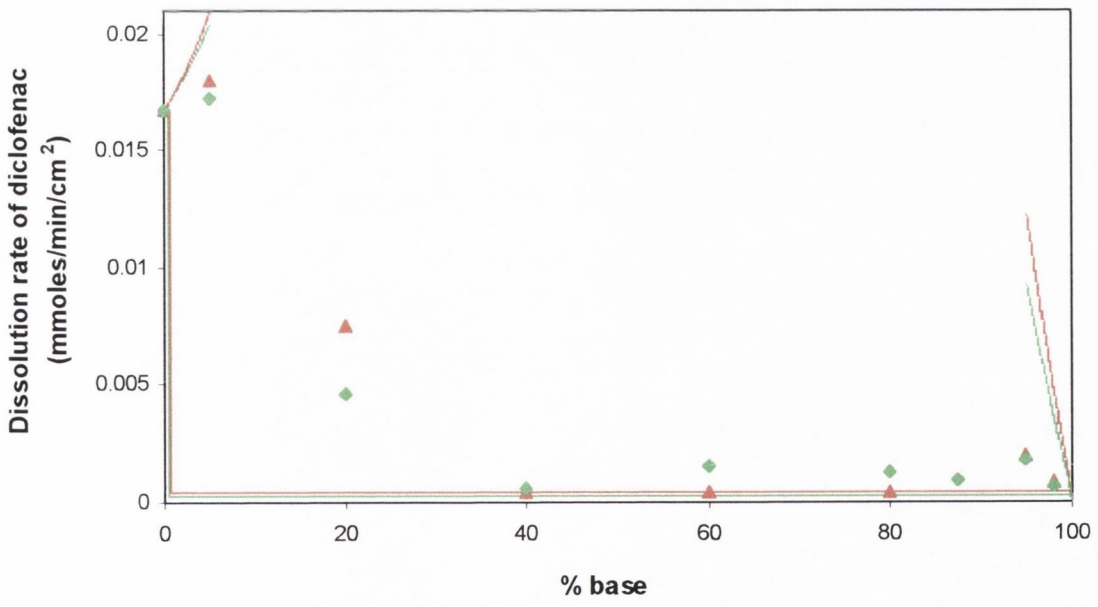

Figure 8. 4 Composition versus dissolution profiles for AMPD:DDNL (▲) and TRIS:DDNL (♦) systems. For each base:salt system, the line of the corresponding colour represents the rates calculated from the two component (salt conversion) model. The rates predicted for carrier dissolution in the systems containing ≤5% or ≥95% base are represented by the dashed lines.

The three component salt conversion model was developed to predict dissolution when the % conversion from SALT1 to SALT2 (P) was less than 100%. When the % conversion was below a certain threshold value, the model predicted dissolution rates identical to those predicted by the two component non-interacting model. When the % conversion was above this threshold value, the simulated rates were identical to those predicted by the two component (salt conversion) model. Accurate prediction by the two component (salt conversion) model of dissolution rates from AMPD:DtBA, AMPD:DDNL and TRIS:DDNL systems indicated that the % conversion was above the threshold values that were estimated for each system. Application of the three component (salt conversion) model demonstrated that complete conversion from SALT1 to SALT2 was not necessary for the generation of dissolution rates similar to those predicted by two component (salt conversion) model. In the case of the TRIS:DtBA mechanical mixes, the observed dissolution rates resulted in a better fit to the two component non-interacting model than to the two component (salt conversion) model. However, XRD analysis of the surface of the discs after dissolution indicated some conversion from DtBA to DTRIS in the discs. Examination of the three component salt conversion model for varying values of P revealed that simulated dissolution rates were identical to those predicted by the two component non-interacting model when P fell between 0 and 36.4%.

As discussed above, the slight enhancement in dissolution rate from DtBA systems and significant retardation of dissolution from DDNL systems in the region of the dissolution profiles corresponding to discs prepared with 20 – 90% base were accounted for by the solubilities of the respective diclofenac:basic excipient salts. However, the dissolution of diclofenac from systems in other regions of the dissolution profiles was shown to be under carrier control and independent of the salt solubilities. Increases in dissolution rate, relative to those predicted by the two component (salt conversion) model, were observed for the DDNL systems containing 5% base and all four systems containing 95% or 98% base. This was attributed to carrier controlled dissolution due to the large solubility difference between the dissolving salt form and the "carrier", DDNL in the case of the 5:95 AMPD:DDNL system and the basic excipient in the case of the systems containing $\geqslant$ 95% base.

The dissolution rates predicted for carrier controlled dissolution of molecularly dispersed drug from systems prepared using 95 – 100% base are presented in Figure 8. 5. As expected, higher dissolution rates were predicted for systems prepared using AMPD, the more soluble of the two bases. For DDNL and DtBA systems prepared using the same base, lower dissolution rates were predicted for DDNL systems. This can be attributed to the higher molecular weight of DDNL, relative to DtBA. The two component (salt conversion) model (Appendix VIII) predicts that a system prepared with 0.5 – 1 mole fraction of base will, after conversion of the salt, contain a

lower proportion of SALT2 the higher the molecular weight of SALT1. The observed dissolution rates were found to deviate significantly from the predicted rates. A ~6-fold difference was observed between predicted and observed dissolution rates for the systems prepared using 95% base. Others have attributed such deviations from predicted rates to the presence of drug as fine particles (Corrigan and Stanley, 1982; Dubois and Ford, 1985). Furthermore, the drug may influence the dissolution rate of the carrier or the diffusivity of the drug may be suppressed due to the high viscosity of the saturated base solutions. The lines of best fit through the experimental data are represented by the dotted lines in Figure 8. 5. The ranking of the slopes of these lines was found to be identical to that of the slopes of the lines corresponding to predicted rates.

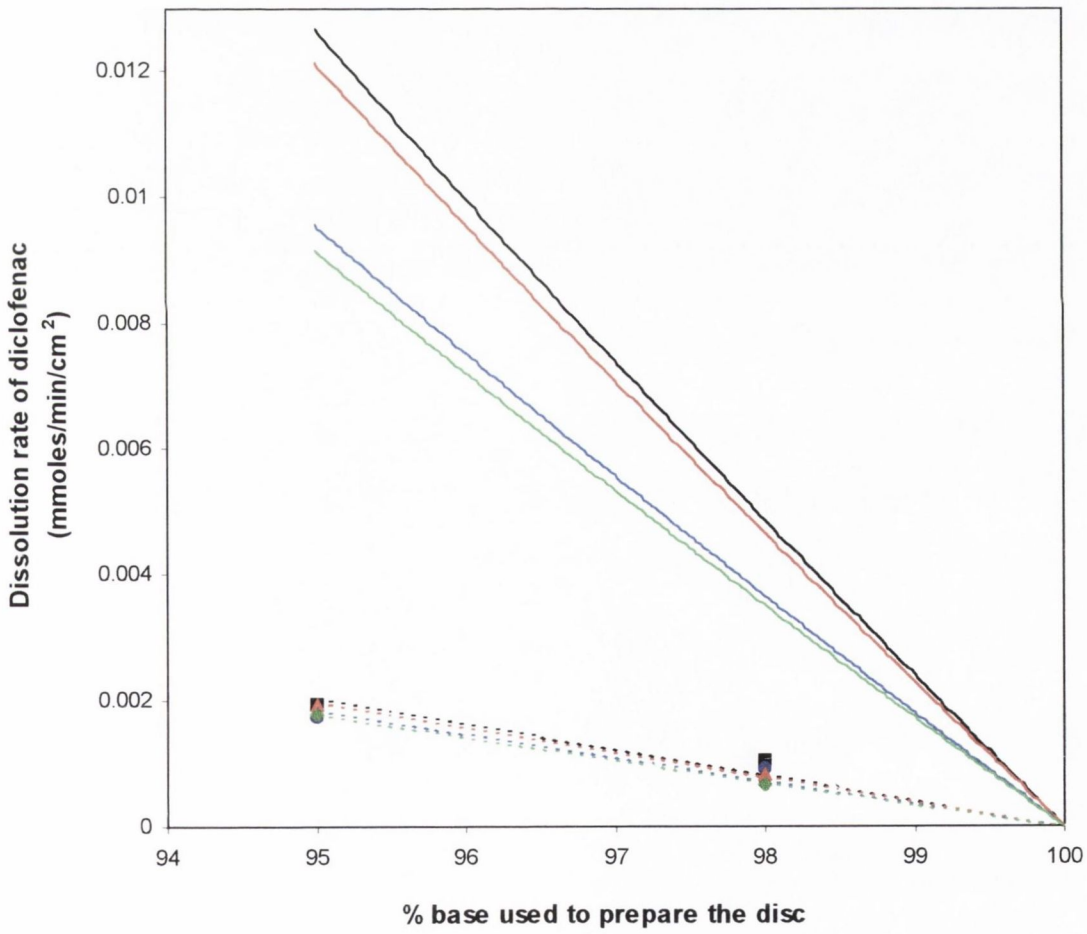

Figure 8. 5 Region of the dissolution profiles showing dissolution under carrier control for AMPD:DtBA (■), AMPD:DDNL (▲), TRIS:DtBA (●), and TRIS:DDNL (♦) systems. The lines of corresponding colour represent the rates predicted from Equation 7.1 (—) and the line of best fit for the experimental data (----)

The dissolution rates predicted for carrier controlled dissolution from DDNL systems prepared using 0 – 5% base are presented in Figure 8. 6. The upward curvature in the lines reflected the nonlinear relationship between the % base used to prepare the disc and the predicted % SALT2 in the disc after conversion. Again, the lower rates were predicted for systems containing TRIS, which is less soluble than AMPD. In accordance with the predictions, the rate of dissolution of diclofenac was lower from the 5% TRIS system than from the corresponding AMPD system. However, as in the case of systems containing ≥95% base, the experimental data for the systems containing 5% base deviated significantly from the predicted rates. The TRIS:DDNL and AMPD:DDNL systems showed 7-fold and 3-fold differences, respectively, between the predicted and observed enhancements in dissolution rate relative to pure DDNL.

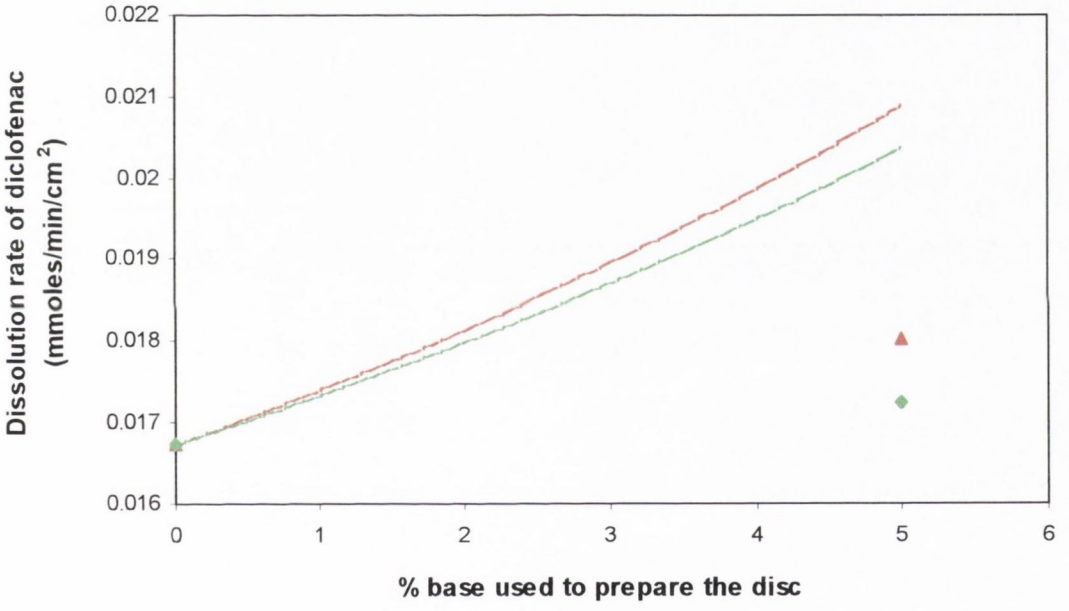

Figure 8. 6 Region of the dissolution profiles of AMPD:DDNL (▲) and TRIS:DDNL (♦) systems showing carrier controlled dissolution of SALT2 by DDNL. The lines of corresponding colour represent the rates predicted from Equation 7.1.

As described in Section 7.3.3, the two component (salt conversion) model involved application of the SALT2:SALT1 two component non-interacting model for discs prepared with 0 – 0.5 mole fraction of base and the BASE:SALT2 two component non-interacting model for discs prepared with 0.5 – 1 mole fraction of base. As observed in the case of the AMPD:DtBA system at mole fractions of base <0.5, addition of the dissolution rates predicted for SALT1 and SALT2 by the SALT2:SALT1 two component non-interacting model resulted in a predicted enhancement in

dissolution rate which was not reflected in the experimental data. In the case of two salts of diclofenac simultaneously dissolving, it was necessary to take into consideration the concentration gradients predicted by the two component non-interacting model (Figure 7. 8). Therefore, the two component (salt conversion) model predicted that the dissolution of diclofenac from these systems equalled that of the diclofenac salt present in the surface layer.

The two component (salt formation) model, proposed by McGloughlin (1989) to quantify dissolution from compacts of acidic drug:basic excipient mechanical mixes, applied the salt:acid two component non-interacting model to systems prepared with mole fractions of base between 0 and 0.5. In this region, the dissolution rate of the drug was calculated from the sum of the acid and salt dissolution rates. The model did not take into consideration the concentration gradients predicted by the model. In order to validate the assumption by the two component (salt conversion) model that the dissolution from discs consisting of two diclofenac salts was limited to the dissolution of the salt present on the surface, the two component (salt formation) model of McGloughlin (1989) was modified so that the predicted drug dissolution rates equalled that of the surface layer for discs prepared with 0 – 0.5 mole fraction base. The rates predicted by the two versions of the two component (salt formation) model for the five acid:base systems studied by McGloughlin (1989) are presented in Figures 8. 7 – 8. 9 and Figures 8.11 – 8.14. The lines in each figure represent the rates predicted from the two component (salt formation) model as originally proposed (----) and as modified (—). Improved goodness of fit parameters were calculated for the TRIS:phenylbutazone, TRIS:benzoic acid and TRIS:naproxen systems following modification of the model (Figures 8. 7 – 8. 9).

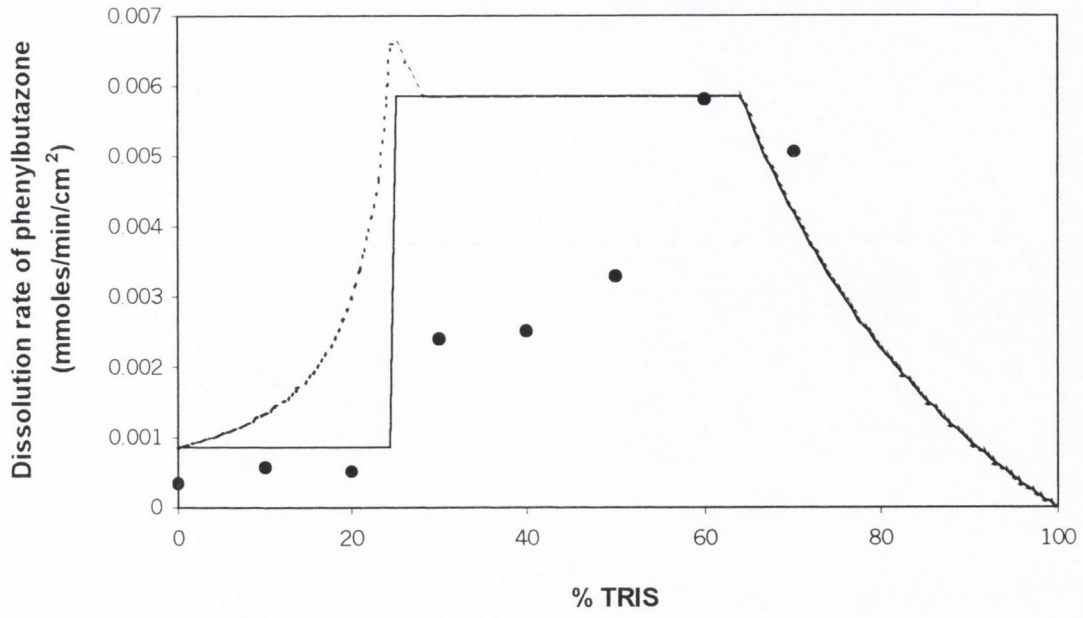

Figure 8. 7 Dissolution of phenylbutazone from TRIS:phenylbutazone discs (McGloughlin, 1989) and dissolution rates predicted from the two component (salt conversion) model, as originally proposed (----) and as modified (—)

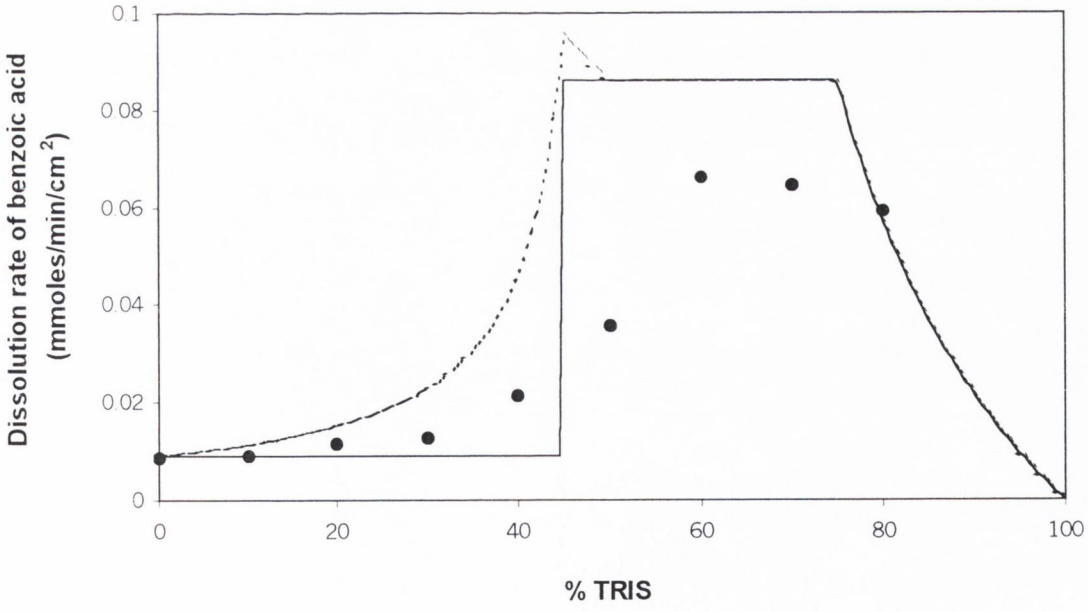

Figure 8. 8 Dissolution of benzoic acid from TRIS:benzoic acid discs (McGloughlin, 1989) and dissolution rates predicted from the two component (salt conversion) model, as originally proposed (----) and as modified (—)

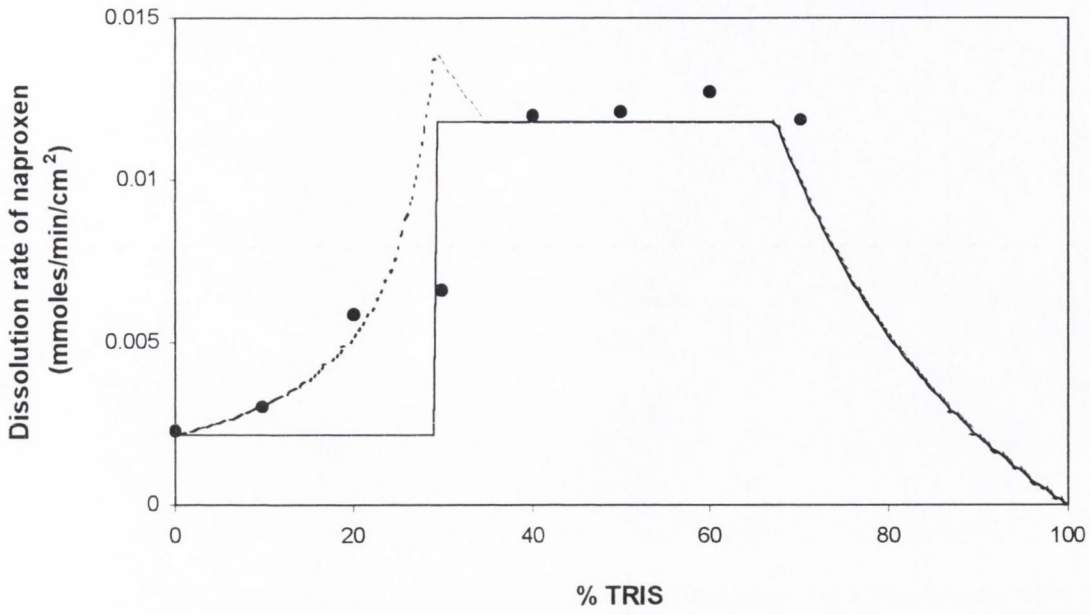

Figure 8. 9 Dissolution of naproxen from TRIS:naproxen discs (McGloughlin, 1989) and dissolution rates predicted from the two component (salt conversion) model, as originally proposed (----) and as modified (—)

The dissolution rates for the three TRIS:acid systems investigated by McGloughlin (1989) are plotted together in Figure 8. 10. The lines represent the dissolution rates predicted from the modified two component (salt formation) model. The predicted dissolution rates occurred in the following order: benzoic acid > naproxen > phenylbutazone. The observed dissolution rates were found to occur in the same rank order. Reasonable agreement was observed between the observed and predicted dissolution rates.

In the region where the two versions of the model differed, observed dissolution rates of naproxen and procaine from procaine:naproxen systems and of benzoic acid and procaine from procaine:benzoic acid systems were closer to those predicted by the original version of the two component (salt formation) model (Figures 8.11 – 8.14).

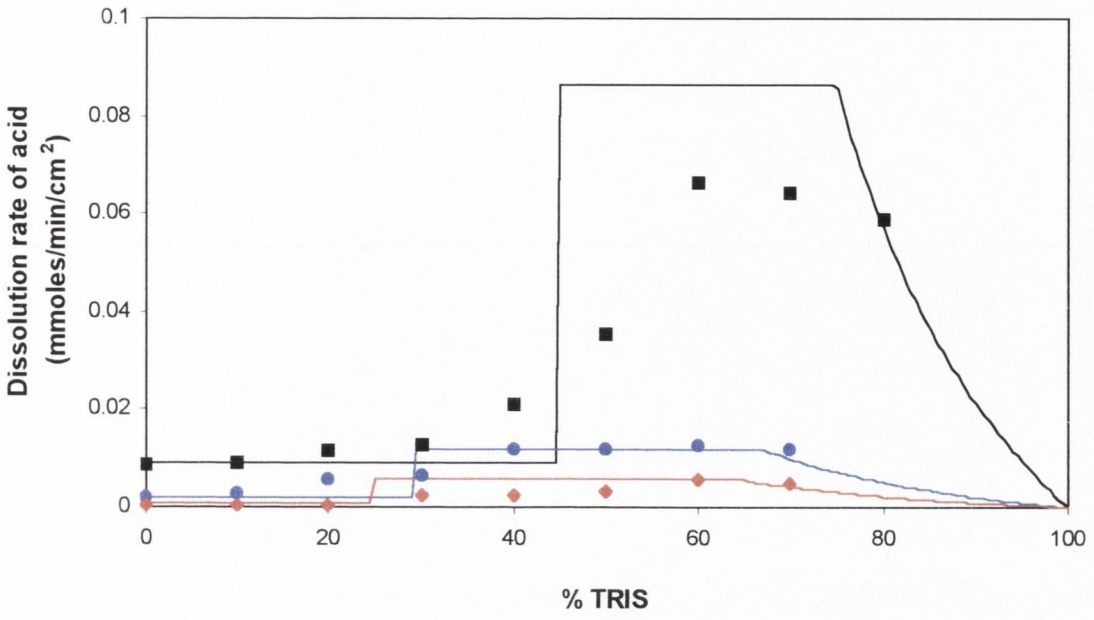

Figure 8. 10 **Dissolution of benzoic acid (■), naproxen (●) and phenylbutazone (◆) from discs prepared with TRIS (McGloughlin, 1989). The lines of corresponding colour represent the dissolution rates predicted from the modified two component (salt formation) model.**

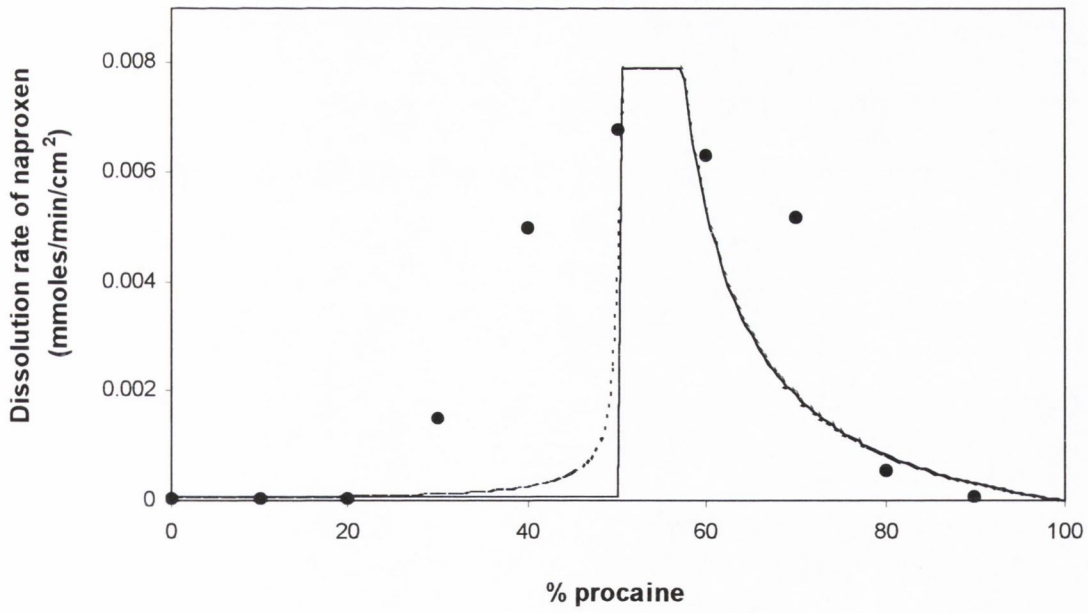

Figure 8. 11 **Dissolution of naproxen from procaine:naproxen discs (McGloughlin, 1989) and dissolution rates predicted from the two component (salt conversion) model, as originally proposed (----) and as modified (—)**

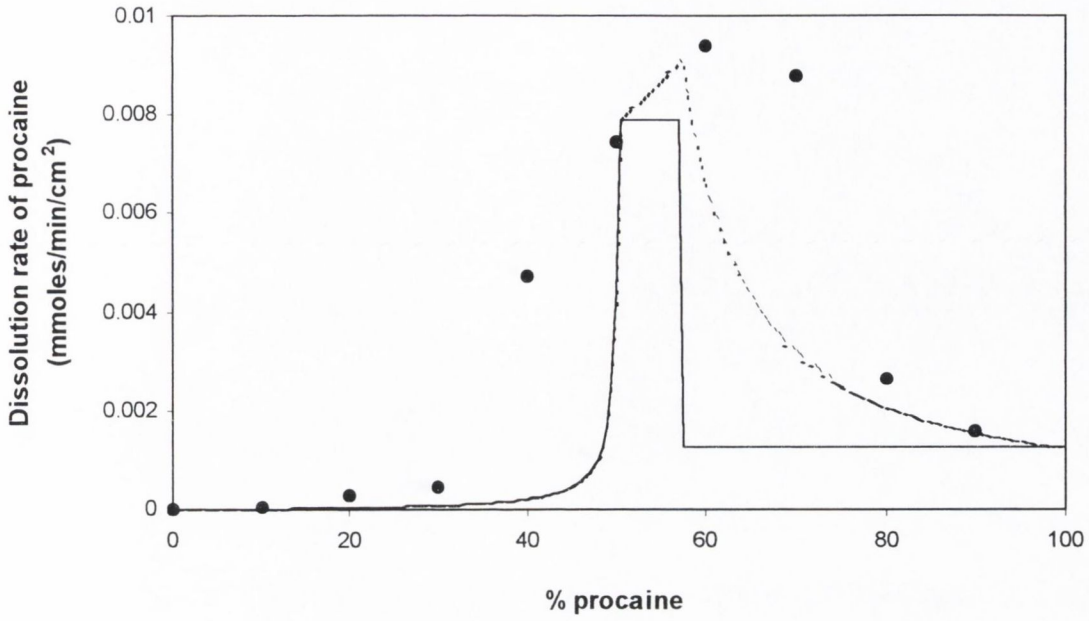

Figure 8. 12 Dissolution of procaine from procaine:naproxen discs (McGloughlin, 1989) and dissolution rates predicted from the two component (salt conversion) model, as originally proposed (----) and as modified (—)

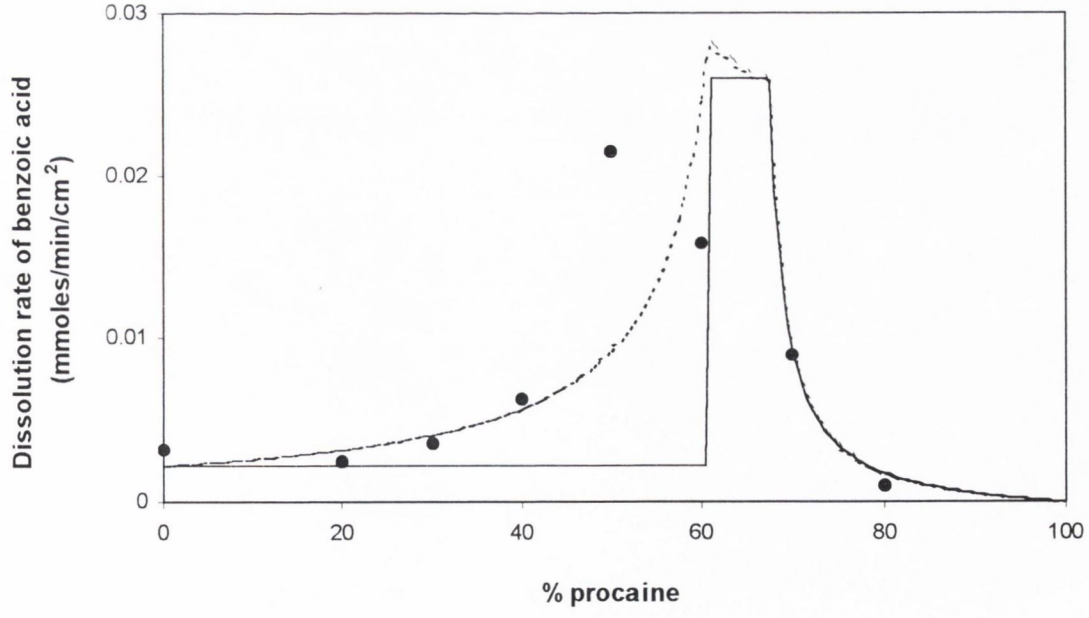

Figure 8. 13 Dissolution of benzoic acid from procaine:benzoic acid discs (McGloughlin, 1989) and dissolution rates predicted from the two component (salt conversion) model, as originally proposed (----) and as modified (—)

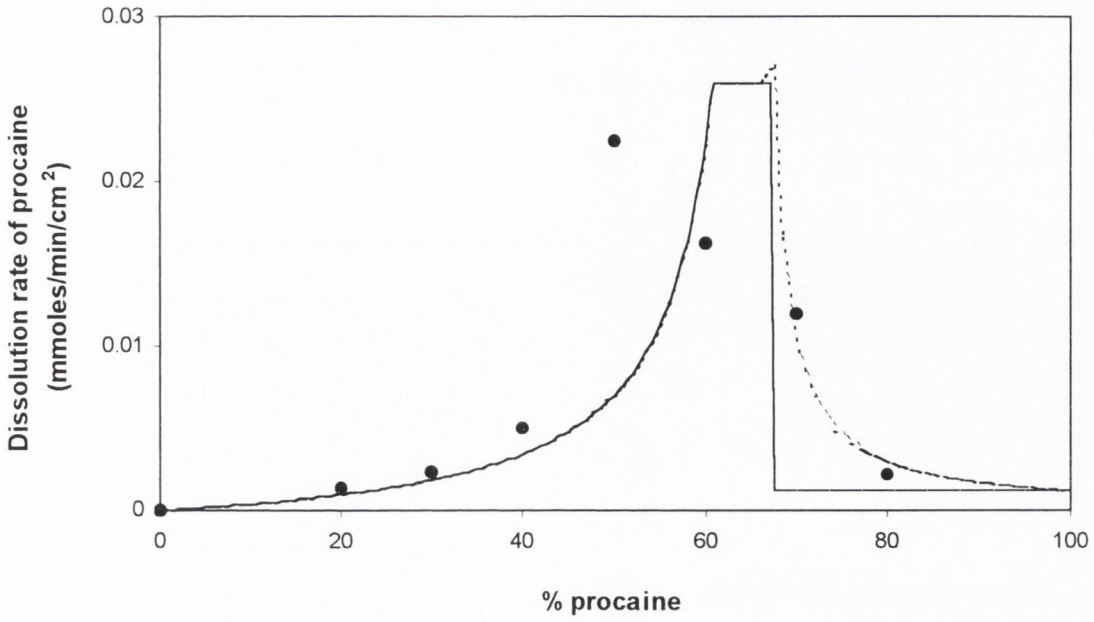

Figure 8. 14 Dissolution of procaine from procaine:benzoic acid discs (McGloughlin, 1989) and dissolution rates predicted from the two component (salt conversion) model, as originally proposed (----) and as modified (—)

The experimental dissolution rates obtained by Cleary (1987) for the dissolution of quinidine from succinic acid:quinidine sulphate discs in normal saline were fitted to the two component (salt conversion) model. The model assumed conversion from quinidine sulphate to the 2:1 quinidine succinate salt. McNamara (1988) prepared the 2:1 quinidine succinate salt and determined its solubility in saline as 70 mg/ml, ~5 times higher than that of quinidine sulphate. The dissolution rates calculated from the two component (salt conversion) model were compared with those predicted by the two component non-interacting model. The observed and predicted rates are presented in Figure 8. 15. The two component (salt conversion) model was found to be superior to the two component non-interacting model in the prediction of the rate of dissolution of quinidine from the systems studied. However, experimental dissolution rates for the discs prepared using 25 – 60% succinic acid were higher than those predicted by the two component (salt conversion) model. Cleary (1987) studied the solubility of quinidine sulphate in the presence of succinic acid and interpreted the data in terms of complex formation between the two components. However, the dissolution rates predicted by the interacting two component model, using an apparent binding constant derived from the results of the solubility study, were up to 4 times higher than those observed (Cleary, 1987).

The solubility of quinidine determined in the presence of succinic acid (Cleary, 1987) exceeded that of the quinidine succinate salt subsequently prepared by McNamara (1988). Whereas Cleary (1987) postulated that a complex was formed between quinidine sulphate and succinic acid, it is possible that this supersaturation relative to the solubility of the salt resulted from self-association of the salt. This situation is analogous to the occurrence of higher dissolution rates than predicted by the two component (salt conversion) model for TRIS:diclofenac salt systems (Figures 8. 3 and 8. 4). The deviation in the case of the diclofenac systems, which occurred in the region of the dissolution profiles for which the model predicted that DTRIS was the surface layer, was thought to result from supersaturated solutions due to self-association of DTRIS.

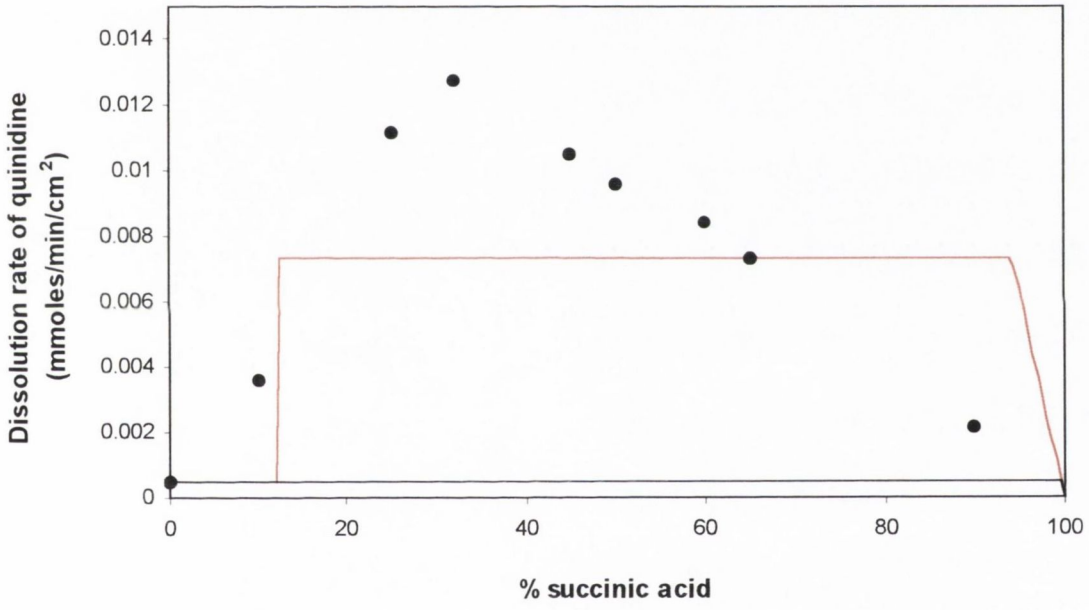

Figure 8. 15 Dissolution of quinidine from succinic acid:quinidine sulphate discs showing actual data (Cleary, 1987) (•) and theoretical rates predicted from the two component non-interacting model (—) and the two component (salt conversion) model (—)

Other studies reporting enhanced dissolution of acidic or basic drugs by the use of ionisable excipients (e.g., Thoma and Zimmer, 1990; Kohri et al., 1991; van der Veen et al., 1991a and 1991b; Gabr, 1992; Thoma and Ziegler, 1998; Streubel et al., 2000) did not involve investigation of an interaction between the drug and excipient to form a salt. To investigate the applicability of the two component (salt conversion) model, further experiments would need to be carried out to

determine the solubility of the salt likely to be formed between the drug and the ionisable excipient.

In conclusion, dissolution of an acidic drug from mechanical mixtures of a basic excipient and a salt of the drug was described by the two component (salt conversion) model. This model was shown to predict dissolution rates more accurately than the two component non-interacting model for three of the salt:base systems studied. This was also found to be the case for mixtures of an acidic excipient and the salt of a basic drug (succinic acid:quinidine sulphate mixes) investigated by Cleary (1987). Examination of the three component (salt conversion) model for each system studied showed that a certain level of conversion from SALT1 to SALT2 was required before application of the two component (salt conversion) model was appropriate. Estimation of the % conversion from the ratios of the base K_b values did not consistently result in accurate prediction of the dissolution rates. The same was observed for estimates of the % conversion calculated from the ratios of the salt solubilities. An extension of this work could involve elucidating a means of predicting the % conversion from SALT1 to SALT2. In the case of TRIS:DtBA mixtures, the two component non-interacting model resulted in a better fit to the model than the two component (salt conversion) model, which suggested a level of conversion from SALT1 to SALT2 of <36.4%. However, deviation of the data from the two component (salt conversion) model may have resulted from supersaturated solutions of DTRIS. Further work may involve investigation of the influence of supersaturation of the salt form present in the discs on the dissolution rate of the drug.

8.5. SUMMARY OF FINDINGS

- A large variation in solubility was observed within the range of diclofenac salts studied, which included five novel salts of diclofenac.
- Correlation was observed between the inverse of salt melting point and the log of salt solubility. Correlation was also displayed between the pH of a saturated salt solution and the log of salt solubility.
- Exploration of relationships between the characteristics of the salt-forming agent and those of the resultant salt form revealed correlation between the base melting point and the melting point of the salt.
- Polymorphic forms of two of the salts and pseudopolymorphic forms of three of the salts were identified. The behaviour in solution of different hydrate forms of DDEA and DHEP were investigated and an estimate obtained for the solubility of the anhydrous form of DDEA.
- The dissolution rate of a diclofenac salt of low solubility was found to be slightly enhanced in the presence of a soluble organic base.
- The inclusion of soluble organic base in compacts of a diclofenac salt of high solubility resulted in a dramatic retardation of dissolution rate.
- The two component (salt conversion) model was developed to account for conversion of the original salt to the salt formed between the drug and the basic excipient. This model accurately predicted dissolution from some of the systems examined.
- The three component (salt conversion) model was developed to predict dissolution rates when the conversion from the original salt form was less than complete.
- Deviation of experimental data from the models at high weight fractions of base, and in the case of DDNL systems, at very low weight fractions of base was attributed to carrier controlled dissolution. Deviation from the model of observed rates from TRIS:DtBA systems was thought to result from the ability of DTRIS to exist as supersaturated solutions.
- The study showed that the inclusion of a basic excipient in the formulation of an acidic drug will not always result in improved dissolution of the drug.

REFERENCES

Adesunloye, T.A. and Stach, P.E., Effect of glycine/citric acid on the dissolution stability of hard gelatin capsules, *Drug Dev. Ind. Pharm.*, 24, 6 (1998) 493-500.

Adeyeye, C.M. and Li, P.K. in *Analytical Profiles of Drug Substances*, Florey, K. (Ed.), Academic Press, San Diego (1990) pp.123-144.

Agharkar, S., Lindenbaum, S. and Higuchi, T., Enhancement of solubility of drug salts by hydrophilic counterions: properties of organic salts of an antimalarial drug, *J. Pharm. Sci.*, 65, 5 (1976) 747-749.

Albert, A. and Serjeant, E.P., *The Determination of Ionisation Constants*, 3rd Edition, Chapman and Hall, New York (1984).

Anderson, B.D. and Conradi, R.A., Predictive relationships in the water solubility of salts of a nonsteroidal anti-inflammatory drug. *J. Pharm. Sci.*, 74, 8 (1985) 815-820.

Anderson, B.D. and Flora, K.P., Preparation of water-soluble compounds through salt formation, in *The Practice of Medicinal Chemistry*, Academic Press, London (1996) pp.739-754.

Anderson, B.D., Prodrugs for improved formulation properties, in *Design of prodrugs*, Bundgaard, H. (Ed.), Elsevier Science, Biomedical Division, Amsterdam (1985) pp.243-269.

Attwood, D. and Florence, A.T., *Surfactant Systems: their Chemistry, Physics and Biology*, Chapman and Hall, London, 1983.

Attwood, D., Aggregation of antiacetylcholine drugs in aqueous solution: monomer concentrations in non-micellar drug systems, *J. Pharm. Pharmacol.*, 28 (1976) 762-765.

Attwood, D., Comparison of the mode of association of amphiphilic phenothiazine and aza-phenothiazine drugs in aqueous solution, *J. Chem. Soc., Faraday Trans.*, 1, 78 (1982) 2011-2016.

Banga, A.K. and Chien, Y.W., Iontophoretic delivery of drugs: fundamentals, developments and biomedical applications, *J. Control. Rel.*, 7 (1988) 1-24.

Bannon, Y.B., A study of the transport processes governing passive and iontophoretic transdermal drug delivery, Ph.D. Thesis, University of Dublin (1989).

Bechgaard, H. and Baggesen, S., Propoxyphene and norpropoxyphene: influence of type of controlled-release formulation on intra- and intersubject variations, *J. Pharm. Sci.*, 69, 11 (1980) 1327-1330.

Benet, L.Z., Biopharmaceutics as a basis for the design of drug products, in *Drug Design*, Vol. IV, Ariens, E.J. (Ed.), Academic Press, London (1973) pp.1-35.

Benjamin, E.J. and Lin, L.-H., Preparation and *in vitro* evaluation of salts of an antihypertensive agent to obtain slow release, *Drug Dev. Ind. Pharm.*, 11, 4 (1985) 771-790.

Berge, S.M., Bighley, L.D. and Monkhouse, D.C., Pharmaceutical salts, *J. Pharm. Sci.*, 66, 1 (1977) 1-19.

Bighley, L.D., Berge, S.M. and Monkhouse, D.C., Salt forms of drugs and absorption, in *Encyclopedia of Pharmaceutical Technology*, Vol. 13, Swarbrick, J. and Boylan, J.C. (Eds.), Marcel Dekker, New York (1996) pp.453-499.

Bogardus, J.B. and Blackwood, R.K. Jr., Solubility of doxycycline in aqueous solution, *J. Pharm. Sci.*, 62, 2 (1979) 188-194.

Bogardus, J.B., Common ion equilibria of hydrochloride salts and the Setschenow equation, *J. Pharm. Sci.*, 71, 5 (1982) 588-590.

Brito, R.M.M. and Vaz, W.L.C., Determination of the critical micelle concentration of surfactants using the fluorescent probe *N*-phenyl-1-naphthylamine, *Analytical Biochemistry*, 152 (1986) 250-255.

Brittain, H.G., Bogdanowich, S.J., Bugay, D.E., DeVincentis, J., Lewen, G. and Newman, A.W., Physical characterisation of pharmaceutical solids, *Pharm. Res.*, 8, 8 (1991) 963-973.

Brittain, H.G., Methods for the characterisation of polymorphs and solvates, in *Polymorphism in Pharmaceutical Solids*, Brittain, H.G. (Ed.), Marcel Dekker, New York (1999) pp.227-278.

Brittain, H.G., Overview of physical characterization methodology, in *Physical Characterization of Pharmaceutical Solids*, Brittain, H.G. (Ed.), Marcel Dekker, New York (1995) pp.1-35.

Brown, M.E., *Introduction to Thermal Analysis – Techniques and Applications*, Chapman and Hall, London (1988).

Bugay, D.E. and Williams, A.C., Vibrational spectroscopy, in *Physical Characterization of Pharmaceutical Solids*, Brittain, H.G. (Ed.), Marcel Dekker, New York (1995) pp.59-91.

Byrn, S.R., *Solid State Chemistry of Drugs*, Academic Press, London (1982).

Cahn, R.W., Internal strains and recrystallization, *Prog. Metal Phys.*, 2 (1950) 151-176.

Carmichael, G.R., Shah, S.A. and Parrott, E.L., General model for dissolution rates of *n*-component nondisintegrating spheres, *J. Pharm. Sci.*, 70, 12 (1981) 1331-1338.

Carr, M.G., Corish, J. and Corrigan, O.I., Drug delivery from a liquid crystalline base across Visking and human stratum corneum, *Int. J. Pharm.*, 157 (1997) 35-42.

Carstensen, J.T., *Theory of Pharmaceutical Systems*, Vol. I, Academic Press, London (1972).

Castellari, C. and Sabatino, P., Anti-inflammatory drugs: 1-(2-hydroxyethyl)-pyrrolidinium salt of diclofenac, *Acta Cryst.*, C50 (1994) 1723-1726.

Chakrabarti, S. and Southard, M.Z., Control of poorly soluble drug dissolution in conditions simulating the gastrointestinal tract flow. 2. Cocompression of drugs with buffers, *J. Pharm. Sci.*, 86, 4 (1997) 465-469.

Chan, H.K. and Doelker, E., Polymorphic transformation of some drugs under compression, *Drug Dev. Ind. Pharm.*, 11, 2-3 (1985) 315-332.

Chiarini, A., Tartarini, A. and Fini, A., pH-solubility relationship and partition coefficients for some anti-inflammatory arylaliphatic acids, *Arch. Pharm. (Weinheim)*, 317 (1984) 268-273.

Chowhan, Z.T., pH-solubility profiles of organic carboxylic acids and their salts, *J. Pharm. Sci.*, 67, 9 (1978) 1257-1260.

Cleary, C., A physicochemical investigation of the dissolution of drug-excipient mixtures containing acids, M.Sc. Thesis, University of Dublin (1987).

Corrigan, O.I. and Stanley, C.T., Dissolution properties of phenobarbitone-β-cyclodextrin systems, *Pharm. Acta. Helv.*, 56, 7 (1981) 204-208.

Corrigan, O.I. and Stanley, C.T., Mechanisms of drug dissolution rate enhancement from β-cyclodextrin-drug systems, *J. Pharm. Pharmacol.*, 34 (1982) 621-626.

Corrigan, O.I., Drug-polyvinylpyrrolidone coprecipitates, in *Percutaneous penetration enhancers*, Smith, E.W. and Maibach, H.I. (Eds.), CRC Press, Boca Raton, U.S.A. (1995) pp.221-232.

Corrigan, O.I., Farvar, M.A. and Higuchi, W.I., Drug membrane transport enhancement using high energy drug polyvinylpyrrolidone (PVP) coprecipitates, *Int. J. Pharm.*, 5 (1980) 229-238.

Corrigan, O.I., Mechanisms of dissolution of fast release solid dispersions, *Drug Dev. Ind. Pharm.*, 11, 2-3 (1985) 697-724.

Corrigan, O.I., Murphy, C.A. and Timoney, R.F., Dissolution properties of polythylene glycols and polyethylene glycol-drug systems, *Int. J. Pharm.*, 4 (1979) 67-74.

Craig, L.C. and Pulley, A.O., Dialysis studies. IV. Preliminary experiments with sugars, *Biochemistry*, 1, 1 (1962) 89-94.

Craig, L.C., Harfenist, E.J. and Paladini, A.C., Dialysis studies. VII. The behaviour of angiotensin, oxytocin, vasopressin, and some of their analogs, *Biochemistry*, 3, 6 (1964) 764-769.

CRC Handbook of Chemistry and Physics, 76th Edition, CRC Press, Boca Raton, U.S.A. (1995).

Cullity, B.D., *Elements of X-ray Diffraction*, 2nd Edition, Addison-Wesley, London, (1978).

Dahlan, R., McDonald, C. and Sunderland, V.B., Solubilities and intrinsic dissolution rates of sulphamethoxazole and trimethoprim, *J. Pharm. Pharmacol.*, 39 (1987) 246-251.

Dean, J.A., *Handbook of Organic Chemistry*, McGraw-Hill Book Company, New York (1987).

Dhanaraj, V. and Vijayan, M., Crystal structures of 1:1 complexes of meclofenamic acid with choline and ethanolamine, *Biochim. Biophys. Acta*, 924 (1987) 135-146.

Dittert, L.W., Higuchi, T. and Reese, D.R., Phase solubility technique in studying the formation of complex salts of triamterene, *J. Pharm. Sci.*, 53, 11 (1964) 1325-1328.

Doff, D.H.D., Brownen, F.L. and Corrigan, O.I., Determination of α-impurities in the β-polymorph of inosine using infrared spectroscopy and X-ray powder diffraction, *Analyst*, 111 (1986) 179-182.

Doherty, C. and York, P., Microenvironmental pH control of drug dissolution, *Int. J. Pharm.*, 50 (1989) 223-232.

Dubois, J.L. and Ford, J.L., Similarities in the release rates of different drugs from polyethylene glycol 6000 solid dispersions, *J. Pharm. Pharmacol.*, 37 (1985) 494-496.

Dunitz, J.D., The entropic cost of bound water in crystals and biomolecules, *Science*, 264 (1994) 670.

Dwight, J.S., *British Patent*, Number 1,291,281 (1972a).

Dwight, J.S., *British Patent*, Number 1,291,282 (1972b).

Edwards, L.J., The dissolution and diffusion of aspirin in aqueous media, *Z. Physik. Chem.*, 23 (1897) 1191-1210.

Eerikäinen, S., Yliruusi, J. and Laakso, R., The behaviour of the sodium salt of indomethacin in the cores of film-coated granules containing various fillers, *Int. J. Pharm.*, 71 (1991) 201-211.

Ekwall, P., Fontell, K. and Sten, A., Micelle formation in bile salt solutions, *Proc. 2nd Int. Congress of Surface Activity*, Vol. I (1957a) 357-373.

Ekwall, P., Rosendahl, T. and Löfman, N., Studies on bile acid salt solutions. I. The dissociation constants of the cholic and desoxycholic acids, *Acta Chem. Scand.*, Vol. II (1957b) 590-598.

Engel, G.L., Farid, N.A., Faul, M.M., Richardson, L.A. and Winneroski, L.L., Salt form selection and characterisation of LY333531 mesylate monohydrate, *Int. J. Pharm.*, 198 (2000) 239-247.

Felmeister, A., Relationships between surface activity and biological activity of drugs, *J. Pharm. Sci.*, 61, 2 (1972) 151-164.

Fini, A., Fazio, G. and Feroci, G., Solubility and solubilisation properties of non-steroidal anti-inflammatory drugs, *Int. J. Pharm.*, 126 (1995c) 95-102.

Fini, A., Fazio, G. and Rabasco, A.M., 1-octanol/water partitioning of diclofenac salts, *Acta Technologiae et Legis Medicamenti*, IV, 1 (1993a) 33-44.

Fini, A., Fazio, G. and Rapaport, I., Diclofenac/*N*-(2-hydroxyethyl) pyrrolidine: a new salt for an old drug, *Drug Exp. Clin. Res.*, 19, 3 (1993b) 81-88.

Fini, A., Fazio, G., Fernández-Hervás, M.J., Holgado, M.A. and Rabasco, A.M., Influence of crystallisation solvent and dissolution behaviour for a diclofenac salt, *Int. J. Pharm.*, 121 (1995b) 19-26.

Fini, A., Fazio, G., Fernández-Hervás, M.J., Holgado, M.A. and Rabasco, A.M., Factors governing the dissolution of diclofenac salts, *Eur. J. Pharm. Sci.*, 4 (1996) 231-238.

Fini, A., Fazio, G., Gonzalez-Rodriguez, M., Cavallari, C., Passerini, N. and Rodriguez, L., Formation of ion-pairs in aqueous solutions of diclofenac salts, *Int. J. Pharm.*, 187 (1999) 163-173.

Fini, A., Fazio, G., Orienti, I., Bertasi, V., Zecchi, V. and Rapaport, I., Self-association and release of diclofenac/*N*-(2-hydroxyethyl)pyrrolidine salt (DHEP), *Proc. 10th Pharm. Tech. Conf.*, Bologna, Italy (1991a) 48-64.

Fini, A., Fazio, G., Orienti, I., Zecchi, V. and Rapaport, I., Chemical properties-dissolution relationship. IV. Behaviour in solution of the diclofenac/*N*-(2-hydroxyethyl)pyrrolidine salt (DHEP), *Pharm. Acta. Helv.*, 66, 7 (1991b) 201-203.

Fini, A., Fazio, G., Rabasco, A.M. and Fernández-Hervás, M.J., Self-association properties of diclofenac, *Il Farmaco*, 49, 2 (1994c) 141-146.

Fini, A., Fazio, G., Rabasco, A.M., Fernández-Hervás, M.J. and Holgado, M.A., Pre-formulation study of diclofenac salts, *Proc. 14th Pharm. Tech. Congress*, Barcelona, Spain (1995a) 82-90.

Fini, A., Fazio, G., Rabasco, A.M., Holgado-Villafuerte, M.A. and Fernández-Hervás, M.J., Influence of the chemical form in the solution behaviour of diclofenac salts, *Proc. 13th Pharm. Tech. Conf.*, Strasbourg, France (1994a) 793-801.

Fini, A., Lualdi, P., Pedemonti-Donati, E. and Rapaport, I., DHEP/plaster: a novel combination for the topical release of diclofenac, *Proc. 13th Pharm. Tech. Conf.*, Strasbourg, France (1994b) 118-130.

Florence, A.T. and Attwood, D., *Physicochemical Principles of Pharmacy*, MacMillan, London (1988).

Flynn, G.L., Yalkowsky, S.H. and Roseman, T.J., Mass transport phenomena and models: theoretical concepts, *J. Pharm. Sci.*, 63, 4 (1974) 479-510.

Forbes, R.T., York, P. and Davidson, J.R., Dissolution kinetics and solubilities of *p*-aminosalicylic acid and its salts, *Int. J. Pharm.*, 126 (1995) 199-208.

Forbes, R.T., York, P., Fawcett, V. and Shields, L., Physicochemical properties of salts of *p*-aminosalicylic acid. I. Correlation of crystal structure and hydrate stability, *Pharm. Res.*, 9, 11 (1992) 1428-1435.

Gabr, K.E. and Borg, M.E., Characterisation of hydrochlorothiazide-trometamol mixtures, *Pharm. Ind.*, 61, 3 (1999) 281-285.

Gabr, K.E., Effect of organic acids on the release patterns of weakly basic drugs from inert sustained release matrix tablets, *Eur. J. Pharm. Biopharm.*, 38, 6 (1992) 199-202.

Ghan, G.A. and Lalla, J.K., Effect of compressional forces on piroxicam polymorphs, *J. Pharm. Pharmacol.*, 44 (1992) 678-681.

Gibaldi, M., *Biopharmaceutics and Clinical Pharmacokinetics*, 4th Edition, Lea & Febiger, Philadelphia (1991).

Giron, D., Thermal analysis and calorimetric methods in the characterisation of polymorphs and solvates, *Thermochimica Acta,* 248 (1995) 1-59.

Goldberg, A.H. and Higuchi, W.I., Improved method for diffusion coefficient determinations employing the silver membrane filter, *J. Pharm. Sci.*, 57, 9 (1968) 1583-1585.

Gould, P.L., Salt selection for basic drugs, *Int. J. Pharm.*, 33 (1986) 201-217.

Grant, D.J.W. and Brittain, H.G., Solubility of pharmaceutical solids, in *Physical Characterization of Pharmaceutical Solids*, Brittain, H.G. (Ed.), Marcel Dekker, New York (1995) pp.321-386.

Grant, D.J.W. and Higuchi, T., *Techniques of Chemistry*, Vol. XXI, Solubility Behaviour of Organic Compounds, Wiley, New York (1990).

Grant, D.J.W., Theory and origin of polymorphism, in *Polymorphism in Pharmaceutical Solids*, Brittain, H.G. (Ed.), Marcel Dekker, New York (1999) pp.1-33.

Grijseels, H., Crommelin, D.J.A. and deBlaey, C.J., Hydrodynamic approach to dissolution rate, *Pharm. Weekblad. Sci. Ed.*, 3 (1981) 129-144.

Gruber, P., Brickl, R., Bozler, G. and Strickler, H., *European Patent*, Number 0032562 (1980).

Gubbins, R.H., Absorption, irritation and formulation aspects of diclofenac, Ph.D. Thesis, University of Dublin (1996).

Gu, L. and Strickley, R.G., Preformulation salt selection. Physical property comparisons of the tris(hydroxymethyl)aminomethane (THAM) salts of four analgesic/antiinflammatory agents with the sodium salts and the free acids, *Pharm. Res.*, 4, 3 (1987) 255-257.

Gu, L., Huynh, O., Becker, A., Peters, S., Nguyen, H. and Chu, N., Preformulation selection of a proper salt for a weak acid-base (RS-82856) – A new positive inotropic agent, *Drug Dev. Ind. Pharm.*, 13, 3 (1987) 437-448.

Guillory, J.K., Generation of polymorphs, hydrates, solvates and amorphous solids, in *Polymorphism in Pharmaceutical Solids*, Brittain, H.G. (Ed.), Marcel Dekker, New York (1999) pp.183-226.

Haleblian, J. and McCrone, W., Pharmaceutical applications of polymorphism, *J. Pharm. Sci.*, 58, 8 (1969) 911-929.

Haleblian, J.K., Characterisation of habits and crystalline modification of solids and their pharmaceutical applications, *J. Pharm. Sci.*, 64, 8 (1975) 1269-1288.

Hamlin, W.E., Northam, J.I. and Wagner, J.G., Relationship between *in vitro* dissolution rates and solubilities of numerous compounds representative of various chemical species, *J. Pharm. Sci.*, 54, 11 (1965) 1651-1653.

Hansch, C. and Leo, A., *Substituent Constants for Correlation Analysis in Chemistry and Biology*, John Wiley & Sons, New York (1979).

Healy, A.M., Investigations of the dissolution mechanisms of acidic drug-excipient compacts, Ph.D. Thesis, University of Dublin (1995).

Heard, D.D. and Ashworth, R.W., The colloidal properties of chlorhexidine and its interaction with some macromolecules, *J. Pharm. Pharmacol.*, 20 (1968) 505-512.

Higuchi, T., Physical chemical analysis of percutaneous absorption process from creams and ointments, *J. Soc. Cosmet. Chem.*, 11 (1960) 85-97.

Higuchi, W.I. and Hamlin, W.E., Release of drug from self-coating surface, *J. Pharm. Sci.*, 52, 6 (1963) 575-579.

Higuchi, W.I., Diffusional models useful in biopharmaceutics. Drug release rate processes, *J. Pharm. Sci.*, 56, 3 (1967) 315-324.

Higuchi, W.I., Lau, P.K., Higuchi, T. and Shell, J.W., Polymorphism and drug availability – solubility relationships in the methylprednisolone system, *J. Pharm. Sci.*, 52, 2 (1963) 150-153.

Higuchi, W.I., Mir, N.A. and Desai, S.J., Dissolution rates of polyphase mixtures, *J. Pharm. Sci.*, 54, 10 (1965b) 1405-1410.

Higuchi, W.I., Mir, N.A., Parker, A.P. and Hamlin, W.E., Dissolution kinetics of a weak acid, 1,1-hexamethylene *p*-tolylsulfonylsemicarbazide, and its sodium salt, *J. Pharm. Sci.*, 54, 1 (1965a) 8-11.

Hill, V.L., Craig, D.Q.M. and Feeley, L.C., The use of modulated temperature differential scanning calorimetry as a tool for the characterisation of pharmaceutical materials, *Proc. 16th Pharm. Tech. Conf.*, Athens, Greece (1997) 124-131.

Hiramatsu, Y., Suzuki, H., Kuchiki, A., Nakagawa, H. and Fujii, S., X-ray structural studies of lomeridine dihydrochloride polymorphs, *J. Pharm. Sci.*, 85, 7 (1996) 761-766.

Hirsch, C.A., Messenger, R.J. and Brannon, J.L., Fenoprofen: drug form selection and preformulation stability studies, *J. Pharm. Sci.*, 67, 2 (1978) 231-236.

Ho, N.F.H., Park, J.Y., Amidon, G.E., Ni, P.F. and Higuchi, W.I., Methods for interrelating in vitro, animal and human absorption studies, in *Gastrointestinal Absorption of Drugs*, Aguiar, A.J. (Ed.), American Pharmaceutical Association, Academy of Pharmaceutical Sciences, Washington, D.C. (1980).

Holgado, M.A., Fernández-Hervás, M.J., Rabasco, A.M. and Fini, A., Characterisation study of a diclofenac salt by means of SEM and fractal analysis, *Int. J. Pharm.*, 120 (1995) 157-167.

Ibrahim, H., Pisano, F. and Bruno, A., Polymorphism of phenylbutazone: properties and compressional behaviour of crystals, *J. Pharm. Sci.*, 66 (1977) 669-673.

Iervolino, M., Raghavan, S.L. and Hadgraft, J., Membrane penetration enhancement of ibuprofen using supersaturation, *Int. J. Pharm.*, 198 (2000) 229-238.

Inagi, T., Muramatsu, T., Nagai, H. and Terada, H., Mechanism of indomethacin partition between *n*-octanol and water, *Chem. Pharm. Bull.*, 29, 8 (1981) 2330-2337.

James, K.C., *Solubility and Related Properties*, Marcel Dekker, New York (1986).

Jasti, B.R., Du, J. and Vasavada, R.C., Characterization of thermal behaviour of etoposide, *Int. J. Pharm.*, 118 (1995) 161-167.

Javaid, K.A. and Cadwallader, D.E., Dissolution of aspirin from tablets containing various buffering agents, *J. Pharm. Sci.*, 61, 9 (1972) 1370-1373.

Jones, P.H., Rowley, E.K., Weiss, A.L., Bishop, D.L. and Chun, A.H.C., Insoluble erythromycin salts, *J. Pharm. Sci.*, 58, 3 (1969) 337-339.

Kalinkova, G.N., Studies of beneficial interactions between active medicaments and excipients in pharmaceutical formulations, *Int. J. Pharm.*, 187 (1999) 1-15.

Kaplan, S.A., Biopharmaceutical considerations in drug formulation design and evaluation, *Drug Metab. Revs.*, 1, 1 (1972) 15-34.

Khalil, E., Najjar, S. and Sallam, A., Aqueous solubility of diclofenac diethylamine in the presence of pharmaceutical additives: A comparative study with diclofenac sodium, *Drug Dev. Ind. Pharm.*, 26, 4 (2000) 375-381.

Khankari, R.K. and Grant, D.J.W., Pharmaceutical hydrates, *Thermochimica Acta*, 248 (1995) 61-79.

Klug, H.P. and Alexander, L.E., *X-ray Diffraction Procedures for Polycrystalline and Amorphous Materials*, 2nd Edition, John Wiley, New York (1974).

Kohri, N., Yatabe, H., Iseki, K. and Miyazaki, K., A new type of pH-independent controlled release tablet, *Int. J. Pharm.*, 68 (1991) 255-264.

Kondo, S., Yamanaka, C. and Sugimoto, I., Enhancement of transdermal delivery by superfluous thermodynamic potential. III. Percutaneous absorption of nifedipine in rats, *J. Pharmacobio-Dyn.*, 10 (1987) 743-749.

Kramer, S.F. and Flynn, G.L., Solubility of organic hydrochlorides, *J. Pharm. Sci.*, 61, 12 (1972) 1896-1904.

Kriwet, K. and Müller-Goymann, C.C., Binary diclofenac diethylamine–water systems: micelles, vesicles and lyotropic liquid crystals, *Eur. J. Pharm. Biopharm.*, 39, 6 (1993) 234-238.

Kriwet, K. and Müller-Goymann, C.C., Diclofenac release from phospholipid drug systems and permeation through excised human stratum corneum, *Int. J. Pharm.*, 125 (1995) 231-242.

Kriwet, K. and Müller-Goymann, C.C., Mutual interactions between diclofenac diethylamine and phospholipids – investigations on the microstructure of the arisen systems, *Pharmazie*, 49 (1994) 187-191.

Ledwidge, M.T. and Corrigan, O.I., Effects of surface active characteristics and solid state forms on the pH solubility profiles of drug-salt systems, *Int. J. Pharm.*, 17 (1998) 187-200.

Ledwidge, M.T., Draper, S.M., Wilcock, D.J. and Corrigan, O.I., Physicochemical characterisation of diclofenac *N*-(2-hydroxyethyl)pyrrolidine: anhydrate and dihydrate crystalline forms, *J. Pharm. Sci.*, 85, 1 (1996) 16-21.

Ledwidge, M.T., The effects of pH, crystalline phase and salt formation on the solubility of ionisable drugs, Ph.D. Thesis, University of Dublin (1997).

Lee, S.J., Kurihara-Bergstrom, T. and Kim, S.W., Ion-paired drug diffusion through polymer membranes, *Int. J. Pharm.*, 47 (1987) 59-73.

Lefebvre, C., Guyot-Hermann, A.M., Draguet-Brughmans, M. and Bouché, R., Polymorphic transitions of carbamazepine during grinding and compression, *Drug Dev. Ind. Pharm.*, 12, 11-13 (1986) 1913-1927.

Leussing, D.L., Solubility, in *Treatise on Analytical Chemistry*, Kolthoff, I.M., Elving, P.J. and Sandell, E.B. (Eds.), The Interscience Encyclopedia, Interscience, New York, Vol. I, Part I (1959) pp.675-732.

Levich, V.A., *Physicochemical Hydrodynamics*, Prentice-Hall, Englewood Cliffs, New Jersey, U.S.A. (1962).

Levy, G., Effect of certain tablet formulation factors on dissolution rate of the active ingredient. I. Importance of using appropriate agitation intensities for *in vitro* dissolution rate measurements to reflect *in vivo* conditions, *J. Pharm. Sci.*, 52, 11 (1963) 1039-1046.

Levy, G., Leonards, J.R. and Procknal, J.A., Development of in-vitro dissolution tests which correlate quantitatively with dissolution rate limited drug absorption in man, *J. Pharm. Sci.*, 54, 12 (1965) 1719-1722.

Lin, S.L., Lachman, L., Schwartz, C.J. and Huebner, C.F., Preformulation investigation. I. Relation of salt forms and biological activity of an experimental antihypertensive, *J. Pharm. Sci.*, 61, 9 (1972) 1418-1422.

Lloyd, G.R., Craig, D.Q.M. and Smith, A., A calorimetric investigation into the interaction between paracetamol and polyethylene glycol 4000 in physical mixes and solid dispersions, *Eur. J. Pharm. Biopharm.*, 48 (1999) 59-65.

Lowes, M.M.J., Caira, M.R., Lötter, A.P. and van der Watt, J.G., Physicochemical properties and X-ray structural studies of the trigonal polymorph of carbamazepine, *J. Pharm. Sci.*, 76, 9 (1987) 744-752.

Magerlein, B.J., *N*-alkylsulfamate salts of lincomycin, *J. Pharm. Sci.*, 54, 7 (1965) 1065-1067.

Maitani, Y., Coutel-Egros, A., Obata, Y. and Nagai, T., Prediction of skin permeabilities of diclofenac and propranolol from theoretical partition-coefficients determined from cohesion parameters, *J. Pharm. Sci.*, 82, 4 (1993a) 416-420.

Maitani, Y., Kugo, M. and Nagai, T., Permeation of diclofenac salts through silicone membrane: a mechanistic study of percutaneous absorption of ionisable drugs, *Chem. Pharm. Bull.*, 42, 6 (1994) 1297-1301.

Maitani, Y., Kugo, M., Nakagaki, M. and Nagai, T., Ionic size and behaviour of diclofenac salts in water and ethanol/water mixtures by conductivity at 25°C, *J. Pharm. Sci.*, 82 (1993b) 1245-1249.

Martin, A., *Physical Pharmacy*, 4th Edition, Lea & Febiger, Philadelphia (1993).

Martindale, The Extra Pharmacopoeia, 32nd Edition, Pharmaceutical Press, London (1999).

McCauley, J.A. and Brittain, H.G., Thermal methods of analysis, in *Physical Characterization of Pharmaceutical Solids*, Brittain, H.G. (Ed.), Marcel Dekker, New York (1995) pp.223-251.

McGloughlin, R.M.R., Dissolution properties of compressed mixtures containing an acidic drug and a basic excipient, M.Sc. Thesis, University of Dublin (1989).

McNamara, M.T., Dissolution of quinidine sulphate from drug-excipient mixtures containing acids, M.Sc. Thesis, University of Dublin (1988).

Merck Index, 12th Edition, Merck & Co., New Jersey (1996).

Mikkelson, T.J., Watanabe, S., Rytting, J.H. and Higuchi, T., Effect of self-association of phenol on its transport across polyethylene film, *J. Pharm. Sci.*, 68, 10 (1980) 133-137.

Miyazaki, S., Inoue, H., Nadai, T., Arita, T. and Nakano, M., Solubility characteristics of weak bases and their hydrochloride salts in hydrochloric acid solutions, *Chem. Pharm. Bull.*, 27, 6 (1979) 1441-1447.

Miyazaki, S., Nakano, M. and Arita, T., A comparison of solubility characteristics of free bases and hydrochloride salts of tetracycline antibiotics in hydrochloric acid solutions, *Chem. Pharm. Bull.*, 23, 6 (1975) 1197-1204.

Miyazaki, S., Oshiba, M. and Nadai, T., Dissolution properties of salt forms of berberine, *Chem. Pharm. Bull.*, 29, 3 (1981a) 883-886.

Miyazaki, S., Oshiba, M. and Nadai, T., Precaution on use of hydrochloride salts in pharmaceutical formulation, *J. Pharm. Sci.*, 70, 6 (1981b) 594-596.

Miyazaki, S., Oshiba, M. and Nadai, T., Unusual solubility and dissolution behaviour of pharmaceutical hydrochloride salts in chloride-containing media, *Int. J. Pharm.*, 6 (1980) 77-85.

Mooney, K.G., Mintun, M.A., Himmelstein, K.J. and Stella, V.J., Dissolution kinetics of carboxylic acids. I. Effect of pH under unbuffered conditions, *J. Pharm. Sci.*, 70, 1 (1981) 13-22.

Morozowich, W., Chulski, T., Hamlin, W.E., Jones, P.M., Northam, J.I., Purmalis, A. and Wagner, J.G., Relationship between *in vitro* dissolution rates, solubilities, and LT_{50}'s in mice of some salts of benzphetamine and etryptamine, *J. Pharm. Sci.*, 51, 10 (1962) 993-996.

Morris, K.R., Fakes, M.G., Thakur, A.B., Newman, A.W., Singh, A.K., Venit, J.J., Spagnuolo, C.J. and Serajuddin, A.T.M., An integrated approach to the selection of optimal salt form for a new drug candidate, *Int. J. Pharm.*, 105 (1994) 209-217.

Mukerjee, P., Micellar properties of drugs: micellar and nonmicellar patterns of self-association of hydrophobic solutes of different molecular structures – monomer fraction, availability and misuses of micellar hypothesis, *J. Pharm. Sci.*, 63, 6 (1974) 972-981.

Mukerjee, P., Mysels, K.J. and Kapauan, P., Counterion specificity in the formation of ionic micelles – size, hydration and hydrophobic bonding effects, *J. Phys. Chem.*, 71, 13 (1967) 4166-4175.

Nagadome, S., Oda, H., Hirata, Y., Igimi, H., Yamauchi, A., Sasaki, Y. and Sugihara, G., Transport of monooleoylglycerol mediated by bile salt micelles across porous membranes, *Colloid Polym. Sci.*, 273 (1995) 701-707.

Nelson, E., Dissolution rate of mixtures of weak acids and tribasic sodium phosphate, *J. Amer. Pharm. Assoc. Sci. Ed.*, 47 (1958) 300-302.

Nelson, E., Knoechel, E.L., Hamlin, W.E. and Wagner, J.G., Influence of the absorption rate of tolbutamide on the rate of decline of blood sugar levels in normal humans, *J. Pharm. Sci.*, 51, 6 (1962) 509-514.

Nelson, E., Solution rate of theophylline salts and effects from oral administration, *J. Amer. Pharm. Assoc. Sci. Ed.*, 46, 10 (1957) 607-614.

Nelson, K.G. and Shah, A.C., Convective diffusion model for a transport-controlled dissolution rate process, *J. Pharm. Sci.*, 64, 4 (1975) 610-614.

Nernst, W. and Brunner, E., Theorie der reaktionsgeschwindigkeit in heterogenen systemen, *Z. Phys. Chem.*, 47 (1904) 52-55; 47 (1904) 56-102.

Newman, A.W. and Brittain, H.G., Particle morphology: optical and electron microscopies, in *Physical Characterization of Pharmaceutical Solids*, Brittain, H.G. (Ed.), Marcel Dekker, New York (1995) pp.127-156.

Nicklasson, M. and Nyqvist, H., Studies on the relationship between intrinsic dissolution rates and rates of water adsorption, *Acta Pharm. Suec.*, 20, 5 (1983) 321-330.

Nicklasson, M., Brodin, A. and Nyqvist, H., Studies on the relationship between solubility and intrinsic rate of dissolution as a function of pH, *Acta Pharm. Suec.*, 18 (1981) 119-128.

Nicklasson, M., Brodin, A. and Stenlander, C., The dependence of intrinsic rates of dissolution on hydrodynamic conditions using a thermodynamic approach, *Acta Pharm. Suec.*, 19 (1982) 25-36.

Nogami, H., Nagai, T., Fukuoka, E. and Yotsuyanagi, T., Dissolution kinetics of barbital polymorphs, *Chem. Pharm. Bull.*, 17, 1 (1969) 23-31.

Noyes, A.A. and Whitney, W., The rate of solution of substances in their own solutions, *J. Am. Chem. Soc.*, 19 (1897) 930-936.

O'Dowd, P.J. and Corrigan, O.I., Dissolution kinetics of three component non-disintegrating compacts: theophylline, benzoic acid and salicylamide, *Int. J. Pharm.*, 176 (1999) 231-240.

O'Reilly, E.B., Mechanism of dissolution of gallstones in cholelitholytic solvents, Ph.D. Thesis, University of Dublin (1990).

Osborne, C.A., A study of the effect of cyclodextrin complexation on membrane transport, M.Sc. Thesis, University of Dublin (1990).

Otsuka, M., Matsumoto, T. and Kaneniwa, N., Effects of the mechanical energy of multi-tableting compression on the polymorphic transformations of chlorpropamide, *J. Pharm. Pharmacol.*, 41 (1989) 665-669.

Pagay, S.N., Use of buffers in matrix capsule formulations, *Drug Dev. Ind. Pharm.*, 14, 7 (1988) 875-894.

Palomo, M.E., Ballesteros, M.P. and Frutos, P., Analysis of diclofenac sodium and derivatives, *J. Pharm. Biomed. Anal.*, 21 (1999) 83-94.

Pandit, N.K., Strykowski, J.M. and Shtohryn, L., The effect of salts on the distribution and solubility of an acidic drug, *Int. J. Pharm.*, 50 (1989) 7-13.

Parrott, E.L., Simpson, M. and Flanagan, D.R., Dissolution kinetics of a three-component solid. II. Benzoic acid, salicylic acid and salicylamide, *J. Pharm. Sci.*, 72, 7 (1983) 765-768.

Parrott, E.L., Wurster, D.E. and Higuchi, T., Investigation of drug release from solids. I. Some factors influencing the dissolution rate, *J. Am. Pharm. Assoc. Sci. Ed.*, 44, 5 (1955) 269-273.

Pederson, A.M., *US Patent*, Number 3,954,959 (1976).

Pellet, M.A., Castellano, S., Hadgraft, J. and Davis, A.F., The penetration of supersaturated solutions of piroxicam across silicone membranes and human skin in vitro, *J. Control. Rel.*, 46 (1997) 205-214.

Pellet, M.A., Davis, A.F. and Hadgraft, J., Effect of supersaturation on membrane transport, *Int. J. Pharm.*, 111 (1994) 1-6.

Pirttimäki, J., Laine, E., Ketolainen, J. and Paronen, P., Effects of grinding and compression on crystal structure of anhydrous caffeine, *Int. J. Pharm.*, 95 (1993) 93-99.

Preechagoon, D., Udomprateep, A. and Manwiwattanagul, G., Improved dissolution rate of poorly soluble drug by incorporation of buffers, *Drug Dev. Ind. Pharm.*, 26, 8 (2000) 891-894.

Qiu, Y., Schoenwald, R.D. and Guillory, J.K., Physicochemical characterization of high- and low-melting phenylephrine oxazolidines, *Pharm. Res.*, 10, 10 (1993) 1507-1515.

Raghavan, S.L., Trividic, A., Davis, A.F. and Hadgraft, J., Effect of cellulose polymers on supersaturation and in vitro membrane transport of hydrocortisone acetate, *Int. J. Pharm.*, 193 (2000) 231-237.

Ramtoola, Z., Dissolution mechanism of drug and acid excipient mixtures in reactive media, Ph.D. Thesis, University of Dublin (1988).

Richards, J.H., Solubility and dissolution rate, in *Pharmaceutics – The Science of Dosage Form Design*, Aulton, M.E. (Ed.), Churchill Livingstone, Edinburgh (1991) pp.62-80.

Rodríguez Bayon, A.M., Corish, J. and Corrigan, O.I., *In vitro* passive and iontophoretically assisted transport of salbutamol sulphate across synthetic membranes, *Drug Dev. Ind. Pharm.*, 19, 10 (1993) 1169-1181.

Roseman, T.J. and Yalkowsky, S.H., Physicochemical properties of prostaglandin $F_{2\alpha}$ (tromethamine salt): Solubility behaviour, surface properties and ionisation constants, *J. Pharm. Sci.*, 62, 10 (1973) 1680-1685.

Rubino, J.T., Solubilities and solid state properties of the sodium salts of drugs, *J. Pharm. Sci.*, 78, 6 (1989) 485-489.

Scientist Handbook, Micromath Scientific Software, Utah, U.S.A (1995).

Senior, N., Some observations on the formulation and properties of chlorhexidine, *J. Soc. Cosmet. Chem.*, 24 (1973) 259-278.

Serajuddin, A.T.M. and Jarowski, C.I., Effect of diffusion layer pH and solubility on the dissolution rate of pharmaceutical bases and their hydrochloride salts. I. Phenazopyridine, *J. Pharm. Sci.*, 74, 2 (1985a) 142-147.

Serajuddin, A.T.M. and Jarowski, C.I., Effect of diffusion layer pH and solubility on the dissolution rate of pharmaceutical acids and their sodium salts. II. Salicylic acid, theophylline and benzoic acid, *J. Pharm. Sci.*, 74, 2 (1985b) 148-154.

Serajuddin, A.T.M. and Jarowski, C.I., Influence of pH on release of phenytoin sodium from slow-release dosage forms, *J. Pharm. Sci.*, 82, 3 (1993) 306-310.

Serajuddin, A.T.M. and Mufson, D., pH-solubility profiles of organic bases and their hydrochloride salts, *Pharm. Res.*, 2 (1985) 65-68.

Serajuddin, A.T.M. and Rosoff, M., pH-solubility profile of papaverine hydrochloride and its relationship to the dissolution rate of sustained-release pellets, *J. Pharm. Sci.*, 73, 9 (1984) 1203-1208.

Serajuddin, A.T.M., Sheen, P.C., Mufson, D., Bernstein, D. and Augustine, M.A., Preformulation study of a poorly water-soluble drug, α-pentyl-3-(2-quinolinylmethoxy)benzenemethanol: selection of the base for dosage form design, *J. Pharm. Sci.*, 75 (1986) 492-496.

Setschenow, J., Über die konstitution der salzlösungen auf grund ihres verhaltens zu kohlensäure, *Z. Phys. Chem.*, 4 (1889) 117-125.

Shah, A.C. and Nelson, K.G., Evaluation of a convective diffusion drug dissolution rate model, *J. Pharm. Sci.*, 64, 9 (1975) 1518-1520.

Shah, J.C. and Maniar, M., pH-dependent solubility and dissolution of bupivacaine and its relevance to the formulation of a controlled release system, *J. Control. Rel.*, 23 (1993) 261-270.

Shah, S.A. and Parrott, E.L., Dissolution of two-component solids, *J. Pharm. Sci.*, 65, 12 (1976) 1784-1790.

Shefter, E. and Higuchi, T., Dissolution behaviour of crystalline solvated and nonsolvated forms of some pharmaceuticals, *J. Pharm. Sci.*, 52, 8 (1963) 781-791.

Silverstein, R.M. and Webster, F.X., *Spectrometric Identification of Organic Compounds*, 6th Edition, J. Wiley & Sons, New York (1998).

Simonelli, A.P., Mehta, S.C. and Higuchi, W.I., Dissolution rates of high energy polyvinylpyrrolidone (PVP)-sulfathiazole coprecipitates, *J. Pharm. Sci.*, 58, 5 (1969) 538-549.

Simpson, M. and Parrott, E.L., Dissolution kinetics of a three-component solid. I. Ethylparaben, phenacetin and salicylamide, *J. Pharm. Sci.*, 72, 7 (1983) 757-764.

Sjökvist Saers, E. and Craig, D.Q.M., An investigation into the mechanism of dissolution of alkyl para-aminobenzoates from polyethylene glycol solid dispersions, *Int. J. Pharm.*, 83 (1992) 211-219.

Small, D.M., *Handbook of Lipid Research. 4. The Physical Chemistry of Lipids*, Plenum Press, New York (1986).

Socrates, G., *Infrared Characteristic Group Frequencies*, 2nd Edition, John Wiley & Sons, New York (1994).

Streng, W.H., Hsi, S.K., Helms, P.E. and Tan, H.G.H., General treatment of pH-solubility profiles of weak acids and bases and the effects of different acids on the solubility of a weak base, *J. Pharm. Sci.*, 73, 12 (1984) 1679-1684.

Streubel, A., Siepmann, J., Dashevsky, A. and Bodmeier, R., pH-independent release of a weakly basic drug from water-insoluble and -soluble matrix tablets, *J. Control. Rel.*, 67 (2000) 101-110.

Summers, M.P., Enever, R.P. and Carless, J.E., The influence of crystal form on the radial stress transmission characteristics of pharmaceutical materials, *J. Pharm. Pharmacol.*, 28 (1976) 89-99.

Suryanarayanan, R., X-ray powder diffractometry, in *Physical Characterization of Pharmaceutical Solids*, Brittain, H.G. (Ed.), Marcel Dekker, New York (1995) pp.187-221.

Takács-Novák, K. and Szász, G., Ion-pair partition of quaternary ammonium drugs: the influence of counter ions of different lipophilicity, size and flexibility, *Pharm. Res.*, 16, 10 (1999) 1633-1638.

Thoma, K. and Ziegler, I., The pH-independent release of fenoldopam from pellets with insoluble film coats, *Eur. J. Pharm. Biopharm.*, 46 (1998) 105-113.

Thoma, K. and Zimmer, T., Retardation of weakly basic drugs with diffusion tablets, *Int. J. Pharm.*, 58 (1990) 197-202.

Thomas, E. and Rubino, J., Solubility, melting point and salting-out relationships in a group of secondary amine hydrochloride salts, *Int. J. Pharm.*, 130 (1996) 179-185.

Tirkkonen, S., Urtti, A. and Paronen, P., Buffer controlled release of indomethacin from ethylcellulose microcapsules, *Int. J. Pharm.*, 124 (1995) 219-229.

Touitou, E. and Donbrow, M., Deviation of dissolution behaviour of benzoic acid from theoretical predictions with lowering of temperature: limitations as a model dissolution substance, *Int. J. Pharm.*, 9 (1981) 97-106.

Tsuji, A., Nakashima, E., Hamano, S. and Yamana, T., Physicochemical properties of amphoteric β-lactam antibiotics. I. Stability, solubility and dissolution behaviour of amino penicillins as a function of pH, *J. Pharm. Sci.*, 67, 8 (1978) 1059-1066.

United States Pharmacopeia 24, United States Pharmacopeial Convention, Rockville, Maryland (2000).

Valenta, C., Siman, U., Kratzel, M. and Hadgraft, J., The dermal delivery of lignocaine: influence of ion pairing, *Int. J. Pharm.*, 197 (2000) 77-85.

van der Veen, C., Buitendijk, H. and Lerk, C.F., The effect of acidic excipients on the release of weakly basic drugs from the programmed release megaloporous system, *Eur. J. Pharm. Biopharm.*, 37, 4 (1991a) 238-242.

van der Veen, J., Bonferoni, C., Buitendijk, H.H. and Lerk, C.F., The influence of acidic excipients on the release of weak basic drugs from programmed release solid dosage forms, *Proc. 10th Pharm. Tech. Conf.*, Vol. 1, Bologna, Italy (1991b) 93-118.

Ventouras, K. and Buri, P., Rôle de l'acidification de matrices hydrophiles sur la libération de principes actifs peu solubles en milieu intestinal, *Pharm. Acta Helv.*, 53, 11 (1978) 314-320.

Ventouras, K., Boucherat, J. and Buri, P., Influence des facteurs technologiques sur la libération de la vincamine incorporée dans des matrices hydrophiles, *Pharm. Acta Helv.*, 52, 5 (1977) 119-123.

Wang, L.H. and Chowhan, Z.T., Drug-excipient interactions resulting from powder mixing. V. Role of sodium lauryl sulphate, *Int. J. Pharm.*, 60 (1990) 61-78.

Wells, J.I., *Pharmaceutical Preformulation – the Physicochemical Properties of Drug Substances*, Ellis Horwood, Chichester (1988).

Williamson, A.T., The exact calculation of heats of solution from solubility data, *Trans. Faraday Soc.*, 40 (1944) 421-436.

Wurster, D.E. and Taylor, P.W., Dissolution rates, *J. Pharm. Sci.*, 54, 2 (1965) 169-175.

Yalkowsky, S.H. and Banerjee, S., *Aqueous Solubility –Methods of Estimation for Organic Compounds*, Marcel Dekker, New York (1992).

Yalkowsky, S.H. and Zografi, G., Potentiometric titration of monomeric and micellar acylcarnitines, *J. Pharm. Sci.*, 59, 6 (1970) 798-802.

Yalkowsky, S.H., Solubility and partitioning. V. Dependence of solubility on melting point, *J. Pharm. Sci.*, 70, 8 (1981) 971-973.

Yu, L., Reutzel, S.M. and Stephenson, G.A., Physical characterization of polymorphic drugs: an integrated characterization study, *Pharmaceutical Science and Technology Today*, 1, 3 (1998) 118-127.

APPENDICES

Appendix I

Assessment of the variability of temperature and enthalpy values determined by DSC analysis

DSC analysis was carried out in replicate (6 scans) on a sample of DHEP using the Mettler Toledo DSC 821^e system. The onset temperature, peak temperature and enthalpy of fusion were determined using STAR^e software. A representative scan is shown below. The values for the 6 scans are presented in the table below.

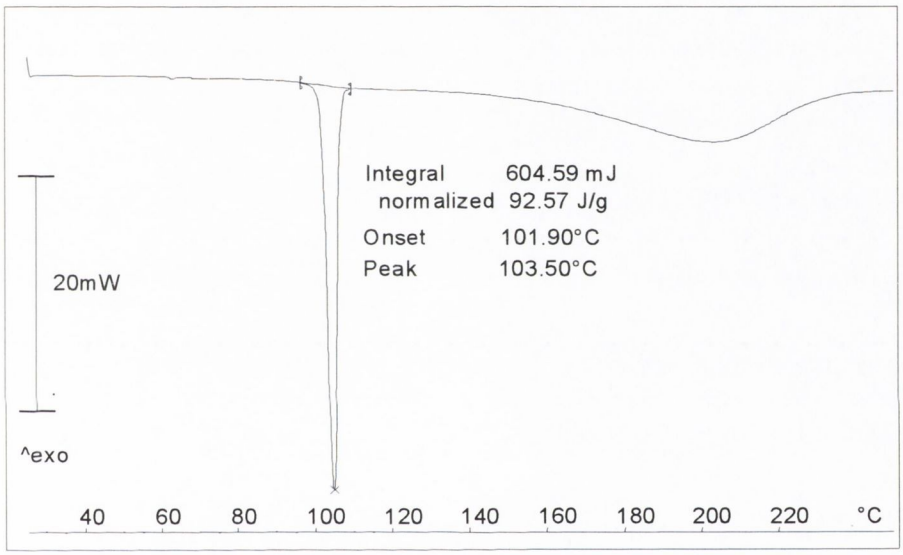

DSC scan for DHEP

Peak and onset temperatures and enthalpy of fusion values for DHEP

Scan	*Peak temperature (°C)*	*Onset temperature (°C)*	ΔH_f *(J/g)*
1	103.50	101.90	92.57
2	103.48	102.00	91.75
3	103.59	102.07	92.24
4	103.51	101.97	92.29
5	103.21	101.84	92.79
6	103.32	101.89	89.08
mean	103.44	101.95	91.79
SD	0.14	0.08	1.37
coefficient of variation	0.14%	0.08%	1.49%

Appendix II

FT-IR scans of diclofenac acid and diclofenac salts prepared, including different polymorphic and pseudopolymorphic forms

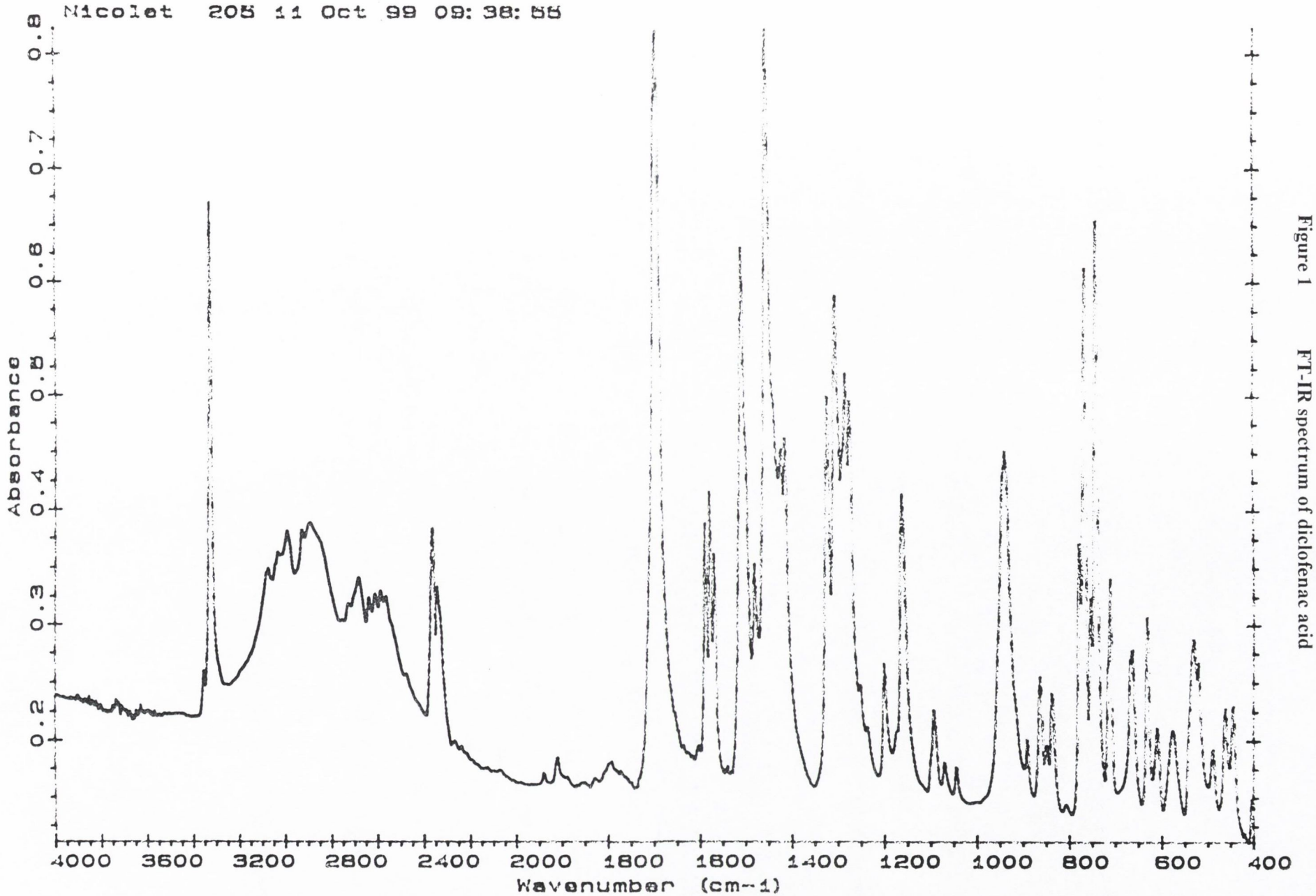

Figure 1 FT-IR spectrum of diclofenac acid

Figure 2 **FT-IR spectrum of DHEP anhydrate**

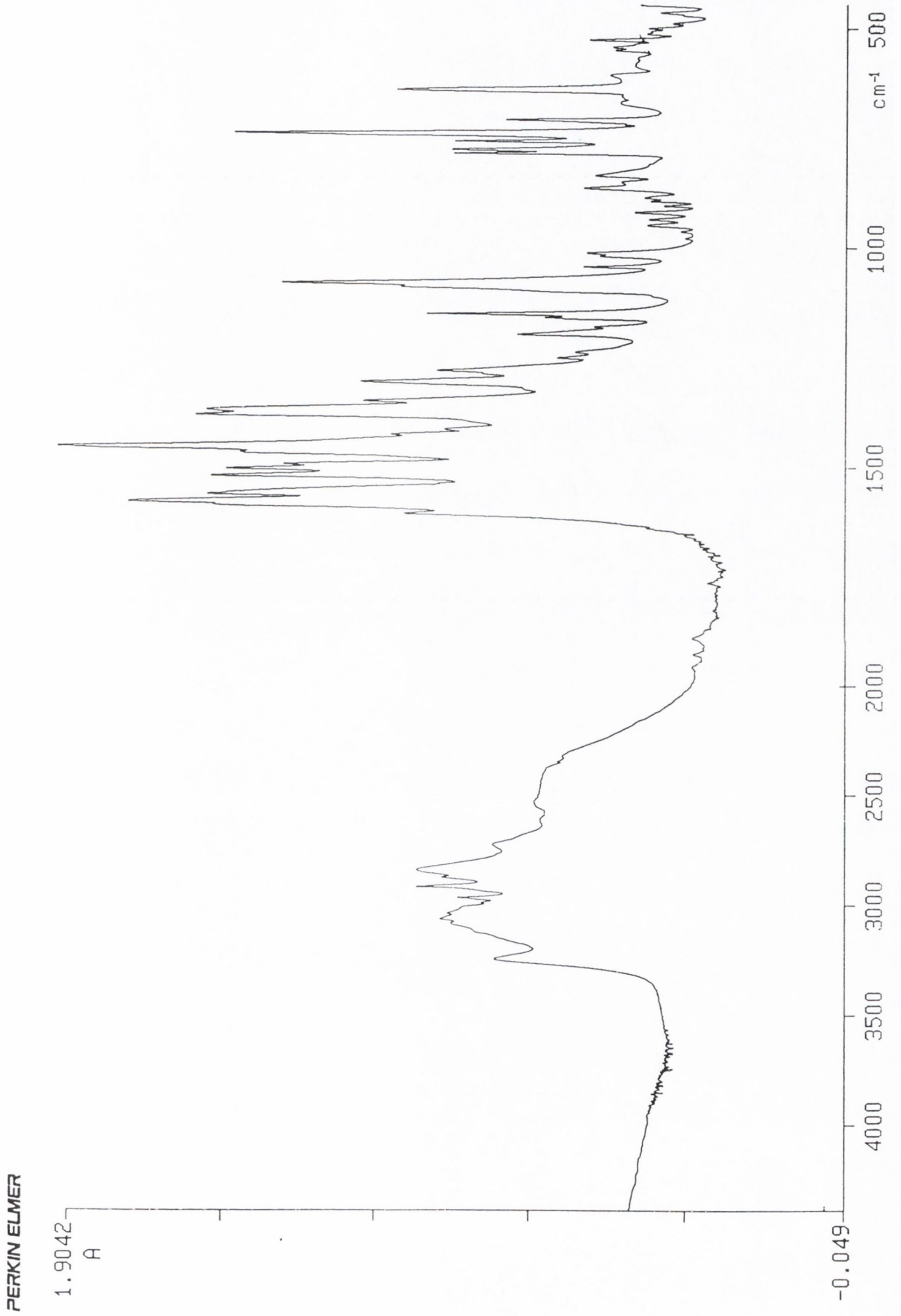

Figure 3 **FT-IR spectrum of DHEP B.N.II recrystallised from water**

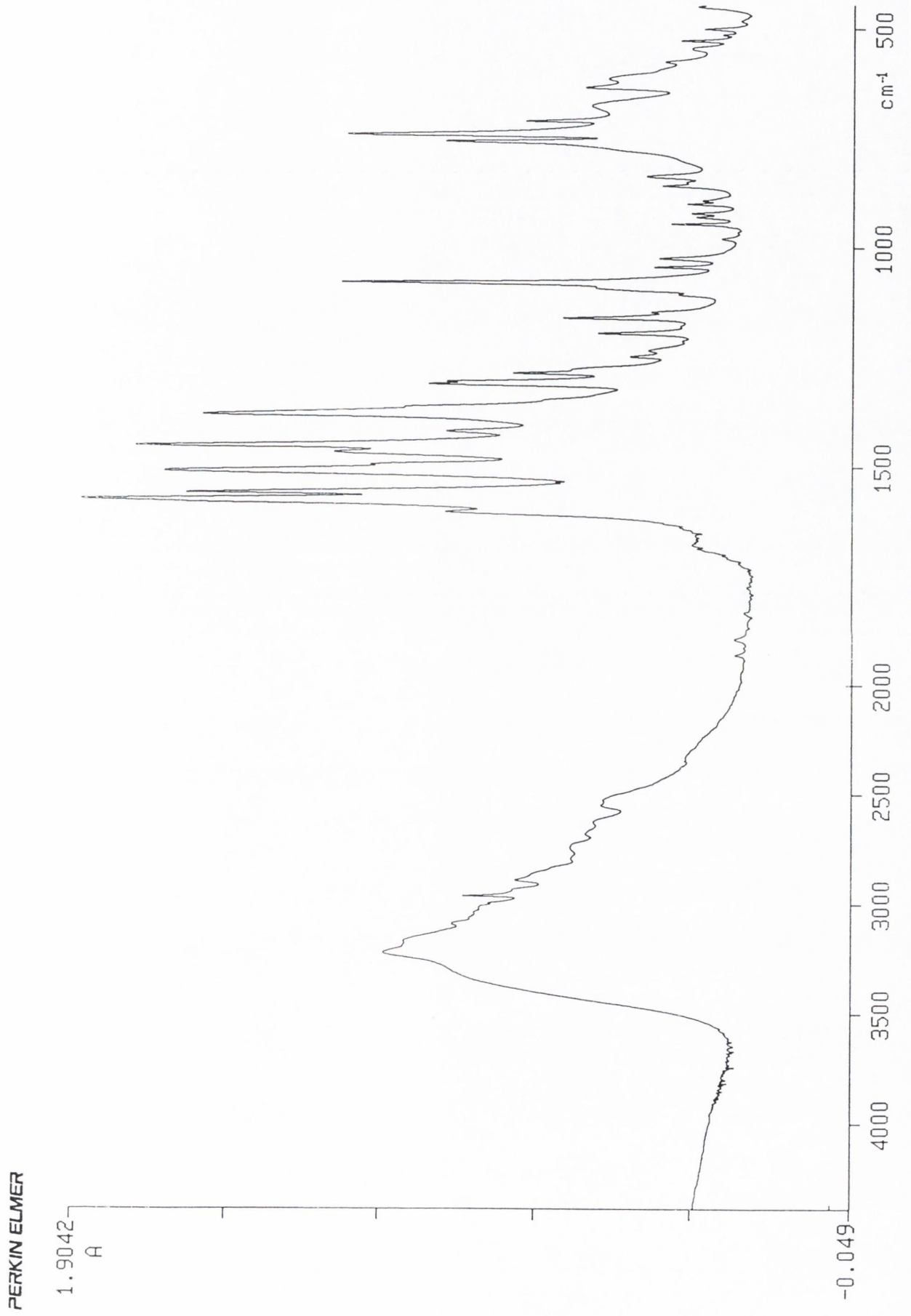

Figure 4 **FT-IR spectrum of DHEP dihydrate**

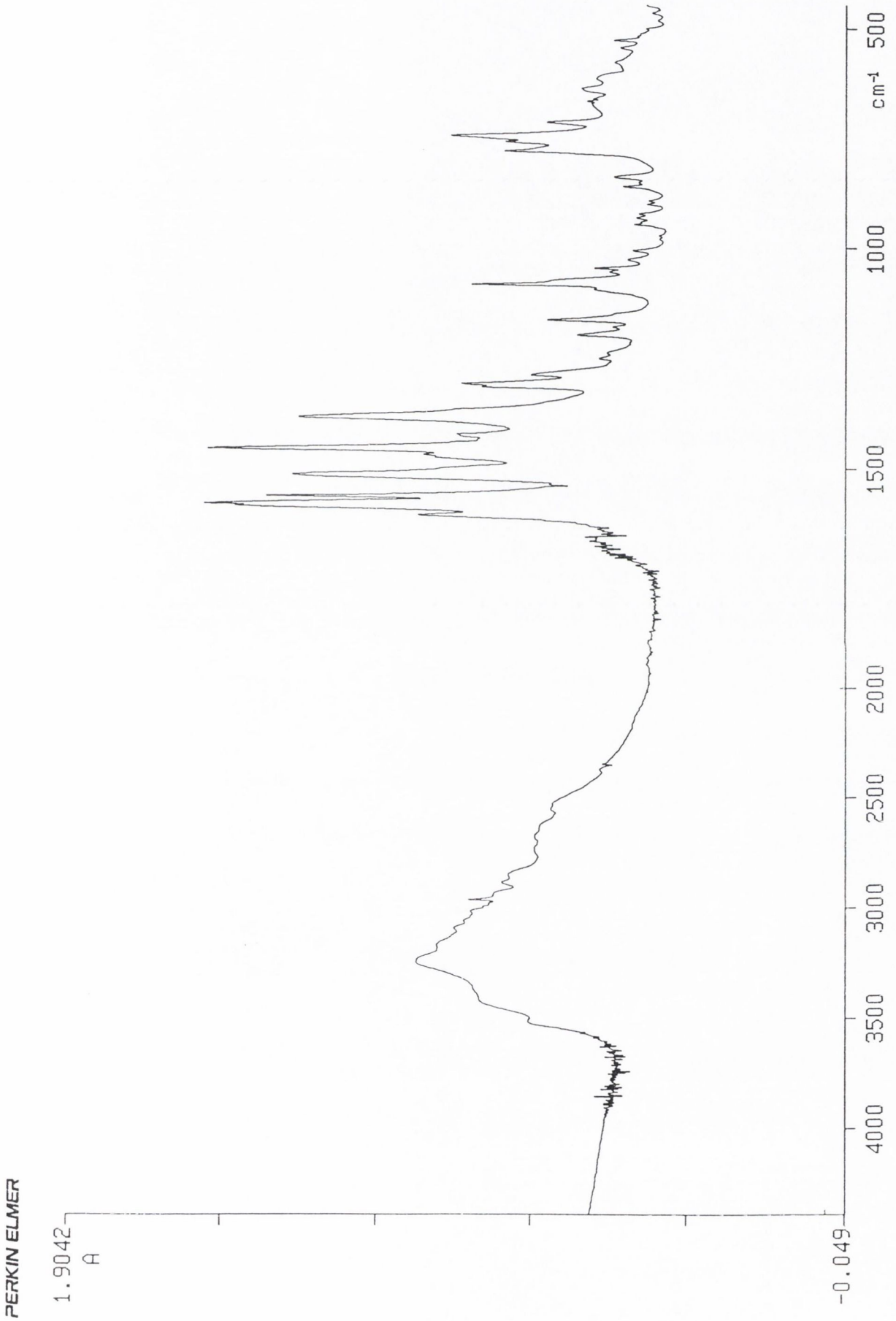

Figure 5 FT-IR spectrum of the commercial sample of DDEA

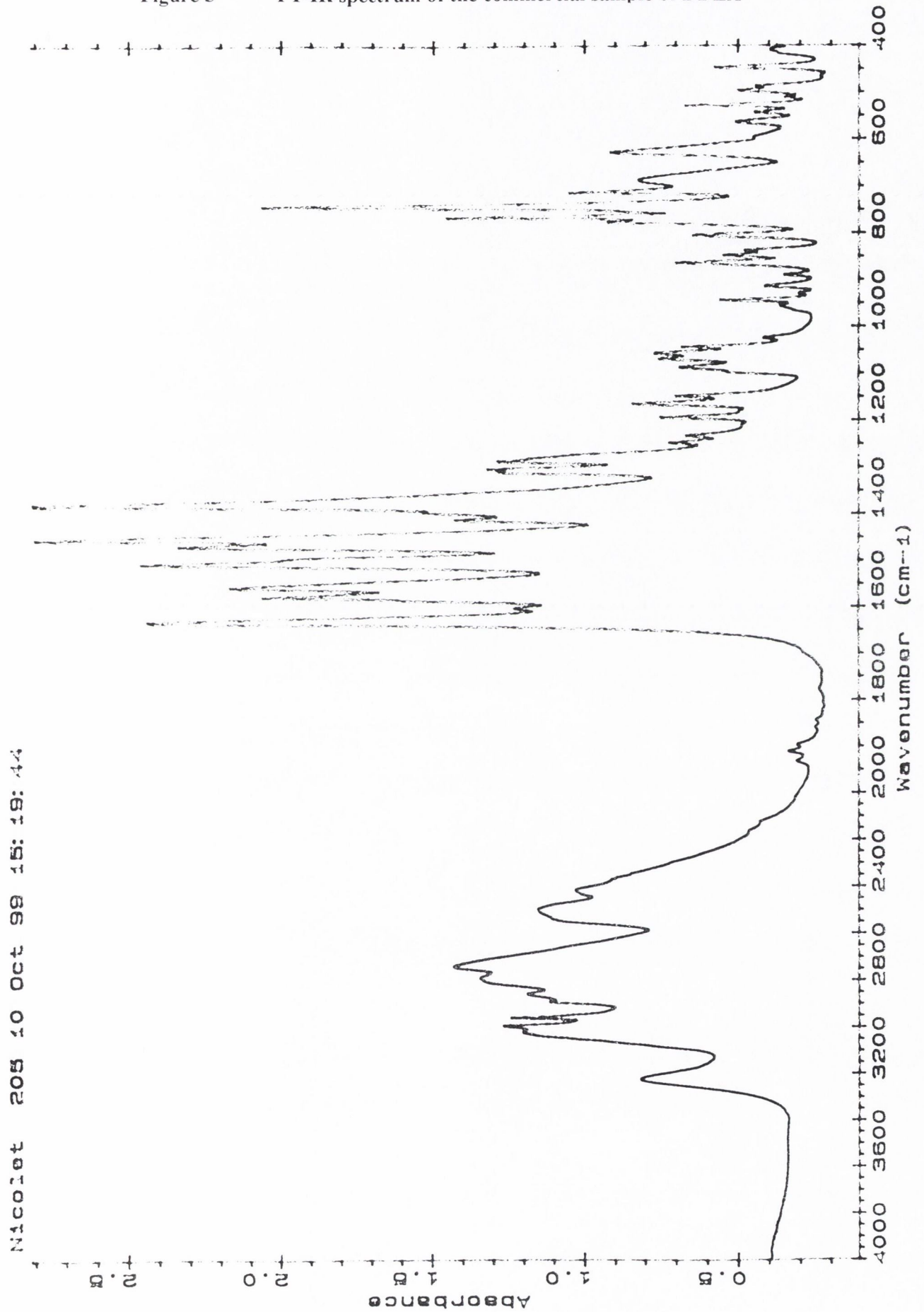

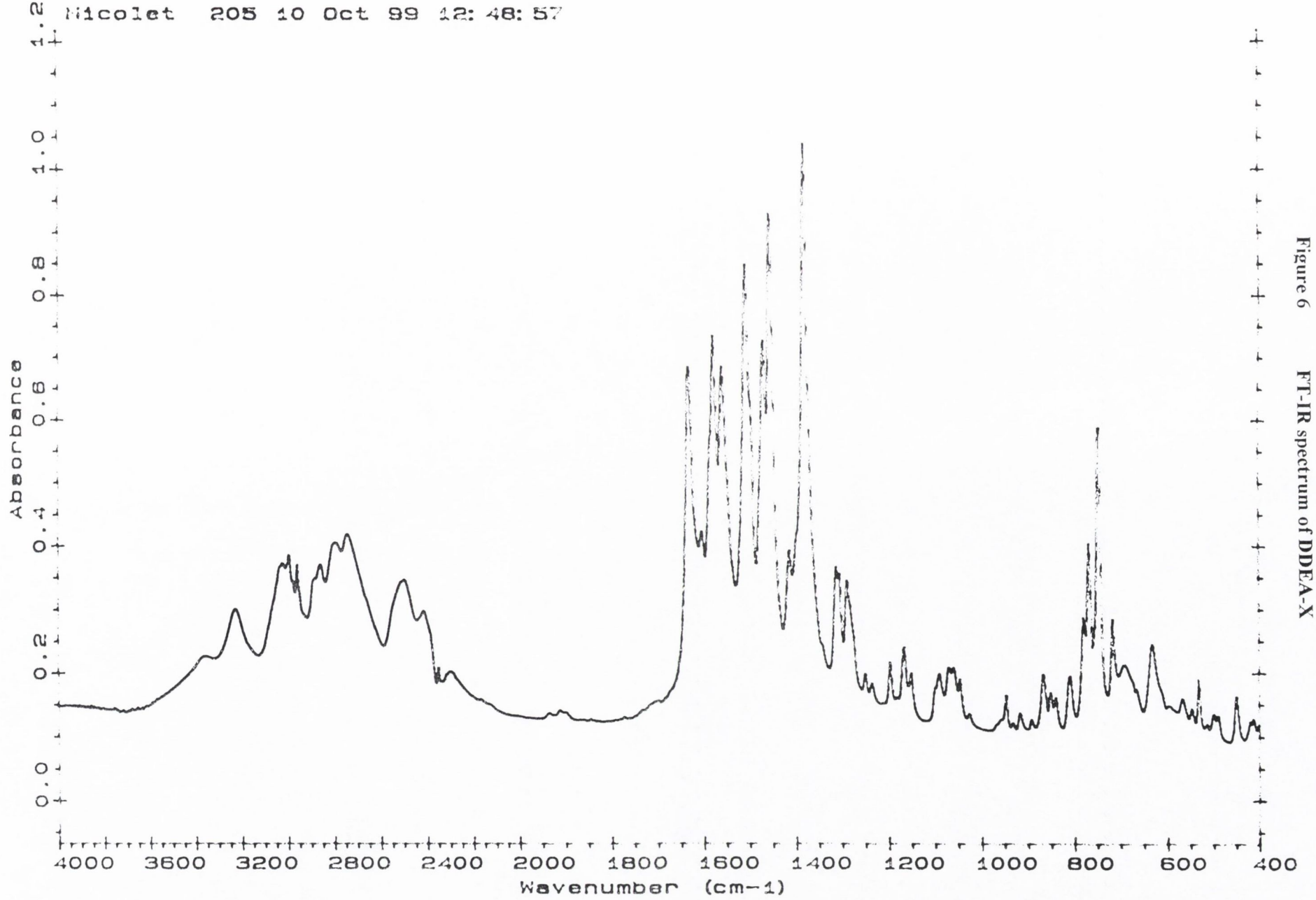

Figure 6 FT-IR spectrum of DDEA-X

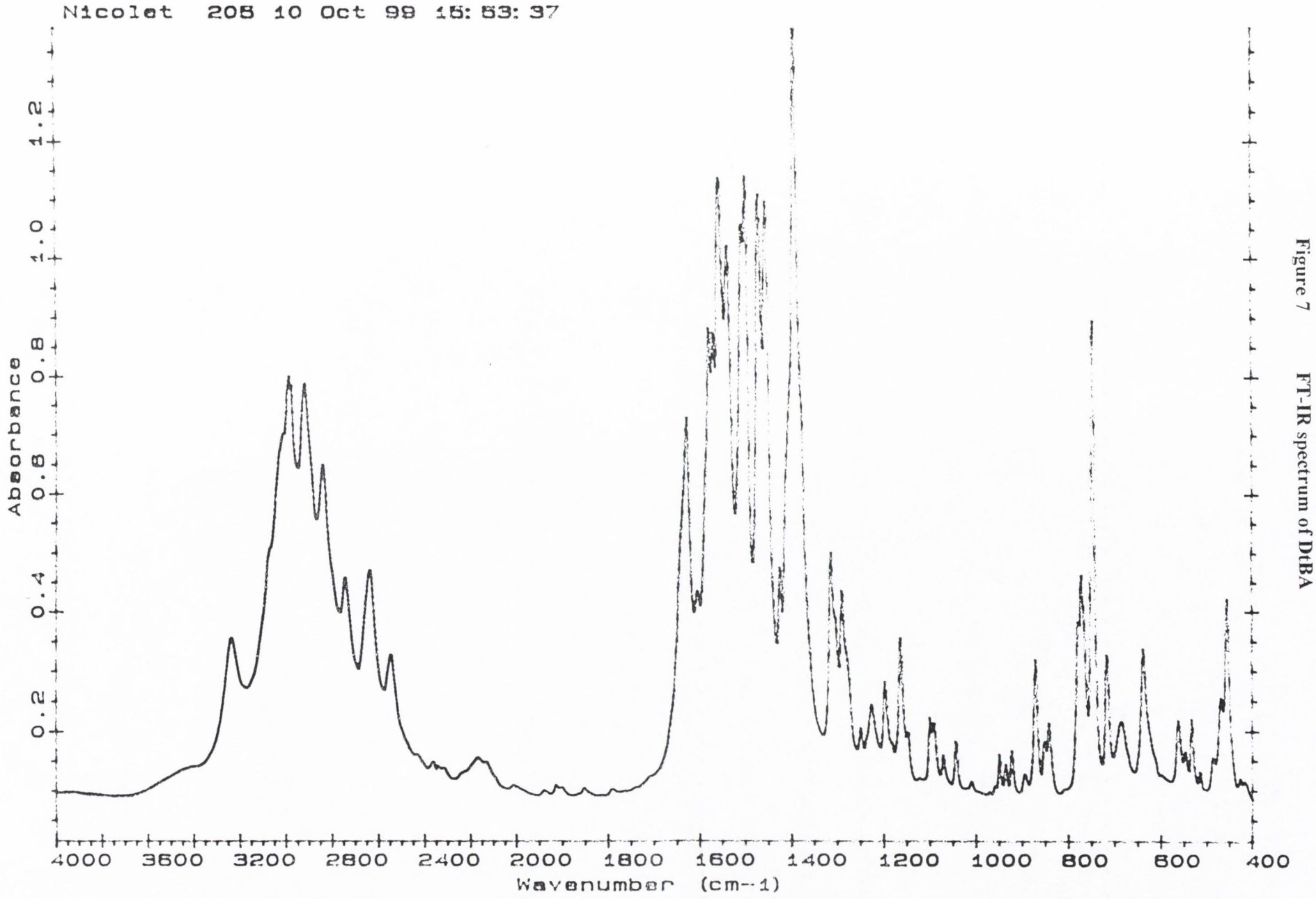

Figure 7 FT-IR spectrum of DtBA

Figure 8 FT-IR spectrum of DAMP-I

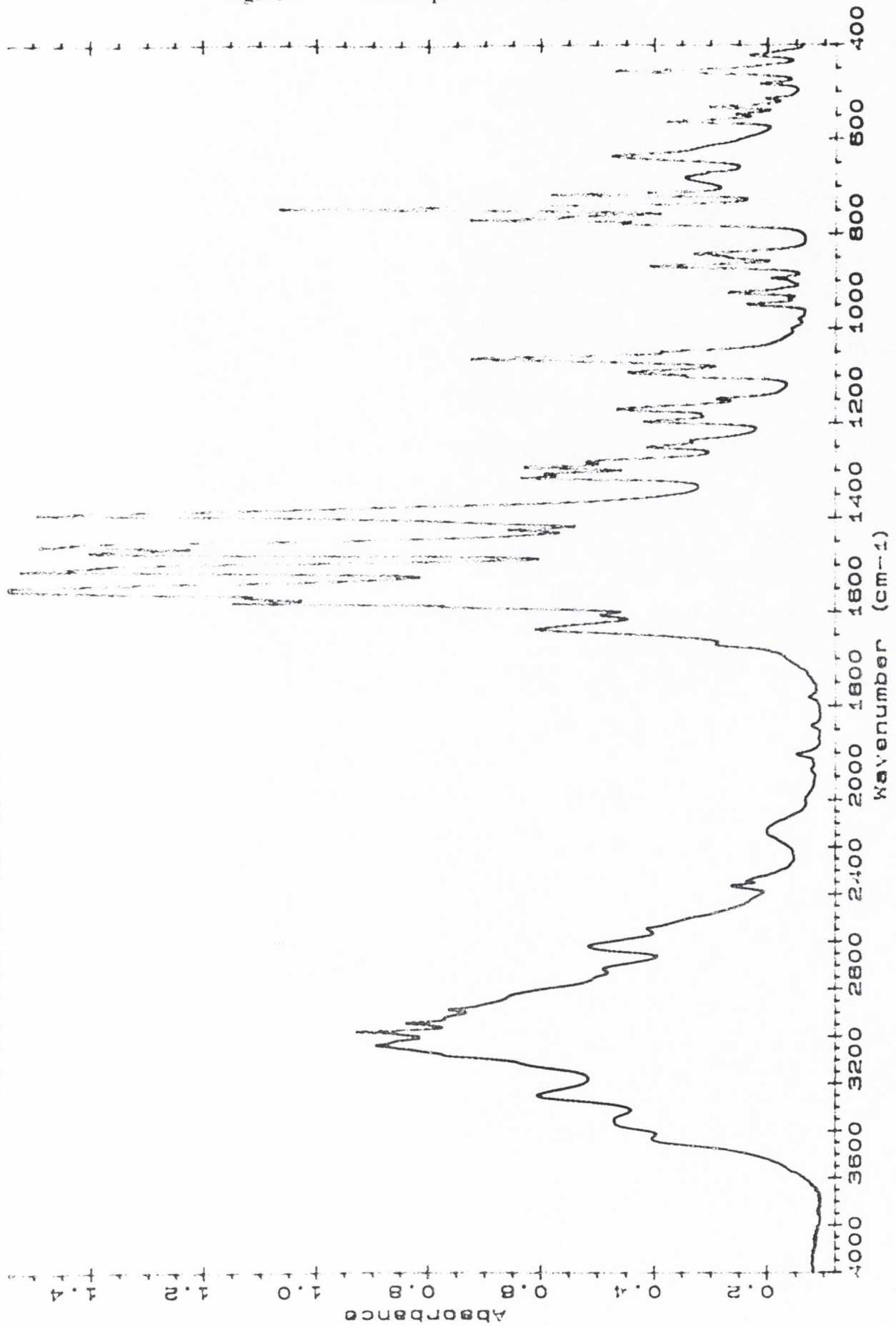

Figure 9 FT-IR spectrum of DAMP-II

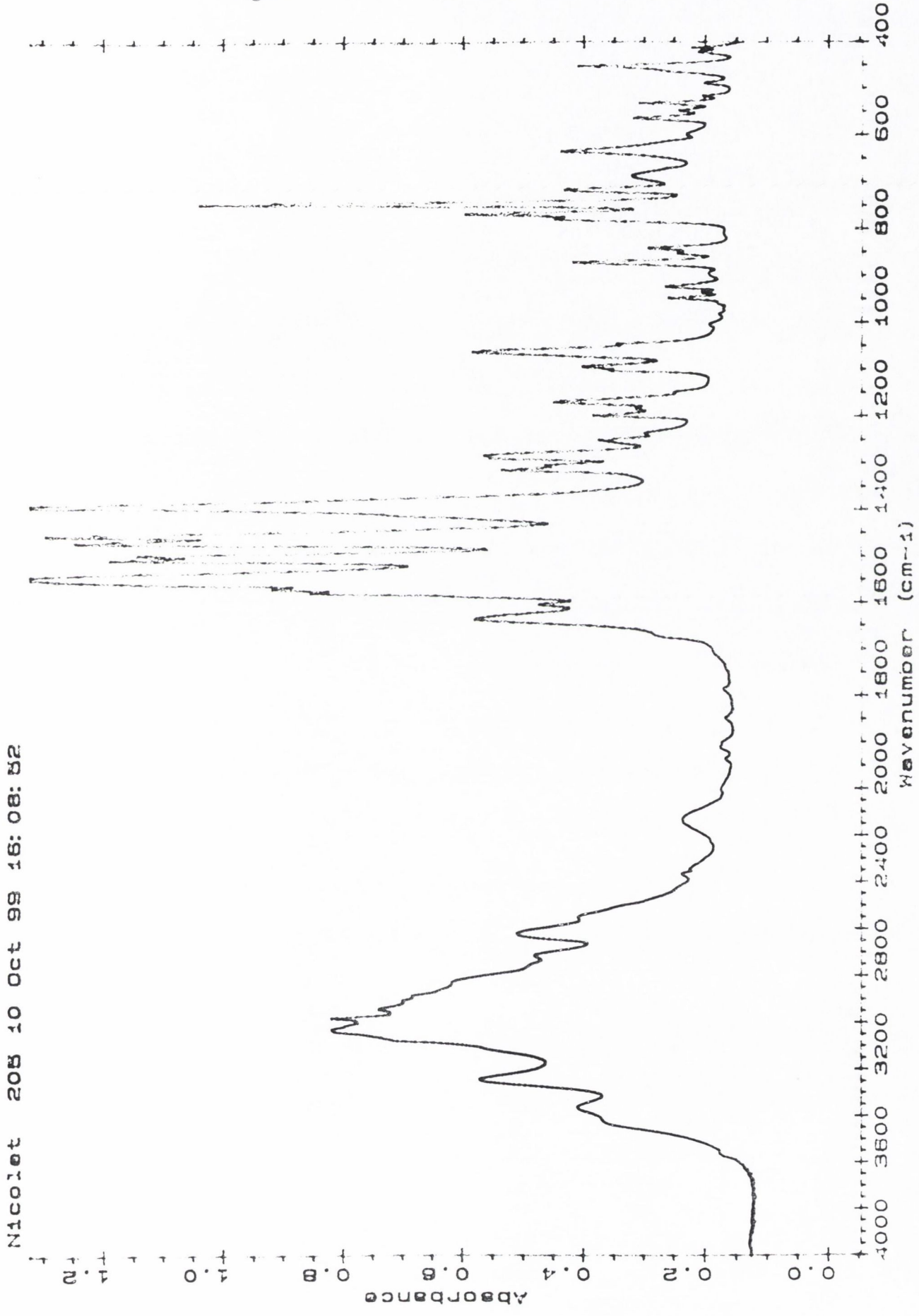

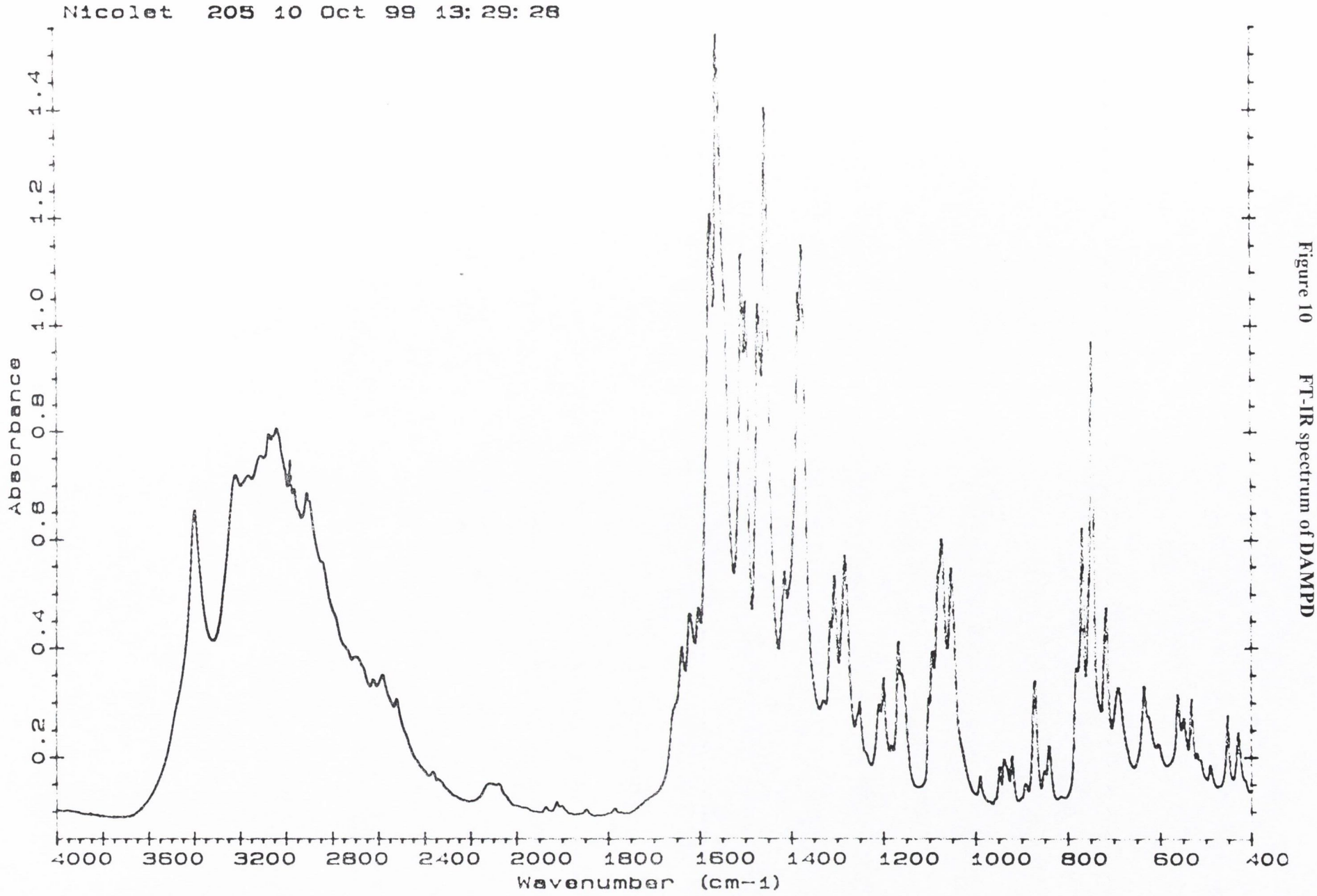

Figure 10 FT-IR spectrum of DAMPD

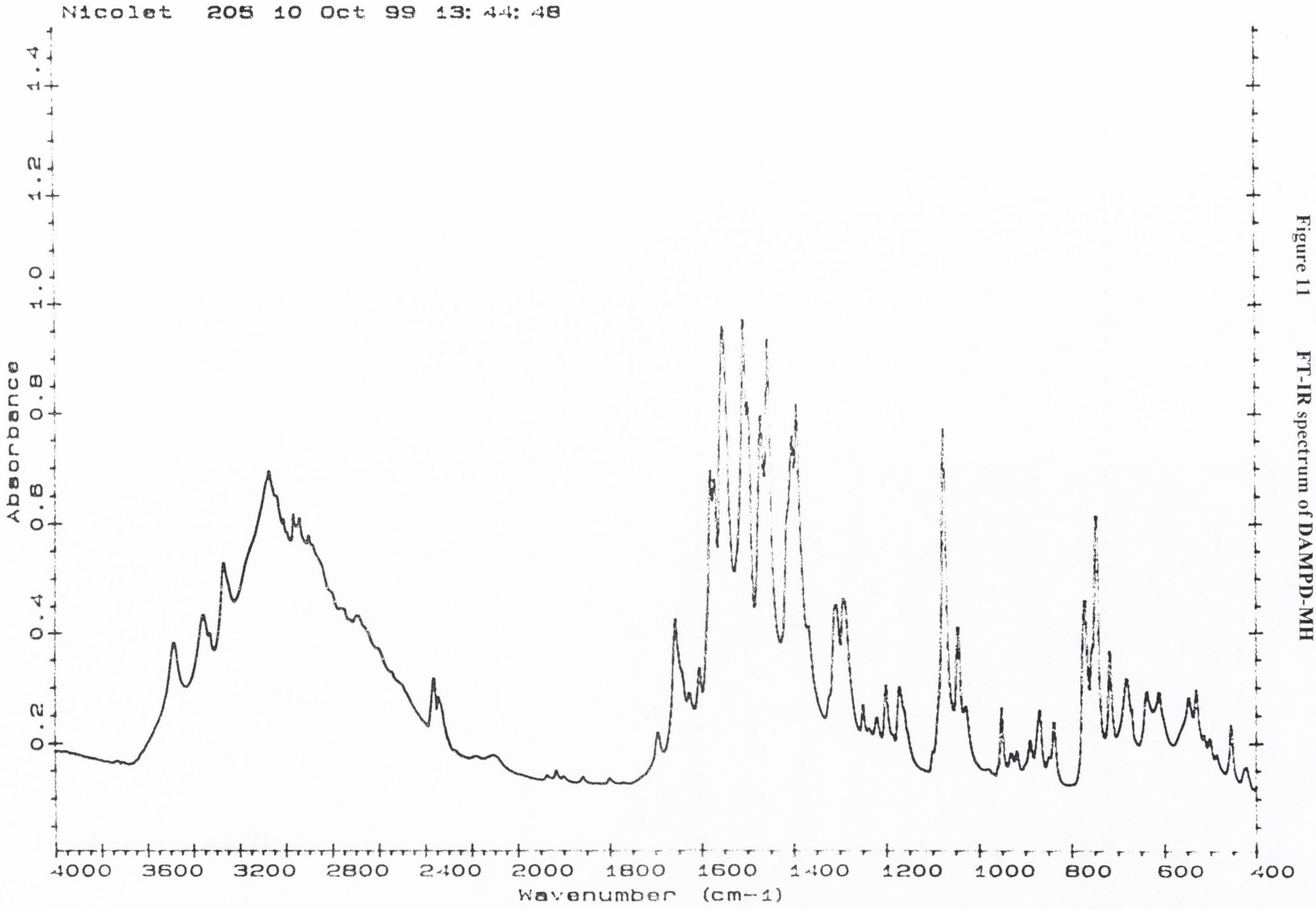

Figure 11 FT-IR spectrum of DAMPD-MH

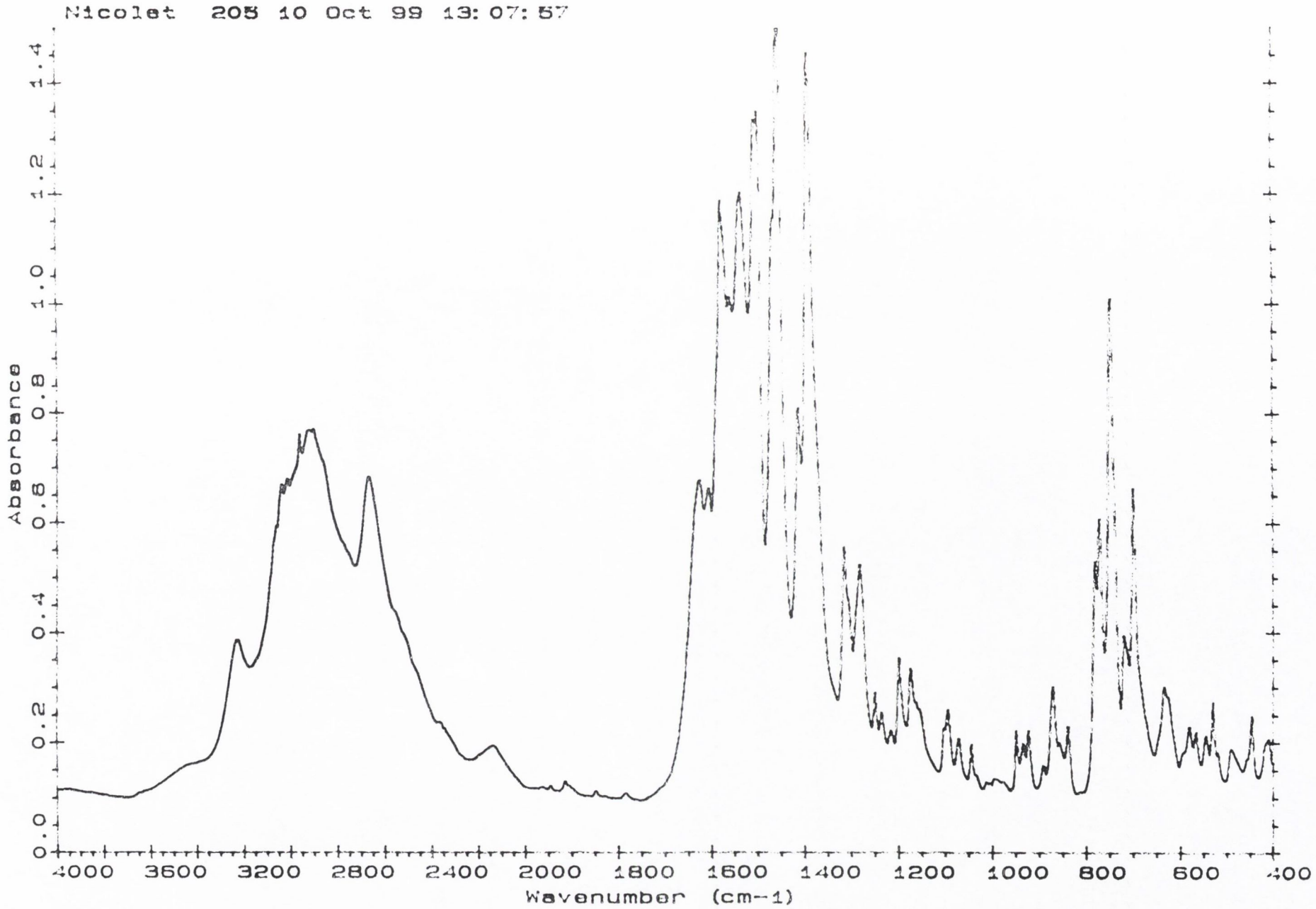

Figure 12 **FT-IR** spectrum of **DBA-I**

Figure 13 FT-IR spectrum of DBA-II

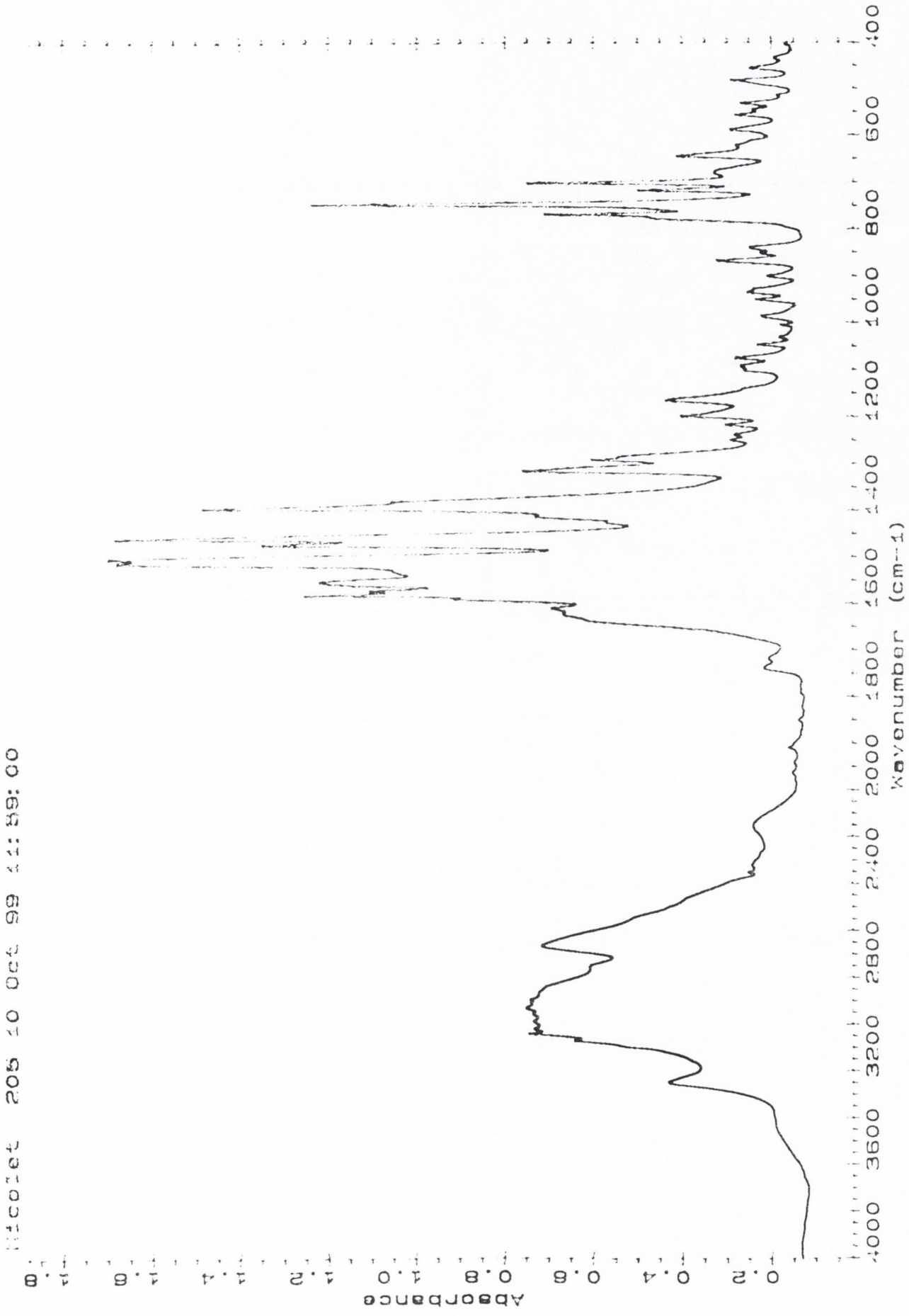

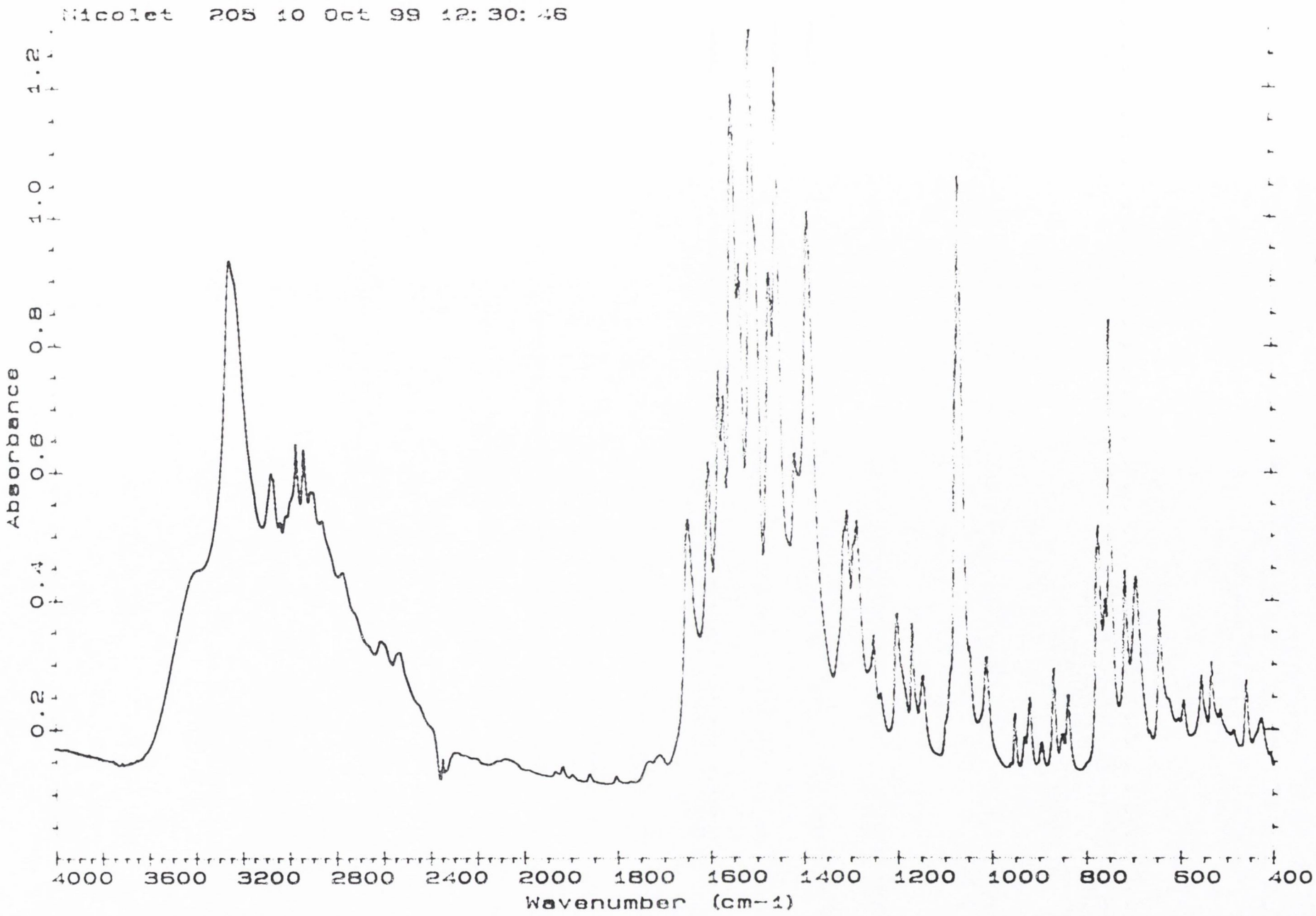

Figure 14 **FT-IR** spectrum of **DTRIS**

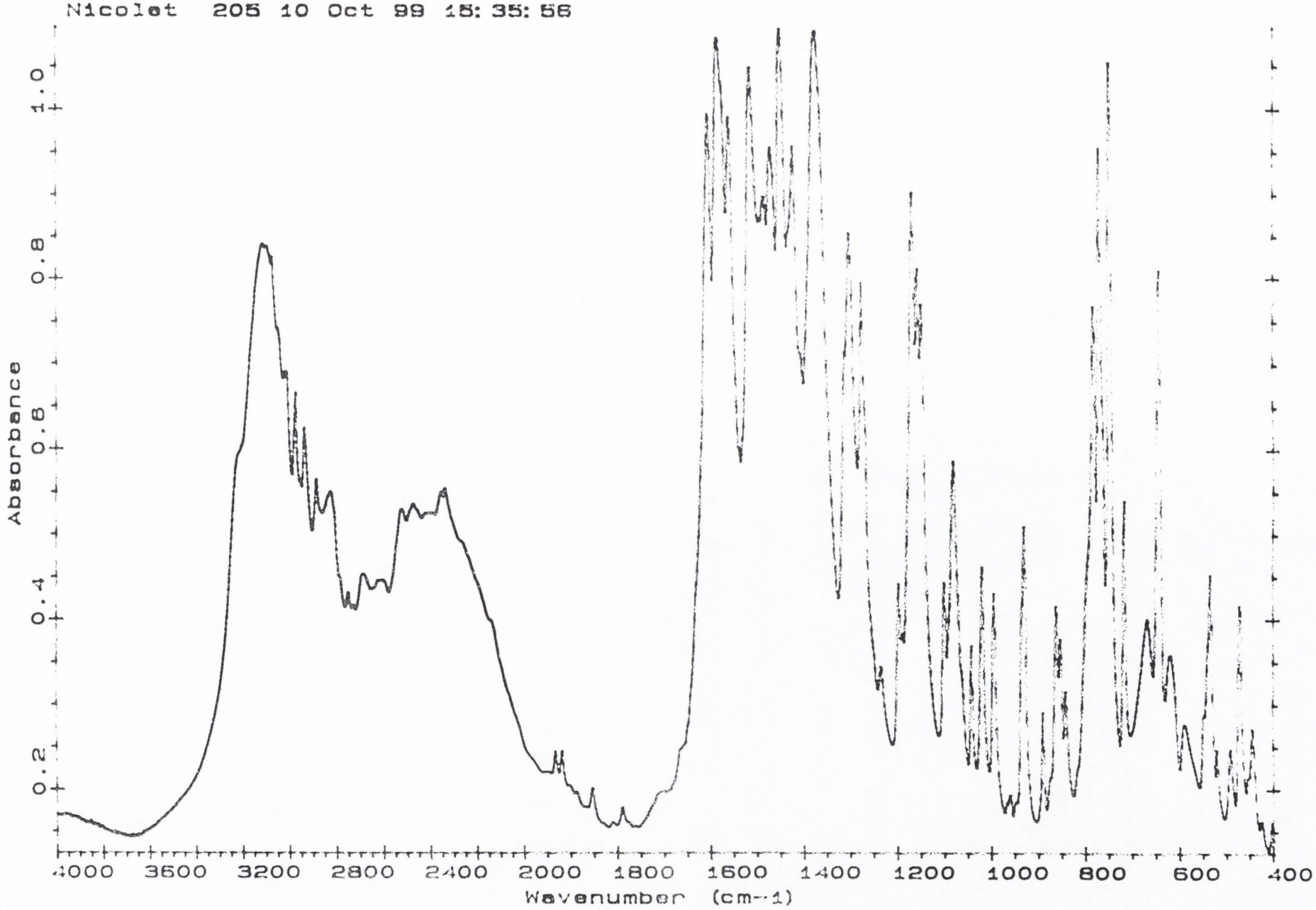

Figure 15 FT-IR spectrum of DDNL

Appendix III

Calibration curves used to determine the concentration of diclofenac in water

The equations are of the form: $y = mx + c$

where y is absorbance at 276 nm and x is concentration (mg/ml).

Concentrations used were in the range 0.004 – 0.04 mg/ml.

Salt	*Equation*	R^2
DAMP	y = 25.573x + 0.0047	0.9999
DAMPD	y = 24.507x + 0.0066	0.9997
DBA	y = 24.748x + 0.0001	0.9998
DtBA	y = 26.660x + 0.0054	0.9999
DDEA	y = 26.938x + 0.0046	0.9999
DDNL	y = 26.040x - 0.0025	0.9997
DHEP	y = 24.283x + 0.0047	0.9999
DNa	y = 31.292x + 0.0132	0.9999
DTRIS	y = 23.724x + 0.0016	1.0000

Appendix IV

Attenuated total reflectance FT-IR spectroscopy in the development of an assay for TRIS and AMPD

Details of calibration curves for TRIS and AMPD

Base	*Characteristic peak* cm^{-1}	*Reference* cm^{-1}	*Calibration curve equation**	R^2
TRIS	1040	1126	y = 0.0295x	0.9881
AMPD	1042	1140	y = 0.0021x	0.9145

* the equations are of the form: y = mx

where y is absorbance and x is concentration (%w/v)

Figure 1 ATR FT-IR spectrum obtained for a 1.0 %w/v aqueous solution of TRIS (corrected for solvent), showing the characteristic peak at 1040 cm^{-1}

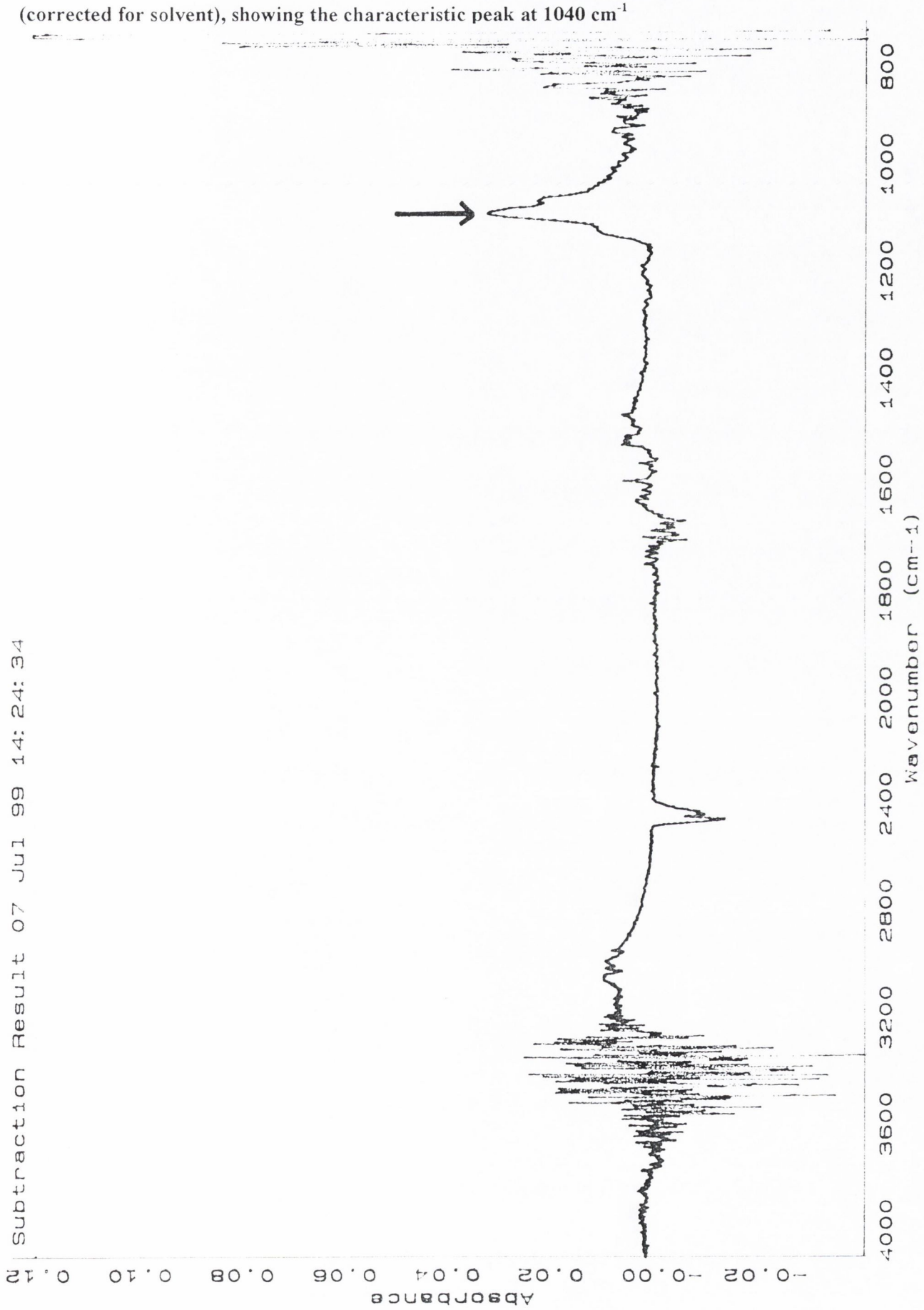

Figure 2 ATR FT-IR spectrum obtained for a 1.0 %w/v aqueous solution of AMPD (corrected for solvent), showing the characteristic peak at 1042 cm^{-1}

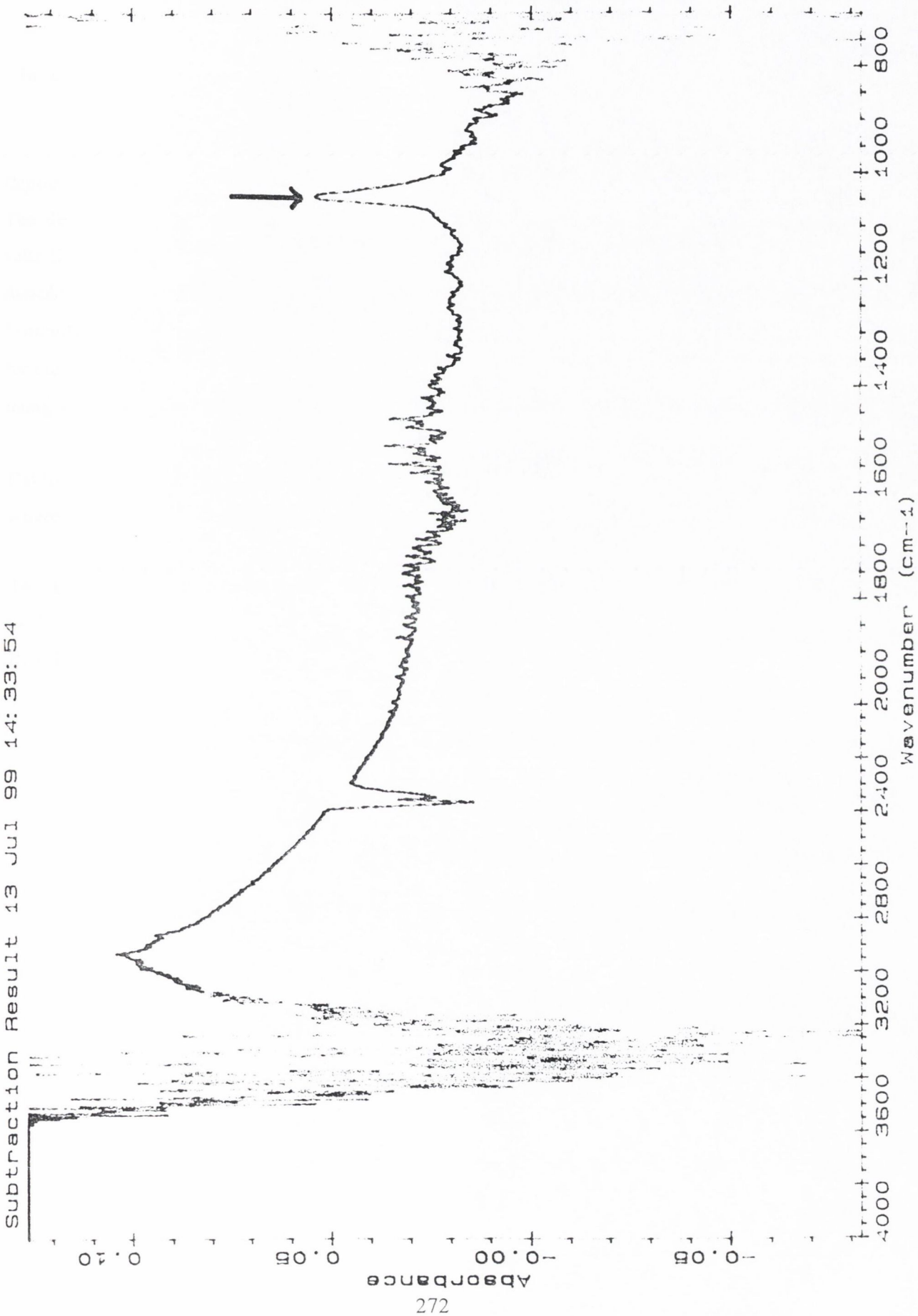

Appendix V

Investigation of the reproducibility of the dissolution method used for intrinsic dissolution rate determinations and dissolution studies on mixed discs

Replicate dissolution runs of benzoic acid (6 discs)

The discs were prepared and mounted in stainless steel disc holders as described for diclofenac salts (Section 3.2.13.1). The dissolution runs were carried out in deionised water in a Sotax AT7 dissolution bath at 37°C (Section 3.2.13.1). Samples were taken after 5, 7.5 and 10 minutes and at 5-minute intervals thereafter up to 60 minutes. The concentration of benzoic acid was determined by measuring the UV absorbance at λ226 nm. A calibration curve for benzoic acid was obtained using a method similar to that employed for diclofenac salts (Section 3.2.10) (λ = 226 nm).

Calibration curve equation: $y = 71.254x + 0.0083$ $R^2 = 0.9992$

where y is absorbance at 226 nm and x is concentration (mg/ml).

The dissolution profiles for the six discs are presented below. The lines shown represent the lines of best fit (linear regression analysis). The slopes of these lines were used to calculate the dissolution rates (mg/min/cm^2), listed in the table below.

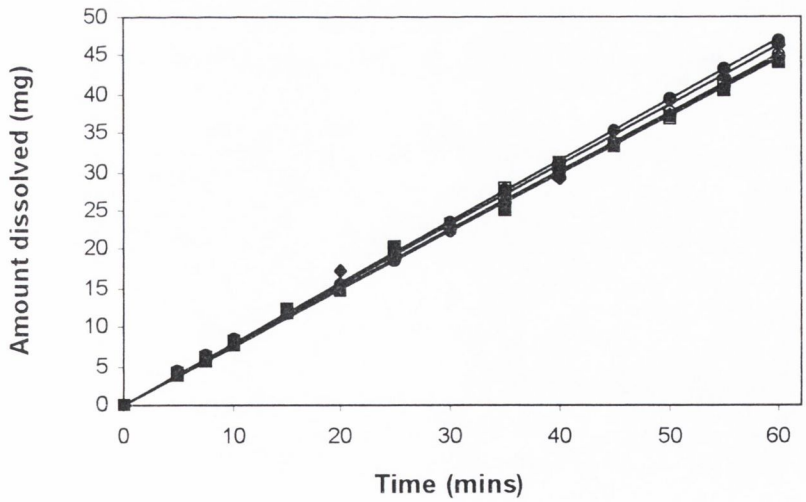

Dissolution profiles for the six benzoic acid discs

Dissolution rates obtained for six benzoic acid discs

Run #	*Dissolution rate* $mg/min/cm^2$	R^2
1	0.5675	0.9967
2	0.5932	0.9994
3	0.5829	0.9971
4	0.5585	0.9981
5	0.5629	0.9989
6	0.5644	0.9994
mean	0.5716	
SD	0.0135	
coefficient of variation	2.36%	

Appendix VI

Determination of the diffusion layer thickness value for the dissolution method used for intrinsic dissolution rate determinations and dissolution studies on mixed discs

The dissolution of benzoic acid was shown by Touitou and Donbrow (1981) to be diffusion-controlled at 37°C. The dissolution rate obtained for benzoic acid at 37°C (0.5716 mg/min/cm^2, Appendix V) was used to calculate the diffusion layer thickness, h, from the Nernst-Brunner equation (Equation 1.25). The value used for the solubility of benzoic acid in water at 37°C, calculated from the solubility values quoted by Edwards (1897) at 35°C and 40°C, was 5.12 mg/ml. A value of 7.42 x 10^{-4} cm^2/min, was used for the diffusion coefficient of benzoic acid (Ramtoola, 1988).

The diffusion layer thickness for the dissolution assembly was calculated to be 66.46 x 10^{-4} cm. This value is higher than the value of 63 x 10^{-4} cm reported by Ramtoola (1988). The static disc, overhead stirrer dissolution method employed by Ramtoola involved coating the disc with paraffin wax such that one side was exposed to the dissolution medium and fixing it to the base of a flat-bottomed vessel, at a distance of 6 cm from the stirrer. In the present work, the disc, held in a stainless steel holder, was positioned on the base of a spherical-bottomed vessel, 1.3 cm from the stirrer, resulting in different hydrodynamics in the system and therefore a different h value.

Appendix VII

Table 1 Rates of dissolution of diclofenac from AMPD:DtBA discs

AMPD:DtBA weight ratio	*Dissolution rate (mean ± SD, n = 3) mmol/min/cm²*
0:100	$3.86 \times 10^{-4} \pm 0.09 \times 10^{-4}$
12:88	$4.45 \times 10^{-4} \pm 0.02 \times 10^{-4}$
20:80	$4.60 \times 10^{-4} \pm 0.04 \times 10^{-4}$
40:60	$4.72 \times 10^{-4} \pm 0.03 \times 10^{-4}$
60:40	$4.62 \times 10^{-4} \pm 0.03 \times 10^{-4}$
80:20	$4.86 \times 10^{-4} \pm 0.04 \times 10^{-4}$
90:10	$4.41 \times 10^{-4} \pm 0.40 \times 10^{-4}$
95:5	$1.95 \times 10^{-3} \pm 0.09 \times 10^{-3}$
98:2	$1.05 \times 10^{-3} \pm 0.03 \times 10^{-3}$

Table 2 Rates of dissolution of diclofenac from TRIS:DtBA discs

TRIS:DtBA weight ratio	*Dissolution rate (mean ± SD, n = 3) mmol/min/cm²*
0:100	$3.86 \times 10^{-4} \pm 0.09 \times 10^{-4}$
20:80	$4.27 \times 10^{-4} \pm 0.01 \times 10^{-4}$
40:60	$4.28 \times 10^{-4} \pm 0.02 \times 10^{-4}$
60:40	$4.65 \times 10^{-4} \pm 0.05 \times 10^{-4}$
80:20	$4.92 \times 10^{-4} \pm 0.02 \times 10^{-4}$
90:10	$5.94 \times 10^{-4} \pm 0.05 \times 10^{-4}$
95:5	$1.75 \times 10^{-3} \pm 0.06 \times 10^{-3}$
98:2	$9.23 \times 10^{-4} \pm 0.02 \times 10^{-4}$

Table 3 Rates of dissolution of diclofenac from AMPD:DDNL discs

AMPD:DDNL weight ratio	*Dissolution rate (mean ± SD, n = 3) mmol/min/cm²*
0:100	$1.67 \times 10^{-2} \pm 0.03 \times 10^{-2}$
5:95	$1.80 \times 10^{-2} \pm 0.02 \times 10^{-2}$
20:80	$7.52 \times 10^{-3} \pm 0.34 \times 10^{-3}$
40:60	$3.96 \times 10^{-4} \pm 0.03 \times 10^{-4}$
60:40	$3.94 \times 10^{-4} \pm 0.05 \times 10^{-4}$
80:20	$3.88 \times 10^{-4} \pm 0.03 \times 10^{-4}$
95:5	$1.95 \times 10^{-3} \pm 0.07 \times 10^{-3}$
98:2	$8.23 \times 10^{-4} \pm 0.44 \times 10^{-4}$

Table 4 Rates of dissolution of diclofenac from TRIS:DDNL discs

TRIS:DDNL weight ratio	*Dissolution rate (mean ± SD, n = 3) mmol/min/cm²*
0:100	$1.67 \times 10^{-2} \pm 0.03 \times 10^{-2}$
5:95	$1.73 \times 10^{-2} \pm 0.03 \times 10^{-2}$
20:80	$4.61 \times 10^{-3} \pm 0.24 \times 10^{-3}$
40:60	$6.38 \times 10^{-4} \pm 0.84 \times 10^{-4}$
60:40	$1.55 \times 10^{-3} \pm 0.07 \times 10^{-3}$
80:20	$1.24 \times 10^{-3} \pm 0.07 \times 10^{-3}$
87.5:12.5	$9.79 \times 10^{-4} \pm 1.25 \times 10^{-4}$
95:5	$1.78 \times 10^{-3} \pm 0.10 \times 10^{-3}$
98:2	$6.82 \times 10^{-4} \pm 0.48 \times 10^{-4}$

Appendix VIII

Models applied to fit experimental dissolution data using the non-linear curve fitting program Micromath® Scientist™ for Windows™

Two component (salt conversion) model

Below is a schematic representation of the two component (salt conversion) model for a BASE:SALT1 system, which assumes complete conversion from SALT1 to SALT2.

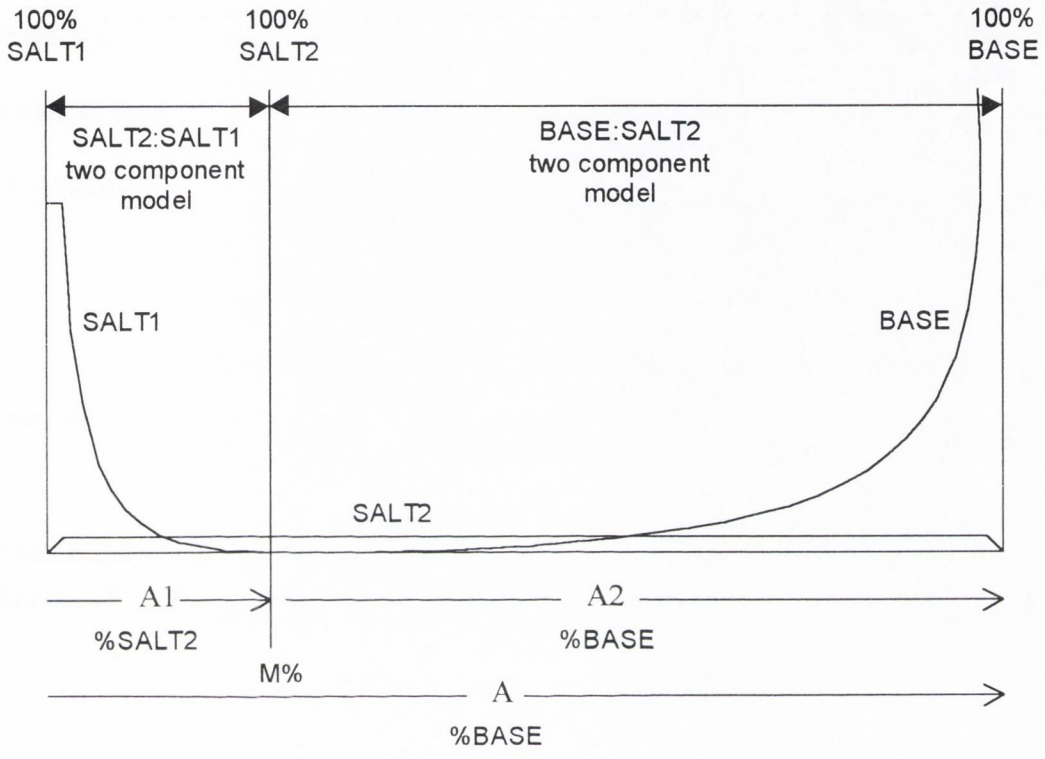

A represents the %BASE used to prepare the disc, A1 represents the %SALT2 in the SALT2:SALT1 two component system and A2 represents the %BASE in the BASE:SALT2 two component system. M represents the %BASE in the initial disc corresponding to a 1:1 BASE:SALT1 molar ratio.

The following derivations were applied to convert from A to A1 at A < M% and to A2 at A > M%.

When A < M%:

Number of moles of SALT2 formed = number of moles of BASE added to disc

$$= \frac{A\,W}{100\,Y}$$

where W is the total weight of the disc

and Y is the molecular weight of BASE.

Weight of SALT2 formed (g) = $\frac{A\ W\ Z}{100\ Y}$

where Z is the molecular weight of SALT2.

Number of moles of SALT1 remaining = number of moles of SALT1 added to disc –number of moles of SALT2 formed = $\frac{(100 - A)\ W}{100\ X} - \frac{A\ W}{100\ Y}$

where X is the molecular weight of SALT1.

Weight of SALT1 remaining (g) = $\frac{(100 - A)\ W\ Y - A\ W\ X}{100\ Y}$

A1 = %SALT2 in the system after conversion

$$= \frac{\text{Weight of SALT2 formed}}{\text{Weight of SALT1 remaining} + \text{Weight of SALT2 formed}}$$

Thus, A1 = $\frac{100\ A\ Z}{A\ Z + (100 - A)\ Y - A\ X}$

When A > M%:

Number of moles of SALT2 formed = number of moles of SALT1 added to disc

= $\frac{(100 - A)\ W}{100\ X}$

Weight of SALT2 formed (g) = $\frac{(100 - A)\ W\ Z}{100\ X}$

Number of moles of BASE remaining = number of moles of BASE added to disc – number of moles of SALT2 formed = $\frac{A\ W}{100\ Y} - \frac{(100 - A)\ W}{100\ X}$

Weight of BASE remaining (g) = $\frac{A\ W\ X - (100 - A)\ W\ Y}{100\ X}$

A2 = %BASE in the system after conversion

$$= \frac{\text{Weight of BASE remaining}}{\text{Weight of BASE remaining} + \text{Weight of SALT2 formed}}$$

Thus, A2 = $\frac{100\left[A\ X - (100 - A)\ Y\right]}{A\ X - (100 - A)\ Y + (100 - A)\ Z}$

```
// MicroMath Scientist Model File
// Two component (salt conversion) model
IndVars: A
DepVars: GD
Params: DA, DB, DC, CSA, CSB, CSC, H, X, Y, Z
A1=(100*A*Z)/(((100-A)*Y)-(A*X)+(A*Z))
CMA1=(DA*CSA)/(DB*CSB)
CMAP1=(CMA1*100)/(1+CMA1)
GA1=(DA*CSA)/H
GB1=(DB*CSB)/H
A2=(100*((A*X)-((100-A)*Y)))/
((A*X)-((100-A)*Y)+((100-A)*Z))
CMA2=(DC*CSC)/(DA*CSA)
CMAP2=(CMA2*100)/(1+CMA2)
GC1=(DC*CSC)/H
GA3=(GC1*(100-A2))/A2
CMAP3=(100*Y*CMAP1)/
((100*Z)+(CMAP1*Y)+(CMAP1*X)-(CMAP1*Z))
CMAP4=((-100*Y*CMAP2)+(100*Z*CMAP2)+(10000*Y))/
((100*X)+(100*Y)-(CMAP2*X)-(CMAP2*Y)+(CMAP2*Z))
FLAG3=UNIT(A-CMAP3)
FLAG4=UNIT(A-CMAP4)
GBX=((1-FLAG3)*GB1)
GB=IFEQZERO(A,GB1,GBX)
D=100-A
GAX=(GA1*FLAG3*(1-FLAG4))+(GA3*FLAG4)
GA=IFEQZERO(D,GA3,GAX)
GD=GA+GB
***
```

Three component (salt conversion) model

Below is a schematic representation of the three component (salt conversion) model, which assumes partial conversion of SALT1 to SALT2.

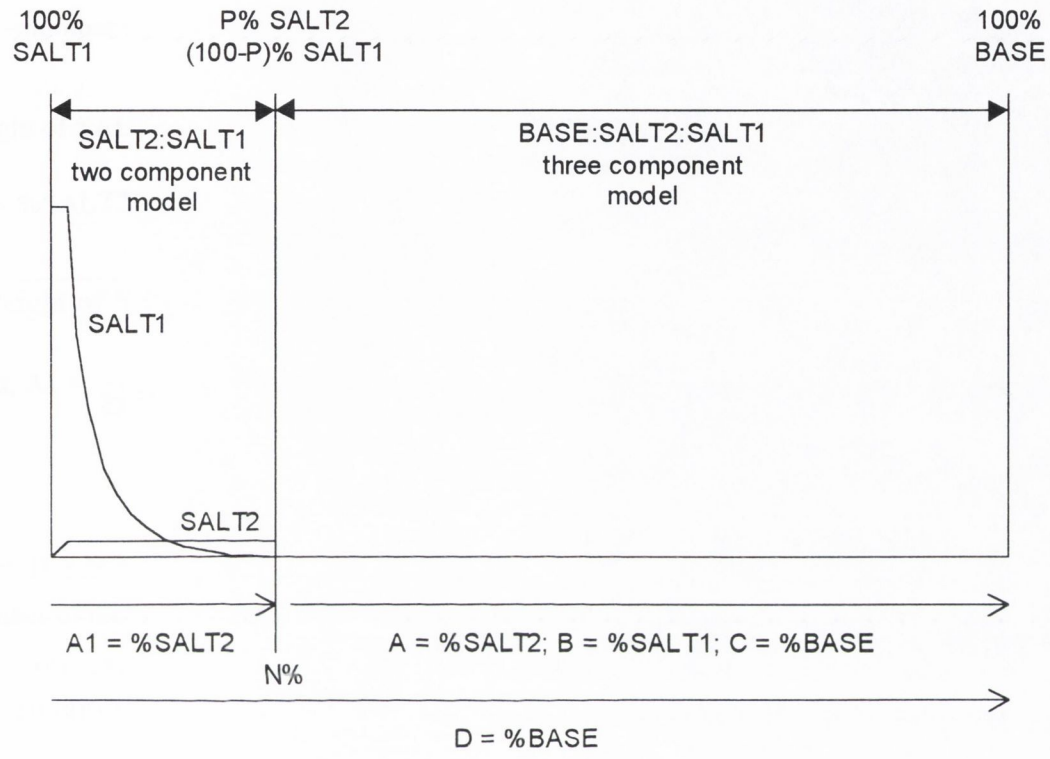

D represents the %BASE used to prepare the disc.

P represents the percentage of diclofenac acid present which converts to SALT2.

A1 represents the %SALT2 in the SALT2:SALT1 two component system.

A, B and C represent the %SALT2, %SALT1 and %BASE, respectively, in the BASE:SALT2:SALT1 three component system.

When D = N%:

There is sufficient BASE present to convert P% of the diclofenac acid to SALT2, i.e. number of moles of BASE added to disc = P% number of moles of SALT1 added to disc

$$\frac{N\,W}{100\,Y} = \frac{P\,(100 - N)\,W}{10{,}000\,X}$$

$$\text{Thus, } N = \frac{100\,P\,Y}{100\,X + PY}$$

When D < N%:

Number of moles of SALT2 formed = number of moles of BASE added to disc = $\frac{D\,W}{100\,Y}$

Weight of SALT2 formed (g) = $\frac{D\,W\,Z}{100\,Y}$

Number of moles of SALT1 remaining after conversion = number of moles of SALT1 added to disc – number of moles of SALT2 formed = $\frac{(100-D)\,W}{100\,X} - \frac{D\,W}{100\,Y}$

Weight of SALT1 remaining after conversion (g) = $\frac{(100-D)\,W\,Y - D\,W\,X}{100\,Y}$

A1 = %SALT2 after conversion

$$= \frac{\text{Weight of SALT2 formed}}{\text{Weight of SALT2 formed} + \text{Weight of SALT1 remaining}}$$

Thus, A1 = $\frac{100\,D\,Z}{D\,Z + (100-D)\,Y - D\,X}$

When D > N%:

Number of moles of SALT2 formed = P% number of moles of SALT1 added to disc

= $\frac{P\,(100-D)\,W}{10{,}000\,X}$

Weight of SALT2 formed (g) = $\frac{P\,(100-D)\,W\,Z}{10{,}000\,X}$

Number of moles of SALT1 remaining after conversion = (100-P)% number of moles of SALT1 added to disc

= $\frac{(100-P)\,(100-D)\,W}{10{,}000\,X}$

Weight of SALT1 after conversion (g) = $\frac{(100-P)\,(100-D)\,W}{10{,}000}$

Number of moles of BASE remaining after conversion = number of moles of BASE added to disc – number of moles of SALT2 formed = $\frac{D\,W}{100\,Y} - \frac{P\,(100-D)\,W}{10{,}000\,X}$

Weight of BASE remaining after conversion (g) = $\frac{100\,X\,D\,W - P\,Y\,W\,(100-D)}{10{,}000\,X}$

A = %SALT2 after conversion =

$$\frac{\text{Weight of SALT2 formed}}{\text{Weight of SALT2 formed} + \text{Weight of SALT1 remaining} + \text{Weight of BASE remaining}}$$

$$= \frac{100\,P\,Z\,(100 - D)}{P\,Z\,(100 - D) + (100 - P)\,(100 - D)\,X + 100\,X\,D - P\,Y\,(100 - D)}$$

B = %SALT1 after conversion =

$$\frac{\text{Weight of SALT1 remaining}}{\text{Weight of SALT2 formed} + \text{Weight of SALT1 remaining} + \text{Weight of BASE remaining}}$$

$$= \frac{(100 - P)\,(100 - D)\,100\,X}{P\,Z\,(100 - D) + (100 - P)\,(100 - D)\,X + 100\,X\,D - P\,Y\,(100 - D)}$$

C = %BASE after conversion = 100 – (A + B)

```
// MicroMath Scientist Model File
// Three component (salt conversion) model
IndVars: D
DepVars: GD
Params: DA, DB, DC, CSA, CSB, CSC, H, P, X, Y, Z
N=(100*P*Y)/((100*X)+(P*Y))
A1=(100*D*Z)/((D*Z)+((100-D)*Y)-(D*X))
FLAG1=UNIT(N-D)
CMA=(DA*CSA)/(DB*CSB)
CMAP=(CMA*100)/(CMA+1)
GA1=(DA*CSA)/H
FLAG2=UNIT(A1-CMAP)
GATW1=(FLAG2*GA1)
GATW2=IFEQZERO(D,0,GATW1)
GB1=(DB*CSB)/H
GBTW1=((1-FLAG2)*GB1)
GBTW2=IFEQZERO(D,GB1,GBTW1)
GDTW=GATW2+GBTW2
A2=(100*P*Z*(100-D))/
((P*Z*(100-D))+((100-P)*(100-D)*X)+(100*D*X)-(P*Y*(100-D)))
B2=((100-P)*(100-D)*100*X)/
((P*Z*(100-D))+((100-P)*(100-D)*X)+(100*X*D)-(P*Y*(100-D)))
C2=100-(A2+B2)
A3=(DA*CSA*100)/((DA*CSA)+(DB*CSB)+(DC*CSC))
B3=(DB*CSB*100)/((DA*CSA)+(DB*CSB)+(DC*CSC))
C3=(DC*CSC*100)/((DA*CSA)+(DB*CSB)+(DC*CSC))
A4=(B2*DA*CSA)/(DB*CSB)
B4=(C2*DB*CSB)/(DC*CSC)
C4=(A2*DC*CSC)/(DA*CSA)
A5=(DA*CSA*100)/((DA*CSA)+(DB*CSB))
B5=(DB*CSB*100)/((DB*CSB)+(DA*CSA))
C5=(DC*CSC*100)/((DC*CSC)+(DA*CSA))
A6=(DA*CSA*100)/((DA*CSA)+(DC*CSC))
B6=(DB*CSB*100)/((DB*CSB)+(DC*CSC))
C6=(DC*CSC*100)/((DB*CSB)+(DC*CSC))
GC1=(DC*CSC)/H
GA3=(A2*GB1)/B2
GB3=(B2*GA1)/A2
GC3=(C2*GA1)/A2
GA4=(A2*GC1)/C2
GB4=(B2*GC1)/C2
GC4=(C2*GB1)/B2
F1=UNIT(A2-A3)+UNIT(A3-A2)
F2=UNIT(B2-B3)+UNIT(B3-B2)
F3=UNIT(C2-C3)+UNIT(C3-C2)
F4=UNIT(A2-A4)+UNIT(A4-A2)
F5=UNIT(B2-B4)+UNIT(B4-B2)
F6=UNIT(C2-C4)+UNIT(C4-C2)
F7=UNIT(C3-C2)
F8=UNIT(A3-A2)
F9=UNIT(B3-B2)
F10=UNIT(C2-C3)
F11=UNIT(A2-A3)
F12=UNIT(B2-B3)
F13=UNIT(B4-B2)
F14=UNIT(A2-A4)
F15=UNIT(B2-B4)
F16=UNIT(C4-C2)
```

```
F17=UNIT(C2-C4)
F18=UNIT(A4-A2)
F19=UNIT(A2-A5)+UNIT(A5-A2)
F20=UNIT(B2-B5)+UNIT(B5-B2)
F21=UNIT(A2-A6)+UNIT(A6-A2)
F22=UNIT(C2-C5)+UNIT(C5-C2)
F23=UNIT(B2-B6)+UNIT(B6-B2)
F24=UNIT(C2-C6)+UNIT(C6-C2)
F25=UNIT(A2-A5)*UNIT(B5-B2)
F26=UNIT(A2-A6)*UNIT(C5-C2)
F27=UNIT(B2-B6)*UNIT(C6-C2)
F28=UNIT(B2-B5)*UNIT(A5-A2)
F29=UNIT(C2-C5)*UNIT(A6-A2)
F30=UNIT(C2-C6)*UNIT(B6-B2)
E=100-A2
F=100-B2
G=100-C2
J=100-D
GAC=((1-F1)*(1-F2)*(1-F3)*GA1)+((1-F4)*F7*GA1)+((1-F6)*F9*GA1)
+((1-F4)*F10*GA4)+((1-F5)*F11*GA1)+(F11*F16*F13*GA1)
+(F14*F17*F9*GA4)+(F14*F7*F15*GA1)
GBC=((1-F1)*(1-F2)*(1-F3)*GB1)+((1-F4)*F7*GB1)+((1-F5)*F8*GB1)
+((1-F4)*F10*GB4)+((1-F6)*F12*GB1)+(F12*F18*F16*GB1)
+(F8*F15*F17*GB1)+(F13*F10*F18*GB4)
GCC=((1-F1)*(1-F2)*(1-F3)*GC1)+((1-F4)*F7*GC3)+((1-F5)*F8*GC1)
+((1-F6)*F9*GC1)+((1-F4)*F10*GC1)+((1-F5)*F11*GC3)+((1-F6)*F12*GC4)
+(F11*F16*F13*GC3)+(F14*F17*F9*GC1)+(F14*F7*F15*GC3)
+(F12*F18*F16*GC4)+(F8*F15*F17*GC4)+(F13*F10*F18*GC1)
GAX=((1-F19)*(1-F20)*GA1)+(F25*GA1)
GBX=((1-F19)*(1-F20)*GB1)+(F28*GB1)
GAY=((1-F21)*(1-F22)*GA1)+(F26*GA1)+(F29*GA4)
GCY=((1-F21)*(1-F22)*GC1)+(F26*GC3)+(F29*GC1)
GBZ=((1-F23)*(1-F24)*GB1)+(F27*GB1)+(F30*GB4)
GCZ=((1-F23)*(1-F24)*GC1)+(F27*GC4)+(F30*GC1)
GAB=IFEQZERO(A2,0,GAC)
GBB=IFEQZERO(A2,GBZ,GBC)
GCB=IFEQZERO(A2,GCZ,GCC)
GAA=IFEQZERO(B2,GAY,GAB)
GBA=IFEQZERO(B2,0,GBB)
GCA=IFEQZERO(B2,GCY,GCB)
GAD=IFEQZERO(C2,GAX,GAA)
GBD=IFEQZERO(C2,GBX,GBA)
GCD=IFEQZERO(C2,0,GCA)
GATH=IFEQZERO(E,GA1,GAD)
GBTH=IFEQZERO(F,GB1,GBD)
GCTH=IFEQZERO(G,GC1,GCD)
GDTH=GATH+GBTH
GA=(FLAG1*GATW2)+((1-FLAG1)*GATH)
GB=(FLAG1*GBTW2)+((1-FLAG1)*GBTH)
GC=(1-FLAG1)*GCTH
GDX=(FLAG1*GDTW)+((1-FLAG1)*GDTH)
GD=IFEQZERO(J,0,GDX)
***
```